University of Strathclyde

Faculty of Engineering

Department of Biomedical Engineering

EEG Signatures and Directional Information in Planning and Execution of Arm Isometric Exertions

by

Bahman Nasseroleslami

Submitted in partial fulfilment of the requirements for the degree of

Doctor of Philosophy

2013

Declaration of Authenticity and Author's Rights

This thesis is the result of the author's original research. It has been composed by the author and has not been previously submitted for examination which has led to the award of a degree.

Part of the author's work has been published externally. The published papers are listed in Appendix F.

Bahman Nasseroleslami

May 13, 2013

to the Universe ...

and

to Science ...

Acknowledgement

I would like to thank everyone who has provided assistance in my PhD research and in preparation of the thesis at the University of Strathclyde: my supervisors, Heba Lakany and Bernie Conway; technical staff of the Biomedical Engineering Department, John MacLean, Stephen Murray and David Robb; post-doctoral researchers, Bruce Carse, Sujay Galen, Campbell Reid and Gopal Valsan; postgraduate students, Pauline Axford, Celia Clarke, Bartek Grychtol, Lucy Jones, Hin Chung Lan, Catherine MacLeod, Federica Menotti, Niall McKenzie, Bilal Nasser and Ange Tano; and also the academic staff overseas, John Kalaska (Département de physiologie, Université de Montréal), Ali Sanjari (Faculty of Rehabilitation, Tehran University of Medical Sciences) and Rhea Eskew (Department of Psychology, Northeastern University). Especially, I am grateful for assistance in data collection, the language proof-reading of the thesis, technical assistance and discussions.

I should hereby acknowledge the Scottish Funding Council (SFC) and Glasgow Research Partnership in Engineering (GRPE) for the PhD studentship scholarship.

I am grateful to all of the staff at the University of Strathclyde and to those within the academic networks of Glasgow, Scotland and the rest of the United Kingdom for all the training and support I have received during my research.

I should also mention the hospitality and friendly support of the people in Scotland which has been a great source of encouragement for me.

I appreciate the role of my previous supervisors, professors, teachers, intellectuals and friends in Iran during my previous studies and degrees, that have given me the skills and opportunity to pursue this research, especially, Mohamad Parnianpour.

I would also like to thank my wife, Sahar; my father, Mohsen; my mother, Zari; my sisters, Parvaneh and Banafsheh; and my nephew, Omid for their support during my studies.

The contributions of staff and volunteers to the open-source writing systems and the relevant tools, especially the developers and maintainers of LaTeX , are greatly appreciated.

Contents

Abstract

The motor-related electroencephalographic (EEG) activity pattern in humans during motor behaviour is of interest to provide insight into normal motor control processes and for development of brain-computer interfaces (BCI), brain stimulation and rehabilitation systems. While the patterns preceding brisk voluntary movements, and especially movement execution, are well described, there are few EEG studies that address the cortical activation patterns seen in isometric exertions, and their planning. Furthermore, the effect of exertion direction on EEG signatures needs investigation. This study explores and reports on the time and time-frequency surface EEG signatures in isometric task experiments in normal subjects (n=8). Multichannel EEG is recorded during motor preparation, planning and execution of directional centre-out arm isometric exertions performed at the wrist in the horizontal plane, in response to instruction-delay visual cues. The directional information of surface EEG and modulation of EEG signatures by cue direction are investigated by statistical measures and linear classifiers. The observations suggest that isometric force exertion is accompanied by transient and sustained forms of event-related potentials (ERP) and event-related (de-)synchronisations (ERD/ERS), comparable to those of a movement task. Furthermore, the ERP and ERD/ERS are observed not only during execution, but also during preparation and planning of the isometric task. Transient synchronisation in 2-7 Hz frequency band and both transient and sustained desynchronisation in α (μ) and β frequency bands were observed. Low-γ (30-50 Hz) ERD is observed in all areas, except over the parietal region where ERS is seen. While ERP and ERD/ERS are not consistently modulated by task direction, the direction of exertion can be predicted by single-trial classification. Classification rates reach 69% and 83% in planning and execution stages, respectively. As no physical displacement happens during the task, it can be hypothesised that the underlying mechanisms of motor-related ERD/ERS and the directional information do not only depend on limb coordinate change or target coordinates. The results contribute to the current understanding of different brain region functions during voluntary motor tasks and can help to clarify the relationships between invasive brain recordings and large-scale recordings such as EEG in this context. Ultimately, this will contribute to further clinical applications, including (BCI-)rehabili-

tation and electrical/magnetic brain stimulation research.

List of Tables

List of Figures

Nomenclature and Abbreviations

AC	Attention Cue
ALS	Amyotrophic Lateral Sclerosis
ANOVA	Analysis of Variance
ARMA	Auto-Regressive Moving Average
BCI	Brain-Computer Interface
BMI	Brain-Machine Interface
BP	Bereitschaftspotential
CAR	Common-Average Reference
CLIS	Completely Locked-In State
CNS	Central Nervous System
CNV	Contingent Negative Variation
CP	Cerebral Palsy
CRT	Cathode Ray Tube
CWT	Continuous Wavelet Transform
DC	Direction Cue
DCR	Direct Current Removal
DFT	Discrete Fourier Transform
ECG	Electrocardiography
ECoG	Electrocorticography
ECR	Extensor Carpi Radialis
ECU	Extensor Carpi Ulnaris
EDC	Euclidean Distance Classifier
EEG	Electroencephalography

ELR	Ear-Lobe Reference
EMG	Electromyography
EOG	Electrooculography
EP	Error Potential
ERD	Event-Related Desynchronisation
ERP	Event-Related Potential
ERS	Event-Related Synchronisation
ERSP	Event-Related Spectral Perturbation
FCR	Flexor Carpi Radialis
FCU	Flexor Carpi Ulnaris
FES	Functional Electrical Stimulation
FFT	Fast Fourier Transform
GUI	Graphical User Interface
ICA	Independent Component Analysis
ITC	Inter-Trail Coherence
KNN	K-Nearest Neighbour
LDA	Linear Discriminant Analysis
LFP	Local Field Potential
LIS	Locked-In State
LPF	Low-Pass Filtering
MEG	Magnetoencephalography
MEP	Motor Evoked Potential
M1	Primary Motor Cortex
MI	Motor Imagery
MRP	Movement/Motor-Related Potential
MS	Multiple Sclerosis
NIRS	Near Infra-Red Spectroscopy
PC	Principal Component
PCA	Principal Component Analysis
PD	Preferred Direction

PMd	Pre-Motor Cortex-dorsal
PSD	Power Spectral Density
RC	Rest Cue
RP	Readiness Potential
rTMS	repetitive Transcranial Magnetic Stimulation
SCI	Spinal Cord Injury
SCP	Slow Cortical Potential
sEMG	surface Electromyography
SL	Surface Laplacian
SMA	Supplementary Motor Area
SMR	Sensorimotor Rhythm
SSEP	Somatosensory Evoked Potential
SSVEP	Steady State Visual Evoked Potential
STFT	Short-Time Fourier Transform
SUA	Single Unit Activity
SVD	Singular Value Decomposition
tACS	transcranial Alternative Current Stimulation
tDCS	transcranial Direct Current Stimulation
TMS	Transcranial Magnetic Stimulation
TNT	Tensor Network Theory
tSDCS	transcranial Sinusoidal Direct Current Stimulation
VEP	Visual Evoked Potential
WVD	Wigner-Ville Distribution
ZPCA	Z-score and Principal Component Analysis

Chapter 1

Introduction

This first chapter of the thesis explores the general context, innovation of the research and structure of the subsequent chapters. First, the general context of research is described in Section 1.1. Then, based on the general research context, the long-term objectives of thesis are highlighted in Section 1.2. The organisation of the thesis is explained in Section 1.3 and finally Section 1.4 summarises the chapter.

1.1. Research Context

As a multidisciplinary research study in biomedical engineering, rehabilitation and motor control, the present research can be viewed to emerge from three major research contexts: (1) the motor neuroscience of large-scale brain recordings, (2) communication and control in severely disabled people who require assistive technologies for communication with the external world and for control of external devices and prosthetics and (3) rehabilitation research for improving sensorimotor functions in neuromuscular disabilities such as stroke, brain lesion and spinal cord injury (SCI).

1.1.1. Large-Scale Brain Recording

Recording of the brain's neural activity is paramount to understanding the brain functional mechanisms. Recordings can be achieved using various invasive and non-invasive techniques and each method has different positives and negatives (Waldert et al., 2009). From a purely neuroscientific viewpoint, identification of signatures of large-scale brain recording techniques, e.g. electrocorticography (ECoG), magnetoencephalography (MEG) and electroencephalography (EEG)[1], provides high time-resolution information about the ac-

[1] In this text, the term EEG is used for non-invasive surface EEG and does not include invasive EEG recording techniques.

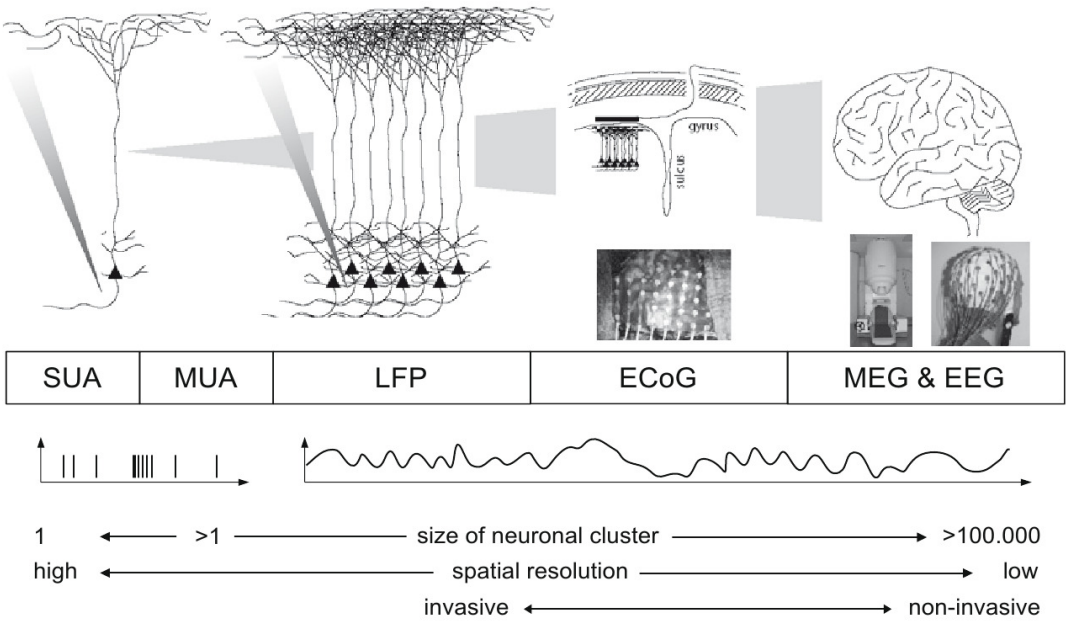

Figure 1.1. Schematic comparison of the different recording techniques: SUA/MUA, LFP, ECoG, and MEG/EEG. From top to bottom: The spatial scale of recording, the characteristics of the signal (spikes vs. continuous analogue signal) and different scales of the methods. From Waldert et al. 2009. Permission to reproduce this figure has been granted by Elsevier.

tivity of pools of neurons during various cognitive and sensorimotor tasks. Although their spatial resolution is lower than local field potentials (LFP) and single unit activity (SUA) recordings (see Figure 1.1 for clarification), they provide good information about brain connectivity and ensemble neural activity. Specifically, they can reveal signatures and measures of interaction between neuronal pools and different neural circuitries. This also facilitates the study of synchronous brain activity. This knowledge can be used for clinical purposes and to study the planning and execution of human movement. It can also be used to find the relationship between different task parameters and neural activities in different brain regions and at different time-instances. This knowledge not only improves the understanding of the brain's sensorimotor function, but would significantly help in healthcare and rehabilitation research as later explained in Sections 1.1.2 and 1.1.3. Figure 1.1 gives a brief overview of the common techniques for recording electrical brain activity.

1.1.2. Communication in Severely Disabled Patients

Communication with and control of an external (i.e. not part of the human body) machine, computer, device, etc. by the human brain is referred to as brain-computer interfacing (BCI). The BCI systems can be categorized based on the way they make this connection. BCI systems pick up some neural activity generated by individuals and translate it to a

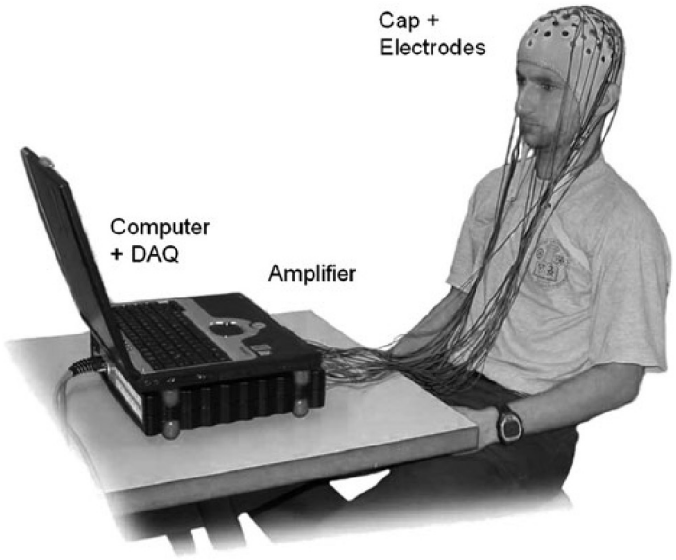

Figure 1.2. An example of a common EEG-based BCI. It consists of EEG electrodes and cap, cables that transmit the recorded EEG to a signal amplifier, digitizer and computer. The computer processes the data and controls the visual output of the BCI, based on the signal processing translation algorithm. From Graimann et al. 2010. Permission to reproduce this figure has been granted by Springer Science+Business Media.

message, command, action or movement of a prosthetic or orthotic device. They effectively act as a new information channel from the central nervous system (CNS) (Wolpaw, 2007). BCI systems are discussed in Section 2.1.

BCIs are potentially considered a communication solution for patients suffering from extreme neuromotor diseases that lead to a locked-in state (LIS) or completely locked-in state (CLIS). These include: progressive neurodegenerative diseases such as amyotrophic lateral sclerosis (ALS), non-progressive non-contagious diseases such as cerebral palsy (CP), autoimmune neural conditions such as multiple sclerosis (MS), and severe disabilities due to spinal cord injury (SCI) (Birbaumer and Cohen, 2007). Figure 1.2 shows a common EEG-based BCI system.

In short, EEG-based brain-computer interface systems are the most feasible BCIs to date, due to clinical, economical, safety and implementation considerations. Consequently, they have been of great interest to researchers. They have also been shown to have a matching performance to invasive BCIs in terms of information transfer rate, when comparing the recent advances in both these areas of research (Birbaumer et al., 2008). BCI systems that use the EEG associated with human motor activity are the most widely studied class of BCI (McFarland et al., 2006; Pfurtscheller and Neuper, 2006). However, development of new electrode manufacturing technologies, such as flexible bio-compatible micro-electrode arrays (Lin et al., 2011; Minev et al., 2011), may boost invasive BCI research in the future. While this will improve the information transfer rates,

the dry electrode technology (Zander et al., 2011) will make the non-invasive BCI more practical. The mentioned role of EEG-based BCIs suggests that a good knowledge about motor related EEG is required for the development of such systems. Contrarily, if the research efforts to develop functional EEG-based BCI systems fail, the knowledge gained through the research is invaluable for other areas of research including: neuromuscular rehabilitation, neurofeedback and motor neuroscience. Furthermore, the algorithms developed dealing with large scale, real-time, high-density, time-variant signals are also invaluable in the field of signal processing and real-time implementation.

1.1.3. Neuromuscular Rehabilitation

1.1.3.1. Enhancement of Rehabilitation Training

Originally, neuro-biofeedback research has been the path to BCI initiation (See Birbaumer, 2006, for review). In Section 1.1.2 it was briefly noted that BCI systems can be used for communication and control of external devices and that many systems use the non-invasive motor-related activity in EEG.

BCI systems can be used as rehabilitation devices, not only for LIS patients but also for people with partial paralysis, motor disorders, incomplete SCI and stroke for improving sensorimotor functions. There are potential uses of BCIs for motor rehabilitation that may help partially paralysed patients (Birbaumer and Cohen, 2007). An example is to set the external movement/output of the BCI system to the original intended motor task which the subject attempts. In such arrangements tiny targeted and successfully generated neural activity results in the physical movement of a robot (controlled by BCI). This can potentially facilitate sensorimotor repair, plasticity and rehabilitation (Birbaumer et al., 2008; Daly and Wolpaw, 2008). Figure 1.3 shows an example of a BCI-controlled robot/orthosis being used for rehabilitation (referred to as BCI-aided Rehabilitation).

Another approach to rehabilitation uses functional electrical stimulation (FES) as the output of the BCI system to artificially apply electrical stimulation to paralysed muscles (Pfurtscheller et al., 2003). The hypothesis behind this strategy is based on the Hebbian learning theory (Hebb, 1949). It is expected that simultaneous activation of motor cortical areas and muscles (probably with the involvement of sensory cortical regions, e.g. S1, and sensory pathways) strengthens or facilitates the repair of the neural connectivity of the lost corticospinal connections. There are however only a few studies which use this approach. Figure 1.4 shows an example of BCI-aided FES rehabilitation.

Again, a detailed knowledge about motor related EEG and its relationship with various motor tasks is required to develop a functional rehabilitation setup and protocol.

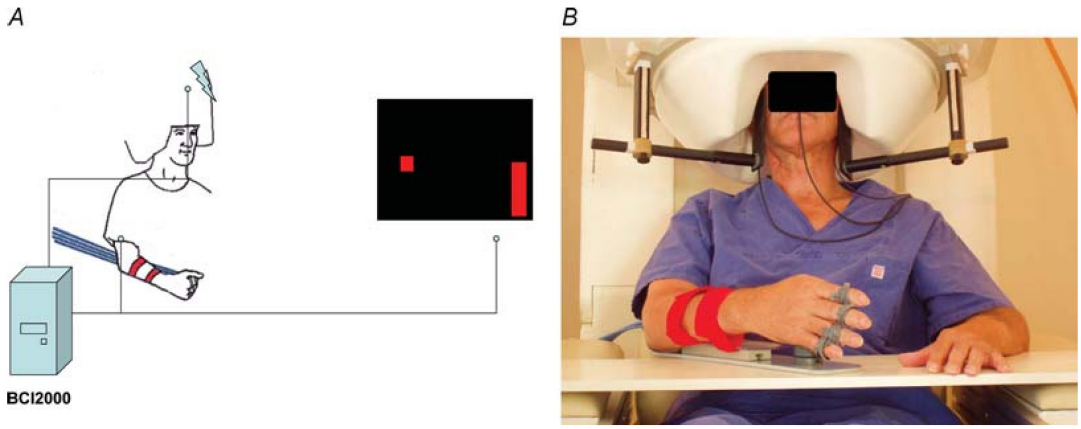

Figure 1.3. MEG BCI-aided rehabilitation using robot/orthosis for chronic stroke. A) Patients receive visual feedback on the generated SMR activity after instruction to increase or decrease the SMR. Decrease in SMR closes and increase in SMR opens the hand gradually. B) Patient during training using the system. From Birbaumer and Cohen 2007. Permission to reproduce this figure has been granted by John wiley & Sons.

1.1.3.2. Targeted Brain Stimulation

Various brain stimulation methods, that are considered as non-invasive techniques, have been used in sensorimotor control and motor learning research (Reis et al., 2008). Transcranial magnetic stimulation (TMS) (Ljubisavljevic, 2006) and repetitive TMS (rTMS) (Lazzaro et al., 2010) use electric impulses generated by a transient, focused and large magnetic field to stimulate groups of neurons transcranially. Recently, transcranial direct current stimulation (tDCS) (Stagg and Nitsche, 2011), has gained more attention among research groups, as a potential non-invasive inducer of plasticity (Cambiaghi et al., 2010). Other variants of transcranial stimulation of the brain using electrical currents are under active research: transcranial alternating current stimulation (tACS) and transcranial sinusoidal direct current stimulation (tSDCS) (Hunter et al., 2009).

Knowledge of oscillatory brain activity is essential to develop a systematic framework for research on the aforementioned methods. The ensemble behaviour of neurons in the brain, appears as brain oscillations with different characteristics. EEG as one of the large-scale brain recording techniques can reflect oscillatory behaviour of the brain that may help us to identify the oscillators involved in motor tasks. This knowledge could aid electrical brain stimulation research by revealing some oscillatory characteristics of the brain during motor tasks. One of the hypotheses is that region, polarity, current flow direction and oscillation frequency of electrical-current brain-stimulation can be inferred partially from large scale brain recordings and imaging (See for example Feurra et al., 2011; Jin et al., 2011; Thut et al., 2011).

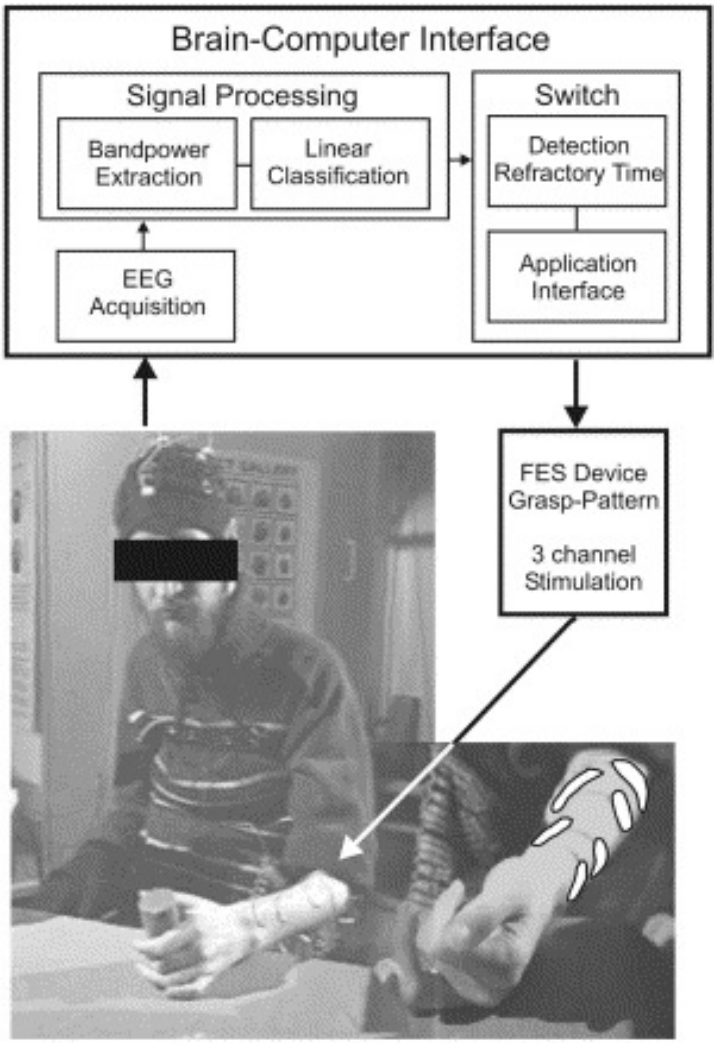

Figure 1.4. EEG-based BCI system activates an FES device with 3 pairs of surface electrodes. Beta band activity burst, generated by foot motor imagery, activates the muscles to help the patient grab the cylinder. From Pfurtscheller et al. 2003. Permission to reproduce this figure has been granted by Elsevier.

1.2. Long-Term Research Objectives

In the previous sections the different contexts in which motor-related EEG can play a significant role were introduced. In this section, more specific research objectives in these contexts are discussed. Theese objectives eventually lead to the reseaerch hypotheses and the novel contributions of the thesis in Section 2.4.

1.2.1. Understanding Motor-Related Brain Activity

Motor-related electrical brain activities are key to man's understanding of motor neuroscience, as a basic and fundamental science. Obviously, this has numerous applications in rehabilitation, medicine, sports science and many other subjects. More specifically, the

following issues are of interest as fundamental concepts: The involvement of different brain regions such as supplementary motor area (SMA), pre-motor cortex (PM), primary motor cortex (M1), parietal cortex; their laterality in motor tasks (ipsilateral, contralateral or bilateral activity in different motor tasks); their activation sequence and timing; range and type of activity; the variation among different types of tasks (reaching vs. isometric tasks). In Section 2.2, a more detailed literature review and analysis address the gaps in the current understanding of motor function.

1.2.2. Identification of Voluntarily Generated Brain Signals

As discussed in Sections 1.1.1, 1.1.2 and 1.1.3.1, a major area of interest is the tasks (primarily motor tasks) that are suitable for BCI applications. These tasks should be repeatable and similar to daily neuromuscular activities as well as have signal features that are spatially and/or temporally modulated by task parameters, so that more information can be extracted from the EEG signals. Ideally, features that can represent several task parameters simultaneously (e.g. direction, speed and endpoint of a reaching task) are sought. These features may be time, time-frequency, or non-linear features. Therefore, the spatial and temporal variations of the candidate features during the task are to be determined as these features are supposed to translate into BCI control commands. The spatial distribution reveals where BCI electrodes should be placed for optimum recordings. Temporal information determines the delays, speed, required signal processing and algorithms of a corresponding BCI system. The dimension of the control commands and the information transfer rate of the BCI is determined by the degree of freedom and separability of the features. The BCI system can be used for communication and control, and if designed according to physically relevant motor task features, for BCI-aided rehabilitation. It is also noteworthy that the desired features are different voluntarily generated EEG features, that accompany normal daily tasks and do not require (re)learning or conditioning of the EEG by user. EEG conditioning and relearning (through biofeedback) can be of interest and studied as an alternative approach to BCI applications and as a diferent window for assessing and understanding the neurophysiology of motor control and learning.

1.2.3. Assessment of Oscillatory Brain Activity

As discussed in Section 1.1.3.2, EEG recordings can give an indication of activity characteristics of brain oscillators. The sinusoidal components in electrical brain stimulation can be potentially applied on different brain regions, with various polarities, various current flow directions, various frequencies, in different time windows, and with different

stimulation protocols. Preliminary results imply that excitation and inhibition of corticospinal pathways may be modulated by the stimulation parameters such as frequency, region, polarity, direction and timing (Axford, 2010). As an example, EEG recordings over motor cortical regions exhibit increased (ERS), decreased (ERD) and decreased (ERD) frequency powers at 5Hz, 10Hz and 20Hz respectively during voluntary movement tasks. Early findings (Axford, 2010) suggest that applying transcranial sinusoidal direct current stimulation (tSDCS) with 10Hz frequency leads to the same facilitatory/inhibitory effect of 20Hz stimulation, but different to that of applying 5Hz stimulation (Axford, 2010). Deeper knowledge about brain oscillators, their location, frequency, interconnections and their exact role and timing in motor planning and execution can pave the way for brain stimulation research. EEG recording is a potential source for knowledge on brain oscillators. Consequently, time-frequency representations of EEG signals taken from different stages of the motor tasks can provide essential information on oscillatory brain activity for designing and implementing brain stimulation and other neuroscientific and clinical purposes.

1.3. Thesis Structure

The thesis is organised into 5 chapters. Chapter 1, Introduction, is the present chapter. Chapter 2, Literature Review and Analysis, focuses mainly on the analysis of the relevant literature and leads to the research hypothesis of the thesis and the philosophy behind the undertaken research. Chapter 3, Materials and Methods, describes *why* and *how* the experiments were performed and the details of the data analysis methods. Chapter 4 is the results chapter and the observations and output of the data analysis are presented from different aspects of interest. Chapter 5, Discussion and Conclusions, is the last chapter and discusses innovations, new insights and limitations, according to the results and concludes with the stand of past, present and future research in the context of the literature.

There are also seven appendices that give the technical details of the implemented data recording setup (Appendix A), the computational algorithms and implementations (Appendix C), the screenshots of custom developed software and GUI tools (Appendix B), the supplementary statistics on overal significance levels (Appendix D), supplementary results (Appendix E), the publications from this research (Appendix F) and also the subject information sheets and consent form (Appendix G).

1.4. Chapter Summary

In this chapter, the research context and motivation of the thesis was introduced: Large-scale brain recording, communication in severely disabled patients, and neuromuscular rehabilitation (training enhancement, targeted stimulation).

In the next chapter, the relevant literature is reviewed in detail and the philosophy behind the research and the thesis statement is discussed in detail.

Chapter 2

Literature Review and Analysis

In this chapter, the BCI literature, motor neurophysiology and modulation of EEG signatures by motor task parameters are reviewed and analysed. Research statement, hypotheses and contributions, conclude the chapter afterwards.

2.1. Brain-Computer Interfaces

2.1.1. Introduction to Brain-Computer Interfaces (BCI)

From a historical standpoint (See Birbaumer, 2006, for review), neuro-biofeedback research has been the source of BCI initiation, particularly in regard to slow cortical potentials (SCP) use (see Section 2.1.2.1). People can change signatures of different neural activities, regardless of the fact that they *learn* to change the neural signal or they just find out how it changes along with already learned daily activities (see Section 2.1.3). If an external computer, machine, or device can pick up and detect such changes, the engineers can establish a mapping between the occurrence or type of the generated signal signatures and an external command, action or output. This external output or action can be the movement of a cursor or the control of a prosthetic or orthotic device. This intention-to-action translation enables the user to interact with their environment or a device using their brain activity. Consequently, any BCI has a recording subsystem to acquire the activity in part of the brain. The acquired signal is pre-processed, analysed and interpreted. The intention of the brain, is extracted from the acquired signal through classification or decoding algorithms, and translated to a machine command using appropriate algorithms. Consequences of the actions on the external environment are fed back to the user via existing or synthetic sensory modalities (Daly and Wolpaw, 2008). This communication loop enables the user to continuously interact with the environment, using their brain activity. Figure 2.1 illustrates this sequence.

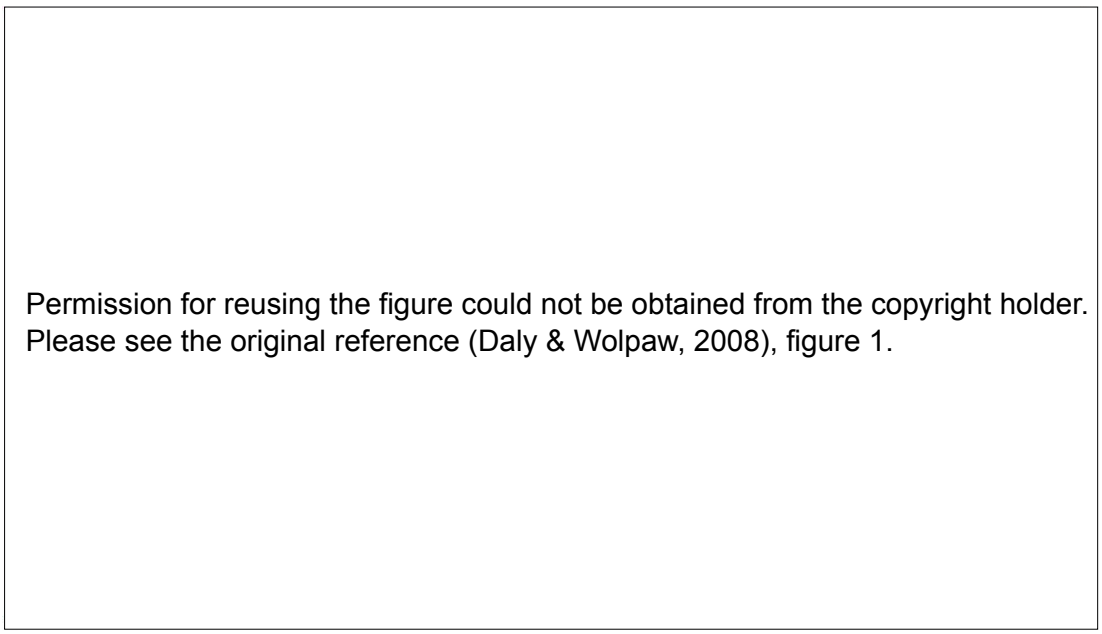

Figure 2.1. A) Schematic of a BCI, showing signal acquisition from the nervous system, signal processing, feature extraction and translation to commands toward external devices (left). B) Different levels of invasion for recording brain activities for different recording techniques including EEG, ECoG, LFP and spikes (right). From Daly and Wolpaw 2008.

2.1.2. Different Types of Brain-Computer Interfaces

It is difficult to further describe and discuss BCI systems without specifying the BCI specifications, as there are many classes of BCI. The major classes and categories of BCI are briefly described in this section.

The BCI system may use the existing neural pathways and existing brain signals evoked by external stimuli for interfacing (e.g. the VEP or SSVEP signals evoked from altered visual stimuli, as a result of altered visual field and encoded optical information, due to change in visual focus). Conversely, the BCI system may use novel neural outputs to make this connection without relying on existing stimuli for initiating brain activity. These are usually termed dependent and independent BCI systems respectively (Wolpaw et al., 2002). An example for the latter is using single unit activity (SUA) spikes (Velliste et al., 2008) or certain frequency powers in EEG to drive a cursor on a monitor (McFarland et al., 2010).

The BCI systems can be classified according to sensory or functional modality, invasiveness, and mental tasks. This classification corresponds to answering the following questions, respectively:

- Modality (Nature of bio-signal): What activity is the source of bio-signal (e.g. visual, motor, cognitive) ?
- Tasks (What modulates the changes in bio-signal): What does the subject do during

recording (e.g. motor imagery of different limbs, motor imagery of movements to different directions) ?

- Recording Technique (invasive vs. non-invasive): How is the bio-signal recorded (e.g. ECoG vs. EEG and MEG) ?

- Cues: What is the timing and the trigger of the recorded signals (cued vs. self-paced) ?

It is noteworthy that these classifications are not necessarily applicable simultaneously, nor are mutually exclusive for a specific system.

2.1.2.1. Recorded Signals and Modalities in Brain Computer Interfaces

The type of neural activity, from which the elicited neural signals are collected, varies and includes visual, cognitive, and motor activity. The major modalities in BCI may be described as follows:

Slow Cortical Potentials (SCP): The slow cortical potentials (SCP), are operantly controllable activities with a slow rate of variation. SCPs are generated from multiple sources and can be controlled toward positive or negative states in surface EEG. While these potentials were used in the first BCI attempts (see Birbaumer, 2006 for a review) they are relatively slow regarding the information transfer rate. Figure 2.2 shows an example of SCPs.

P300: The P300 potential is an ERP seen in response to the incidence of a known unexpected rare event or stimulus. A classic example is seeing or hearing a rare known type of cue (target) among many cues that are not relevant to the individual's intention. It is used to develop BCI systems suitable for spelling applications (Farwell and Donchin, 1988, cited in Birbaumer and Cohen, 2007) by using arrays of flashing LEDs that each represents an alphabet. Although it is the external visual stimulus that generates the P300 potential about 300ms after the stimulus, the nature of signal is cognitive and dependent on the user's attention. Figure 2.3 shows the P300 potential.

Visual Evoked Potentials (VEP): Visual evoked potentials (VEP) are large scale brain activities (for example from EEG, MEG and ECoG) generated mainly in the occipital brain area where the visual cortex shows activity in response to different types of visual stimuli (Drissi et al., 2000). As a common practice, the response to observation of a blinking light source with various frequencies appears as a steady state visual evoked potential

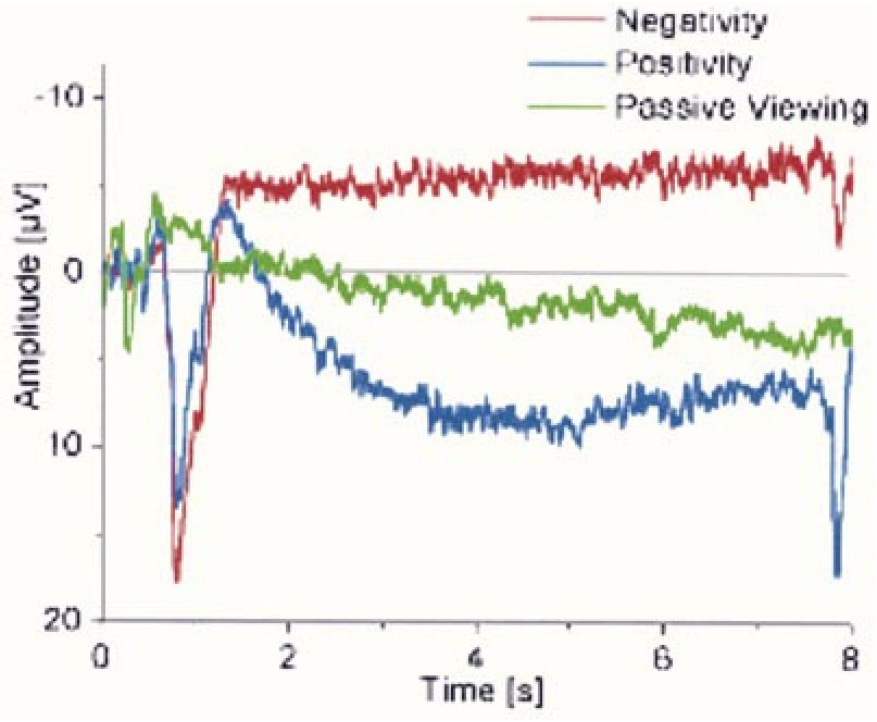

Figure 2.2. Slow Cortical Potentials (SCP) can be voluntarily controlled to reach the top or bottom target according to the desired task. From Birbaumer et al. 2003. Permission to reproduce this figure has been granted by IEEE.

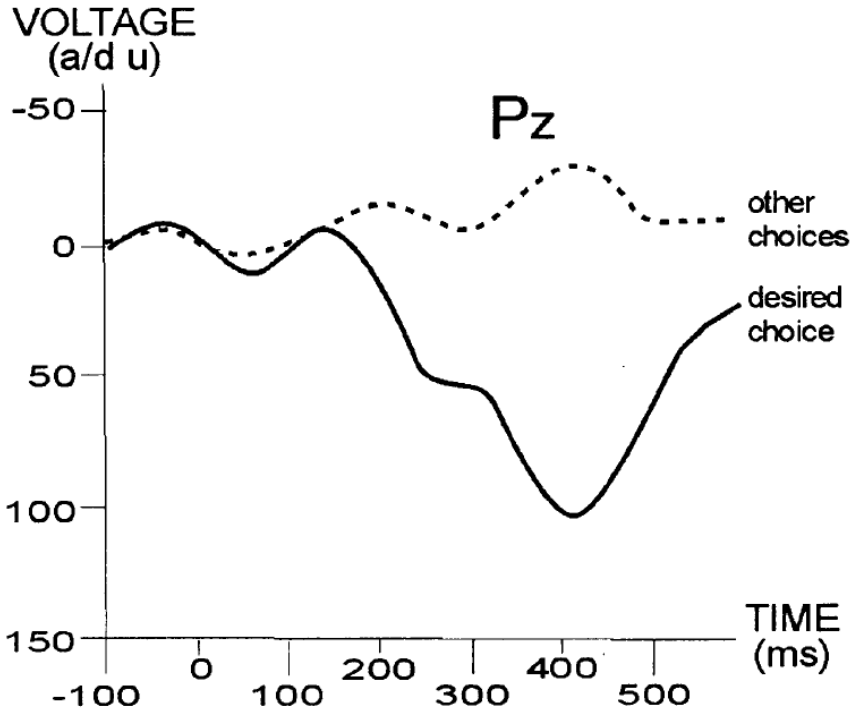

Figure 2.3. P300 potentials that appear after occurrence of a rare target event (desired choice) compared to occurrence of common non-target events (other choices). a/d u: analogue-to-digital unit. From Donchin et al. 2000; Wolpaw et al. 2002. Permission to reproduce this figure has been granted by IEEE.

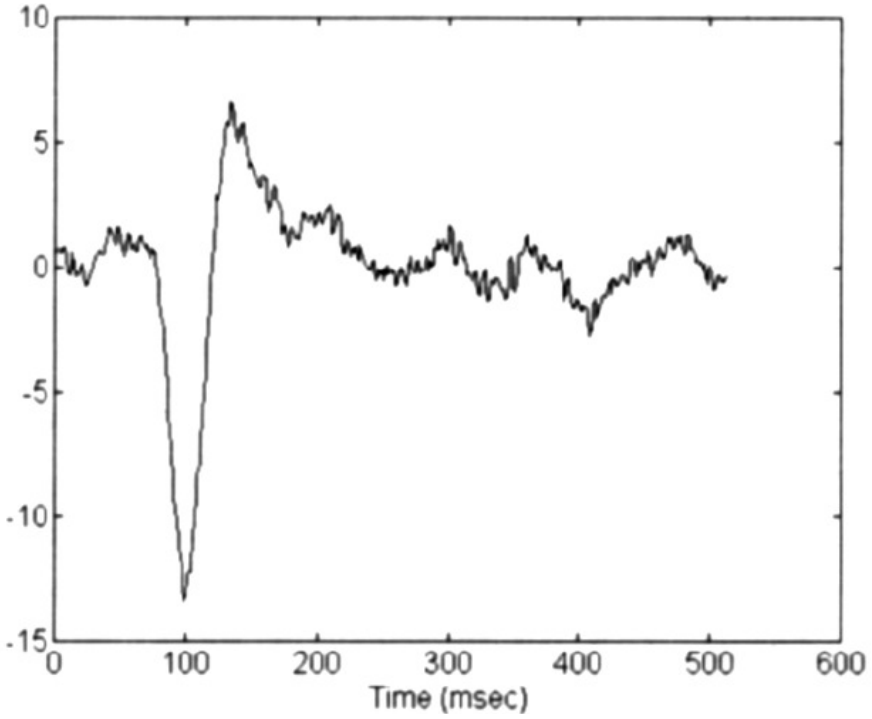

Figure 2.4. An example of a visual evoked potential (VEP) from a single visual stimulus (checker-board flashing in this case). Data is the trial-averaged VEP (μV) from bipolar $O_z - C_z$ recording. Notice the waveforms and timings of a visually evoked potential in EEG. From Drissi et al. 2000. Permission to reproduce this figure has been granted by Elsevier.

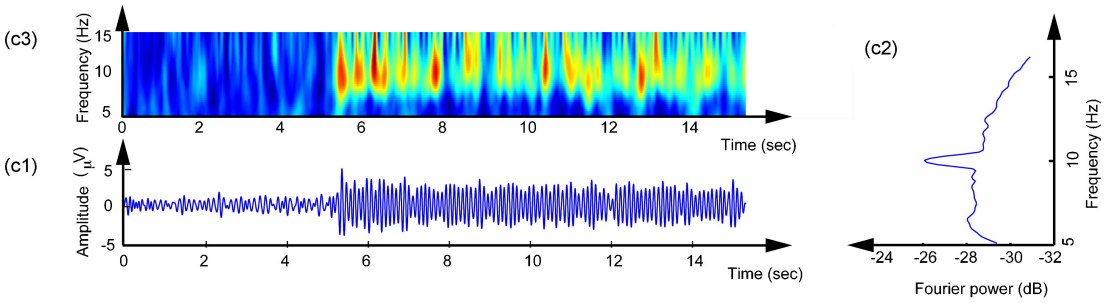

Figure 2.5. Steady State Visual Evoked Potential (SSVEP) elicited by a black-white square flickering at 10Hz. Data are 20-trial averaged values. c1, c2 and c3 show time, frequency and time-frequency domains, respectively. Notice the pattern of appearance of repetitive visual components in EEG. From Vialatte et al. 2010. Permission to reproduce this figure has been granted by Elsevier.

(SSVEP) with distinguished frequencies equal to that of the light source (Allison et al., 2008). Another type of VEP that can be used for BCI applications is the motion-onset VEP (mVEP) in response to a moving visual cue (Guo et al., 2008b). Figures 2.4 and 2.5 and 2.6 show examples of VEP, SSEVP and mVEP waveforms.

Motor-Related Potentials (MRP) & Sensorimotor Rhythms (SMR): The other signals that have been a great source of attention for BCI, motor-related potentials (MRP),

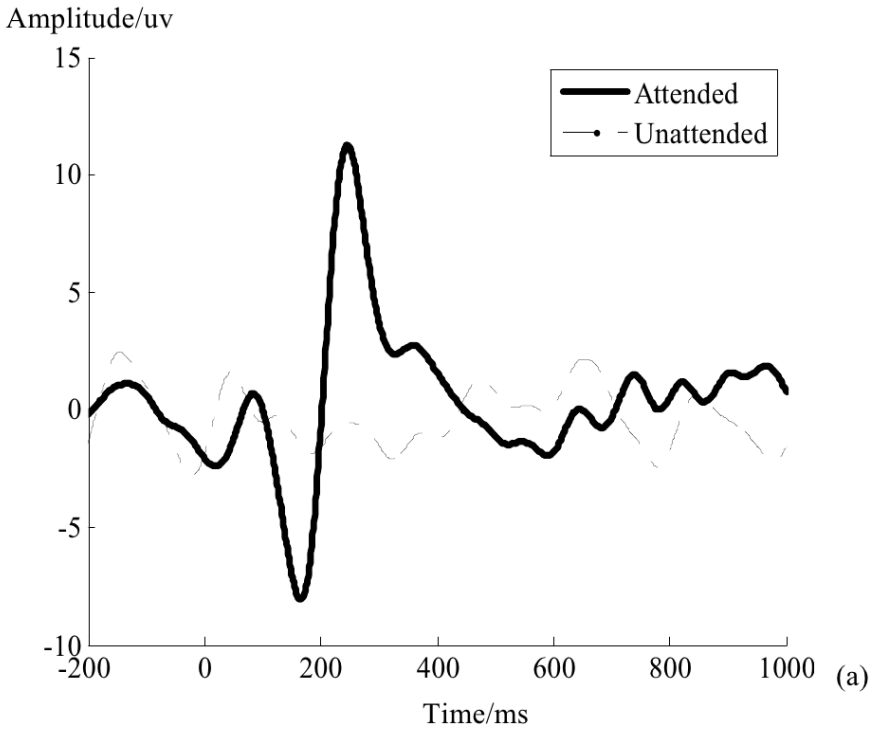

Figure 2.6. An example of motion-onset visual evoked potential (mVEP) at electrode P_z when an attended line starts moving, compared to non-attended moving visual objects. Zero indicated the motion onset instance. From Guo et al. 2008a. Permission to reproduce this figure has been granted by IEEE.

are discussed in more detail in Section 2.1.3. These potentials, including Bereitschaftspotential (BP) and contingent negative variation (CNV), appear mostly in central regions above the motor cortical areas as well as frontal and parietal regions (Shibasaki and Hallett, 2006). The oscillations related to motor activity are referred to as sensorimotor rhythms (SMR) and the relative changes in frequency content are called event-related (de-)synchronisation (ERD/ERS) (Neuper et al., 2006b). It has been shown that imagination of motor tasks (Motor Imagery or MI) produces similar patterns of motor activity as well (Herman et al., 2008). As these types of signals are the main focus of this dissertation, they are elaborated on in Section 2.2.4.

Error Potentials (EP): One of the other cognitive potentials is the error potential (EP). When people interact with BCI systems, they try to generate commands. When they see the effect and feedback of the detected action by BCI translator, the correctness of the performed action compared to the original intended action affects the elicited potential after feedback observation. The difference between the elicited feedback-related potentials in correct vs. incorrect actions is referred to as error potential. Figure 2.7 is an example of an EP.

In closed loop BCIs, error potentials can be potentially used for correcting the classi-

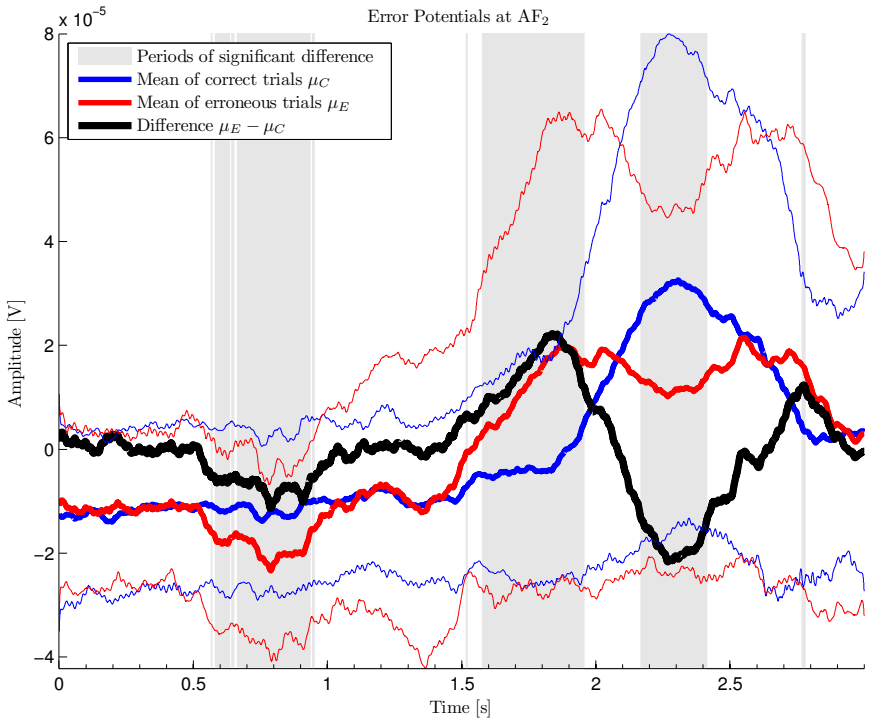

Figure 2.7. An example of potentials (ERPs and EP) after observation of feedback in case of correct and incorrect detected actions by BCI system and the Error Potential. The thick blue line shows the average of ERPs after the subject observes the correctly-detected action of the BCI. The thick red line shows the average of ERPs after the subject observes the incorrectly-detected action of the BCI. The difference between these two mean signals is the error potential (EP) and its significance (shown by shaded regions) is determined by statistical comparison of ERPs in the correct and incorrect detection groups. Thin lines show the ranges. From Grychtol et al. 2010. Permission to reproduce this figure has been granted by IEEE.

fier's misclassification after the wrong detection.

2.1.2.2. Invasive vs. Non-Invasive Brain-Computer Interfaces

An obvious BCI classification can be distinguished in the literature as invasive and non-invasive. Figure 2.1 shows the different levels of electrode penetration used for recording brain activity in different recording techniques. The electrical activity can be recorded directly from SUA neuronal spikes, ensemble recording of population of neurons such as local field potentials (LFP), electrocorticography (ECoG) recordings, or recording this electrical activity over the scalp with surface EEG or MEG. Other recording techniques can indirectly represent neural activity, among which are the blood oxygen level dependent (BOLD) response in functional magnetic resonance imaging (fMRI) and near infrared spectroscopy (NIRS) of brain tissue (Birbaumer, 2006).

For generation of control commands in any class of BCI, some signal features need to be identified, defined and extracted to be translated to a control command. Signal features

may be spike counts, time domain analogue values, frequency contents in different bands, non-linear and model-based features, spatial presence of these features or a combination of these features. If the features vary among different classes and types of tasks in a discrete fashion, they can be classified. If the features are continuously modulated by continuous variable parameters, they can be decoded to appropriate continuous variables according to the task. Examples of discrete classes are movement or motor imagery in different limbs (Morash et al., 2008) and examples of continuously changing variables are end-point limb coordinates (Bradberry et al., 2010).

All recording techniques, except fMRI and NIRS provide good temporal resolution, as the electrical/magnetic activity is reflected in recording electrodes with little delay. Invasive recordings, and fMRI thereafter provide high spatial resolution regarding localisation of the generated activity. While the SUA and the needle electrode-arrays give perfect temporal and spatial resolution, due to its invasive nature it cannot be applied simultaneously to many recording sites. Large scale recordings (EEG, MEG, ECoG) give little spatial resolution, but can capture large-scale behaviours of the brain in the form of brain oscillations that cannot be easily captured by SUA methods. Figure 2.8 compares the spatial and temporal resolution of different brain imaging techniques.

The invasive BCIs, i.e. single cell recording, LFP and ECoG, require implantation of recording electrodes and have attracted much attention for animal experiments and studies, but there are very limited clinically plausible applications for human beings to date (Lebedev and Nicolelis, 2006).

In general, EEG-based BCIs tend towards high level goal-prediction (Wolpaw, 2007), while invasive BCI, ignoring the risk and implementation issues, may target low-level muscle-level control according to the current trend of research and development (Santucci et al., 2005; Velliste et al., 2008).

2.1.2.3. Synchronous vs. Asynchronous Brain-Computer Interfaces

Patients and BCI users may generate voluntary control signals to control an external device, without relying on external stimulation or cues. These BCI systems are called asynchronous or self-paced BCIs. Conversely, BCI systems may selectively operate based on the type of responses that arise from human responses to external stimuli or cues. These BCI systems are called synchronous or cued BCI.

P300-based BCI is a synchronous BCI with regard to the external cues, but operates asynchronously regarding the cognitive intention of the subject. The same holds for many VEP-based BCIs. If motor-related activity is used for BCI, then synchronous or cue-based systems can be considered as the first step in research towards self-paced systems. This is obviously because motor tasks signal an intention rather than a passive

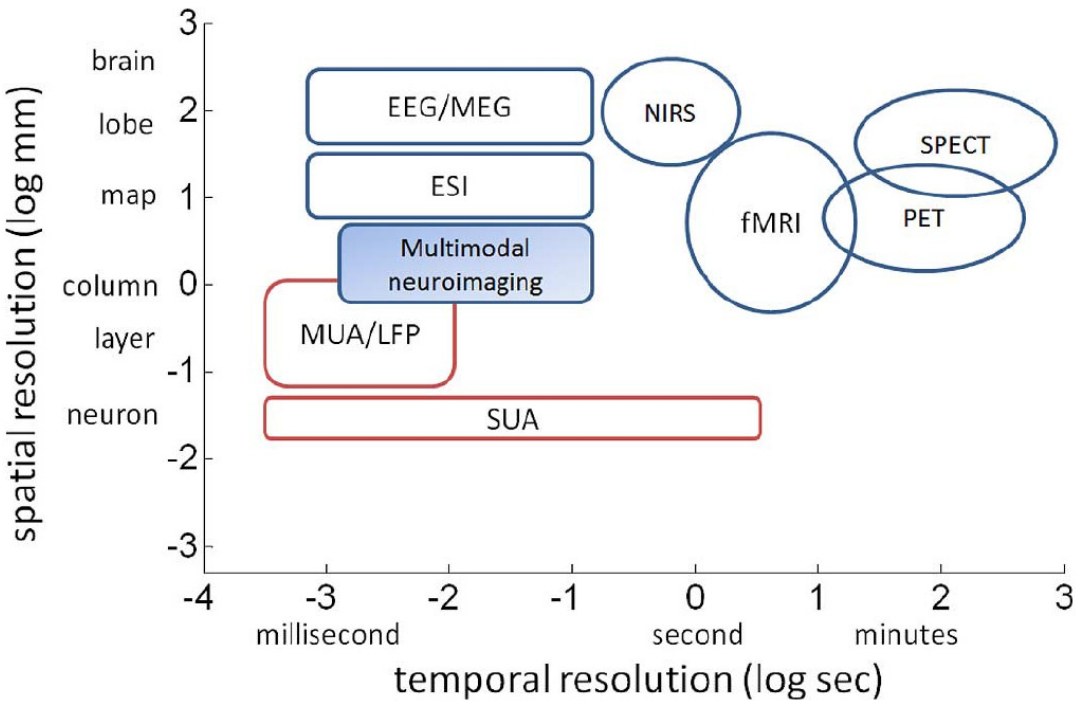

Figure 2.8. Comparison of temporal and spatial resolution of selected invasive (in red) and non-invasive (in blue) brain recording/imaging techniques. EEG: electroencephalography, ESI: electromagnetic source imaging, fMRI: functional magnetic resonance imaging, LFP: local field potentials, MEG: magnetoencephalography, MUA: multi-unit activity, NIRS: near infra-red spectroscopy, PET: positron emission tomography, SPECT: single-photon emission computed tomography, SUA: single-unit activity. From He and Liu 2008. Permission to reproduce this figure has been granted by IEEE.

response. This issue is not the case if the BCI system is used for motor rehabilitation rather than communication or device control.

2.1.2.4. Mental Tasks (Different Limbs vs. Different Directions)

In all of the abovementioned BCI classes, the user performs a mental task. Many cognitive tasks can be used in the context of expectation, differentiation and focus (e.g. P300), and imagination of different sensory modalities. There are also examples of doing mental arithmetic tasks (Power et al., 2010).

For BCI systems based on motor (or motor imagery) activity, there has been different ranges of motor tasks: movement of right and left wrist, arm, leg, foot, and tongue (Morash et al., 2008; McFarland et al., 2010); the arm (Waldert et al., 2008) and wrist (Valsan, 2007) movement to different directions and their imagination or observation (Valsan, 2007); isometric contraction of leg (Gu et al., 2009) and also many similar tasks but in the form of motor imagery (do Nascimento and Farina, 2008).

2.1.3. Motor related activity in EEG, MEG and ECoG based Brain-Computer Interfaces

As discussed in Section 2.1.2, non-invasive BCI systems based on motor related activity are very practical and reasonable options for humans, especially with recent BCI developments (McFarland et al., 2010). In this section, the major BCI reviews and surveys with focus on non-invasive and EEG-based BCI are listed and analysed. The motor related EEG activity is reviewed from a neurophysiological viewpoint in Section 2.2.4.

Table 2.1 lists the major reviews on BCI or BMI from 2002 to mid 2011. The different aspects of literature that each review addresses are mentioned in the table.

Based on the review in Section 2.1 and the reviews listed in Table 2.1, two main approaches to motor-related BCI research can be considered: (1) normal activity based and (2) re-learning/conditioning based.

2.1.3.1. Normal Activity Based Brain-Computer Interfaces

Some studies (Neuper et al., 2006a; Scherer et al., 2007; Valsan, 2007; Daly and Wolpaw, 2008; Waldert et al., 2008; Bradberry et al., 2009; Valsan et al., 2009; Waldert et al., 2009; Bradberry et al., 2010) try to read an already existing activity or pattern of activity in the nervous system. This approach is based on the fact that the neural activity during normal daily movement tasks, such as moving the hand, foot, tongue, or directional wrist or arm tasks, produces specific patterns of motor activity. It is assumed that the pattern may be picked up from EEG, MEG or any recording method. In this approach the subject produces already learned (real or imagery-based) motor activity. Although adaptation and co-adaptation may occur (Daly and Wolpaw, 2008), the target tasks are external motor tasks that users have already learned and know how to do (such as finger or wrist movement). The only difference in BCI use of such tasks is that the recording point of the generated activity is changed from muscles to EEG, MEG or ECoG. Examples of these approaches are multi-class movement (imagination) BCIs (Scherer et al., 2007; Neuper et al., 2006a) where the user's imagined movement is classified into one of several movement classes (left/right hand/arm and tongue movement) and the detected class is assigned to the control signal values. In another series of studies, the different detected classes are assigned to different directions of movement. The direction-specific classes (Waldert et al., 2009) have been used for arm (Waldert et al., 2008) and wrist movements (Valsan, 2007; Valsan et al., 2009). The studies that try to decode continuous variables such as end-point hand trajectory from EEG (Bradberry et al., 2009, 2010) also fall into this category, as the subjects do not have to learn the intended task which is part of their daily activity.

Table 2.1. List of selected recent reviews on motor BCI between 2002 and mid 2011 .

Study	Focus of Review
Wolpaw et al. (2002)	Introduction to basic components of BCI; Major non-invasive motor-BCI systems; performance and technical considerations
Andersen et al. (2004)	Invasive methods, spike count and LFP; Cognitive aspects
Birbaumer (2006)	History of biofeedback, operand conditioning, and BCI; SCP and motor-BCI use in patients for communication and rehabilitation; Psychological aspects of BCI applications
Lebedev and Nicolelis (2006)	Invasive vs. non-invasive BCI with focus on invasive studies, invasive recording techniques, signal processing, decoding and interfacing; Animal studies and underlining the role of feedback
Birbaumer and Cohen (2007)	Comparison of recording methods, modalities and mental tasks; Clinical applications
Dobkin (2007)	Usability considerations of BCI for communication and neurorehabilitation
Fagg et al. (2007)	Considerations for invasive BCI: advanced decoding techniques, system dynamics and somatosensory feedback
Wolpaw (2007)	Performance measures of invasive and non-invasive BCI systems and their suitability for high vs. low level motor control
Birbaumer et al. (2008)	Motivations for BCI research; Advantages of non-invasive approaches
Daly and Wolpaw (2008)	Overview of brain activity and BCI methods; User-BCI interaction and learning; BCIs for high vs. low level motor control
van Gerven et al. (2009)	General review on the BCI control and feedback loop, including recording, mental tasks, algorithms, sensory feedback and applications
Leuthardt et al. (2009)	Overview of invasive and non-invasive BCI; Brain regions, their laterality and the recorded signals in normal, stroke and prosthetic motor control
Waldert et al. (2009)	Reflection of directional tuning of neurons and the decodable directional information in different brain recording modalities

The majority of reviews on non-invasive BCI, as well as few selected reviews on invasive BMI are included.

2.1.3.2. Relearning/Conditioning Based Brain-Computer Interfaces

The relearning or conditioning based approach to BCI, does not rely on normal (already learned) activity patterns. It does not explicitly deal with known external daily tasks and consequently the picked up signal is not another reading of motor commands that generate normal daily tasks. Instead, subjects are trained through practice and biofeedback to control and modulate specific signal features and parameters. These signal features (such as μ or β rhythm band amplitudes) are correlated with motor tasks, but subjects aim to control the features (selected by the BCI designer) directly and more independently of external tasks, task parameters and other signal features. Consequently, a conditioning

or relearning happens. Although this approach comes from the seminal neurofeedback studies and conditioning of non-motor slow cortical potentials (SCP) (Birbaumer et al., 2006), it has been a successful method. Examples of this approach are studies by Wolpaw and McFarland (2004) and McFarland et al. (2010) where BCI users learned to control the μ and/or β band amplitudes from several different brain regions to realise 2D or 3D control signals for BCI.

2.2. Motor Neurophysiology

Motor-related brain activity is of interest not only from physiological and neuroanatomical points of view, but also from a neural and rehabilitation engineering perspective. How different regions of brain are activated during various motor tasks can give valuable insight into the possible mechanisms of neural control. Brain activity has been widely studied using various recording and imaging techniques for clinical or scientific purposes (Hatsopoulos and Donoghue, 2009). An introduction on the computational processing and integration stages in a motor task is provided in Section 2.2.1. Following this, single neuron activity characteristics, fMRI signatures and large-scale brain recording characteristics of movements and motor tasks are discussed in Sections 2.2.2, 2.2.3 and 2.2.4, respectively. As the primary interest in this study is the large-scale electrophysiological correlates of motor control, many of the behavioural and clinical studies on human motor control are not explicitly addressed in the review.

2.2.1. Introduction to Motor Neurophysiology Experiments

Figure 2.9A shows the computational stages through which location of hand or end effector (Figure 2.9B), as well as the target locations are computed through different block sets: from the *location maps*, passed to *displacement map* (a motor planning job) and finally to the *dynamics map* which does the job of a dynamic model of body-environment and calculates the required joint torques. Figure 2.10 shows a more complete control scheme along with feedback loops and delays. These diagrams are not completely accurate and they are probably slightly controversial in some parts (e.g. the inverse dynamics). Specifically, the author is not supportive of the idea of explicit calculation of force and torque by CNS. They are being amended and modified day by day (Green and Kalaska, 2011). Nevertheless, they show the overall information flow and computations which are required for a voluntary motor task.

Logically, each computational stage in the control loop (Figure 2.10), depends on the computations in previous stages. Therefore it is quite logical to consider a sequential

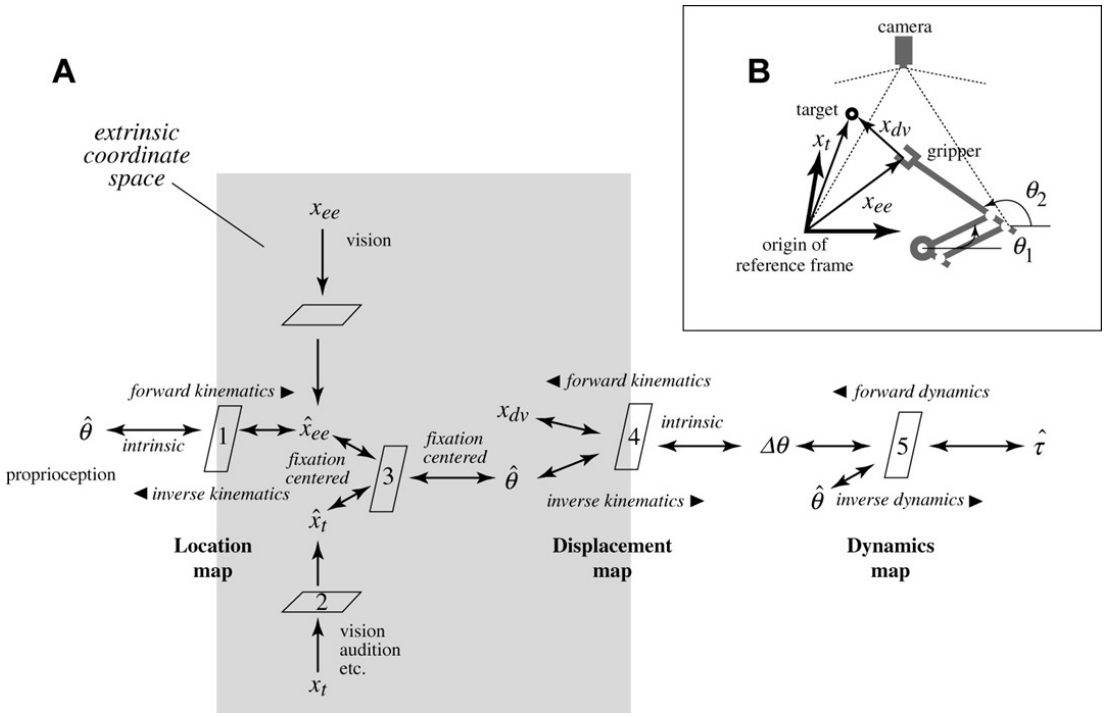

Figure 2.9. Computational processing stages in CNS for motor control, based on logical sequence of information processing stages and results from neurophysiological and behavioural studies. The information processing paths (A) show how the information in neural activity that represnt joint angles θ, end-effector coordinates x_{ee}, target coordinates x_t, difference vector x_{dv} and torques τ of a (bio-)mechanical system (B), flow through different hypothetical processing blocks in brain. These blocks may represent the function of some neuroanatomical circuitries in brain. From Shadmehr and Wise 2005. Permission to reproduce this figure has been granted by MIT Press.

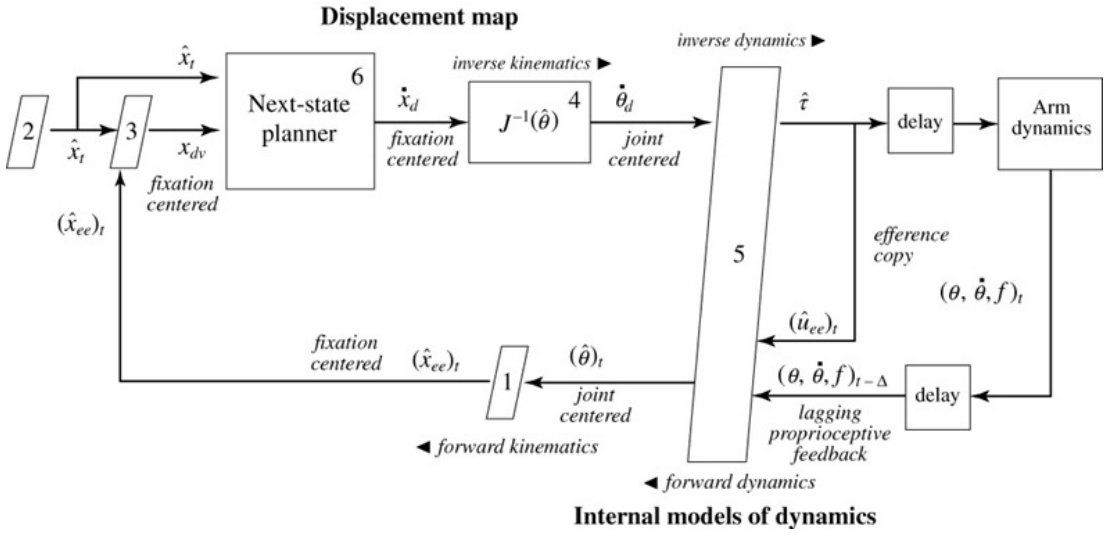

Figure 2.10. Computational motor control scheme, based on the building blocks in Figure 2.9A, along with feedback loops. Joint angles θ, end-effector coordinates x_{ee}, target coordinates x_t, difference vector x_{dv}, muscle/joint force f, instantaneous difference vector $\dot{x}_d$ and torques τ of the controlled bio-mechanical system (Figure 2.9B) are shown. From Shadmehr and Wise 2005. Permission to reproduce this figure has been granted by MIT Press.

processing of events in the indicated control loop. In contrast to such an assumption, integrated processing schemes such as optimal feedback control, have also been suggested (Todorov, 2004). In this context, many motor outputs are described as the output of a large black box that is fed only with abstract task goals. However, based on the forthcoming evidence, this large black-box can be broken down to many smaller black boxes attached to each other with at least one path for flow of sensorimotor information: from abstract goals to detailed control commands.

Consequently, the logical order can also be artificially lengthened in experiments for more detailed neurophysiological and neuroanatomical analysis. To be precise, this means separating the presentation time of the readiness signal, directional cue, and go command. This separation provides a delay between various neural processing stages of Figures 2.9 and 2.10. In other words, determination of limb position, readiness for movement, determination of potential reach targets or tasks, decision on the real target and the go command, along with their delay and wait periods, all have their own specific neural activity (see Figure 2.9) and at least partially distinguished neural processing regions. The forthcoming electrophysiological recording studies in Section 2.2.2 demonstrate some of the above-mentioned concepts and illustrate the neural characteristics of these computational stages.

Before focusing on EEG correlates of neuromotor activity, it is useful to highlight some key characteristics of the human sensorimotor system by reviewing some electrophysiological evidences from experiments on primates (Section 2.2.2) and some human fMRI findings (Section 2.2.3). Single cell activity, LFP and ECoG of primates and humans in specific, reveal invaluable information about motor computations in CNS. These neural activities are more direct reflections of generators behind EEG signals and by careful analysis of these evidences, potential EEG-based BCI designs may be enhanced.

2.2.2. Single Neuron Cortical Activity

In this section, a series of invasive recording studies, primarily on non-human primates, are presented, discussed and analysed. Movement studies, isometric tasks and spatio-temporal distribution patterns of single-neuron activity are reviewed.

2.2.2.1. Neural Activity in Movements

The neural activity correlates of voluntary movements have been known for many years, at least when the population coding of hand movement direction in motor cortex was reported (Georgopoulos et al., 1986). Some early theoretical descriptions of this directional tuning have been documented under the term of tensor network theory (TNT)

(Pellionisz and Llinas, 1979; Pellionisz, 1988). This theory, describes the coordinates of movement, musculature and motor output in terms of sine and cosine tensor components of each other. The equivalence of TNT and the cosine tuning studies has been discussed elsewhere (Gaal, 1993). This has been followed by further studies in the level of single cell firing rates at that time (Kettner et al., 1988; Schwartz et al., 1988). Examples are the population coding patterns in 3D with respect to movement direction (Georgopoulos et al., 1988) and dynamic movements (Sergio et al., 2005).

2.2.2.2. Neural Activity in Isometric Tasks

A directional tuning pattern, very similar to that of movements, has been reported for isometric tasks as well (Sergio and Kalaska, 2003). Figure 2.11 shows the electromyographic (EMG) and single cell motor cortex firing rate activity that accompanies the hand isometric force exertions in different directions in various hand-arm configurations. It shows that the firing rate of the corresponding neuron is cosine-tuned to the direction and is maximum at its *preferred direction*, Furthermore, this tuning and preferred direction is modulated by the arm configuration/position during the exertion. For the purpose of this study, i.e. tracing the reflection of this activity in EEG, the directional tuning as a function of force level and direction is of most importance.

2.2.2.3. Spatial and Temporal Distribution of Neural Activity

In this section, the neural activity patterns in different movement and isometric tasks (different temporal patterns) are more closely studied. The recording sites on ipsilateral or contralateral primary motor cortex or pre-motor cortex (spatial distribution) are also indicated.

The projections from motor cortex cells to spinal motor-neurons or spinal inter-neurons have direct influence on muscle activation patterns (Schieber and Santello, 2004) and therefore on the generated muscle force. Based on this, this close relationship between isometrically exerted force, EMG activity and single neuron activity is more easily understood. This, however, does not mean that motor cortex neurons *encode* muscle force (Scott and Norman, 2003), as this is not the behaviour for all motor cortex cells. Furthermore, except for the upper motor-neurons, the M1 neuronal activities can be dissociated from muscle activities in (re)learning (Schieber, 2011). In short, for static exertions, the force magnitude and direction are highly *correlated* with motor cortical neural activity. This is held for muscle force increase (or rate of change of force) and M1 (primary motor cortex) activity during dynamic movements (Ashe, 1997a).

The other significant data on M1 neural activity describes the firing behaviour of neurons and their directionality during step tracking movements of hand in primates (Sergio

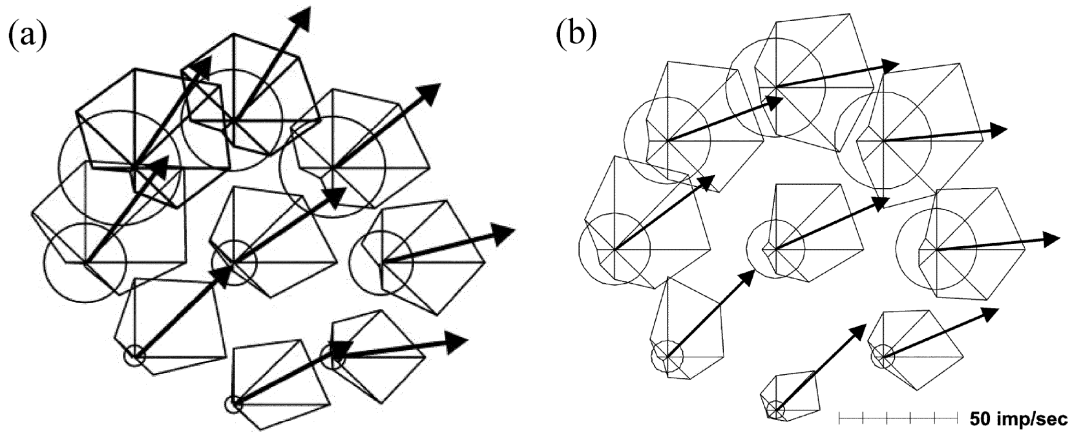

Figure 2.11. a) Polar-plot representations of electromyographic (EMG) activity of the right infraspinatus muscle in monkey, at nine hand locations, during isometric force production. The position of each polar plot corresponds to the relative location of the hand on the planar work surface. The polar plots for the hand locations at 0° and 180° are reproduced on the right and left, respectively, and the upper-most polar plot corresponds to the hand location furthest away from the monkey's body (90°). The radius of the circle in the polar plot represents the mean muscle activity. The length of each of the 8 axes in the polar plot represents the mean activity over the 5 trials of force production in each direction during the peripheral target hold epoch. The heavy arrow corresponds to the preferred direction of the muscle during target hold epoch. b) Polar plot representations of discharge pattern of a primary motor cortex cell of a monkey during isometric force production while the hand was held at 9 different locations. The radius of the circle in the polar plot represents the mean cell discharge rate during the centre hold epoch. The length of each axis represents the mean discharge rate (firing rate) over the 5 trials in that direction during the peripheral target hold epoch. The heavy arrow corresponds to the preferred direction of the cell. Display format is the same as for the EMG polar plots in part (a). From Sergio and Kalaska 2003. Permission to reproduce this figure has been granted by American Physiological Society.

et al., 2005). Figure 2.12 shows this direction-dependent activity along with the corresponding EMG activity.

Figures 2.11 and 2.12 present a behaviour which contains important and useful features as follows:

1. There is high correlation between the EMG activity and the selected neuron. Although the neuron is not known to project directly to the same muscle, it can be concluded that for reasonably synergistic muscle-neuron pairs, a high correlation exists. This holds for both isometric exertions and movements and over the time course of trials.

2. The directional tuning can be identified for both isometric exertions and movements and this directional tuning is valid through the time course of trial.

3. The three-burst pattern (Brown and Cooke, 1981) seen in ballistic movements (Brown and Gilleard, 1991) is present in both EMG and single neuron activity. This can be seen by considering the bi-phasic activity in the preferred direction (PD) which consists of the first and third bursts of agonistic activity, and the mono-phasic activity in the opposite direction of PD, which is in fact the second burst of antagonistic activity.

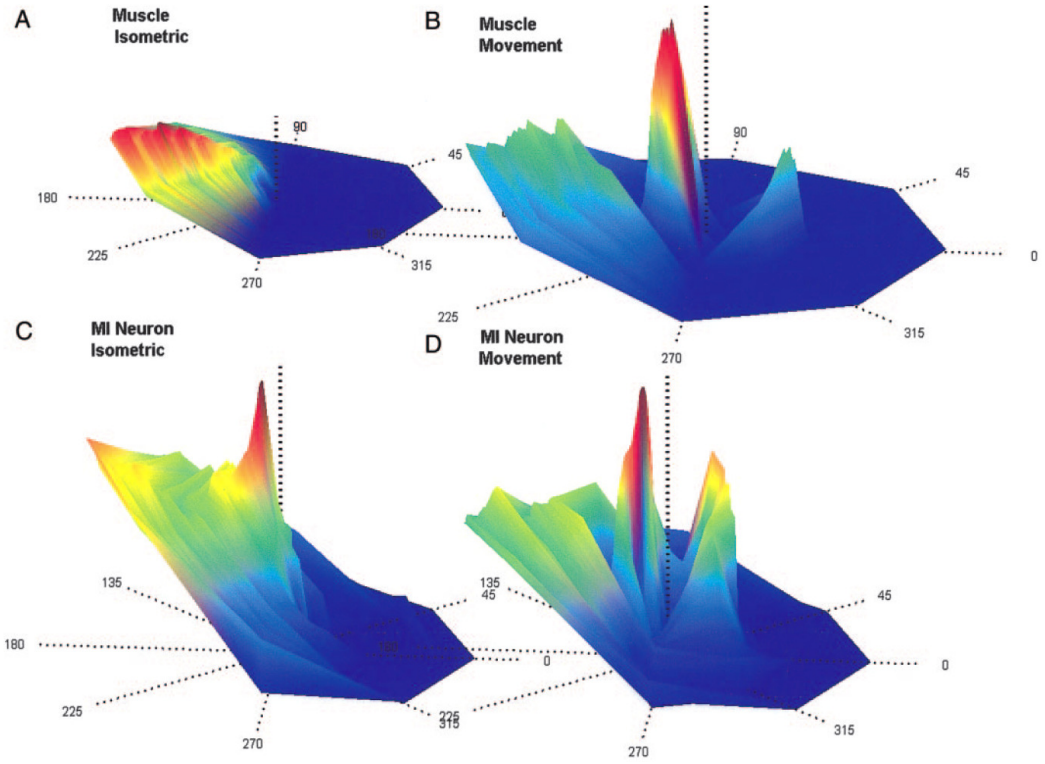

Figure 2.12. EMG and M1 neuronal activity for directional movements and isometric tasks as a function of time and direction of task. EMG is from the right pectoralis muscle of a monkey and neural activity from a co-varying contralateral M1 cell. (A) shows EMG for isometric exertions and (B) the EMG for movement tasks. In (C) the neuronal activity for isometric tasks and in (D) the neuronal activity of movement tasks are shown. Plots are shown from -200 to +1400 ms, measured from force onset. Distance from the plot centre represents time, and the activity level is shown by the height and colour. Data are obtained from trials in 8 centre-out trials. From Sergio et al. 2005. Permission to reproduce this figure has been granted by American Physiological Society.

These phenomena help to interpret the behaviour of BCI devices in this section and are a base for the forthcoming observations on non-invasive recordings. To this point, it can be assumed that there is a coding-like behaviour in the neuronal activity of M1 cells that reflect parameters such as direction of activity. Similar concepts about joint-space, muscle-space, the corresponding coordinates and representation conversions, as shown in Figures 2.9 and 2.10 (Hwang and Shadmehr, 2005), can be traced back to earlier studies (Pellionisz and Llinas, 1979).

An immediate emerging question is about the activity of other significant contributors to motor related neural activity during static or dynamic exertions. The activity of primary motor and dorsal/ventral pre-motor cortices (M1, PMd, PMv) seem to be key features to look for during the time course of movement or exertion. Below is a short review of recording studies that reflect these parameters, as well as directional tuning of recorded cells during trials.

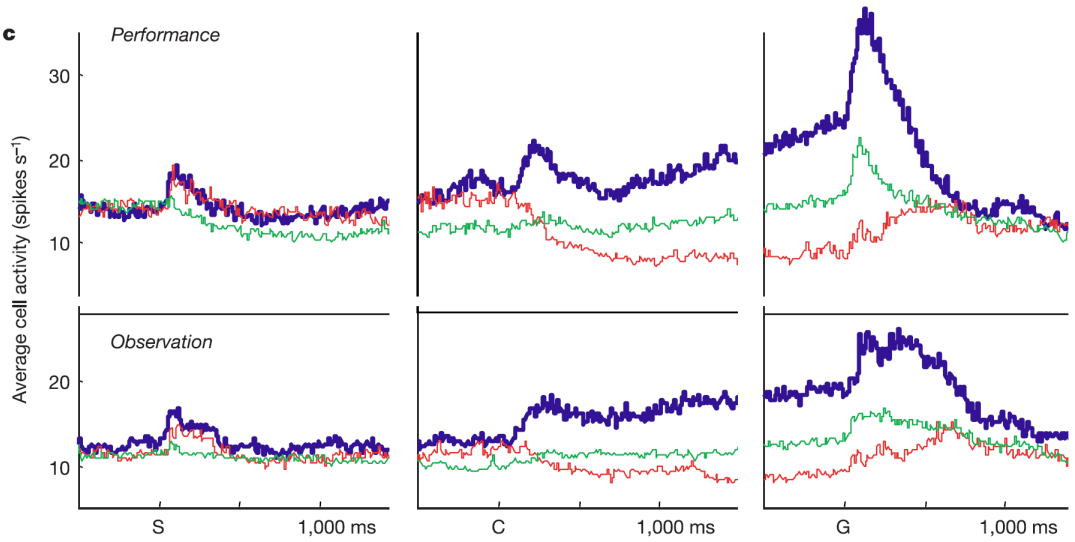

Figure 2.13. Average neural activity of contralateral PMd cells during movement trial and observation of movement. Spatial cue onset of multiple-target readiness (S), colour cue onset of single-target planning (C) and GO command (G) are shown on time axis. The average activity of cells during trials to each cell's best tested direction (blue), opposite direction (red) or orthogonal directions (green) are shown. From Cisek and Kalaska 2004. Permission to reproduce this figure has been granted by Nature Publishing Group.

In instructed delay tasks, where there are three distinct phases of movement: no action, movement planning (roughly corresponding to the processing in and after map 3 in Figure 2.9), and motor execution (roughly corresponding to the processings that include map 5 in Figure 2.9); the M1 and PMd activities have been studied in contralateral and ipsilateral areas (Cisek et al., 2003). There is considerable activity in PMd areas of both hemispheres, especially in the contralateral hemisphere. This activity is maintained during the execution of movement. In M1, activity is seen only during motor execution and not planning. The activity is considerably higher in the contralateral than ipsilateral hemisphere. Directional tuning features are found for active cells in both regions (Cisek et al., 2003).

Existence of multiple reach targets causes the PMd cells to become directionally tuned toward all targets simultaneously in the form of modified PD curves of cell (Cisek and Kalaska, 2002). This can be the simultaneous presence of neural activity for several reach plans when the target is not completely determined (Cisek and Kalaska, 2002).

A very good description of PMd neuronal activity during movement trials that reflects the activity as a function of preferred direction (PD) during silence, multiple-target readiness, single-target planning, and motor execution is replicated from the report by Cisek and Kalaska (2004) in Figure 2.13.

This is complemented by Cisek and Kalaska (2005), with an excellent illustration which is replicated in Figures 2.14 and 2.15. The time course of activity in M1 and PMd

is shown when movement planning takes place mostly in the PM cortex. Additionally, the effect of a multi-target task, which creates multiple motor plans, are shown in two states. When presentation of spatial cues introduces the potential targets, the motor plans for both become activated. Upon presentation of the colour cue, which indicates what the actual target is, the final motor plan is defined. The go signal instructs the execution of movement.

In Figure 2.15, the match-to-sample (MS) task acts as a control experiment in which the effect of the first colour cue is negligible as it provides no planning or movement information to the subject. However, the second (spatial) cue directly activates the final motor plan. It can be seen that its features are similar to the superimposed activity of the single-target task. As shown, these superimposed components include transient (phasic) and sustained (tonic) components, where a transient component appears upon the introduction of movement direction and the sustained activity is movement plan readiness. This is more explicitly shown for reaction-time (RT) trials versus direct-delay (DD) tasks where planning and its neural activity happens directly after the go signal which also instructs the motor execution. It supports the superposition interpretation of chronologically separated stages of movement planning and execution (Crammond and Kalaska, 2000).

Motor cortex neuronal activity has been extensively studied and correlations between the firing rate and force level, as well as rate of force development are reported in the literature (Ashe, 1997a; Sergio and Kalaska, 1998). Figure 2.16 briefly shows the M1 activity during isometric force development.

Despite a rather rich literature on M1 and PM activity during movement (usually reaching tasks), and extensive M1 activity in isometric conditions, little explicit information is available on PM activity during isometric tasks (personal communication, John F. Kalaska, Département de physiologie, Université de Montréal). For statically maintained torques there are near-proportional relationships between PM (area 6) activity and the exerted wrist torque with slight modulation by wrist configuration (Werner et al., 1991). This activity is observed in smaller number of cells compared to M1 (area 4). However, to the best of the Author's knowledge there are no instruction-delay or directional studies.

The data for other non-primary motor areas show that not only is transient activity in M1 not seen in posterior parietal area 5, but the directionally-tuned activity seen during movement is considerably attenuated in isometric exertions (Hamel-Paquet et al., 2006).

A very qualitative summary of the activity in PM and M1 areas for isometric and movement tasks in different stages of planning and execution can be seen in Table 2.2.

While the laterality of cortical innervations are still under investigation, the corticomuscular innervations from M1 are mostly contralateral (Soteropoulos et al., 2011).

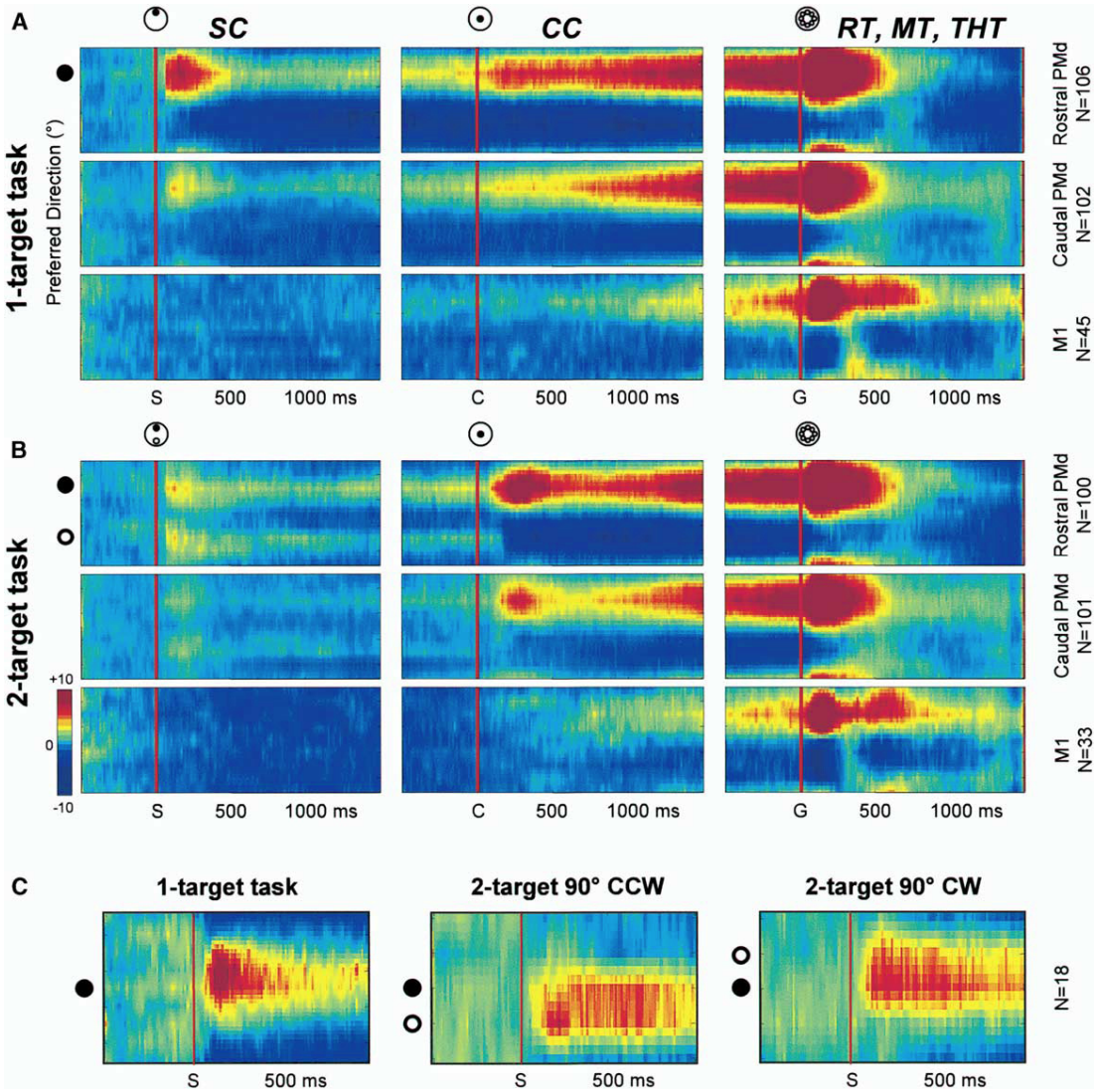

Figure 2.14. PM and M1 population activity. (A) one-target tasks (B) two-target tasks. Each row represents the average activity of group of neurons which have the same specific preferred directions relative to movement direction. i.e. the vertical axis is the preferred direction, the horizontal axis is time, and color shows the relative change in firing rate. Circles on top and left of contour plots show the tasks and direction references. Spatial cue onset, colour-cue onset, and GO signal onset are shown by (S), (C) and (G), respectively. Firing rates are relative to the 500 ms time window prior to spatial cue onset. (C) PMd activity in the 90° variant of the two-target task: SC activity in the one-target task (Left), when a second spatial cue appeared 90° counter-clockwise from a cue in each cell's PD (Middle), and when a second spatial cue appeared 90° clockwise from the PD (Right). From Cisek and Kalaska 2005. Permission to reproduce this figure has been granted by Elsevier.

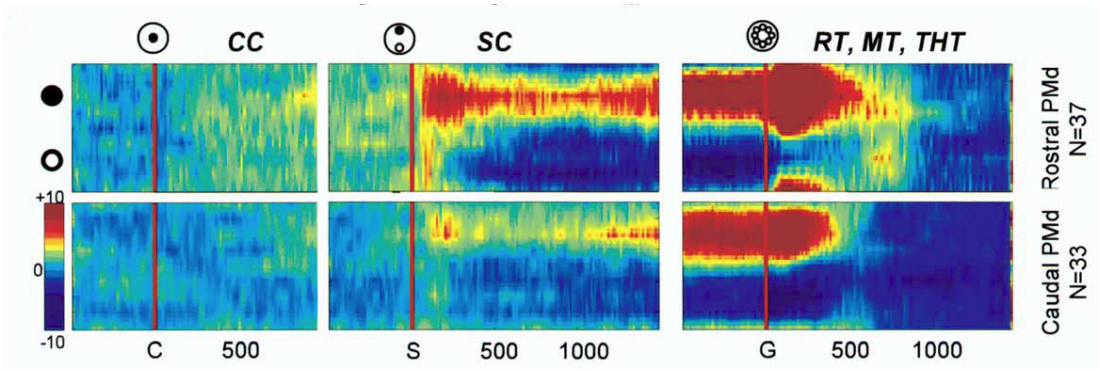

Figure 2.15. Population activity in the match-to-sample (MS) task. Same format as Figure 2.14. From Cisek and Kalaska 2005. Permission to reproduce this figure has been granted by Elsevier.

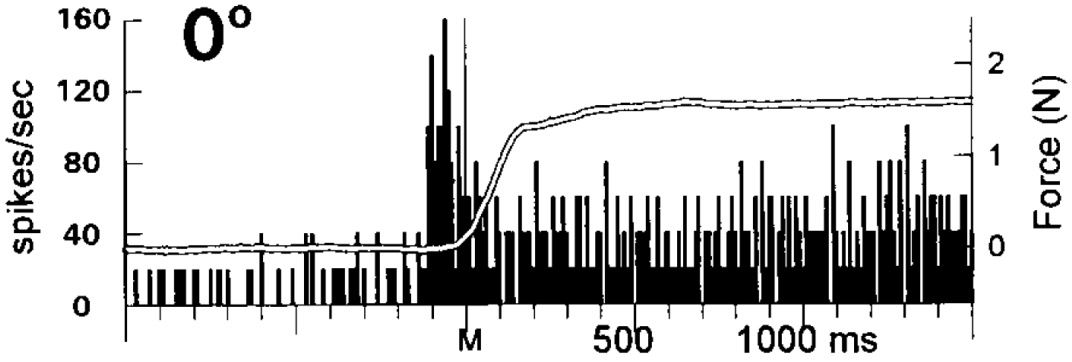

Figure 2.16. Firing rate of a selected M1 neuron, during an isometric exertion arm task to a 0° target direction. Primate experiment data. Notice the increased firing rate during force development stage. From Sergio and Kalaska 1998. Permission to reproduce this figure has been granted by American Physiological Society.

Table 2.2. Qualitative comparison of involvement of contralateral pre-motor (PM) and primary motor (M1) cortices in preparation, planning and execution stages of isometric and reaching movement tasks, based on single unit neural activity literature review .

Task	Area	Readiness	Planning	Execution
Movement	PM	PT	PPTTT	PPPT
Movement	M1	0	T	PPTT
Isometric	PM	?	?	?TT
Isometric	M1	0	T	TTTPP

P and T repetitions indicate phasic and tonic activity intensity respectively. 0 means no activity and ? shows lack of studies.

However, based on the type of task, contralateral M1, ipsilateral M1 and ipsilateral PM get activated for the position control of non-rhythmic tasks (Schaal et al., 2004), although the innervation and primary activation is from contralateral M1.

2.2.3. Brain Activity of Overt and Covert Motor Tasks in fMRI

This short section is included to establish the functional and neurophysiological similarities of overt (real) and covert (imaginary) motor tasks and addresses some findings in functional magnetic resonance imaging (fMRI) studies. It is of importance as the MEG/EEG studies on both overt and covert motor tasks are taken into account in the same context in Section 2.2.4.

Motor imagery, as the internal covert rehearsal of movement without overt motor execution, is believed to share the same neural circuitries with motor control and most neuroanatomical regions involved in motor control are believed to be active in motor imagery as well. The evidence is stronger for pre-frontal areas and pre-motor cortex (Decety, 1996). As seen in Figure 2.13, observation-induced imagery produces a neural activity very similar to actual movement in PMd area. This includes the phases of activity, amplitude and directionality in primate electrophysiological recording (Cisek and Kalaska, 2004).

fMRI studies have shown that motor imagery more or less activates the areas involved in actual motor tasks (motor and pre-motor cortices and supplementary motor areas) for repetitive tongue, toe and finger movements. This happens contralaterally or bilaterally with various degrees of intensity (Ehrsson et al., 2003). Figures 2.17 and 2.18 show a comparison between spatial patterns of activity and activity levels seen in actual movements and motor imagery. As depicted, most motor related centres are active from moderate to high levels during motor imagery compared to the activity levels observed in actual movement. M1 is an exception and shows lower level of activity compared to actual execution of movement. The motor imagery signature becomes more similar to actual movement for skilled movement, though not completely with the same intensity (Lacourse et al., 2005).

2.2.4. Motor Activity in EEG, MEG and ECoG

The single cell recording and many invasive recording techniques provide good spatial resolution and sharp signal features. Though neural activity is the source of EEG activity, the acquired EEG signal differs in nature due to ensemble effects and low-pass and spatial filtering effect of tissues between neural tissues and EEG electrodes (Daly and Wolpaw, 2008; Sanei and Chambers, 2007). For human studies non-invasive recordings such as EEG are often the most practical.

There are various studies on how the motor-related activity appears in EEG (Babiloni et al., 1999). Recent BCI research has significantly contributed to the understanding of motor-related EEG. The motor-related EEG can provide useful information on temporal

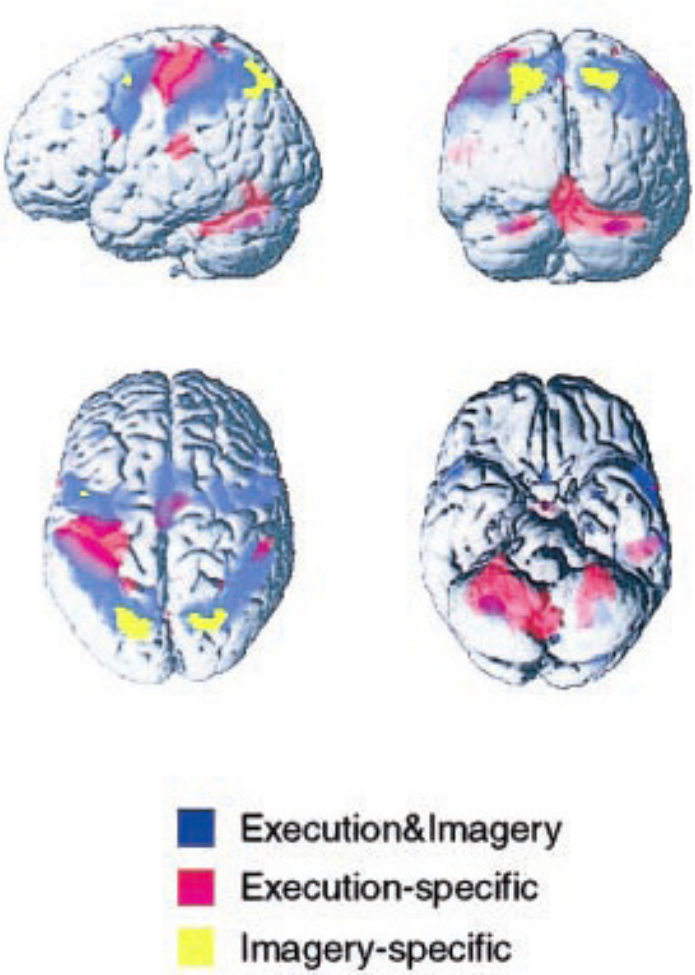

Figure 2.17. Regions activated in actual movement, motor imagery, and both in fMRI during finger movement. From Hanakawa et al. 2003. Permission to reproduce this figure has been granted by American Physiological Society.

characteristics of motor-related electrical brain activity (Waldert et al., 2009). In addition, recording the activity of pools of neurons, albeit without high spatial resolution, can provide insight into large-scale activity of different neuro-circuitries and how they are temporally and spatially activated, in the context of synchronous brain oscillators (Siegel et al., 2012). This can be of interest for clinical diagnostics, neuro-feedback training, therapy and maybe for future large-scale therapeutic interventions (Reis et al., 2008). This is of special interest for the BCI community as it can provide a framework to develop BCI communication systems or BCI-aided rehabilitation (McFarland et al., 2006; Wolpaw, 2007; Birbaumer et al., 2008).

In the following sections, the time domain correlates of human motor tasks in EEG or motor-related potentials (MRP) and time-frequency specifications of motor related EEG are briefly described. The time-frequency features are described by event-related (de-)synchronisation (ERD/ERS) by means of event-related spectral perturbation (ERSP)

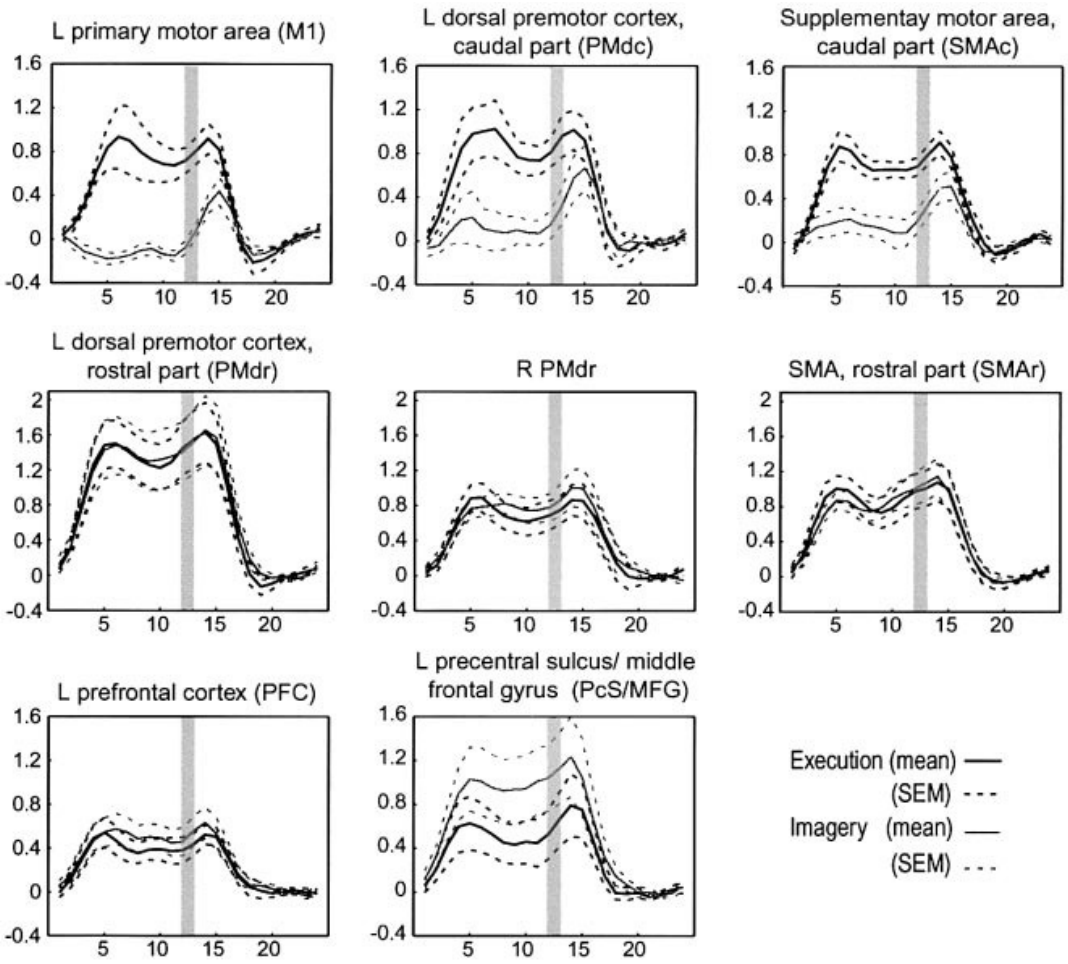

Figure 2.18. Change of activity in various brain regions in actual movement and motor imagery vs. time from fMRI study during finger movement. The horizontal axes indicate the number of scans (each lasts 2.6 s), aligned at the onset of task. The vertical axes show the mean and standard error of signal change (%) across 10 subjects. From Hanakawa et al. 2003. Permission to reproduce this figure has been granted by American Physiological Society.

or similar techniques. More details, can be found in Chapter 5.

2.2.4.1. Motor Related Potentials (MRP)

Evoked potentials, time-locked to an external trigger can be studied in the time domain and are referred to as event-related potentials (ERP). In the case that the event or activity is motor-related, ERPs are actually movement/motor-related potentials (MRP).

Motor-Related Potentials in Movement Tasks: The earliest known MRP is probably the contingent negative variation (CNV) which is a negative potential before externally-triggered predictable movements (Walter et al., 1964). The readiness potential (RP) or the bereitschaftspotential (BP), is a potential observed mostly as a pre-movement neg-

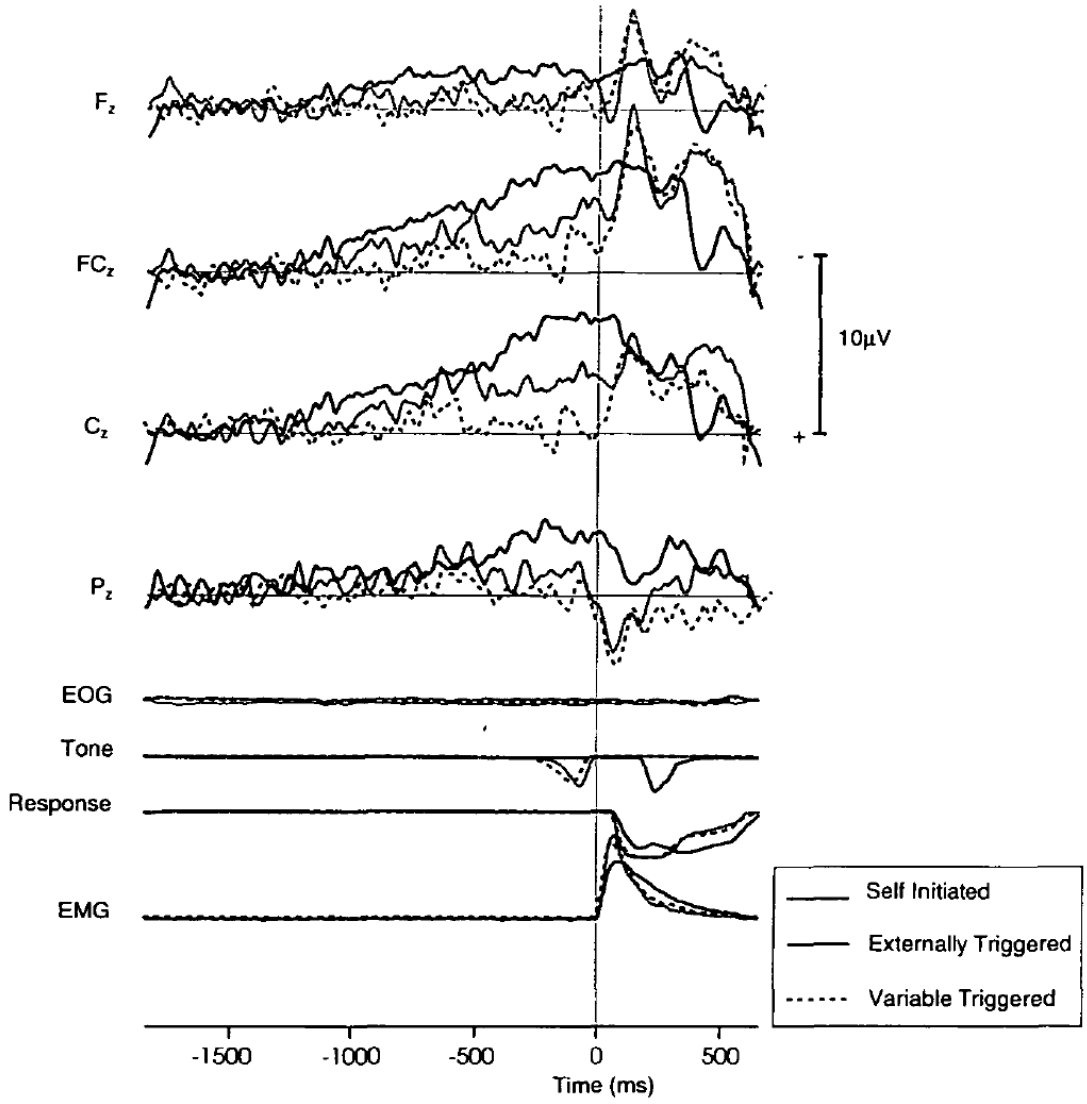

Figure 2.19. EEG recordings for self-initiated movements, externally triggered movements, and movements in response to a variably timed trigger signal. Bereitschaftspotential (BP), contingent negative variation (CNV), and movement potentials are shown. From Jahanshahi et al. 1995. Permission to reproduce this figure has been granted by Oxford University Press.

ativity in self-initiated movements (Kornhuber and Deecke, 1965); it has 2 early and late phases (BP1 and BP2) which start about $1.2s$ and $0.5s$ before movement onset respectively, and their generating sources are considered to be supplementary motor area (SMA) and contralateral M1 (Colebatch, 2007). Figure 2.19 depicts important variation characteristics of BP and CNV in various movement initiation states. From the early discovery of BP and CNV (see Shibasaki and Hallett, 2006, for a review), various studies have investigated the movement-related activity in EEG (Neuper et al., 2006b). The BP is observed for various limb movements (Colebatch, 2007). Further detailed nomenclature for movement-related potentials and their waveform peaks has also been suggested (Cui and Deecke, 1999).

The earliest findings on motor-related potentials (MRP) of self-paced impeded arm movement tasks (Wilke and Lansing, 1973) report bipolar recordings from centro-parietal regions: pre-movement negative potential followed by a large positive potential during exertion followed by two smaller negative and positive waveforms.

The other study on MRPs during thumb movements (Shibasaki and Kato, 1975) reports the ipsilateral and contralateral central ELR EEG during self-paced left, right or bi-manual thumb movement. In this case, MRPs are in the general form of N1-P1-N2-P2 sequence of waveform negativities (N) and positivities (P) with some of the peaks absent in some subjects, tasks, or electrode regions.

The ELR motor-related potentials during an impeded arm movement with cue and pre-cue (MacKay and Bonnet, 1990) include a rather similar pattern for most electrodes, including F_z, C_z, and P_z: small positivity-negativity followed by greater positivity-negativity after an attentional cue (the cue may also include information about force direction and, or magnitude). The information provided about the requested force is reported to intensify the magnitude of the peaks but does not change the activity pattern. The execution of movement induces a positivity-negativity peak sequence according to MacKay and Bonnet (1990).

Motor-Related Potentials in Isometric Tasks: The majority of EEG studies that address EEG correlates of voluntary force generation are probably groups of studies that reflect different task parameters in EEG, such as force magnitude of arm (Siemionow et al., 2000), foot (do Nascimento et al., 2005, 2006) and fingers (Oda et al., 1996; Shibata et al., 1997; Slobounov et al., 2002). The only EEG study on isometric finger tasks with planning pre-cues before exertion (Ulrich et al., 1998) provides some time-domain results only (see Figure 2.20). This self-paced isometric finger force generation task (Ulrich et al., 1998) provides similar results compared to those of movement (Wilke and Lansing, 1973; Shibasaki and Kato, 1975; Hink et al., 1983), with the last two activity peaks partially suppressed. These studies and various other Electrocorticographic (ECoG) studies relevant to motor task planning and execution are addressed in Chapter 5.

2.2.4.2. Event-Related (De-)Synchronisation (ERD/ERS)

The relationship between cortical and muscular activity can be studied in different ways. The co-variation of similar frequency components of EMG and EEG/MEG during motor tasks, first reported by Conway et al. (1995), is referred to as corticomuscular coherence (CMC) (Mima and Hallett, 1999). However, the neural activity can be studied with regard to motor tasks, without direct reference to or dependence on muscular activity. This is especially useful in the planning stage and motor imagery where there is no muscular

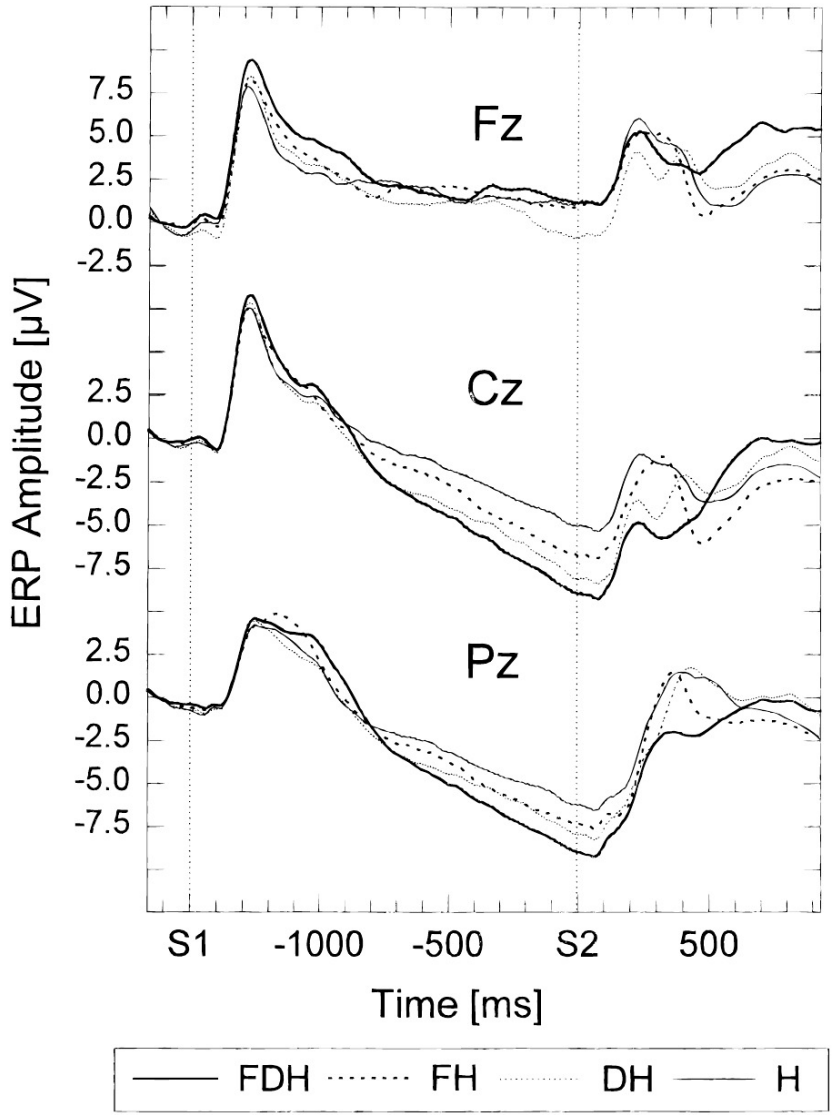

Figure 2.20. Motor-related potentials (MRPs) at F_z, F_z and P_z electrodes during index finger isometric task planning and execution. The pre-cues contain instruction information about the force generation task: right/left hand (H), hand and flexion/extension direction (DH), hand and low/high force level (FH), all the force, direction and hand information (FDH). S1 shows the pre-cue and S2 the GO signal. From Ulrich et al. 1998. Permission to reproduce this figure has been granted by John wiley & Sons.

activity, but there is still considerable brain activity. The relative increase/decrease in time-frequency components of EEG with respect to rest-time EEG is called event-related (de-)synchronisation (ERD/ERS) (Pfurtscheller and Aranibar, 1977); it can be used to find the EEG time-frequency patterns associated with various motor tasks through different analytical techniques (Pfurtscheller and da Silva, 1999).

Event-Related (De-)Synchronisation in Movement Tasks: Sensorimotor rhythms (also called μ-rhythms especially in the alpha range) over the motor cortex, have been

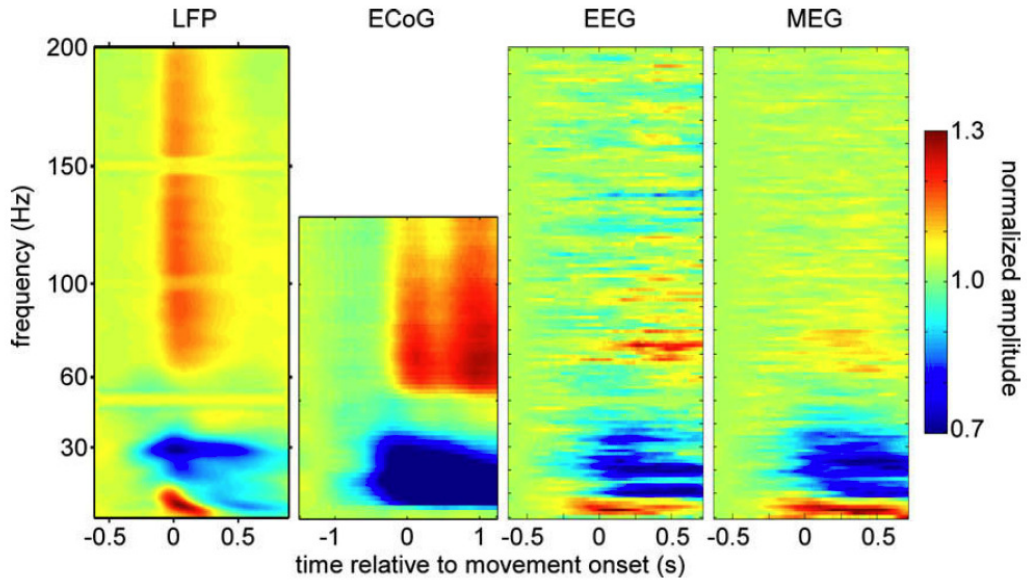

Figure 2.21. Normalised time-frequency representations or event-related spectral perturbations (ERSP) in large-scale recordings (LFP, ECoG, EEG and MEG) during a movement task. Zero time indicates the movement initiation point. From Waldert et al. 2009. Permission to reproduce this figure has been granted by Elsevier.

studied in α (μ) (8-13 Hz), β (14-26 Hz), and γ (30 Hz and above) bands (Neuper et al., 2006b). The rhythms are studied using frequency domain techniques such as ERD and ERS (Pfurtscheller and da Silva, 1999). While MRPs may indicate more local event-related neural activity on specific recording areas, the ERD/ERS may indicate a more distributed background motor activity in motor areas (Babiloni et al., 1999). The results show that oscillations at each frequency and time point can be associated with certain recording sites in each task (Babiloni et al., 1999).

The μ-rhythm is probably the most prominent feature in EEG during movements (da Silva, 2006). It is observed mostly over contralateral and also ipsilateral motor cortical regions. The movement-related activity has also been studied using time-frequency techniques. The ERS in δ (0.5-4 Hz) and θ (4-7.5 Hz) bands and ERD in α (μ) and β frequency bands have been reported in various studies (Graimann and Pfurtscheller, 2006; Waldert et al., 2009). Figure 2.21 shows the ERD/ERS in different large-scale recordings. Figure 2.22 shows the ERD/ERS in point to point wrist movements and for 4 different directions.

Also, a time-frequency MEG spatial distribution map during cue-based arm movement can be seen in Figure 2.23.

Event-Related (De-)Synchronisation in Isometric Tasks: ECoG studies of the human sensorimotor cortex in isometric contractions of the tongue, hand, and leg suggests

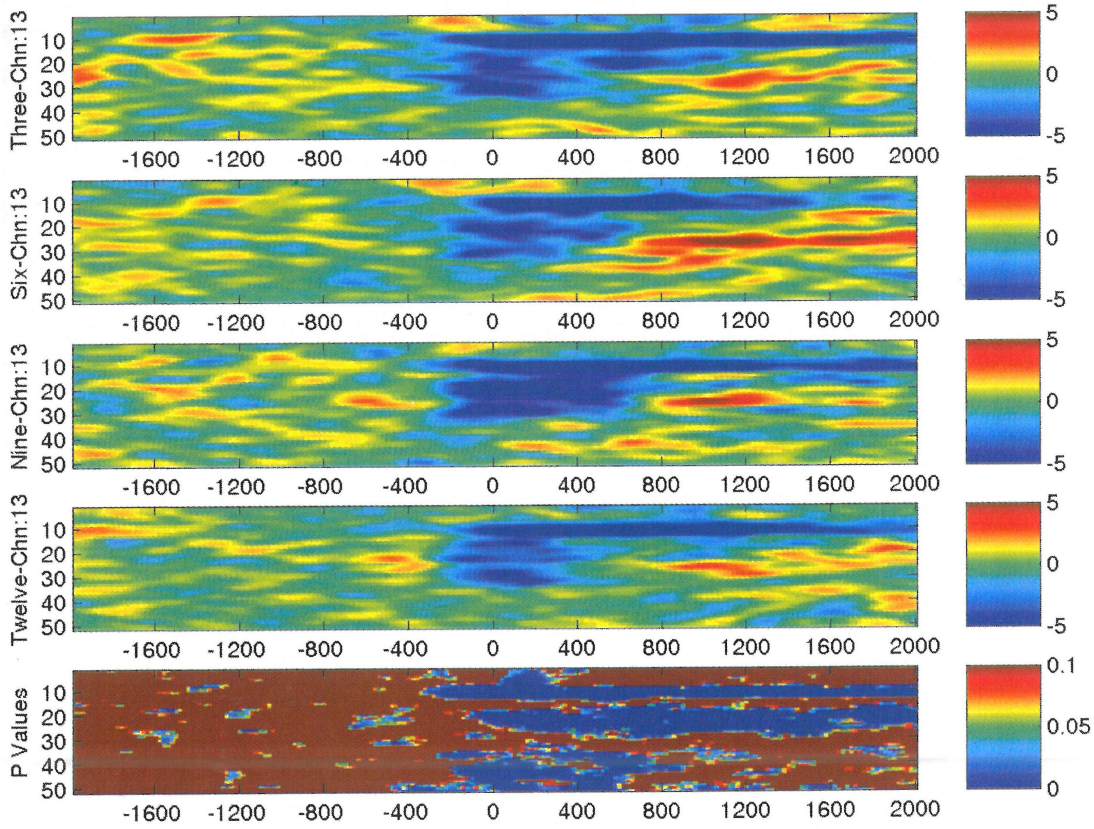

Figure 2.22. Normalised time-frequency representations or event-related spectral perturbations (ERSP) in C_3 EEG electrode during point to point wrist movements to 4 different directions (right, down, left, up; indicated by 3, 6, 9, 12). Zero time indicates the movement initiation point. The bottom panel shows the significance levels for inter-group (between directions) variance. From Valsan 2007. Permission to reproduce this figure has been granted by Gopal Valsan.

that there is alpha, and to a lesser extent beta range ERD in contralateral and also ipsilateral sides (Crone et al., 1998a). The somatotopically distributed activities in the alpha frequency band and especially in early stages of motor activity, and to a lesser extent in later phases of activity and beta band activity are notable. This map is not very close to the stimulation somatotopic map except in the late exertion phase (Crone et al., 1998b). It is reported that different gamma band activities are also present during these tasks: (1) A low gamma band ERS between 35 and 50 Hz with sustained (tonic) properties which accompanies alpha band ERD, (2) A high gamma band ERS between 75 and 100 Hz with transient (phasic) characteristics. These gamma band ECoG activities appears in a more somatotopically organised fashion (Crone et al., 1998a). However, these results are for sustained isometric co-contractions, rather than isometric force generation toward a specific direction.

A study on EEG features during planning of impeded elbow flexion/extension task (MacKay and Bonnet, 1990), which is to some extent closer to isometric exertion, re-

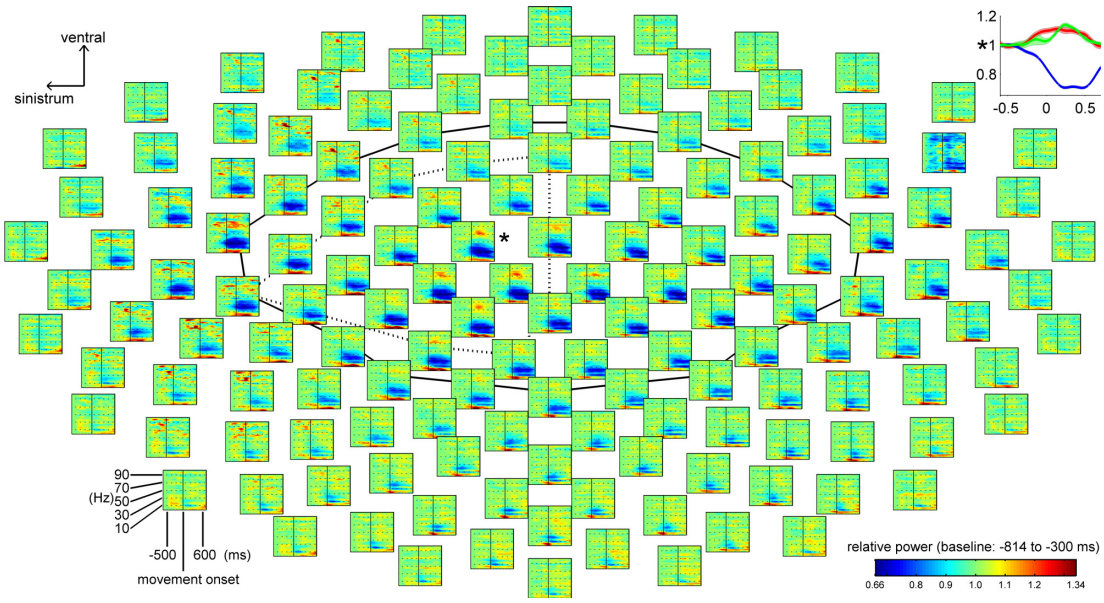

Figure 2.23. Normalised time-frequency representations (ERSP), plotted for all MEG electrodes during cued arm movement task. Data are average across 9 subjects and across 4 movement directions. The motor cortical areas are indicated by a black solid line. The top right plot is the band power changes for indicated sensor $*$ for below 7Hz (red), 10-30Hz (blue) and 62-87Hz (green). From Waldert et al. 2008. Permission to reproduce this figure has been granted by Society for Neuroscience, Journal of Neuroscience.

ports on the potentials after an attentional cue that may also include information about force direction and/or magnitude. These studies do not include thorough analysis on time-frequency features and their spatial distributions.

There is considerable documented research about EEG correlates of isometric force generation or movement, but most of them approach the EEG from the corticomuscular coherence (CMC) point of view (Conway et al., 1995; Salenius and Hari, 2003; Schoffelen et al., 2008; Chakarov et al., 2009), and consequently there is no systematic data about ERD/ERS available. This demands new investigations and as expanded in Section 2.4 will be a basis for this study.

Motor Execution and Imagery in EEG: Motor imagery EEG recordings show similar features of activity as in real motor tasks in the corresponding neural structures (Caldara et al., 2004; do Nascimento and Farina, 2008). This is expected according to the previously mentioned fMRI studies (Hanakawa et al., 2003).

2.3. Decoding Motor Task Parameters from EEG, MEG and ECoG

As discussed in Section 2.2, different motor tasks are accompanied by different changes and patterns of activity in virtually any kind of brain imaging/recording. The next emerging question would be:

How much information about different motor task parameters can be decoded from EEG, MEG, or ECoG ?

High information rates from invasive single unit recordings or LFP are expected with the emergence of multi-electrode arrays (Stieglitz et al., 2009). To summarise the available knowledge about the decodable information from large scale recording techniques, Table 2.3 lists selected previous studies, decoded information and decoding accuracies. Studies that review the signal processing methods rather than the BCI or decoding concepts are not included in the table.

It is noteworthy that the term *decoding* may not necessarily reflect the one-to-one mapping and the reverse concept of *encoding*. The author prefers the term *extracted*, rather than the common *decoded* term in the literature.

2.3.1. Decoding Movement Task Parameters from EEG, MEG and ECoG

Detection of wrist movement direction for cued actual and imagery movements (Valsan, 2007) and also arm movement direction decoding from EEG/MEG (Waldert et al., 2008) has been successfully accomplished. The average reported accuracies are 72% and up to 67%, respectively. Directional information has also been found in the planning and execution stages of reaching tasks (Hammon et al., 2008).

In multi-class classification, the information rate and the chance levels depend on the number of classes. Figure 2.24 shows the chance levels versus the number of classes and how the selected studies compare against each other.

While Valsan (2007) reports high single channel average decoding rates (see Table 2.3), i.e. 52%-62%, the single channel decoding rates are relatively low according to Waldert et al. (2008): decoding rates up to 30% from time-frequency features and up to 36% from time domain features (above central and contralateral motor cortex). This is relatively low for a 4-class task and 25% chance level.

Table 2.3. Decoded motor task parameters from large-scale brain recording techniques (EEG/MEG/ECoG) .

study	recording method	task	cue	decoded information	mean decoding accuracy	maximum decoding accuracy
Valsan (2007)	single channel EEG	ballistic point to point centre-out wrist movement	cued	movement direction	52.2% @4 class	85 % @ 4 class
Valsan (2007)	single channel EEG	ballistic point to point centre-out wrist movement	self-paced	movement direction	61.8% @4 class	75 % @ 4 class
Valsan (2007)	single channel EEG	point to point centre-out wrist motor imagery	cued	movement direction	72.2 % @ 4 class	95 % @ 4 class
Hammon et al. (2008)	multichannel EEG	centre-out reaching (plan, execution) tasks	cued	movement direction	(58.85%,63.0%) @ 3 class plan/reach	n/a
do Nascimento and Farina (2008)	single channel EEG	imaginary isometric plantar flexion	cued	rate of force development	82.6% @ 2 class	91% @ 2 class
Waldert et al. (2008)	multichannel EEG (contralateral)	point to point centre-out arm movement	cued	movement direction	55.0% @ 4 class	69.2% @ 4 class
Gu et al. (2009)	single channel EEG	imaginary isometric plantar flexion	cued	target torque	79.0% @ 2 class	100.0% @ 2class
Gu et al. (2009)	single channel EEG	imaginary isometric plantar flexion	cued	rate of force development	82.5% @ 2 class	100.0% @ 2class
Bradberry et al. (2010)	multichannel EEG	3D centre-in/out reaching movements	self-paced	3D hand velocity	r=0.296 @ 6 class	r=0.51 @ 6 class
Lv et al. (2010)	multichannel EEG	continuous drawing task in 4 directions	tracking	2D end point position	r=0.315	r>0.67
Yuan et al. (2010)	multichannel EEG	left/right hand repetitive clenching	cued	clenching speed of right/left hand	r=0.32, 74% @ 2 class	r=0.58, 93% @2 class
Bradberry et al. (2011)	multichannel EEG	Imaginary tracking fingertip movements	tracking	2D end point position	r=0.59	n/a
Waldert et al. (2008)	multichannel MEG	point to point centre-out arm movement	cued	movement direction	67.0% @ 4 class	85.0% @ 4 class
Bradberry et al. (2009)	multichannel MEG	tracking centre-out tool/hand movements	tracking	2D end point position	r=0.40 @ 4 class	n/a
Schalk et al. (2007)	multichannel subdural unilateral ECoG	impeded circular arm movements in horizontal plane	tracking	2D end point position	r=0.697	r=0.90
Ball et al. (2009)	Multichannel contralateral subdural ECoG	centre-out arm reaching movement	self-paced	movement direction	(75%, 45%) @ 4 class total/plan (55%, 45%) @ 8 class total/plan	(80%,70%) @ 4 class total/plan n/a
Reddy et al. (2009)	Multichannel unilateral subdural ECoG	directional arm movements & keypress	cued	direction of movement and key press	73.5% @ 5 class	86.0 % @ 5 class

r: correlation coefficient

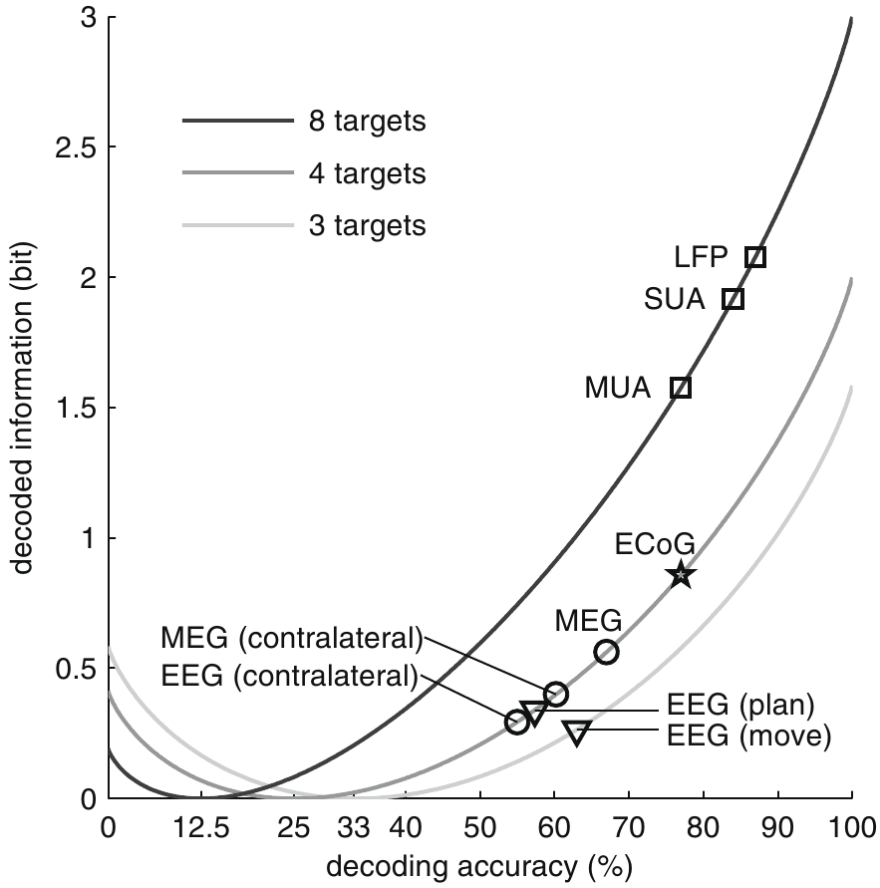

Figure 2.24. Decoded information (information transfer rate) in bits (Information theoretic definition, Shannon, 1948) versus decoding accuracy (%), as a function of the number of classes. Squares: (Mehring et al., 2003); Star: (Ball et al., 2009); Circles: (Waldert et al., 2008); Triangles: (Hammon et al., 2008). contra-lateral: only contralateral sensors/electrodes are used for decoding. From Waldert et al. 2009. Permission to reproduce this figure has been granted by Elsevier.

Also, continuous decoding of 3D hand kinematics (Bradberry et al., 2010), 2D tool endpoint position (Bradberry et al., 2009; Lv et al., 2010; Bradberry et al., 2011), and movement speed (Yuan et al., 2010) are reported.

Further evidence for possibility of decoding movement parameters, is the ECoG decoding of kinematic movement parameters including the direction (Reddy et al., 2009) and 2D endpoint position (Schalk et al., 2007).

2.3.2. Decoding Isometric Task Parameters from EEG, MEG and ECoG

Detection of contraction intensity and in its classical form as isometric force levels are present in the literature for both actual isometric contractions (do Nascimento et al., 2005) and imaginary isometric contractions (do Nascimento et al., 2006).

Another set of studies try to decode force or rate of torque development in real or imaginary isometric tasks (Romero et al., 2000; do Nascimento and Farina, 2008; Gu et al., 2009). Most of the signal characteristics and features in this category are not directly related to the accompanying ERS/ERD phenomena.

The very few EEG studies mentioned above and also listed in Table 2.3, are practically the only available documentation on isometric tasks that seek to decode or extract task parameters from EEG. This shows the inadequacy of experimental data and knowledge in this area and the need for further research.

2.4. Thesis Statement

In Section 1.1, a wide perspective on large-scale motor neurophysiology and neuro-rehabilitation was explored. In Section 1.2 some of the larger picture objectives in this perspective were highlighted.

Based on the review on motor neurophysiology in Section 2.2, it is concluded that the role of pre-motor cortex, supplementary motor area (SMA) and also the activation of ipsilateral (vs. contralateral) M1, pre-motor cortex and SMA are not adequately studied in isometric tasks. Although the signal features in time and time-frequency domain can reflect valuable information about the spatial and temporal characteristics of brain activity, much more information about the underlying mechanism of neural control of movement can be obtained. Using the sequenced execution protocols (Cisek and Kalaska, 2004; Hammon et al., 2008) such as instruction-delay (versus reaction-time paradigm), and using restricted or specific tasks such as isometric exertion (where no physical coordinate change of limb happens), can help in this regard. There are several single cell recording studies on primates for complex planning-execution paradigms in movements (Cisek and Kalaska, 2004, 2005; Sergio et al., 2005) and for isometric exertions (Sergio and Kalaska, 2003; Sergio et al., 2005). However, there are a few EEG studies in this context (see Section 5.2.2 in Discussion for details and examples). An exception for movement tasks is an EEG study on instruction-delay reaching tasks (Hammon et al., 2008) where the signal during planning and execution stages are used to decode movement direction. Based on this, the knowledge about EEG signatures in planning and execution of isometric tasks is incomplete. Even in single cell recording or other imaging modalities the available literature does not address the role of all brain regions nor are the planning-execution stages studied separately. Large-scale recordings (e.g. EEG) can provide insight not only about the involvement of different brain regions in planning and execution of motor tasks, but also about the activity characteristics (specifically MRP and oscillatory ERD/ERS) of these centres.

Directional isometric tasks have not been used before in a BCI context. Precisely, directional isometric tasks are exertion of force toward a specific direction, without any displacement. This is different from sustained isometric contraction in which only static co-contraction happens. Directional isometric tasks, in comparison to movement tasks, lack the extrinsic change of limb coordinates that can potentially alter the patterns of activity and the amount of directional information in specific brain regions and in the whole. They, however, retain the muscle activation specificity better than directional movements, due to lack of three-phasic pattern (Berardelli et al., 1996; Hoffman and Strick, 1999) in isometric tasks (Sergio et al., 2005). Furthermore, as the variability of isometric tasks tend to be much lower in kinematic and kinetic task parameters, they can potentially provide a more accurate and predictable inter-class variance in the accompanying EEG. Additionally, for BCI-aided rehabilitation, isometric tasks are much more desirable in stroke and SCI rehabilitation, due to practical and clinical considerations such as comfort, ease of measurement and feedback and relative ease of coordination and control. According to the review on motor parameter decoding in Section 2.3 and reviews on directional information (Waldert et al., 2009), this information can be enhanced by extracting direction-specific features, and directional information across the spatial surface EEG map. This adds to the understanding of motor planning and execution. Furthermore, it paves the way for potential applications in BCI research and development.

Based on the discussed motivation, research philosophy and potential applications, the intended research and expected observations can be summarised as follows:

2.4.1. Research Statement

1. It is of interest to determine the EEG signal features in time (MRP) and time-frequency representations (ERD/ERS) associated with planning and execution of directional arm isometric exertions. The spatial distribution of the identified signals in surface EEG is the next question to be investigated.

2. It is of interest to find out the directional information in the whole EEG electrode set, in different stages of planning and execution of isometric tasks and to assess the contribution of different regions to directional information.

2.4.2. Research Hypotheses

2.4.2.1. The Role of Different Brain Regions in Various Tasks

It is of interest to explore whether there are consistent signal features associated with planning and execution of isometric tasks, as there are for movement tasks and move-

ment imagery (McFarland et al., 2000; Caldara et al., 2004; Neuper et al., 2006b). It is also of interest to explore whether the observed signal parameters in planning and execution are similar to or different from those of movement or movement imagery and to what extent; also if the planning stage has as significant features as execution. When an isometric motor task is attempted, the spatial distribution of surface EEG signal can reveal what brain regions (e.g. ipsilateral/contralateral motor cortex, pre-motor cortex, supplementary motor area or parietal cortex) are responsible for the observed activity and to what extent. Both the time and time-frequency features can provide insight about the characteristics, timing and region of neural activity in different stages of task. This hypothesis tries to verify if ERP and ERD/ERS originate from the extrinsic coordinate change of limb position or simply from the pattern/intensity of the involved active muscles.

If the hypothesis is proved, most of the applications of movement related activities in EEG (ERPs and SMRs) can be generalised for isometric tasks. This includes BCI applications, BCI-rehabilitation, and potentially useful rhythm characteristics for brain stimulation and rehabilitation. Additionally, the planning and execution stages can be properly decided for, in such applications.

2.4.2.2. Presence and Spatial Distribution of Directional Information in Different Stages of Tasks in Surface EEG

It can be hypothesised that directional information is found in both stages of planning and execution. According to the current understanding of the function of M1 and other motor areas, it is expected to see directional information coming mostly from electrodes above M1 during planning and execution. It is also expected that the electrodes above SMA and PM contribute to direction decoding mostly during planning and to some extent during execution. In general, improved directional decoding in comparison to movement studies are expected, due to decreased variability. However, a lack of target point encoding in motor processing (extrinsic coordinates), may have a contradicting effect. This hypothesis targets the potential source of directional information: extrinsic coordinates vs. muscles activity *per se*. It can also reveal if directional information is provided through a cosine-tuning pattern, as in SUA in movement and isometric tasks (Sergio et al., 2005) and movement related ERPs and ERSP (Valsan, 2007).

This is of significant help for the design of BCI and BCI-rehabilitation systems, as isometric task planning and execution are more practical for patients with neuromuscular disabilities. Furthermore, the current opinion about the role of different brain regions in planning and execution of directional tasks can be verified.

2.4.3. List of Contributions

This section summarises the main contributions of this thesis to knowledge. To the best of the author's knowledge, the following contributions have not been explored before and recorded in literature.

- Identification of event-related (de-)synchronisation (ERD/ERS) of directional arm isometric exertions during planning stage that distinguishes the type and region of oscillatory neural activity.
- Identification of event-related (de-)synchronisation (ERD/ERS) of directional arm isometric exertions during execution stage that distinguishes the type and region of oscillatory neural activity.
- Identification of directional information in EEG recordings of directional arm isometric exertions during planning stage that reflects the directional neural processing and achievable information transfer rate.
- Identification of directional information in EEG recordings of directional arm isometric exertions during execution stage that reflects the directional neural processing and achievable information transfer rate.
- Comparison of the directional information of isometric exertions with movements in the planning and execution stages that can justify the application of isometric tasks instead of movements in BCI and rehabilitation.

Potential Impacts:

ERD/ERS patterns help to identify the generating sources of the brain for different sensorimotor integrations and their relationship with task parameters during motor planning and execution, especially the tasks without extrinsic coordinate change. This implies that in many applications, isometric tasks (which can be exercised easily with less variability) can be used instead of reaching or pointing movements. They are of interest for targeted brain stimulation (e.g. tDCS and tACS) and for rehabilitation research where an elementary prediction about the stimulation polarity, frequency and direction can be made based on EEG signatures. The ERD/ERS patterns and sources may also provide clinicians valuable clues about normal and abnormal motor activity.

Furthermore, the identification of directional information in each step adds another layer of information about the sensorimotor integration and implies which brain regions are involved in the determination of motor plans, task direction and muscles activity.

This is of interest for BCI-rehabilitation research where robot or FES-assisted rehabilitation for each muscle group or direction can be triggered by the corresponding BCI class. Knowledge about the directional information content during planning and execution is paramount to developing better designs and further exploitation of different BCI and rehabilitation paradigms and protocols. An example can be the proper selection of the time windows involving the planning or execution of motor tasks.

The detailed justification and the philosophy behind the contributions are discussed in Sections 1.1 and 1.2 and are further elaborated, in Chapter 2, specifically in Sections 2.4.1 and 2.4.2.

2.5. Chapter Summary

In this chapter, the basic motor neurophysiology was briefly introduced, the basic characteristics of motor related potentials in time and time-frequency representations were discussed, and the research statement and hypotheses were established. In the next chapter the requirements and chosen implementation of experimental setup are discussed.

Chapter 3

Materials and Methods

In this chapter, the requirements for the experiment and the considerations for the study are discussed in Section 3.1 followed by Section 3.2 where the experiment setup and protocol are described. The data analysis methods are explained in Section 3.3, and finally Section 3.4 summarises the chapter.

3.1. Requirements and Design of Experimental Setup

Following the research statement in Section 2.4, this section discusses the requirements for successfully investigating the EEG signatures in isometric exertions. The different implementation aspects of the experiments are discussed and the required setup is designed.

3.1.1. Experiment Task Specifications

Humans can make sustained voluntary contractions (in the form of increased co-contraction of agonist and antagonist muscles) or directional isometric tasks in different body parts. While any body part can be chosen the upper limb is a better choice for this study. Upper limb, while smaller in size compared to lower limb, receives roughly the same corticospinal innervations from M1 and the corresponding cortical area is close to the skull (Patestas and Gartner, 2006). It is therefore expected that the more accurate muscle control will provide more distinct EEG patterns.

For this study, directional isometric tasks are favoured over sustained isometric co-contractions. The directional tasks are accompanied by surface EEG patterns that can potentially reflect the direction of task (see Chapter 2). When analysed by statistical and pattern classification techniques on time and time-frequency EEG signatures, the directional information of the task could be extracted. This would give a much better under-

standing of CNS mechanisms in the planning and control of tasks. In Section 2.2 the role of direction on the neural activity was discussed.

By selecting directional wrist tasks the fine individual muscle activations may be targeted, although the contributing sources of activity to the overall EEG are smaller and fewer. Doing an arm task brings more muscles of the upper limb in to play and observation of more pronounced activity features are expected. This probably gives a larger but mixed activity pattern; that is, many sources (that correspond to different muscle innervations) get activated simultaneously. As the first approach in this thesis the arm isometric tasks are chosen; however, the same experiment on wrist isometric tasks would be as important and may be explored in future works. The arm isometric tasks are more suitable in practice as participants can grab a manipulandum (similar to a gear knob), as they would in daily activities, which provides a convenient and natural grip position.

Since the dominant and non-dominant hands can result in slightly different neural activity patterns (Bagesteiro and Sainburg, 2002; Martin et al., 2011), especially in laterality of the observed activity, for the first approach in this work, experiments on dominant hand or arm were selected.

The directional tasks limited to horizontal plane, are easy to control and suitable for this study.

The isometric exertion should be large enough to induce detectable changes while, at the same time, it should not cause posture disruption, EMG artefact or, most importantly, muscle fatigue. The force limit was chosen, for each participant, to be 30% of the maximum voluntary contraction (MVC) limit of the task.

As subjects need to react to cues and, at the same time, keep a minimum level of consciousness for a long time, then a sitting posture is the most suitable choice against standing or lying.

3.1.2. Stages and Timing of the Experiment

Similar to many previous studies (see Section 2.2.2 for SUA experiments on primates), different stages of preparation, planning and execution of the task need to be slightly delayed. Although in practice these stages follow each-other without a delay, by separating them, different patterns of activity associated with each stage can be inspected. The subjects were therefore asked to prepare for exertion in the first stage; this is the motor readiness stage, but no information about the task direction was known to the participants. In the planning stage a cue about the type of task (direction) was introduced, but the participant did not start it; in this stage, planning for the specific task direction is reflected in the recordings. During execution the recordings have less preparation-activity and can be mostly attributed to the execution of the task.

A 0.5s to 1.0s time (See Figure 3.5) needs to be considered for the transient effects of motor planning or execution in the EEG, and at least 1.0s for the sustained state in which there is stable neural activity specific to the task stage (observations from the pilot study on subject S0). A minimum of 2.0s in the preparation and planning stage, and 3.0s for the physical exertion are allowed as development of force requires some more time.

It is essential that the cues and the stages of the task are not predictable as this can corrupt the nature of signal in each stage. For this reason a random time is added to the duration between cues in each stage.

A separate time window is added for complete rest of subjects between trials, to enhance the quality of the task execution, reduce the error rates and prevent muscle fatigue. Additionally, longer rest times are added between different experiment sets.

3.1.3. Visual Cues

The timing and direction of exertions need to be signalled to the subjects by a sensory cue. Visual cues are straightforward and very close to many daily activities and tasks that are visuo-motor in nature. Cathode ray tube (CRT) displays were chosen to signal the visual cues to the subjects. The eye-display distance should be large enough to prevent eye-movement artefacts. The visual cues should be small so that they do not induce large VEPs. The background and cues should not be of very high contrast either. The magnitude of exerted force has to be fed back to participants so that they can adjust their exerted force level.

3.1.4. Subjects and Ethics

Adult able-bodied right-handed participants with normal or corrected to normal vision (inclusion criteria) without any history of neuromuscular disease (exclusion criteria) qualify for the experiment. Subjects of normal neuromusculoskeletal ability were expected to feel comfortable with the experiment. Subjects were provided with an information sheet along with a consent form prior to the experiment (see Appendix G). The procedures comply with the Declaration of Helsinki (Association, 2001).

3.1.5. Recording Requirements

There were several considerations for the experiment regarding the visual stimuli presentation and digitisation, capturing and recording of EEG, EMG and force. The recordings had to be synchronised to each other and to the visual stimuli.

EEG has physiological components up to 120 Hz and in some specific cases up to

600 Hz (van Drongelen, 2006); however the frequencies above 50Hz are harder to detect and quantify due to temporal and spatial filtering through the skull and scalp, recording noise and artefacts. Surface EMG (sEMG) has physiological components up to 500Hz (Merletti and Parker, 2004). The digital recording should have a sample rate well above twice the signal's frequency content (Oppenheim et al., 1999), and, consequently, the recording should be at minimum of 1000Hz, preferably higher. While EEG is the main concept of study, EMG is recorded for verification purpose only.

3.1.6. EEG Electrodes and Recording

Multi-electrode arrangements, such as the 10-20 international system or its extended version, the 10-10 international system (Society, 2006), have been used as standards for surface EEG electrode placement. As the interest here is to investigate the EEG signatures over the whole spatial surface EEG map, no electrodes are excluded from the 10-10 system. While the electrode count can be chosen from 18 to 256, it should be emphasised that too few electrodes cannot properly capture the spatial features of the signal. Nevertheless, too many electrodes are difficult to setup and maintain successfully before and during the experiment. This also increases the chance of two or more electrodes electrically shorting by the conductive gel. Hammon et al. (2008) show an example of practicability. 64-128 surface EEG channel arrangements are practical and either can be chosen according to the experiment and its circumstances.

Recording direct current (DC) unfiltered EEG looks fascinating; however, due to large varying potentials at interfaces, artefacts and the limitation of digitising or recording systems, alternating current (AC) recording is more practical.

For referencing, regions with minimum active electrical activity, such as the nose or earlobes, are preferred as they provide a relatively symmetric and neutral location in comparison to many recording electrodes. They have little muscle activity in normal recording experiments. For grounding, any surface EEG electrode gives a potentially appropriate ground as no significant electrophysiological activity (e.g. ECG, EMG) affects the reported differential EEG and no other physiological signals (except the bipolar EMG) need to be recorded.

3.1.7. EMG Recording from Muscles

Many muscles contribute to arm isometric exertions or movements including trunk muscles and upper limb muscles. The major muscles that get activated in gear shifting positions include (but are not limited to) extensor carpi radialis (ECR), extensor carpi ulnaris (ECU), flexor carpi radialis (FCR), flexor carpi ulnaris (FCU) in forearm; biceps brachii

and triceps brachii in upper arm; and trapezius in the neck-shoulder (Huysmans et al., 2006). Unfortunately, there are experiment and recording limitations and so, for approximate monitoring purposes, EMG recording of some of the muscles should suffice.

3.1.8. Inclusion Criteria for Trials

There are techniques, such as independent component analysis (ICA) and its variants, that are used for decomposing EEG to artefacts and brain activities (Delorme and Makeig, 2004). The applicability of ICA for decomposition of EEG components and artefacts requires different independence conditions; however, the author does not find the arguments for statistical independence of ICA sources in EEG analysis (Onton and Makeig, 2006) strong enough. As the EEG characteristics and exact specifications of MRPs and SMRs are just being explored in this study there is some chance that ICA distorts the actual EEG rather than only removing the artefacts. Besides, the EEG in this experiment is primarily investigated for new neurophysiological phenomena rather than BCI applications. Consequently, rejection of contaminated trials seems to be the safer option compared to artefact removal by source separation techniques.

3.2. Experiments

3.2.1. Experimental Setup and Recording

3.2.1.1. EEG

EEG was recorded by Synamps^2® System (Compumedics Neuroscan, Charlotte, NC, USA), using an electrode cap with BIO-S-200 Ag/AgCl sintered ring electrode set (EASYCAP GmbH, Herrsching-Breitbrunn, Germany), referenced to the earlobes and with a forehead location (AF_z) used as the ground. EEG was band-pass filtered between 0.05 - 500 Hz, digitally sampled at 2000 Hz and captured using SCAN® software (Compumedics Neuroscan, Charlotte, NC, USA). A total of 73 surface EEG channels were recorded in full 10% arrangement (Society, 2006). The contact impedances of all recorded electrodes were lowered to $5k\Omega$ before recording and were constantly monitored and maintained during recordings. Figure 3.1 shows the electrodes arrangement.

3.2.1.2. Force

Force was transduced by a Nano25® 6-axial torque and force transducer and power supply/interface box (ATI Industrial Automation, Apex, NC, USA) and was captured by a Power1401 mk1.5 (Cambridge Electronic Design Limited, Cambridge, England, UK),

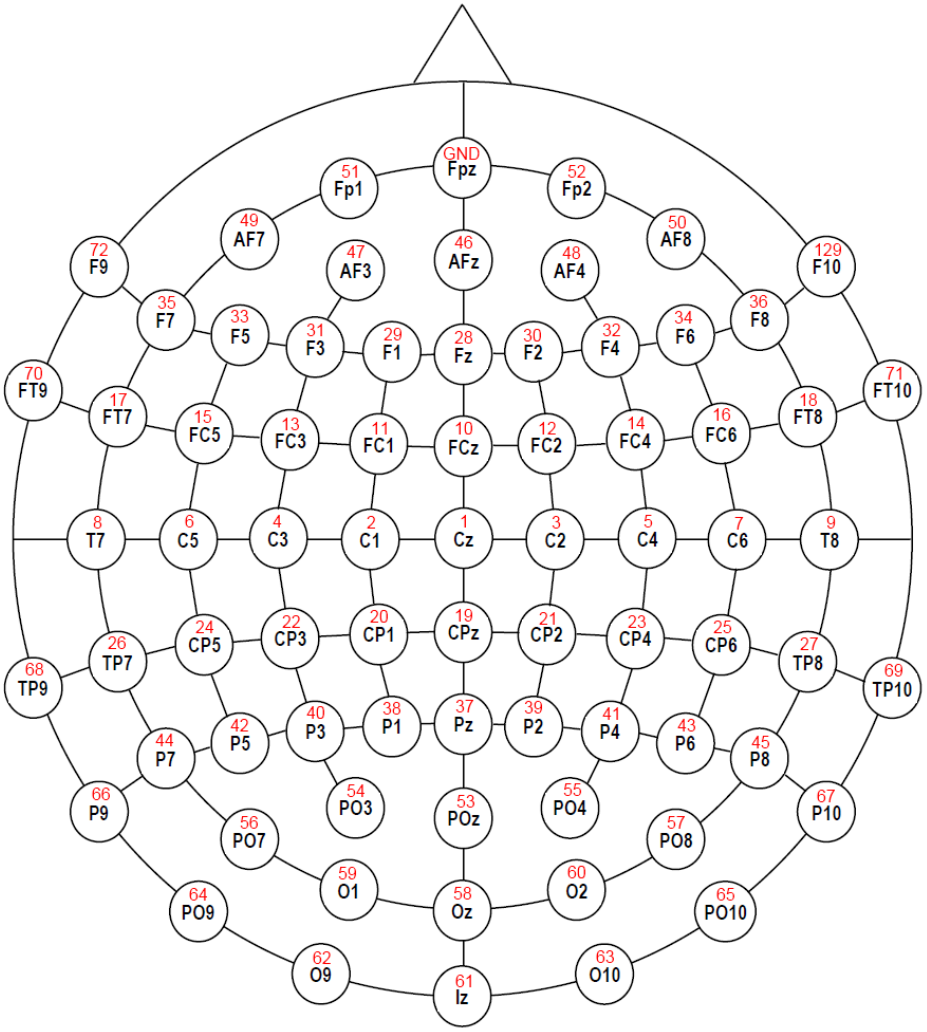

Figure 3.1. 10-10 surface EEG electrode locations and nomenclature (Society, 2006). The numbers indicate conventions for recording and bear no physiological meaning. Image has been modified from the map provided by EASYCAP GmbH, Herrsching-Breitbrunn, Germany.

sampled at 2000 Hz and recorded by Spike2® software (Cambridge Electronic Design Limited, Cambridge, England, UK). A spherical knob (diameter=5.3cm) was attached on top of the sensor and the sensor is fixed to the experiment seat (see Figure 3.2).

The technical drawings for the mechanical parts that fix the sensor and manipulandum to the chair are reproduced in Appendix A. The parts were fabricated in the Mechanical Workshop, Department of Biomedical Engineering , University of Strathclyde. Also the basic diagram for the custom interface box and wiring are reproduced in Appendix A. The interface circuits and boxes were made in the Electronics Lab, Department of Biomedical Engineering, University of Strathclyde.

Subjects were requested to generate three maximal exertions in each direction, and the average of the least strong direction was considered as the MVC value. 30% of this

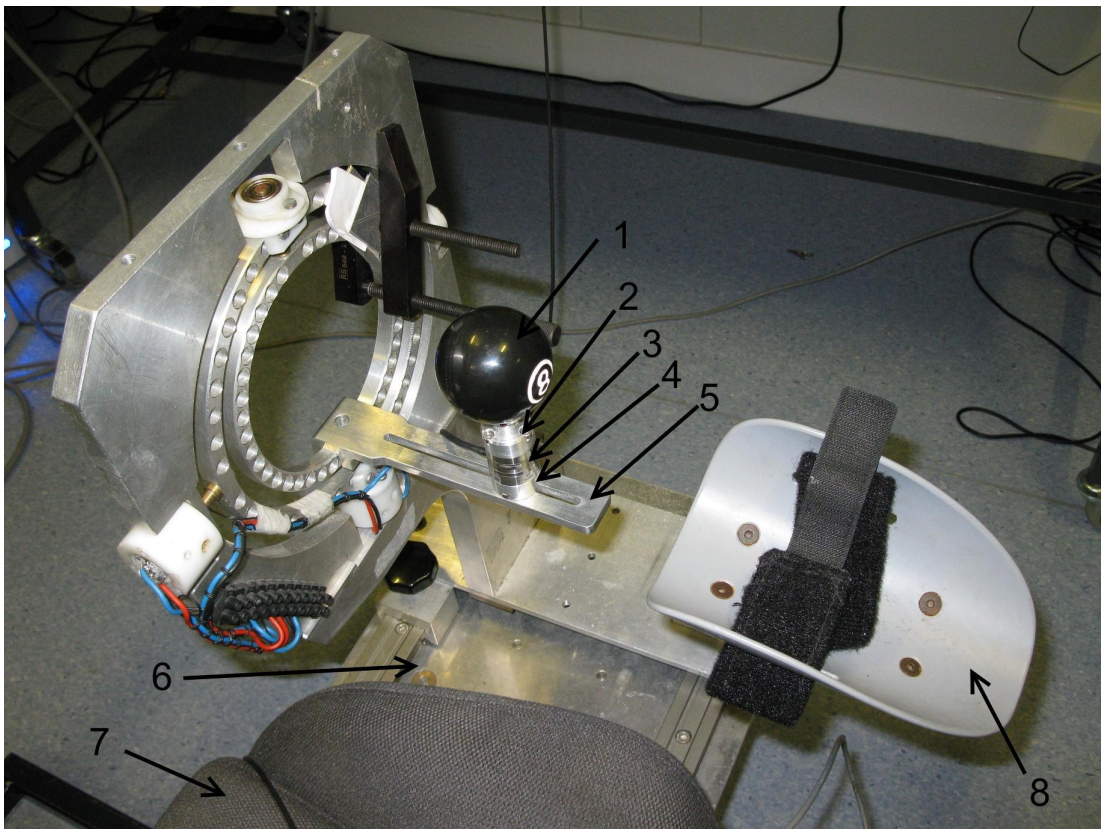

Figure 3.2. The manipulandum used in the experiment. The gear knob (1) is grabbed by the subject to exert force. The knob is attached to the sensor (3) via a top-plate connector (2) and is attached to the base (5) via a bottom-plate connector (4). The assembly and the seat (7) are fixed to the support (6). An elbow and arm rest (8) is used to support the arm's weight.

value was used for the experiment thresholds.

3.2.1.3. EMG

Bipolar EMG was recorded from four forearm muscles: extensor carpi radialis (ECR), extensor carpi ulnaris (ECU), flexor carpi radialis (FCR) and flexor carpi ulnaris (FCU). Figure 3.3 shows the four selected forearm muscles. Blue Sensor N® Ag/AgCl ECG electrodes (Ambu A/S, Ballerup, Denmark) and Synamps^2® System (Compumedics Neuroscan, Charlotte, NC, USA) are used for EMG recordings. An inter-electrode distance of 2.0cm was used based on SENIAM recommendations (Hermens et al., 2000).

To locate the appropriate EMG electrode sites, the guidelines in Table 3.1 were used.

3.2.1.4. Visual Cues

Visual Cues and the force signal feedback were generated by a custom GUI and code (see Appendix B, Figure B.1), using the Psychophysics Toolbox (Brainard, 1997; Pelli,

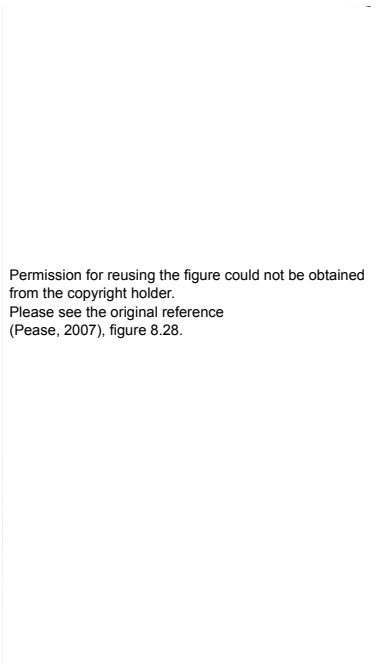

(a) Extensor Carpi Radialis (ECR).

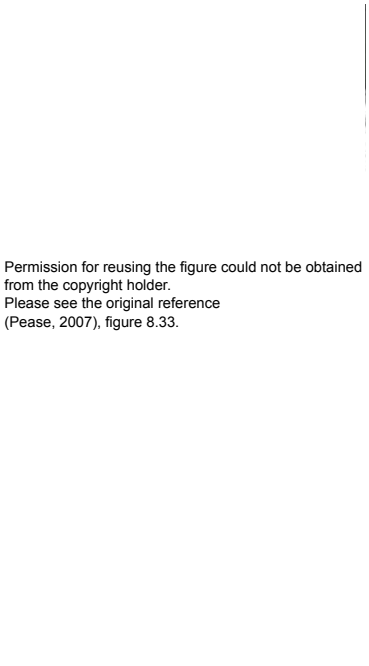

(b) Extensor Carpi Ulnaris (ECU).

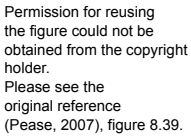

(c) Flexor Carpi Radialis (FCR).

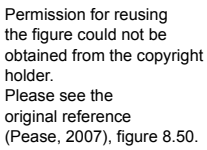

(d) Flexor Carpi Ulnaris (FCU).

Figure 3.3. Four forearm muscles, selected for EMG recording to monitor execution of arm isometric tasks. Figures from Pease 2007.

Table 3.1. Guidelines for locating EMG electrode placement sites .

Muscle Name	Short Muscle Name	Instructions
Extensor Carpi Radialis	ECR	First find the brachioradialis in the fisted semi-pronated situation, by flexing the elbow. Put your thumb in the middle hole of inner elbow and then grab the muscle; ECR is adjacent to this. While keeping the hand in a fist, pronate the forearm, and then extend and, or radially abduct the wrist. The site is 1/3 or 5-7cm proximal of the forearm on the line between the epicondyle and the second metacarpal bone.
Extensor Carpi Ulnaris	ECU	With a pronated forearm, ECU is dorsal to the ulna (a bit radial) in the proximal third of the forearm. It is activated with wrist extension/ulnar adduction (mid to upper forearm).
Flexor Carpi Radialis	FCR	With the forearm supinated, FCR is in 1/3 proximal distance of the line that connects the medial elbow epicondyle to radial styloid. It is activated by wrist flexion (and radial deviation). It is on the medial side of elbow inner side.
Flexor Carpi Ulnaris	FCU	With the forearm supinated, during wrist adduction and flexion FCU is on the medial line that connects the medial epicondyle to the pisiform bone (1/3 proximal distance).

Guidelines from Pease 2007; Lei and Trapani 2000.

1997) and MATLAB® (The Mathworks Inc., Natick, MA, USA). The visual cues and force feedback were presented to the subjects using CRT Monitors at 75Hz. Subjects were seated approximately 175cm away from the CRT display to minimise the effect of eye movement and movement artefacts (see Figure 3.5).

3.2.1.5. Synchronisation

The synchronization between the visual cues, EEG recording system and force recording system was achieved by an event cable. The computer that generated the visual cues, generated and sent digital event signals, via the parallel port to, first, EEG/EMG recording system and, secondly, to the force recording system. The simple diagram of the wiring for this purpose is reproduced in Appendix A. The time delays between the generated event for each visual cue and the recording events were limited to 1ms. The visually

presented feedback of the force had a delay of 15-65ms and a $mode$ of 45ms. This delay is the delay between the acquisition and the visualisation of the force and not between the presented cues, recorded EEG or recorded force.

3.2.2. Subjects and Ethics

All subjects were asked to read the information sheet and sign the written consent form, prior to attending the experiment. The experiments had been approved by the Departmental Ethics Committee of the Biomedical Engineering Department at the University of Strathclyde. A total of 8 (5 male and 3 female) healthy subjects (in addition to 1 subject for a pilot study) from research students and staff community, without a history of neuromuscular disease, volunteered for the experiment. Subjects had normal or corrected to normal vision. After explanation and acquiring written consent, the subjects could get familiar with the experiment environment and the visual feedback of the manipulandum force for a few minutes. Each subject attempted a total of 220 trials in 10 experiment sets of about 7-8 minutes. Subjects were able to rest between the trials sets if required.

3.2.3. Experiment Protocol

Subjects sat in a modified motorsport car seat, which provided a high degree of trunk stability, in front of the monitor while gripping the spherical knob, placed on their right hand side. Subjects were requested to exert centre-out force to left, right, front and back, in the horizontal plane (see Figure 3.4). The requested force was set to 30% of the maximum voluntary contraction (MVC) for each subject. Subjects had a few minutes to practice and learn the task before the recording began.

The sequence of visual cues are presented to the subject as depicted and explained in Figure 3.5. In each trial the subject began in a rest position and was presented with five sequential visual cues:

1. Rest cue (RC): Beginning of trial with a white screen preceding the attention cue.
2. Attention cue (AC): A black circle in the middle of screen, tells the subject to be prepared for planning.
3. Directional cue (DC): Another black circle randomly pointing to one of the four directions, instructs the subject to plan for exertion in the specified direction in the next stage (the subject takes no physical action).
4. GO signal (GO): The middle black circle changes to red and tells the subject to start the isometric exertion towards the indicated direction that was presented in

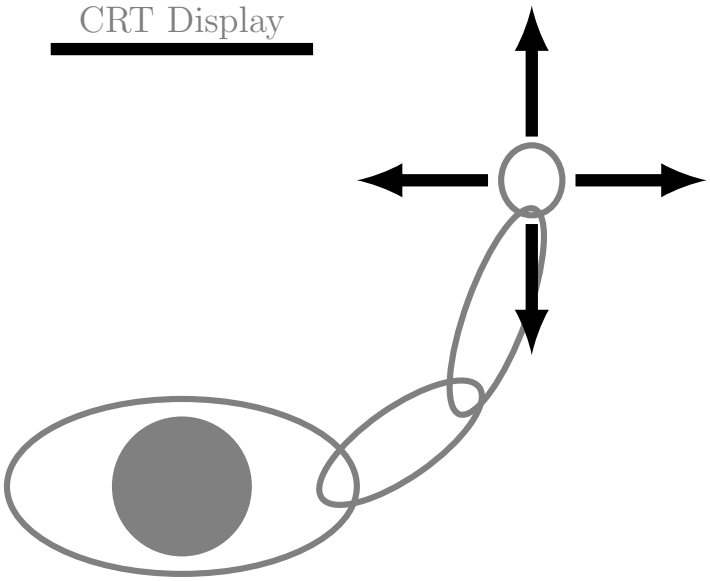

Figure 3.4. Schematic of the experimental setup: Subjects exert isometric arm exertions with the right arm according to the visual cues.

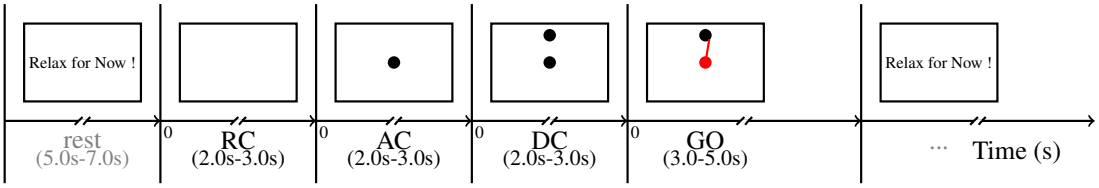

Figure 3.5. Sequence of visual cues and timings (indicated in parentheses). The cues are displayed from left to right: 0. Rest, where the subject takes no action or planning. 1. Rest cue (RC), a white screen preceding the attention cue. 2. Attention cue (AC), a black circle appears in the middle of the screen and tells the subject to be prepared for planning. 3. Directional cue (DC), another black circle, in one of the four random directions, instructs the subject to plan for exertion in the specified direction in the next stage (the subject takes no physical action). 4. GO signal (GO), the middle black circle changes to red and tells the subject to start the isometric exertion towards the indicated direction in the last stage. Simultaneously, the subject sees the direction and magnitude of the exerted force as an orange centre-out line. 5. End of the trial and start of the next trial.

the last stage. Simultaneously, the subject sees the direction and magnitude of the exerted force as an orange centre-out line.

5. "Relax for Now !": End of the trial.

In each trial RC, AC, and DC stages last a random duration of between 2 and 3 seconds, the GO (exertion) stage lasts between 3 and 5 seconds and the rest period lasts between 5 and 7 seconds. The trial consequently lasts between 14s to 21s. Trials are conducted in sets of 7-8 minute recordings with time in between for a complete rest. Each subject attempted a minimum of 220 trials in total (see Figure 3.6).

Figure 3.6. Subjects sat in a chair in front of a monitor where multichannel EEG was recorded. Subjects exerted a force in the horizontal plane according to the visual cues on the monitor. The monitor was situated at a distance of about 175cm from the subject.

3.3. Data Analysis

A custom GUI and scripts were developed to process the recorded data in MATLAB® (Mathworks Inc., Natick, MA, USA).

3.3.1. Data Preprocessing

To prepare the experimental data for further analysis, it was necessary to remove the artefacts and put the data into epochs that correspond to the event of interest. Preliminary preprocessing and time-domain analysis also included baseline removal, averaging and common-average referencing (CAR). Each issue is elaborated on in the following sections.

3.3.1.1. Artefact Removal

The acquired signals are visually inspected for eye movement, jaw clenching, blink, EMG, ECG, sweat, movement and electrode artefacts (Tatum et al., 2011). Using a custom built MATLAB® code and GUI (see Appendix B, Figures B.2 and B.3) the contaminated EEG segments were excluded from the analysis. Trials with early or late subject response were also discarded based on the force profile.

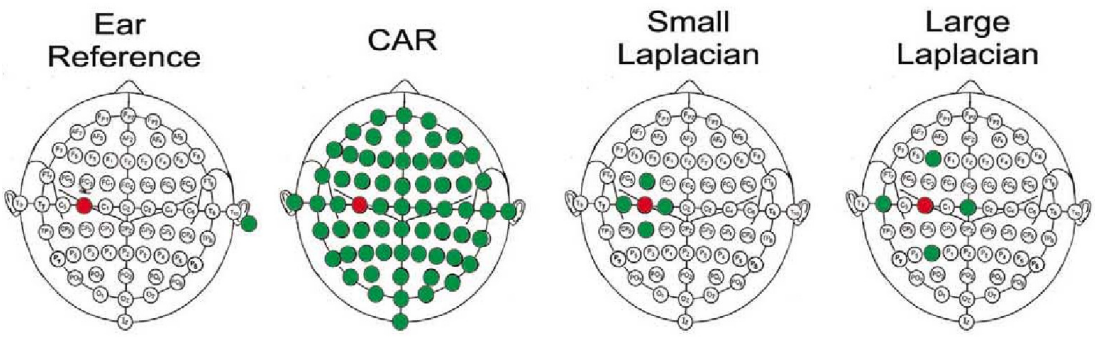

Figure 3.7. Different EEG referencing methods (ELR: ear-lobe referencing, CAR: common-average referencing, SL: surface Laplacian) which provide different spatial filtering levels. In each schematic, the red electrode is measured with respect to the average of the green electrodes. From Wolpaw et al. 2002. Permission to reproduce this figure has been granted by Elsevier.

3.3.1.2. Epoching and Baseline Removal

Data were epoched based on the type of event or cue. To better inspect the relative changes induced by the visual cues, the signals in the RC, AC, DC, and GO stages were baseline adjusted to the signal values at the time of the cues.

It should be noted that because of 0.05Hz high-pass filtering of EEG, the absolute signal values without a defined referencing bear no physiological meaning.

3.3.1.3. Common-Average Referencing and Averaging

Data were common-average referenced (CAR) as needed. The common-average referenced EEG provides a basic spatial filtering by subtracting the common far field EEG activity, and can show some aspects of local activity across subjects (Srinivasan et al., 2006). The CAR data is used to find the time-domain averages to inspect MRP and to further apply time-frequency techniques on the data. Figure 3.7 shows different referencing (spatial filtering) on the recorded EEG.

3.3.2. Time-Frequency Analysis

Different representations can be used to study the time-frequency signatures of signals (Boashash, 2003). The quadratic time-frequency representations such as Wigner-Ville distributions (Ville, 1958), provide sharp and bold representations of signal features but suffer to different extents from cross-terms. The kernel-based variations of quadratic distributions such as smoothed psudo Wigner-Ville distributions and Choi-Williams distributions (see Cohen, 1995 for definitions and in-depth discussions) can provide a compromise between resolution and cross-terms, but include many parameters and require special fine-tuning. Short-time Fourier transform spectrograms and continuous Morlet

wavelet scalograms provide lower levels of resolution, but cause no cross-term effects (Hlawatsch and Auger, 2008). Wavelet scalograms also allow to analyse the signal at any frequency of interest. This feature and lack of cross-terms are desirable and allow exploration for further time-frequency features in addition to the already well documented spectral changes associated with movement planning and execution. In this study wavelet scalograms have been used to get better time-resolution at higher frequencies and better frequency resolution at lower frequencies. Matching pursuit methods (Durka, 2007) were not used due to extreme computational demands.

3.3.2.1. Continuous Wavelet Transform

For time-frequency analysis, continuous Morlet wavelet transform coefficients (Misiti et al., 2007) were calculated using Equation (3.1):

$$\begin{aligned} W(a,b) &= \frac{1}{\sqrt{a}} \int_{-\infty}^{\infty} f(t)\psi^*\Big(\frac{t-b}{a}\Big)\mathrm{d}t \\ \psi(t) &= \frac{1}{\sqrt{2\pi}} e^{-t^2/2+j2\pi b_0 t}, \quad b_0 = 1 \end{aligned} \tag{3.1}$$

where W(a,b) is the wavelet coefficient at frequency $1/a$, b is time, $f(t)$ the signal in time, and * indicates the complex conjugate. Custom MATLAB® codes were developed, along with the time-frequency toolbox (Centre National de la Recherche Scientifique, Paris, France) for the comparison and verification of results.

3.3.2.2. Event-Related Spectral Perturbation (ERSP) or Normalised Scalograms

In order to obtain the normalised scalogram (squared wavelet coefficients moduli), the squared coefficients from the rest time EEG (0.0-0.66s before the appearance of RC cue, i.e. white screen) were averaged over the rest time at each frequency and used to normalise the scalogram coefficients of that frequency in other time windows. This normalised representation is usually referred to as event-related spectral perturbation (ERSP). The normalisation method may vary according to different applications and in different studies. See the report by Pfurtscheller and da Silva (1999) for a list and a discussion of different nomenclature and techniques for reporting the relative changes in spectral power of EEG.

3.3.2.3. Inter-Trial Coherence (ITC)

In order to assess the phase-locking of the signal to the presented cues, inter-trial coherence (ITC) was calculated for all time-frequency representations (Sinkkonen et al., 1995).

This is a measure of the consistency of the wavelet coefficient angles (phase values) across the trials and is defined by Equation (3.2). The minimum theoretical value for ITC, 0, indicates that phases of the wavelet coefficients at a specific time and frequency are totally random from trial to trial. On the other hand, the maximum theoretical value, 1, corresponds to complete consistency and zero variance of the phase of wavelet coefficients in all trials. The ITC values depend on the frequency, experiment, and referencing method with respect to events. High ITC value at a specific frequency and time shows that the corresponding waveforms and oscillations are time-locked to and (most probably) trigerred by an event or their phases get reset due to the event; eventually, indicating the type of involvement of the brain oscillators in the task. Consequently, for those ERSP patterns that do show statistical significance (see Section 3.3.3), ITC provides an additional layer of information about the nature of ERSP in the task. This makes the ITC a supporting measure for time-frequency analysis.

$$ITC(a,b) = \frac{|\sum W(a,b)|}{\sum |W(a,b)|} \tag{3.2}$$

where W(a,b) is defined by Equation 3.1.

3.3.3. Statistical Analysis

In order to assess the statistical significance of the time-frequency distributions the values of each point in the time-frequency plane for all trials have to be compared against the rest-time time-frequency values of that frequency. The simple method is to use parametric statistics, assuming normal distribution for EEG time series which leads to χ^2 distribution for the wavelet moduli (Torrence and Compo, 1998). However, as the squared wavelet coefficients (and consequently their normalised values) have a statistical distribution very far from normal (the author's observation and other reports such as Durka et al., 2004) a general statistical method, different from those with assumptions on the distributions (as in ANOVA), needs to be used.

3.3.3.1. Permutation Test

One of the methods for dealing with non-Gaussian data distributions are re-sampling methods (Erfon and Tibshirani, 1993; Basso et al., 2009). For significance analysis between two non-Gaussian data groups, the null hypothesis is that there is no difference between the two data groups. If the null hypothesis is true, the data points from the two groups (group A with n_a data points and group B with n_b data points) can be mixed into one large group (group C with $n_c = n_a + n_b$ data points) and randomly re-sampled into two new groups with the same number of data points (group A^* with n_a data points

and group B^* with n_b data points). In this case no difference between the test statistic values of the original datasets and the permuted datasets would be expected. A good, common candidate for the test statistic is the difference between the group mean values, as in Equation 3.3, where μ_a is the mean of group A, μ_b is the mean of group B and δ denotes the test statistic. The test statistic reflects a measure of difference between the groups.

$$\delta = \mu_a - \mu_b \tag{3.3}$$

By repeating this re-sampling a large enough number of times, a distribution of δ is generated, which is denoted by δ^*. By comparing this distribution with the original test statistic, δ_0, for groups A and B, the p value can be found. The p value is the ratio of number re-samplings (denoted by $\#\{.\}$) with $\delta > \delta_0$ to the total number of re-samplings (Note that this relationship changes to $\delta < \delta_0$ for $0 > \delta_0$). This is shown in Equation 3.4, where N is the number of permutations.

$$p = \frac{\#\{\delta^* > \delta_0\}}{N} \tag{3.4}$$

As the p value comparison has a binomial distribution in N permutations (Erfon and Tibshirani, 1993), the number of permutations (N) required to give the coefficient of variation COV at p significance level is given by Equation 3.5:

$$N = \frac{1-p}{p.COV^2} \tag{3.5}$$

The permutation test (Erfon and Tibshirani, 1993) is used to check the statistically significant difference between the rest time and the experiment time windows. The rest-time signal values or wavelet moduli at each frequency can be compared. For wavelet moduli, at each frequency, f, the values are chosen from points that are $0.5Ts$ apart (where $T = 1/f$), from all trials. This provides relatively independent samples and at the same time allows for the inclusion of several samples from the rest time duration. The $p = 0.05$ value is used as the significance level with a coefficient of variation of 0.10, which equals 1900 permutations. See Durka et al., 2004 for details of the method and a discussion. The permutation analysis is computationally intensive (e.g. hundreds of hours of processing on an 8-core computer); to overcome this problem the distribution values are computed every $20ms$ (i.e. $0.5T$ at $50Hz$) and GPU computing is used.

3.3.3.2. Permutational ANOVA

In order to find if there is a statistically significant difference between the time-frequency features of 4 trial groups representing 4 exertion directions, a non-parametric method is needed. This is because the distribution of features is far from normal. By choosing an appropriate test statistic the permutation analysis can be applied to multi-class data. The permutational ANOVA (Basso et al., 2009) is applied to the test statistic in Equation 3.6,

$$T = \sum_{i=1}^{G} n_i.(\overline{\mu_i} - \overline{\mu})^2 \tag{3.6}$$

where G is the number of groups, n_i the number of samples in group i, $\overline{\mu_i}$ the corresponding group average and $\overline{\mu}$ the dataset average. The p value is calculated similarly to that of Equation 3.4. By using 2000 permutations to find the p-value at 2.5% significance level the coefficient of variation for the estimated p-value is about 13.9%, according to Equation 3.5 (Erfon and Tibshirani, 1993; Durka et al., 2004). This is equivalent to finding the p-value at 5% with the coefficient of variation of 10.26%. The null hypothesis is that there is no difference between group (direction) labels versus different coefficients for each group (direction). To reduce the computing time the down-sampled scalogram at 100Hz is used. The MATLAB® (Mathworks, Inc., Natick, MA, USA)/C++ permutational ANOVA code on an 8-core x86 64-bit platform at 2.88GHz, took about 190 minutes.

3.3.3.3. Sign Test

To assess if the number of subjects that show a specific EEG signature is different from chance, the siginificance level or p-value of the observation is determined by sign test, using binomial cumulative distribution function (Moore et al., 2010). The derivation and calculation of the correction for the family-wise or multiple-comparison error (Bretz et al., 2011) for the sign test, along with the table of corrected significance levels can be found in Appendix D.

3.3.4. Feature Extraction from Data/Signals

In order to classify the EEG patterns, based on previous EEG trials, the dimension of the time domain signal or the time-frequency representation matrices should be reduced. This makes classification simpler by reducing the dimension of data that are fed to the classifiers. It is noteworthy that most dimension reduction techniques, such as princiapl component analysis (PCA), are in fact combinations of dimension reduction and feature extraction. This is mainly because specifying a criteria for dimension reduction, makes

the data in the reduced dimension to be automatically structured according to the applied criterion. As an example, PCA can be used to reduce the dimension of data based on the variance of original data. While the data are represented by fewer variables, these variables also contain more information about the variance and variance structure of the data.

3.3.4.1. Principal Component Analysis (PCA)

Principal component cnalysis (PCA) is a linear transformation between the space of the actual data and a new space (principal components space or PC space). The new space is defined based on the distribution of the data. Based on the definition (Jolliffe, 2002), the PCA transformation is the one that provides the greatest variance for the first new variable and the greatest variance for the next new variables independent from the previous new variables.

The mathematical description is as follows. If n is the number of trials or observations and p is the number of variables (dimensions) then the raw data matrix is denoted by $\mathbf{X}_{n\times p}$, where the rows correspond to trials or observations and the columns are variables. Without loss of generality, $\mathbf{X}$ is assumed to have zero mean on each column. The transformation is formulated as in Equation 3.7, with $\mathbf{C}_{p\times p}$ as the transformation matrix, $\mathbf{X}_{n\times p}$ as the raw data matrix and $\mathbf{Y}_{n\times p}$ as the transformed data in the PC space.

$$\mathbf{Y}_{n\times p} = \mathbf{X}_{n\times p}\mathbf{C}_{p\times p} \tag{3.7}$$

Based on this definition, $\mathbf{Y}_{n\times p}$ variables should have maximum variance in descending order across observations. At the same time the columns of the transformation matrix $\mathbf{C}_{p\times p}$ are orthogonal independent vectors in the new PC space and representative of maximum variances directions in the raw space. Figure 3.8 shows data samples in raw and PC spaces.

The transformation matrix can be calculated using different methods such as covariance matrix eigen-decomposition or singular value decomposition (SVD) (Jolliffe, 2002) and based on the values of n and p. It is common practice to consider the column vectors of transform as unit vectors. Based on the dimensionality of the data and the number of data points two cases can be considered:

case n>p: The number of trials, or observations, are greater than the number of variables. The transformation finds and sorts the maximum variance combinations of the raw variables.

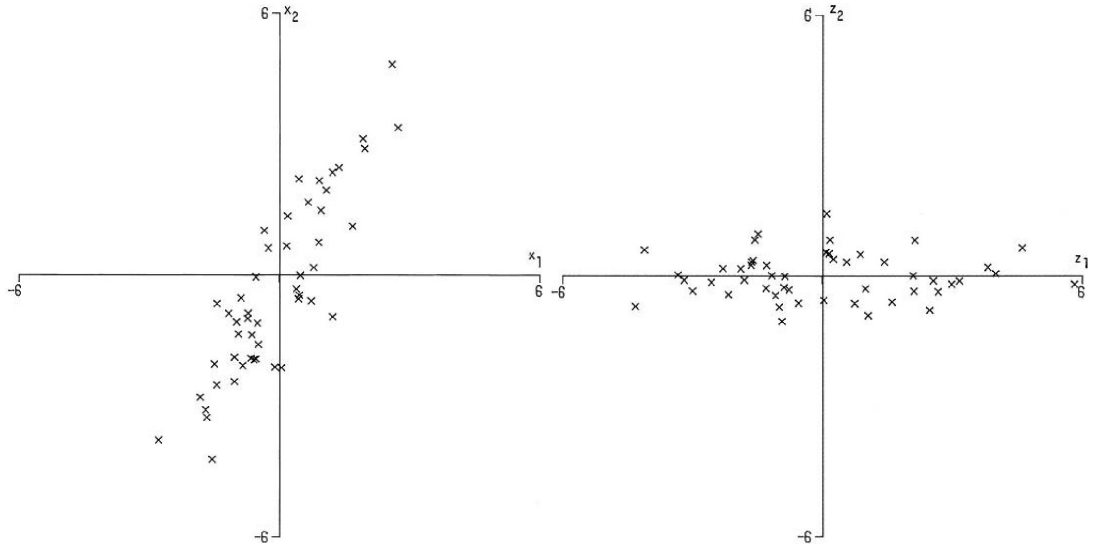

Figure 3.8. Representation of 50 samples of data in raw coordinate space (x_1, x_2) on the left and principal component (PC) space (z_1, z_2) on the right. Notice that PCA transformation is a linear matrix transformation, defined based on the data itself. From Jolliffe 2002. Permission to reproduce this figure has been granted by Springer Science+Business Media.

case n=<p: The number of trials, or observations, are equal to or smaller than the number of variables. The transformation still finds and sorts the maximum variance combinations of raw variables; however, only the first $n-1$ variables of the transformed data in PC space have non-zero values. This property makes this case of PCA a suitable tool for dimension reduction. By using PCA for dimension reduction the data are abstractly represented as a function of their deviation from the mean. It is noteworthy that in this case the data representation is abstracted considerably in $\mathbf{Y}_{n\times p}$ coordinates; however, the $\mathbf{C}_{p\times p}$ matrix also contains considerable information about the data and its variance.

3.3.4.2. Z-Scores

As a normalisation and centring tool the data points can be centred to the mean and normalised by the variance of the data so that the adjusted data have 0 mean and a standard deviation of 1. This adjustment is referred to as z-score calculation (Izenman, 2008) and is described in Equation 3.8:

$$\vec{z}_i = \frac{\vec{x}_i - \vec{\mu}_x}{\vec{\sigma}_x} \tag{3.8}$$

In Equation 3.8, i indicates the i^{th} observation, and $\vec{z}_i$ and $\vec{x}_i$ are the observation vectors in transformed and original coordinates. Also $\vec{\mu}_x$ and $\vec{\sigma}_x$ are the mean and standard deviation across all observations.

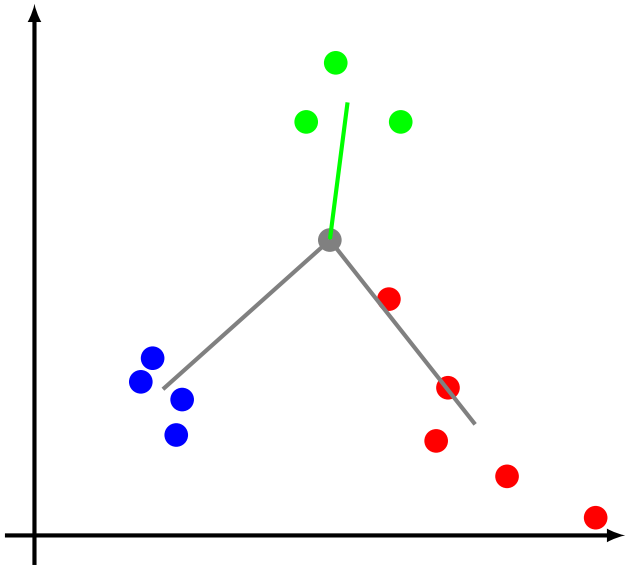

Figure 3.9. Euclidean distance classifiers (EDC) schematic. The gray sample is classified as green because the mean of the group (class) green has the least distance to the new observation.

3.3.5. Pattern Classification of Data Features

Assuming a multi-class observation data set, it is possible to classify single observations based on knowledge from previous observations. This knowledge or data mining from previous data is manifested in the design of different classifiers.

3.3.5.1. Euclidean Distance Classifier (EDC)

Euclidean distance classifier (EDC), or minimum distance classifier (Duda et al., 2000), is a very simple non-parametric classifier. It can be used without an explicit assumption of the distribution of the data or its features. According to EDC, the identified class of an unknown observation is the class whose group average is closest to the observation. The measure for closeness of a group's mean to the new observation is the Euclidean distance between them in data or feature space. Figure 3.9 shows an example of EDC detection.

3.3.5.2. K-Nearest Neighbour Classifier (KNN)

K-nearest neighbour (KNN) is another non-parametric classification method in the classification literature (Fukunaga, 1990; Duda et al., 2000; Izenman, 2008). Instead of comparing the new observation with the group means (as in EDC), the k closest (least distance) previous observations in the neighbourhood of the new observation is found. The

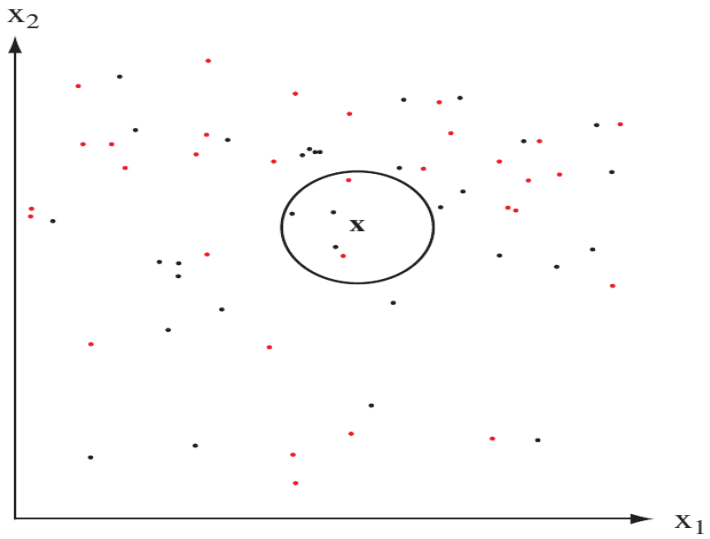

Figure 3.10. The K-nearest neighbour (KNN) search starts at the new observation point and continues until the k closest training samples are found (in this figure $k = 5$). The label with the majority of the k neighbour samples is the detection label for the new observation. In this example the detection is black. From Duda et al. 2000. Permission to reproduce this figure has been granted by John Wiley & Sons.

detected class of the new observation is the one with the highest count in the k nearest neighbour samples. Figure 3.10 shows an example of KNN detection.

3.3.5.3. Validation of Classification

In order to quantify the performance of classifiers, the observations set can be divided into two groups: one group is used to build or *train* the classifier and the other to validate or *test* the classifier. This is essential to ensure the generalization capability of the classification method (Haykin, 1999; Duda et al., 2000). However this reduces the number of observations that can be used for training and testing, because they get divided to 2 groups. In order to maximally exploit the observations in a dataset, k-fold cross-validation methods can be used. In cross-validation methods, the dataset is devided into k subsets; one group is used for testing and the remaining (k-1) groups for training. By cycling through the k subsets, all observations can take the turn to be in the testing set without simultaneously being used in the training set. Averaging the success rate across the k-folds gives the overal classification rate of the designed classifier. In this study, k-fold cross validation with k=1, also known as *leave-one-out* method, is used (Haykin, 1999; Duda et al., 2000).

3.3.6. Data Postprocessing

Custom scripts were coded in MATLAB® (Mathworks Inc., Natick, MA, USA) to produce plots and diagrams to aid in (re)analysing and interpreting results.

3.4. Chapter Summary

In this chapter, first the considerations and requirements for the experiments were stated in Section 3.1, and then the chosen experimental setup was elaborated on in Section 3.2. Data analysis methods were explained in Section 3.3. In next chapter, the results and outputs are presented.

Chapter 4

Results

In this chapter, the raw performance of subjects and the overall statistics on the experimental data are reviewed in Section 4.1, followed by the time domain ERPs in Section 4.2, and the time-frequency signatures of arm isometric exertions in Section 4.3. In each section, the ear-lobe referenced (ELR) and common-average referenced (CAR) potentials and (de-)synchronisations are assessed separately and the significant temporal and spatial features are highlighted. Finally the directional information of isometric exertions in Section 4.4 are explained by (1) significant inter-class variance of time and time-frequency features and (2) classification accuracies and the relative performance of different recording sites and classification methods during the planning and execution stages.

4.1. Performance of the Subjects

4.1.1. Overview and Statistics

This section provides the essential statistics on the experiments and subjects. All the participating subjects have successfully completed the experiment (see Section 3.2). Following on from the pilot study experiment (Subject S0), 8 further subjects were recruited (S1 to S8, in the order of participation) as mentioned in Section 3.2.2. Table 4.1 provides a list of information about each of the subjects.

Table 4.2 shows the number of total recorded trials, and the number of acceptable EEG data after exclusion of bad and contaminated data (see Section 3.3.1 for methods and criteria). The number of acceptable trials or epochs depends on the stage of experiment, electrode position, subjects and other experimental conditions. Generally, however, a relatively large number of trials had to be rejected because of different artefacts (see Section 3.3.1.1). This is necessary to assure the reliability of the EEG signals and not to

Table 4.1. Subject information .

No.	Gender	Handedness	Age	Considerations
S0	F	R	33	Pilot study: 30 electrodes recorded only
S1	M	R	38	none
S2	M	R	26	none
S3	M	R	24	none
S4	F	R	27	none
S5	F	R	24	none
S6	M	R	26	modified MVC value is used.
S7	F	R	25	none
S8	M	R	33	none
Average	5M,3F	R	27.87($\pm$4.99)	

$\pm$in parentheses shows standard deviation

report artefacts as neurophysiological signatures.

A complete list of the acceptable included EEG trials and epochs is available in Appendix E.

4.1.2. Force, EMG and Timings

In this section, the timing, force and EMG data are shown, along with general observations. While the experiment had a monotonous nature (due to long duration of the experiment), none of the subjects reported any feeling of muscular fatigue. Table 4.3 demonstrates the maximum voluntary contraction (MVC) levels which each of the subjects could generate and were used to normalise the requested level of effort.

Figure 4.1 shows the magnitude of force development during the force generation stage GO and the 2D path of the force.

As shown in Figure 4.1, there is a usual trend of overshoot (transient over-exertion of force beyond the requested level before settling to a closer value to target level) and in some cases sustained over-exertion (maintaining a constantly larger force than the requested level with no final settling to target value). In the execution phase, after 2.0s, all the subjects had reached the steady state force values and consequently, the 2.0-3.0s time window shows maintenance of the steady state force.

EMG is used as a potential indicator of muscle fatigue. Median frequency of power spectral density (PSD) of EMG is a relatively established indicator of muscle fatigue (Cifrek et al., 2009). In order to monitor the status of some (but not all) of the muscles active in the task, the median frequency of PSD of the four forearm muscles (ECR, ECU, FCR and FCU) are calculated for 4 different exertion direction trials (right, left,

Table 4.2. Statistics from all of the experimental trials and total number of acceptable EEG epochs for each subject .

Subject	Total	Electrode Number	Electrode	RC	AC	DC	GO
S1	228	1	Cz	58	140	129	131
		4	C3	57	136	125	127
		5	C4	55	126	121	124
		28	Fz	5	13	12	35
		37	Pz	56	146	137	131
S2	223	1	Cz	115	187	159	148
		4	C3	113	186	159	147
		5	C4	111	184	157	148
		28	Fz	103	169	152	137
		37	Pz	114	189	159	147
S3	220	1	Cz	82	138	98	115
		4	C3	82	137	98	114
		5	C4	38	70	49	46
		28	Fz	78	126	95	101
		37	Pz	83	136	102	112
S4	221	1	Cz	32	150	164	146
		4	C3	32	149	162	144
		5	C4	11	70	75	71
		28	Fz	28	141	158	132
		37	Pz	9	56	67	54
S5	222	1	Cz	9	110	110	83
		4	C3	9	104	107	76
		5	C4	8	74	82	66
		28	Fz	2	66	71	34
		37	Pz	11	117	124	104
S6	224	1	Cz	39	114	116	138
		4	C3	31	95	96	115
		5	C4	20	54	55	63
		28	Fz	24	98	102	123
		37	Pz	47	120	119	142
S7	220	1	Cz	68	167	166	148
		4	C3	65	156	161	142
		5	C4	68	165	165	147
		28	Fz	52	148	151	130
		37	Pz	66	143	159	129
S8	260	1	Cz	102	128	126	115
		4	C3	94	121	121	110
		5	C4	101	128	126	114
		28	Fz	86	108	118	110
		37	Pz	67	91	98	83

Total shows the number of all recorded trials and RC,AC, DC and GO show the number of acceptable trials for each recording stage of experiment for each recording electrode. For example, Subject 1 had 126 (of 228 total) acceptable epochs at C4 electrode during the AC stage of experiment.

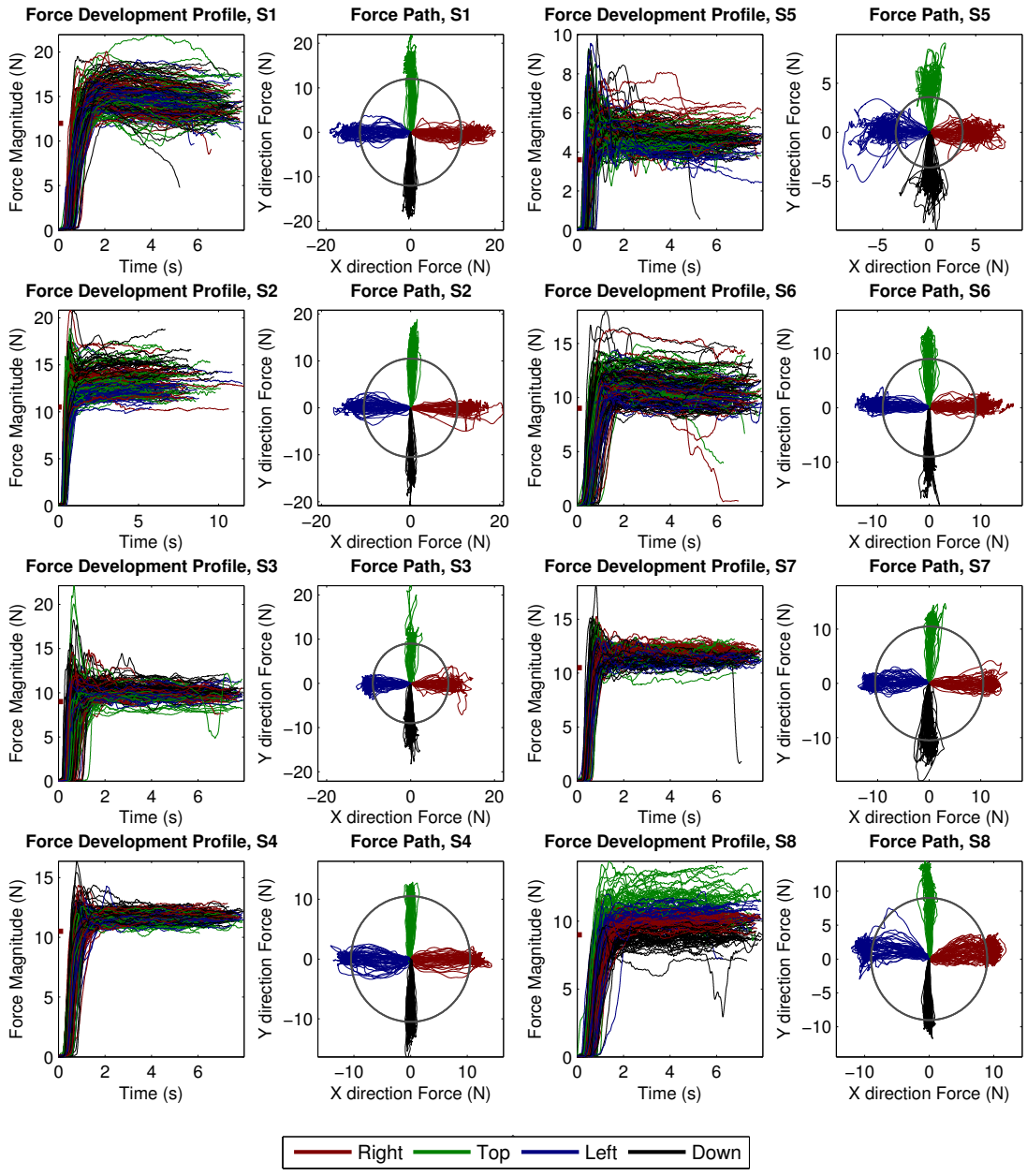

Figure 4.1. Force development profiles for all 8 subjects. Magnitude of the exerted force in GO (execution) stage against time, as well as the 2 dimensional path of generated force are plotted. The 30% MVC level of requested force is shown by a red indicator on Y (Force) axis in the time plots and as a grey circle in 2D path plots. Data is plotted after 15Hz low pass filtering for smoother representation. The rest time bias, usually due to rest-time weight of arm is removed. The number of acceptable trials plotted for each direction are listed in Table E.9, Appendix E.

Table 4.3. Maximum voluntary contraction (MVC) values for all 8 subjects .

Subjects	S1	S2	S3	S4	S5	S6[a]	S7	S8	average(±SD)
MVC (N)	40	35	30	35	12	30[a]	35	30	30.87(±8.39)

[a] Subject 6 was not comfortable with maximum voluntary force generation value (50N) and the corresponding 30% threshold, due to history of mechanical impact pain. The MVC value is considered as the maximum value at which the subject could do the experiment without any discomfort.

forward, backward). EMG data between 2.0-3.0s of the GO stage (where a constant isometric force is being exerted) is used for analysis. Figure 4.2 shows that while the median frequency is variable in different trials, the overall trend is not decreasing. This suggests that the occurrence of fatigue is unlikely. This observation is in agreement with the subjects' reflection on the experiment where it was noted that they all did not experience muscle fatigue during or after the experiment.

4.2. Event-Related Potentials (ERP)

In this section the ERPs as time-domain features of EEG are presented. First, the ear-lobe referenced (ELR) EEG are shown in Section 4.2.1, and then the common-average referenced (CAR) EEG are presented in Section 4.2.2. The major waveform negativity and positivity peaks in the key electrodes are listed in Sections 4.2.1.1 and 4.2.2.1. Finally, the spatial distribution of ERPs in surface EEG in different stages of execution are highlighted in Sections 4.2.1.2 and 4.2.2.2.

4.2.1. Ear-Lobe Referenced Event-Related Potentials

4.2.1.1. Temporal Features of Ear-Lobe Referenced Event-Related Potentials

To inspect the temporal features of ERPs, the per-subject trial-averaged ear-lobe referenced (ELR) event-related potentials (ERP) and across-subject trial-averaged ERPs were studied. Each of the 5 selected electrodes were studied separately. Figures 4.3, 4.4, 4.5, 4.6 and 4.7, show the ear-lobe referenced (ELR) event-related potentials (ERP) for C_z, C_3, C_4, F_z, and P_z electrodes, respectively.

Table 4.4 contains the time domain parameters of the ELR waveform negative and positive peaks for the electrodes C_z, C_3, C_4, F_z, and P_z. Time domain results averaged over trials from individual subjects are visually inspected to verify the occurrence of the reported negative or positive peaks in the majority of subjects. Similar to many neurophysiological recordings, some subjects had some suppressed positive or negative

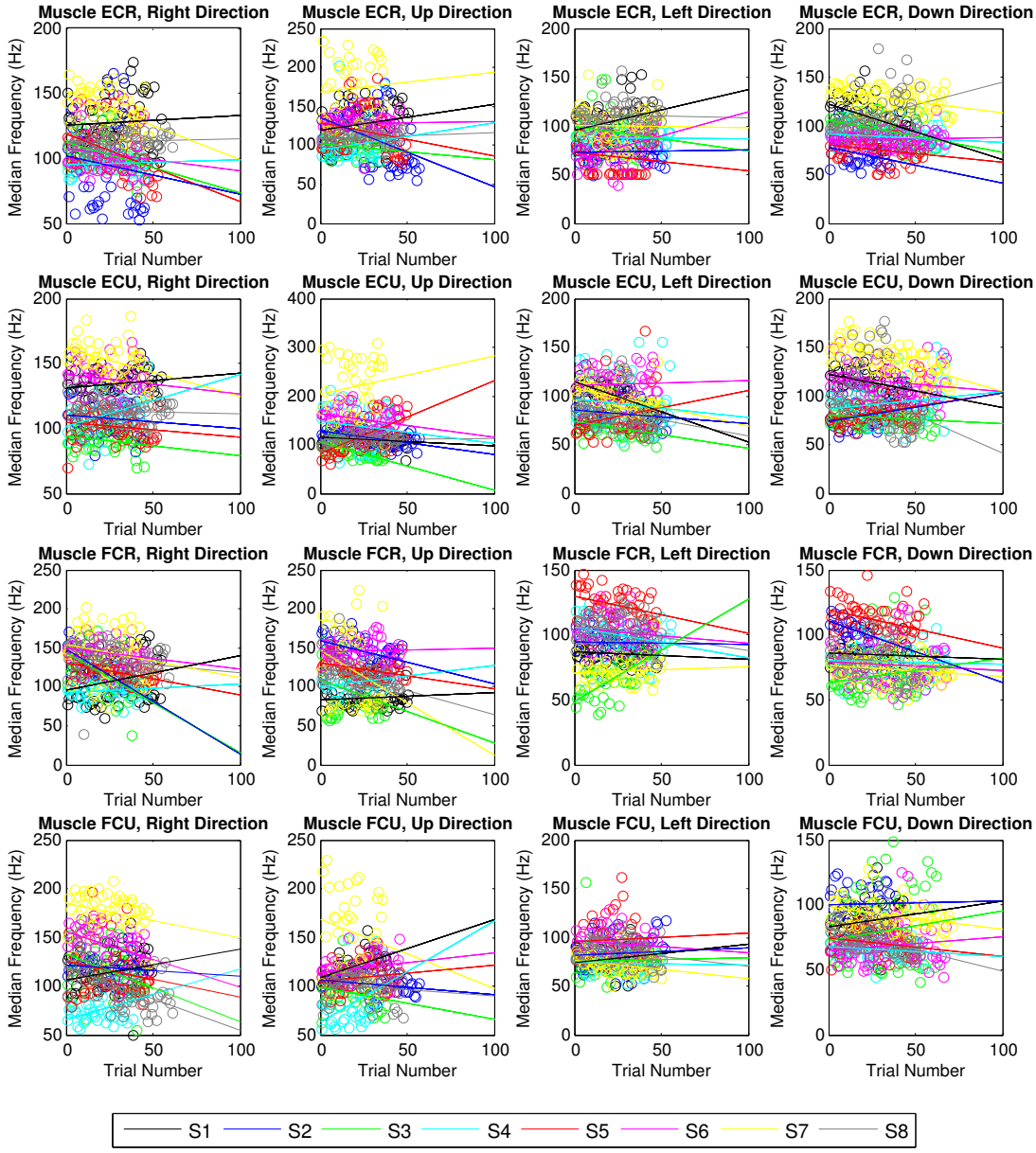

Figure 4.2. Trend of changes for EMG median frequency during execution of trials. Each row of plots corresponds to a muscle and each column of plots corresponds to an exertion direction. In each plot the x-axis is the number of trials and the y-axis is the median frequency (Hz) during $1s$ (2.0-3.0s of GO stage) isometric exertion of force in that trial. Least square lines help to distinguish the overall trend of change for median frequency during the experiments. Each colour corresponds to a different subject. ECR: extensor carpi radialis, ECU: extensor carpi ulnaris, FCR: flexor carpi radialis, FCU: flexor carpi ulnaris.

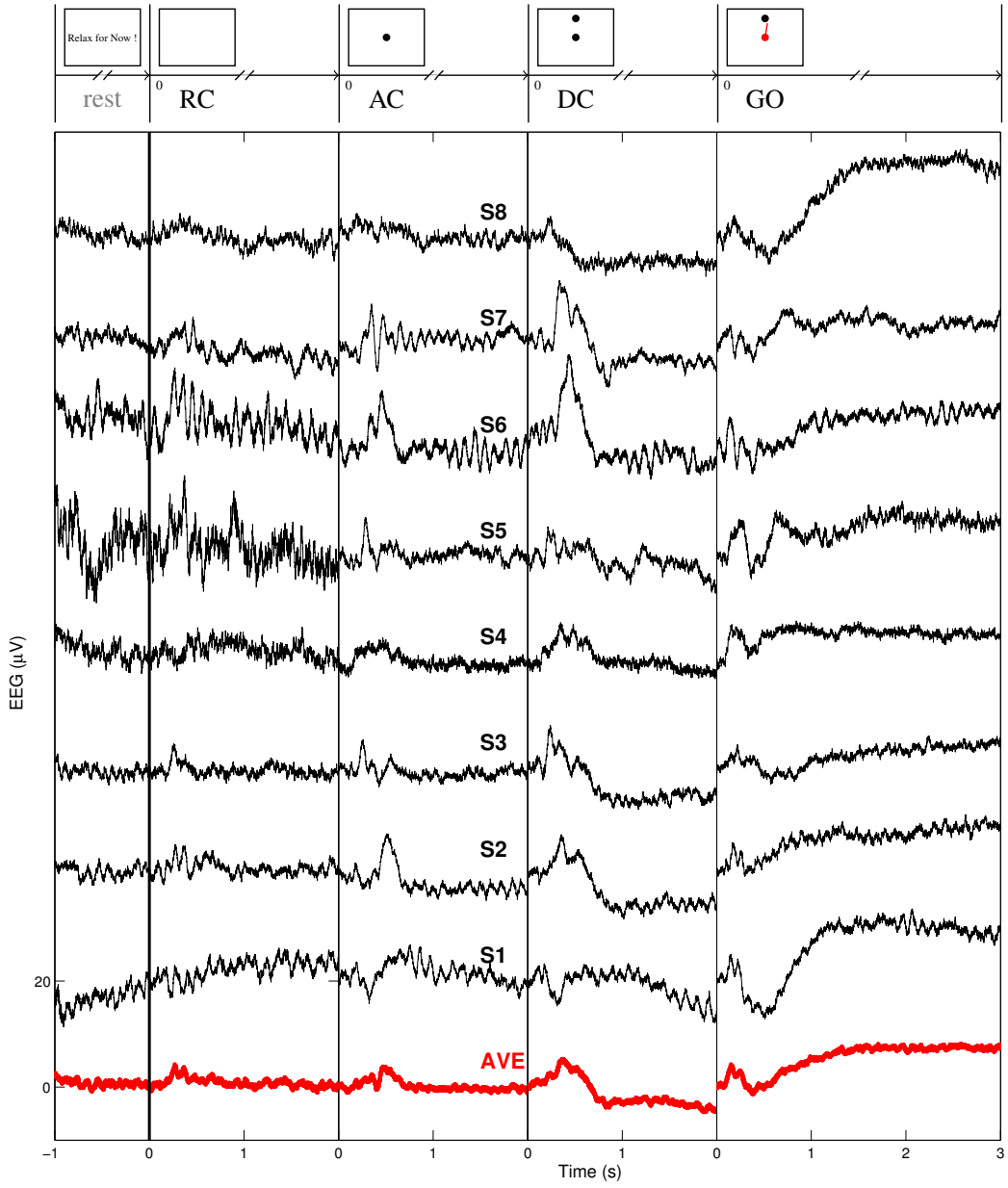

Figure 4.3. Event-related potentials in C_z during different stages of movement, as described in Figure 3.5. Trial-averaged time domain ELR EEG are plotted for all 8 subjects. The thick red plot shows the ERP from averaging all trials from all subjects. The plots for each subject are shifted to distinguish between the plots. The graduation and scale for the grand average applies for all plots.

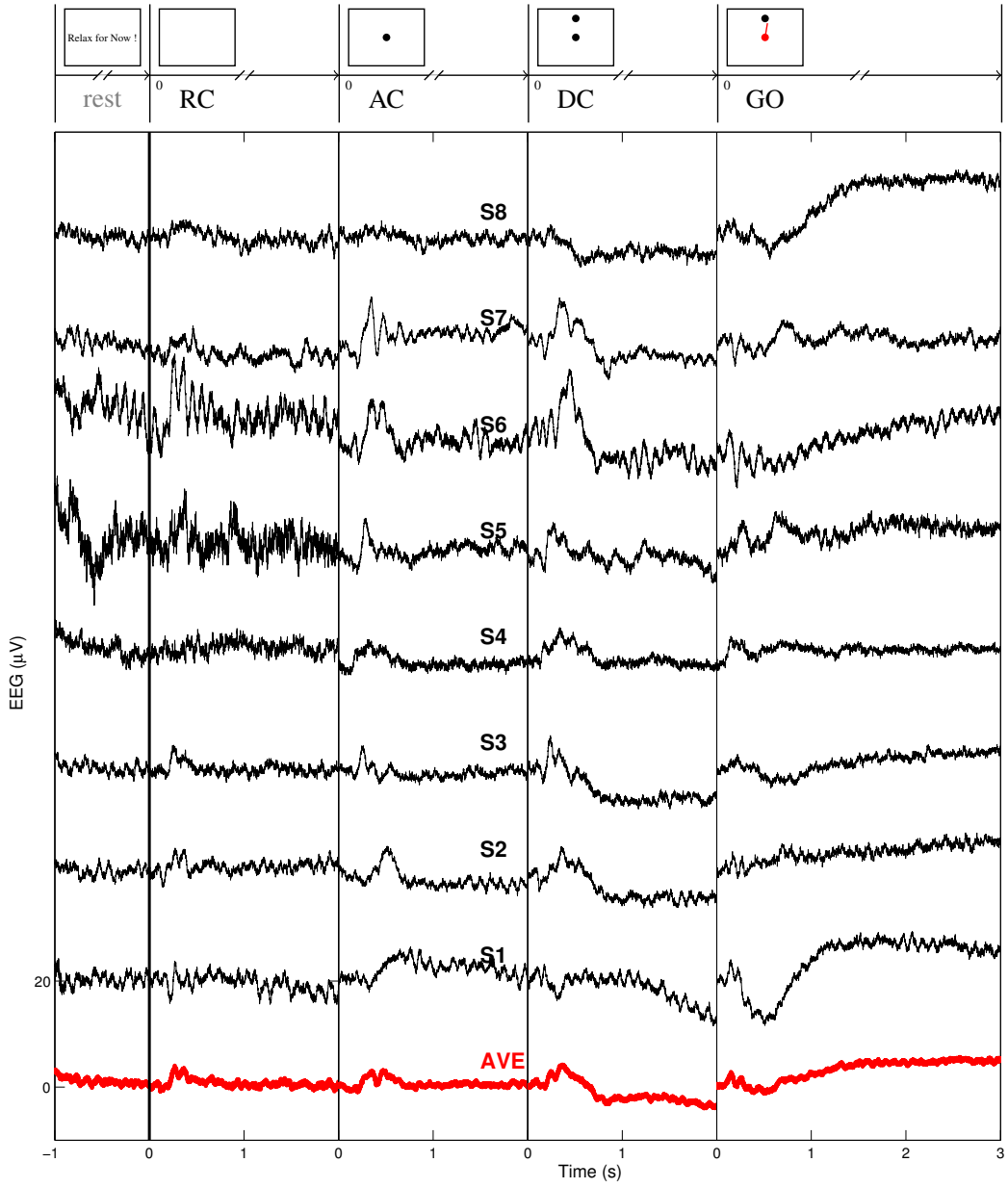

Figure 4.4. Event-related potentials in C_3 during different stages of movement, as described in Figure 3.5. Trial-averaged time domain ELR EEG are plotted for all 8 subjects. The thick red plot shows the ERP from averaging all trials from all subjects. The plots for each subject are shifted to distinguish between the plots. The graduation and scale for the grand average applies for all plots.

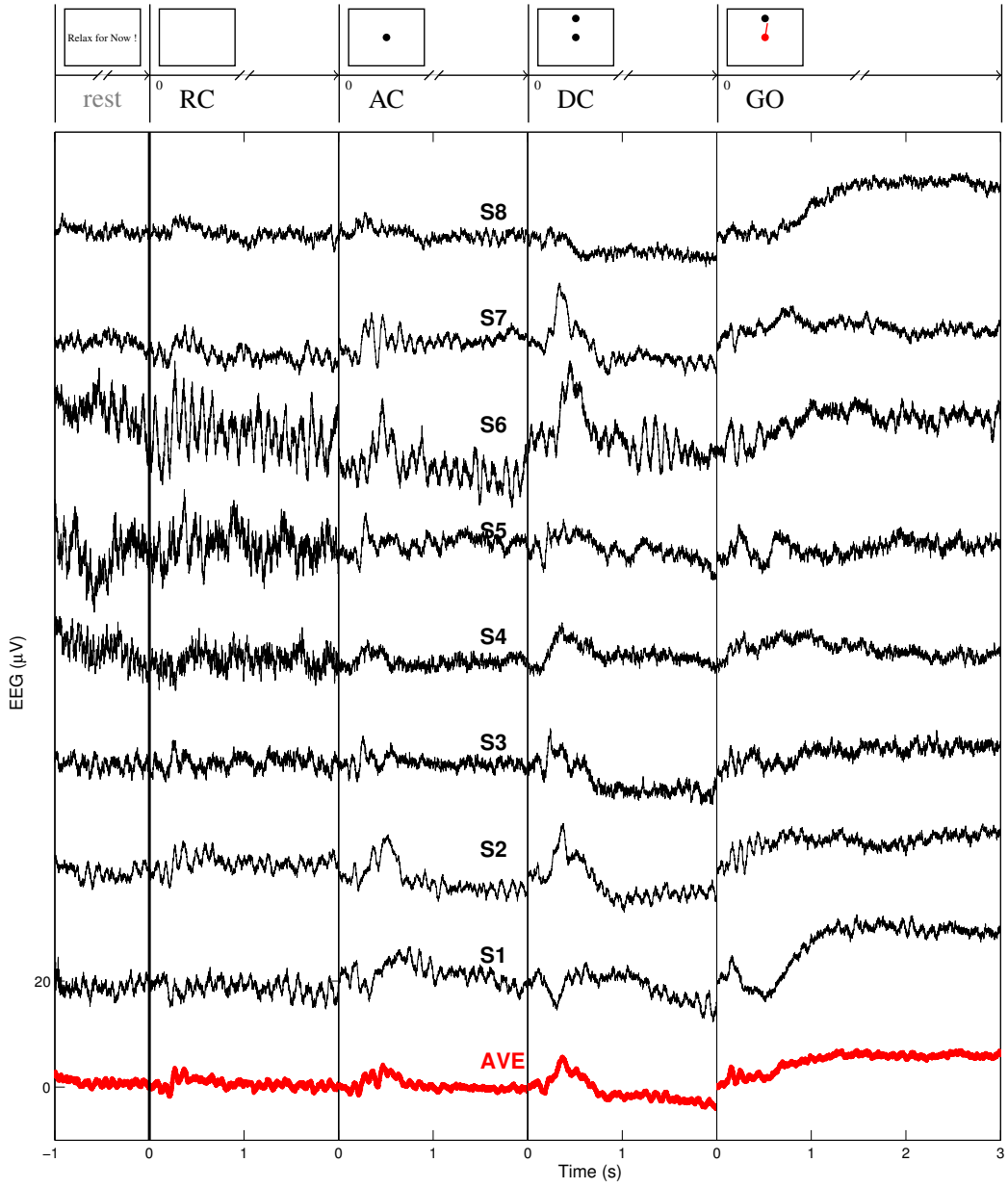

Figure 4.5. Event-related potentials in C_4 during different stages of movement, as described in Figure 3.5. Trial-averaged time domain ELR EEG are plotted for all 8 subjects. The thick red plot shows the ERP from averaging all trials from all subjects. The plots for each subject are shifted to distinguish between the plots. The graduation and scale for the grand average applies for all plots.

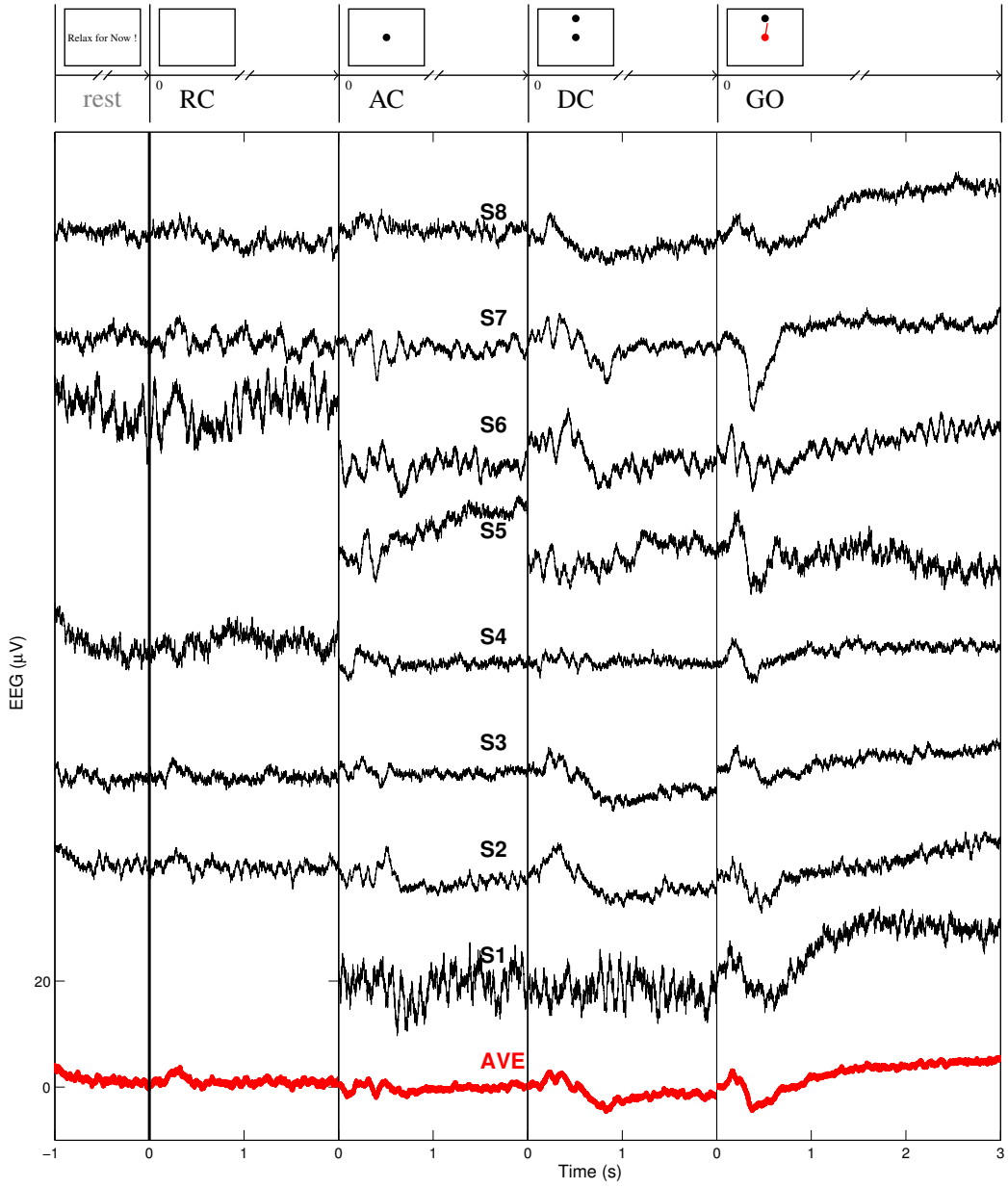

Figure 4.6. Event-related potentials in F_z during different stages of movement, as described in Figure 3.5. Trial-averaged time domain ELR EEG are plotted for all 8 subjects. The thick red plot shows the ERP from averaging all trials from all subjects. The plots for each subject are shifted to distinguish between the plots. The graduation and scale for the grand average applies for all plots. Average segments with too few acceptable trials are not plotted.

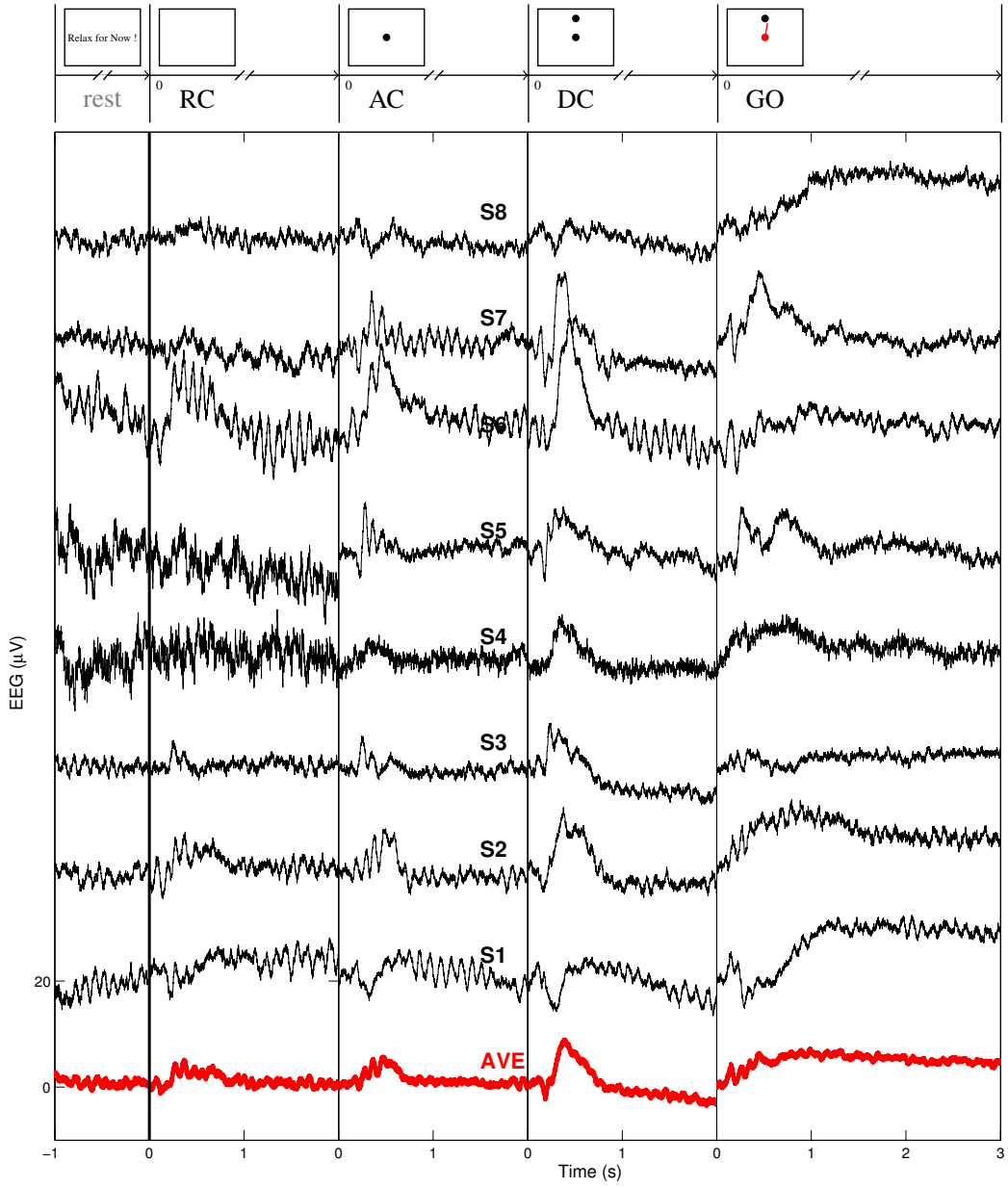

Figure 4.7. Event-related potentials in P_z during different stages of movement, as described in Figure 3.5. Trial-averaged time domain ELR EEG are plotted for all 8 subjects. The thick red plot shows the ERP from averaging all trials from all subjects. The plots for each subject are shifted to distinguish between the plots. The graduation and scale for the grand average applies for all plots.

Table 4.4. Characteristics of ear-lobe referenced event-related potentials waveform positive and negative peaks, observed in the majority (5/8) of subjects in electrodes C_z, C_3, C_4, F_z, and P_z .

Electrode	Time Stage	Peak 1	Peak 2	Peak 3	Peak 4	Sustained Value
Cz	RC	P(268ms,4.31)				0.804^n
	AC	P(353ms,2.38)	N(398ms,-0.48)	P(472ms,3.87)		-0.976^n
	DC	P(378ms,5.297)				-4.5
	GO	P(151ms,4.31)	N(384ms,-1.323)			7.934
C3	RC	N(117ms,-0.827)	P(269ms,4.039)			1.142^n
	AC	N(207ms,-0.8821)	P(348ms,3.005)	N(401ms,0381)	P(471ms,3.194)	0.095^n
	DC	N(185ms,-0.311)	P(366ms,4.209)	N(850ms,-3.206)		-3.799
	GO	P(151ms,2.847)	N(504ms,-1.22)			5.216
C4	RC	N(216ms,-1.767)	P(269ms,3.633)			0.722^n
	AC	P(362ms,3.08)	N(411ms,-0.015)	P(469ms,4.235)		-0.791^n
	DC	P(108ms,1.190)	N(185ms,-1.198)	P(368ms,5.665)		-4.004
	GO	P(152ms,3.87)	N(198ms,0.578)	P(246ms,3.267)		6.571
Fz	RC	P(325ms,3.767)				1.676^n
	AC	N(89ms,-1.903)	P(313ms,1.583)	N(398ms,-2.049)	P(495ms,1.181)	-0.025
	DC	P(242ms,2.887)	P(362ms,2.679)	P(552ms,0.849)	N(834ms,-4.595)	-1.904
	GO	P(165ms,3.128)	N(373ms,-4.444)			5.409
Pz	RC	N(117ms,-1.207)	P(365ms,5.142)			1.099
	AC	P(472ms,5.735)				-0.268^n
	DC	P(112ms,1.89)	N(185ms,-2.283)	P(392ms,8.931)		-3.127
	GO	P(151ms,4.284)				4.945

[a] P and N stand for positive and negative waveform peaks. Numbers in parentheses show the time delay in milliseconds and the value of the peak in the average EEG (μV). e.g. P(184ms,1.288) shows a positive peak of 1.288 μV, 184ms after the relevant visual cue.
[b] The values are referenced to average signal values at the point of appearance of cues. i.e. EEG values at these cues are set to zero. Consequently the sustained values are relative to these values.
[n] Shows non-significant value, based on 3-state positive/neutral/negative.

peaks. However the majority of subjects (5 of 8, equivalent to 4.88% significance level) exhibited the features observed in the average. Positive and negative waveform peaks are represented by *P* and *N* (see Table 4.4).

4.2.1.2. Spatial Features of Ear-Lobe Referenced Event-Related Potentials

Figures 4.8, 4.9, 4.10 and 4.11 illustrate spatial distribution of the average time domain changes in ELR surface EEG signals induced by the different visual cues (RC, AC, DC and GO).

Figure 4.12b demonstrates the trend of ELR EEG changes in the time domain when moving from the frontal regions to parietal regions of the brain (F_z to P_z) whereas Figure 4.12d shows the trend of ELR EEG changes when moving from the ipsilateral to

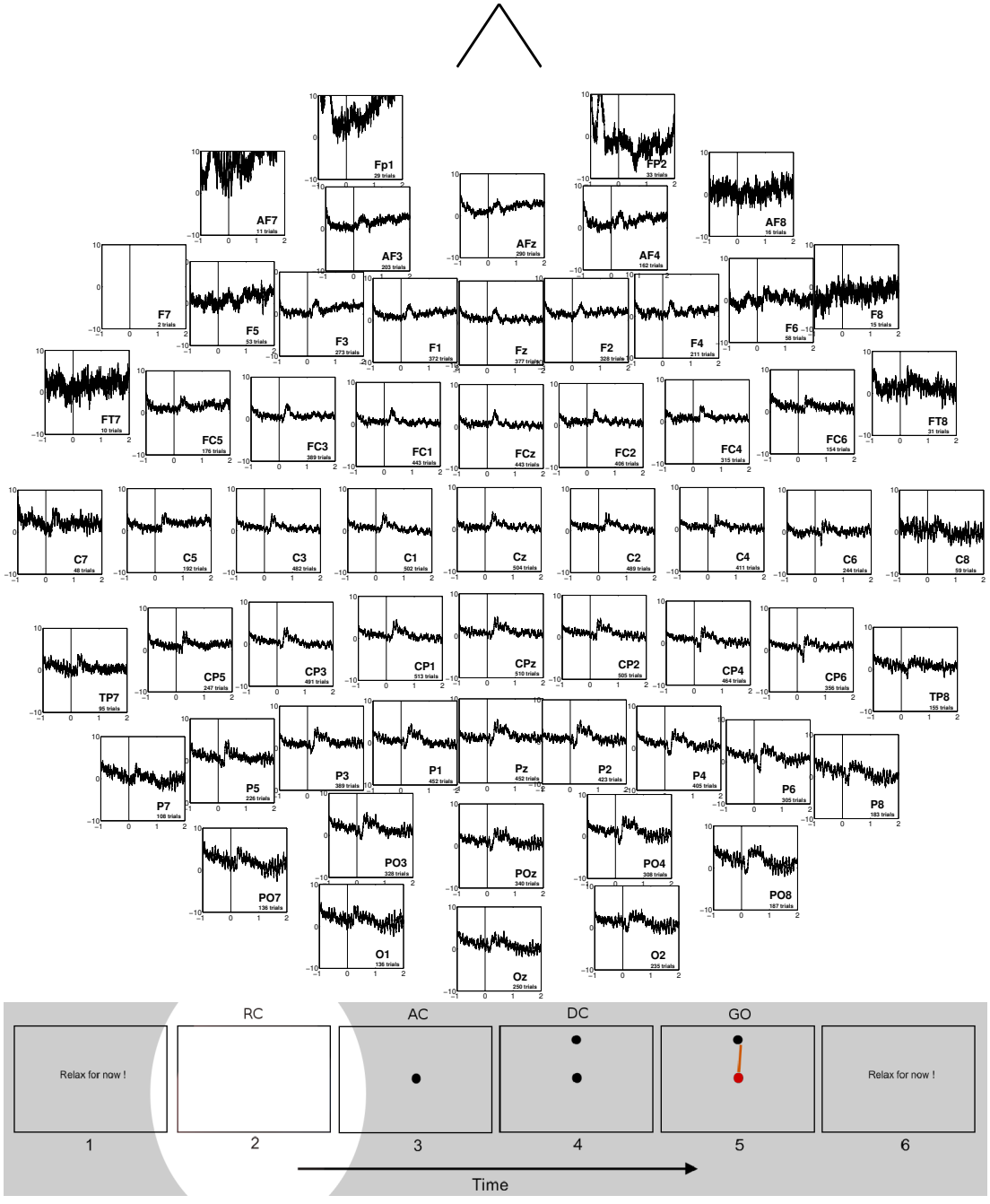

Figure 4.8. Spatial distribution of the time domain variations in surface EEG electrodes. Average ELR EEG (μV) across all trials from 8 subjects during the RC stage.

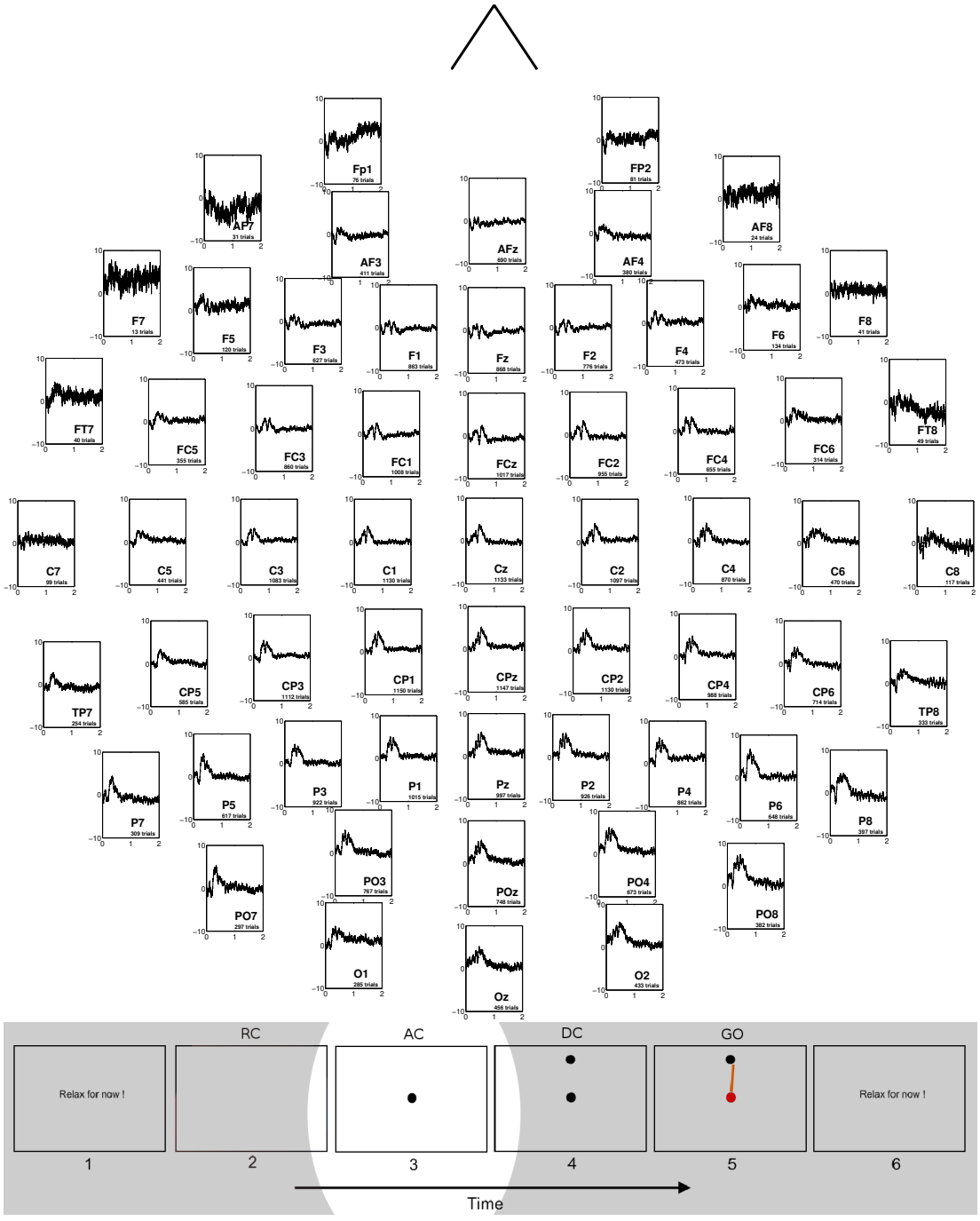

Figure 4.9. Spatial distribution of the time domain variations in surface EEG electrodes. Average ELR EEG (μV) across all trials from 8 subjects during the AC stage.

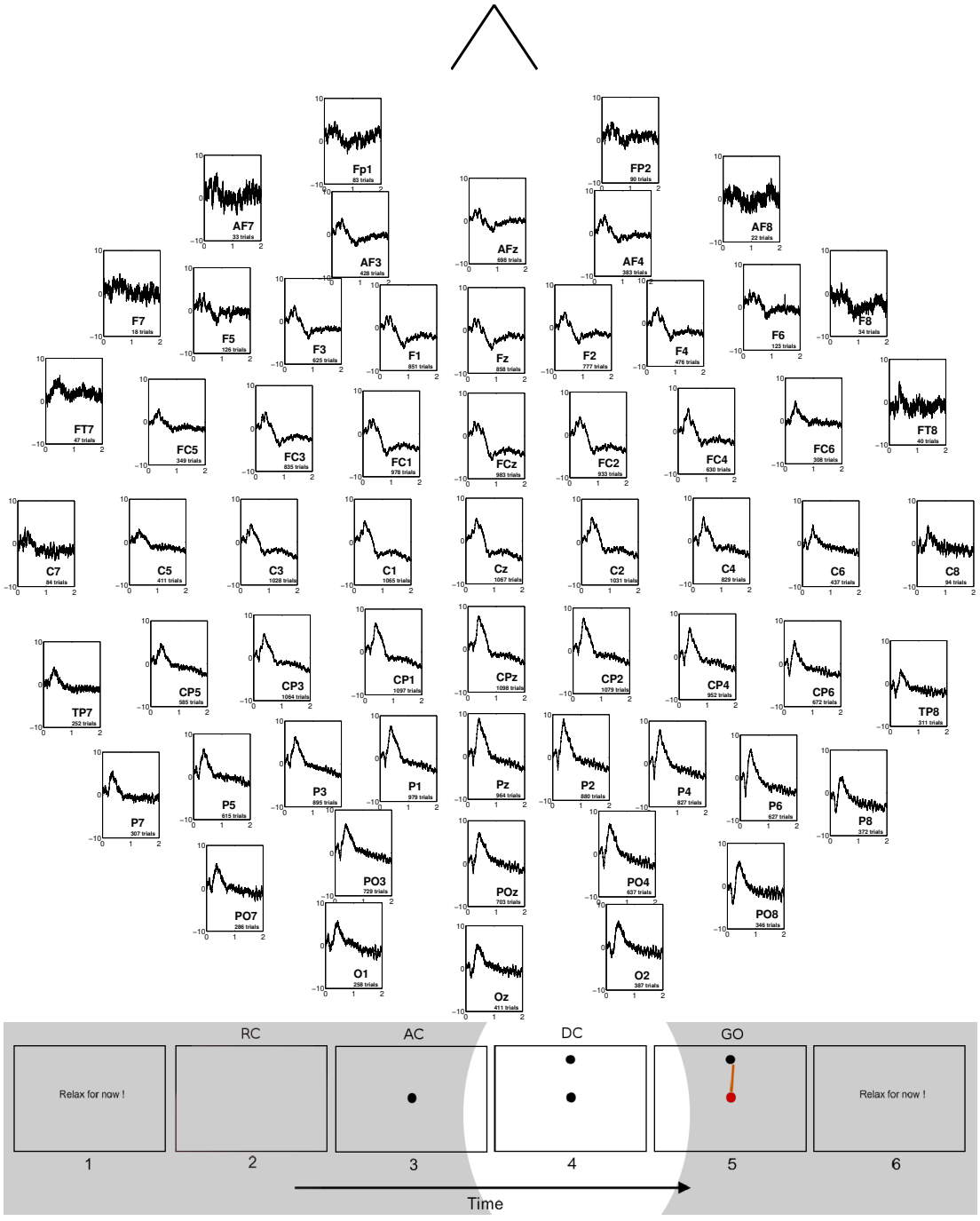

Figure 4.10. Spatial distribution of the time domain variations in surface EEG electrodes. Average ELR EEG (μV) across all trials from 8 subjects during the DC stage.

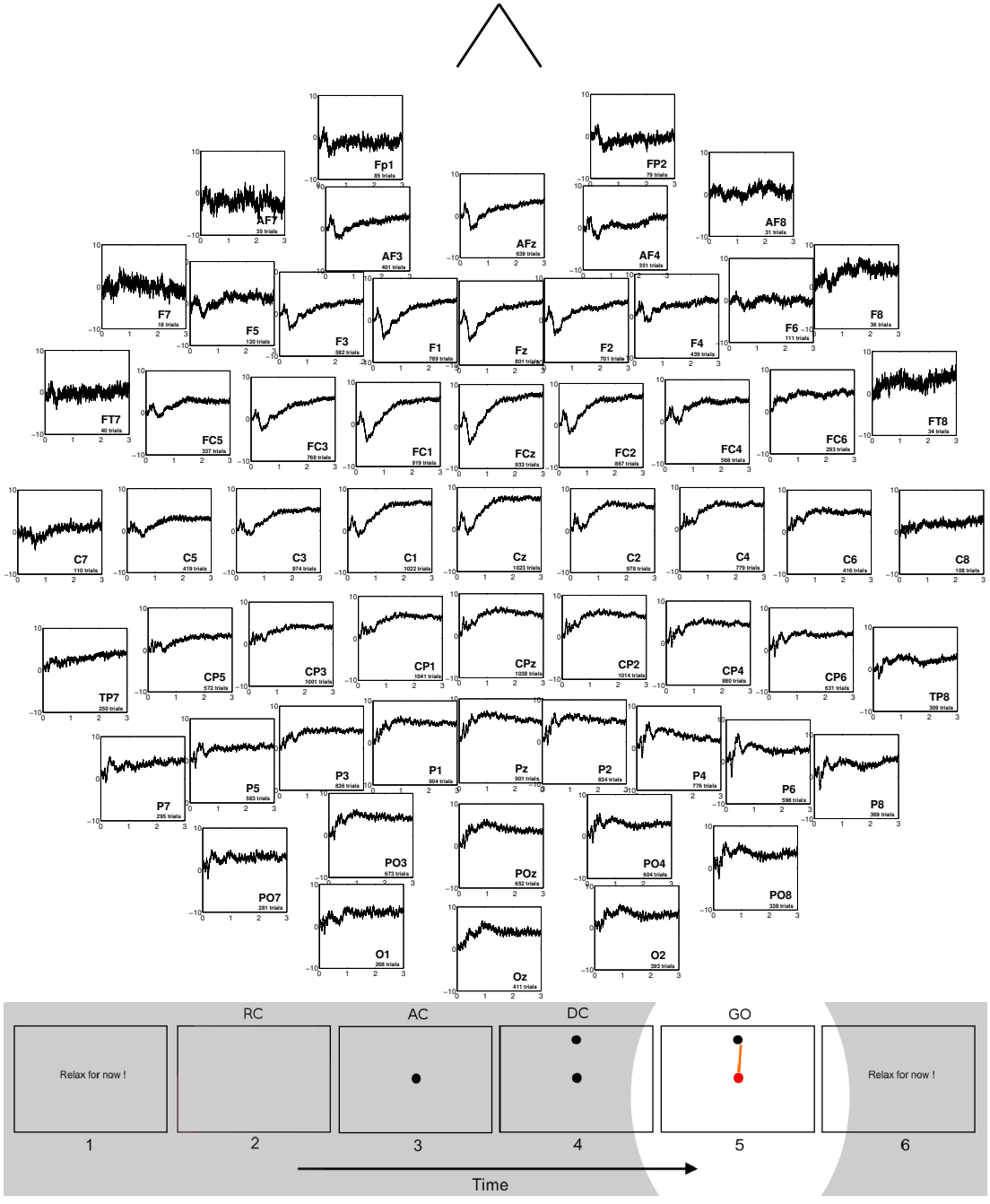

Figure 4.11. Spatial distribution of the time domain variations in surface EEG electrodes. Average ELR EEG (μV) across all trials from 8 subjects during the GO stage.

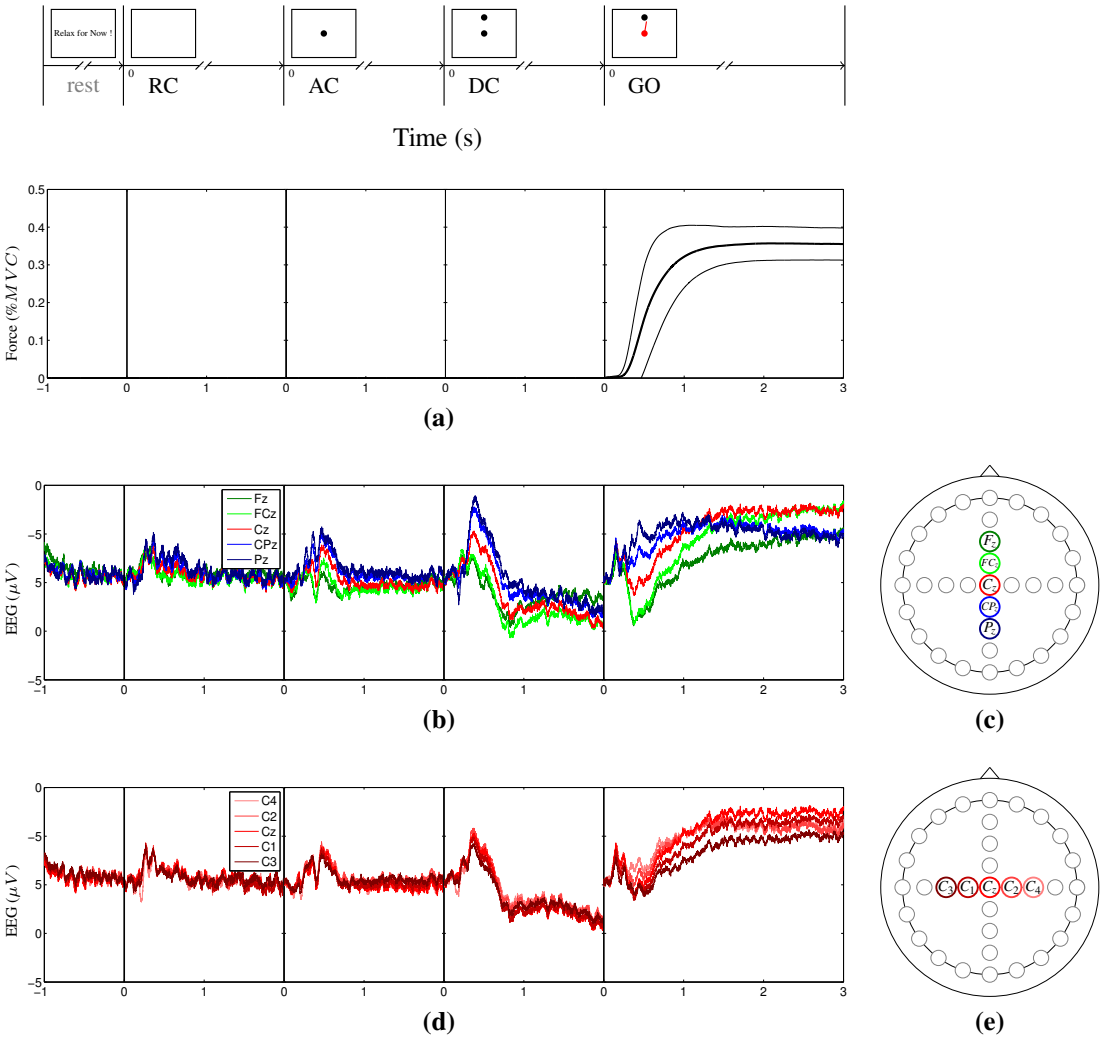

Figure 4.12. Spatial difference of the time domain average of the ELR EEG. Horizontal axes are time in seconds. Zeros from left to right indicate the presentation of visual cues: RC, AC, DC and GO (see Figure 3.5). a) The force development profile (mean $\pm$ 1 SD). b) Trend of EEG changes when moving from frontal to parietal regions from F_z, FC_z, C_z, and CP_z to P_z as depicted in (c). d) Trend of EEG changes when moving from ipsilateral to contralateral motor regions from C_4, C_2, C_z, and C_1 to C_3 as depicted in (e).

contralateral motor regions (C_4 to C_3).

While Table 4.4 provides an accurate description of ear-lobe referenced (ELR) event-related potentials (ERP), the spatial distribution of peaks can be summarised as follows:

RC (Rest) Stage: The activity pattern in parietal regions changes from N-P (negative peak followed by positive peak) to P in frontal regions (N peak is suppressed). However, in central regions there is a N-P pattern where the negative peak (N) is present only in the lateral sides.

AC (Preparation) stage: When moving from parietal regions to frontal areas, the one single positive peak, changes to a more complex pattern of P-N-P at C_z and N-P-N-P at F_z. The P-N-P pattern is common in central regions, except toward the contralateral side with N-P-N-P at C_3.

DC (Planning) stage: The small P-N burst component of P-N-P pattern at P_z is suppressed when moving to C_z location and changes to a complex P-P-P-N overall pattern when moving toward frontal sites (at F_z). The large third P peak at P_z is gradually suppressed towards frontal regions and a sustained N burst appears instead afterwards. The changes in central medial/lateral or ipsilateral/contralateral regions are very small. A sustained negative potential is observed in all electrodes.

GO (Execution) stage: While moving from parietal regions to frontal sites, the first P peak stays unchanged. However, a large secondary Negativity peak is developed. In medial-lateral comparison, the first P peak is again unchanged. The other changes are rather complex. While C_4 shows a transient N-P peak after the first P, there is only a negativity at C_z and another even later negativity at C_3. A sustained positive potential is observed in all electrodes.

4.2.2. Common-Average Referenced Event-Related Potentials

4.2.2.1. Temporal Features of Common-Average Referenced Event-Related Potentials

To inspect the temporal features of ERPs, the per-subject trial-averaged common-average referenced (CAR) event-related potentials (ERP) and across-subject trial-averaged ERPs are studied for the 5 selected electrodes. Figures 4.13, 4.14, 4.15, 4.16 and 4.17 show the common-average referenced (CAR) event-related potentials (ERP) for the C_z, C_3, C_4, F_z, and P_z electrodes, respectively.

Table 4.5 contains the time domain parameters of the CAR waveform negative and positive peaks for the electrodes C_z, C_3, C_4, F_z, and P_z. Time domain results, averaged over trials from individual subjects, were visually inspected to verify the occurrence of the reported negativities or positivities in the majority of subjects. Some subjects had some suppressed positive or negative peaks. However the majority of subjects (5 of 8, equivalent to 4.88% significance level) showed the features observed in the average.

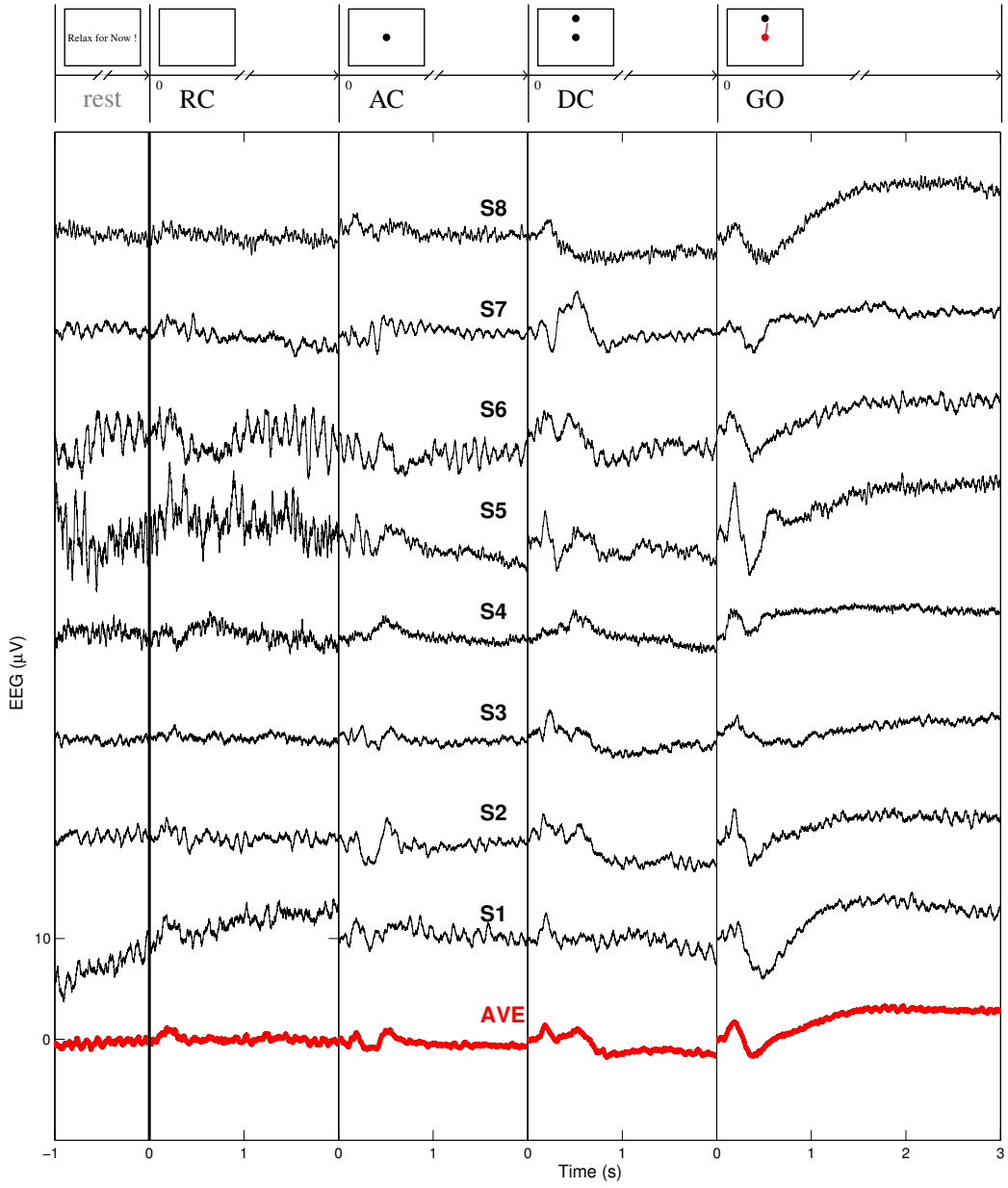

Figure 4.13. Event-related potentials in C_z during different stages of movement, as described in Figure 3.5. Trial-averaged time domain CAR EEG are plotted for all 8 subjects. The thick red plot shows the ERP from averaging all the trials from every subject. The plots for each subject are shifted to distinguish between the plots. The graduation and scale for the grand average applies for all plots.

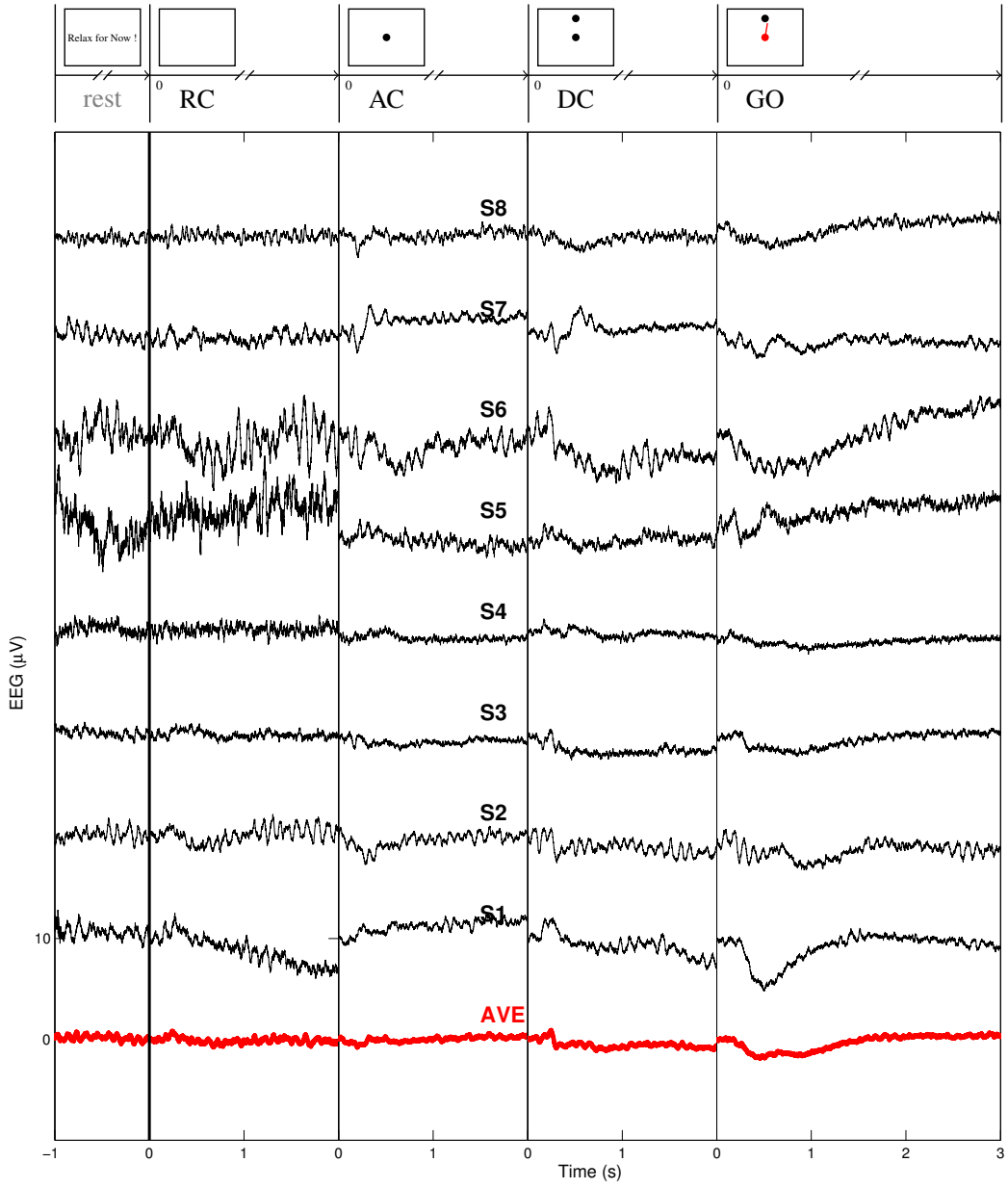

Figure 4.14. Event-related potentials in C_3 during different stages of movement, as described in Figure 3.5. Trial-averaged time domain CAR EEG are plotted for all 8 subjects. The thick red plot shows the ERP from averaging all the trials from every subject. The plots for each subject are shifted to distinguish between the plots. The graduation and scale for the grand average applies for all plots.

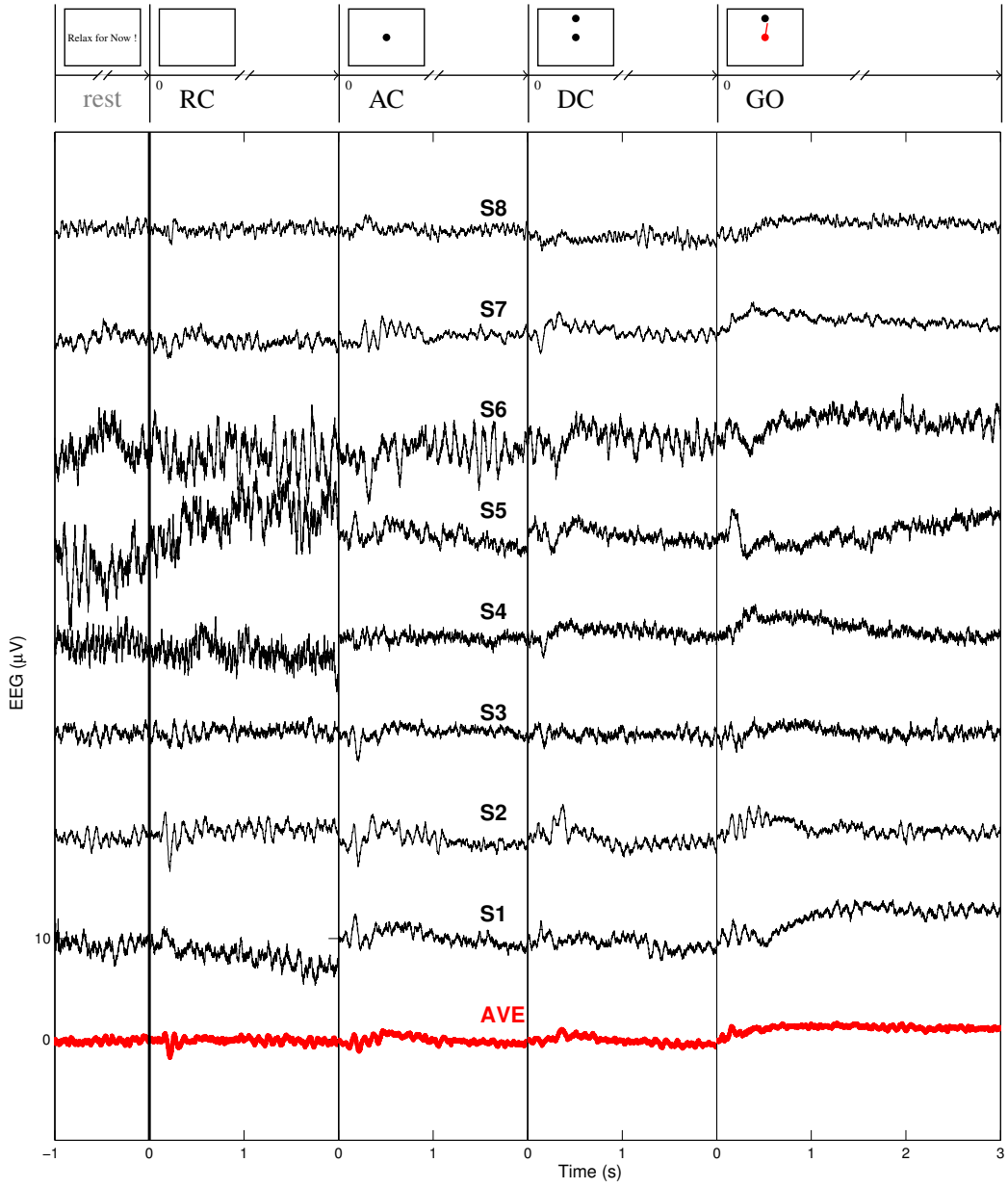

Figure 4.15. Event-related potentials in C_4 during different stages of movement, as described in Figure 3.5. Trial-averaged time domain CAR EEG are plotted for all 8 subjects. The thick red plot shows the ERP from averaging all the trials from every subject. The plots for each subject are shifted to distinguish between the plots. The graduation and scale for the grand average applies for all plots.

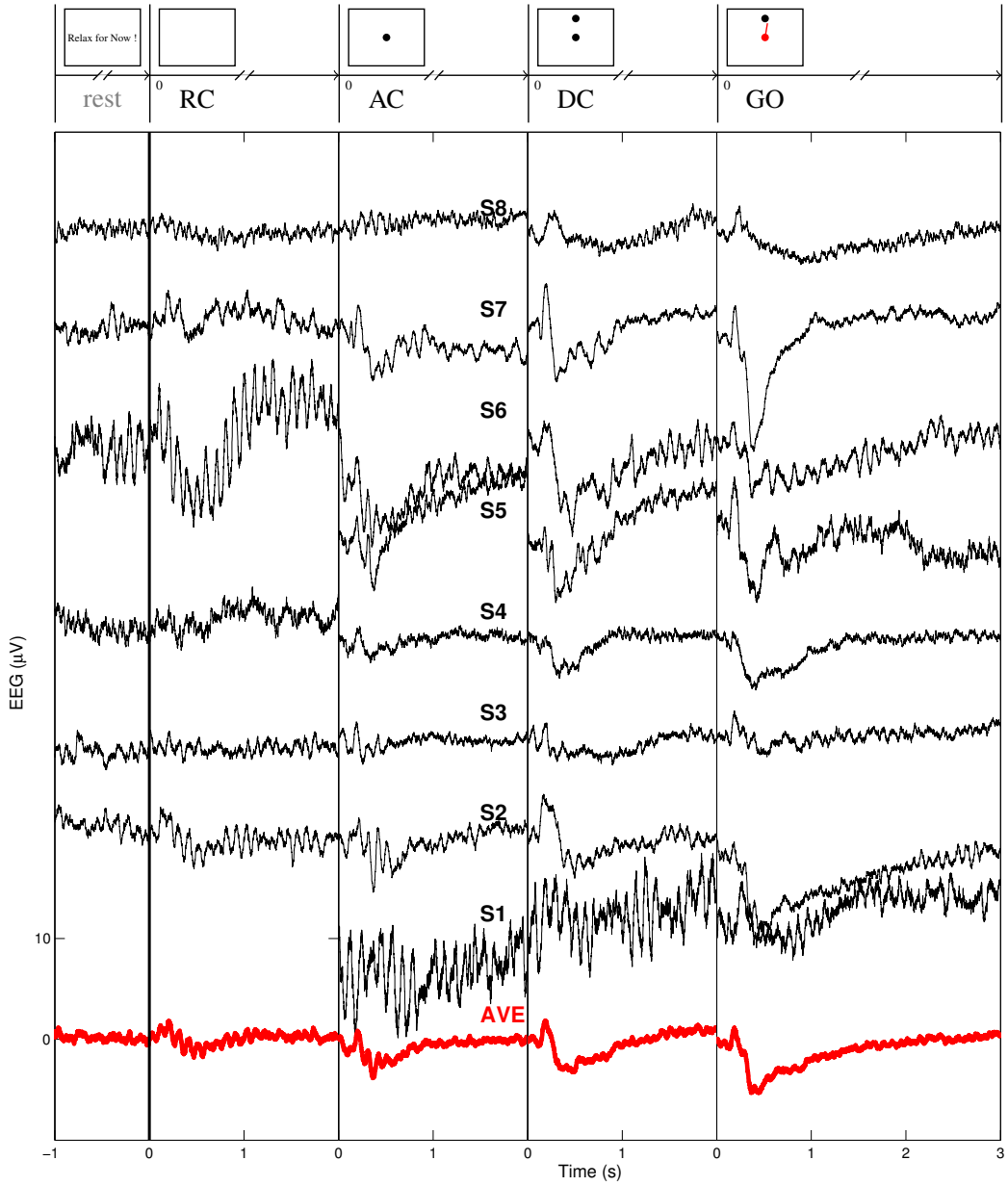

Figure 4.16. Event-related potentials in F_z during different stages of movement, as described in Figure 3.5. Trial-averaged time domain CAR EEG are plotted for all 8 subjects. The thick red plot shows the ERP from averaging all the trials from every subject. The plots for each subject are shifted to distinguish between the plots. The graduation and scale for the grand average applies for all plots. Average segments with too few acceptable trials are not plotted.

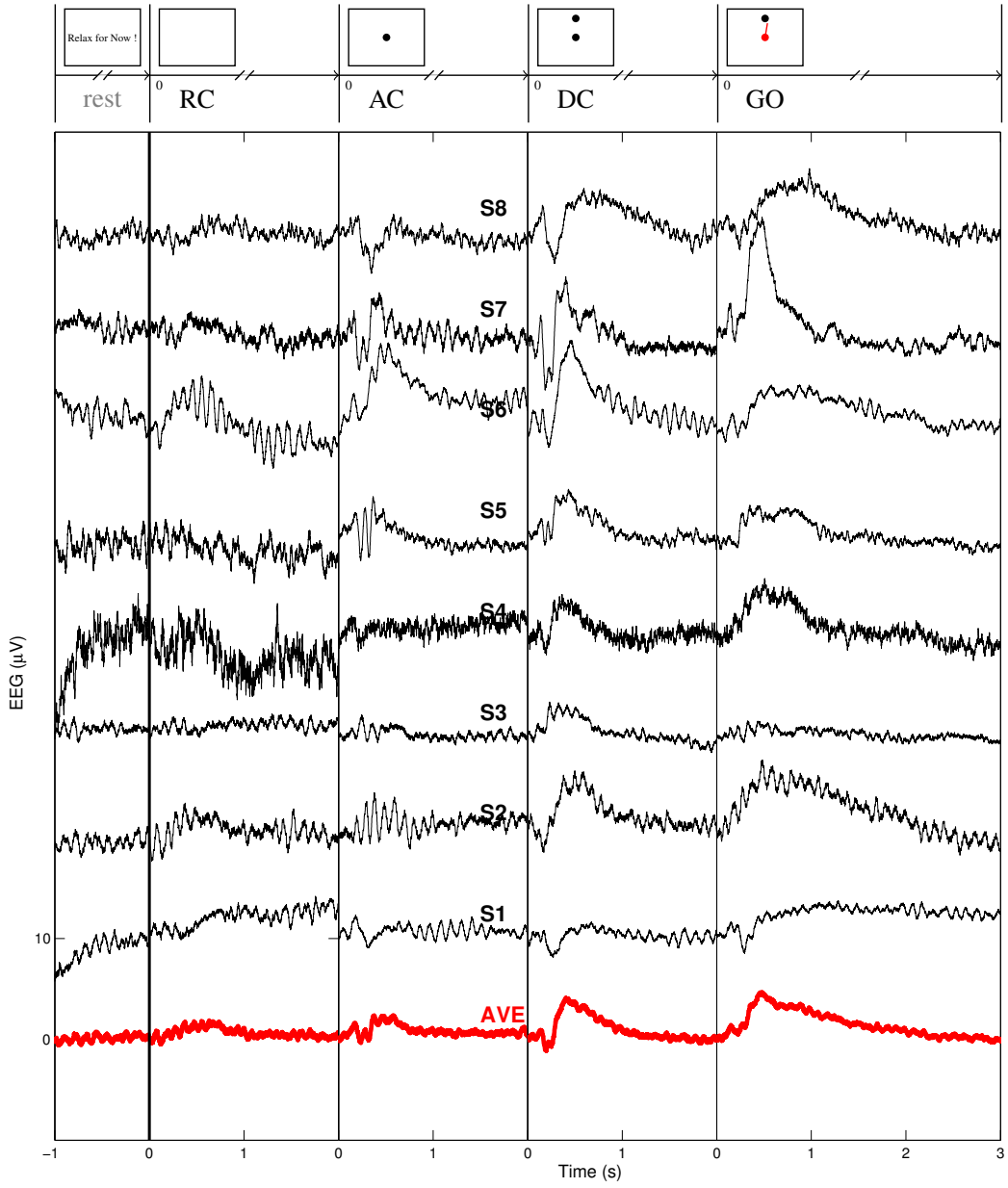

Figure 4.17. Event-related potentials in P_z during different stages of movement, as described in Figure 3.5. Trial-averaged time domain CAR EEG are plotted for all 8 subjects. The thick red plot shows the ERP from averaging all the trials from every subject. The plots for each subject are shifted to distinguish between the plots. The graduation and scale for the grand average applies for all plots.

Table 4.5. Characteristics of the common-average referenced event-related potentials waveform positive and negative peaks, observed in majority (5/8) of subjects in electrodes C_z, C_3, C_4, F_z, and P_z .

Electrode	Time Stage	Peak 1	Peak 2	Peak 3	Peak 4	Sustained Value
Cz	RC	P(184ms,1.288)				-0.185
	AC	N(105ms,-0.804)	P(188ms,0.700)	N(353ms,-0.997)	P(522ms,0.949)	-0.737
	DC	P(179ms,1.420)	N(301ms,-0.232)	P(525ms,1.047)	N(833ms,-1.793)	-1.506
	GO	P(188ms,1.769)	N(381ms,-1.736)			2.951
C3	RC	P(238ms,0.877)				-0.070^n
	AC	N(197ms,-0.812)	P(318ms,0.294)			0.422^n
	DC	P(249ms,0.915)				-0.691^n
	GO	N(458ms,-1.911)				0.276^n
C4	RC	N(217ms,-1.692)				-0.311^n
	AC	P(166ms,0.495)	N(217ms,-1.233)	P(467ms,0.866)		-0.355^n
	DC	P(361ms,1.022)				-0.717
	GO	P(154ms,1.328)				1.127
Fz	RC	P(209ms,1.703)	N(472ms,-1.926)			0.248^n
	AC	N(98ms,-1.567)	P(201ms,0.837)	N(363ms,-3.840)		0.208^n
	DC	N(109ms,-0.724)	P(183ms,1.868)	N(471ms,-3.265)		1.013^n
	GO	N(136ms,-0.974)	P(185ms,1.144)	N(405ms,-5.331)		0.405^n
Pz	RC	P(631ms,1.407)				-0.002^n
	AC	P(177ms,1.632)	N(236ms,-0.350)	P(378ms,2.431)		0.367^n
	DC	P(136ms,0.917)	N(197ms,-1.132)	P(404ms,4.097)		-0.012^n
	GO	P(478ms,4.674)				-0.093

[a] P and N stand for positive and negative waveform peaks. Numbers in parentheses show the time delay in milliseconds and the value of the peak in the average EEG (μV). e.g. P(184ms,1.288) shows a positive peak of 1.288 μV, 184ms after the relevant visual cue.
[b] The values are referenced to average signal values at the point of appearance of cues. i.e. EEG values at these cues are set to zero. Consequently the sustained values are relative to these values.
[n] Shows non-significant value, based on 3-state positive/neutral/negative.

4.2.2.2. Spatial Features of Common-Average Referenced Event-Related Potentials

Figures 4.18, 4.19, 4.20 and 4.21 illustrate the spatial distribution of the average time domain changes in the CAR surface EEG signal induced by the different visual cues (RC, AC, DC and GO).

Figure 4.22b demonstrates the trend of CAR EEG changes in the time domain when moving from frontal to parietal regions (F_z to P_z) and Figure 4.22d shows the trend of CAR EEG changes when moving from the ipsilateral to contralateral motor regions (C_4 to C_3).

While Table 4.5 provides an accurate description of common-average referenced (CAR) event-related potentials (ERP), the spatial distribution of peaks can be summarised

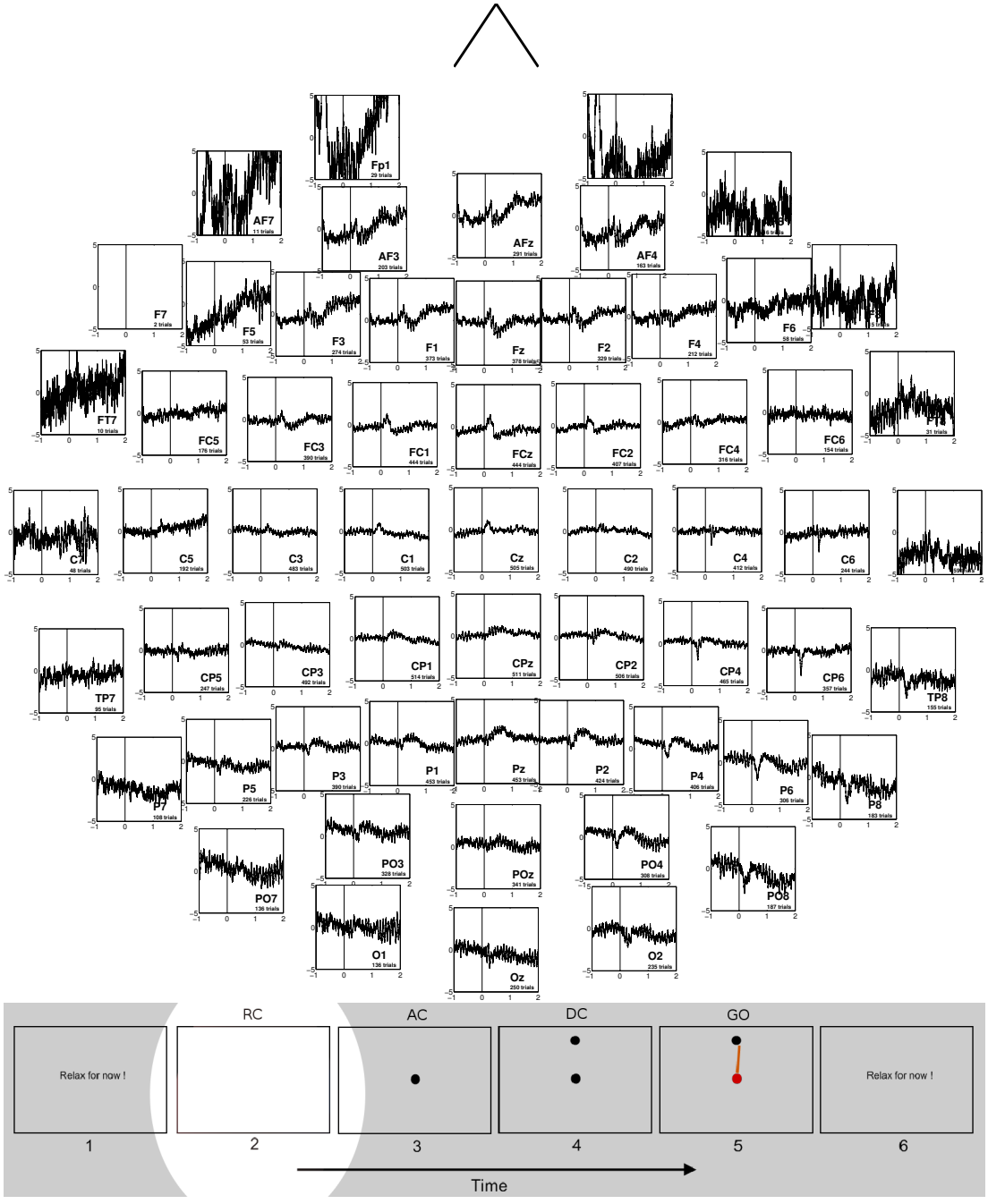

Figure 4.18. Spatial distribution of the time domain variations in surface EEG electrodes. Average CAR EEG (μV) across all of the trials from 8 subjects during the RC stage.

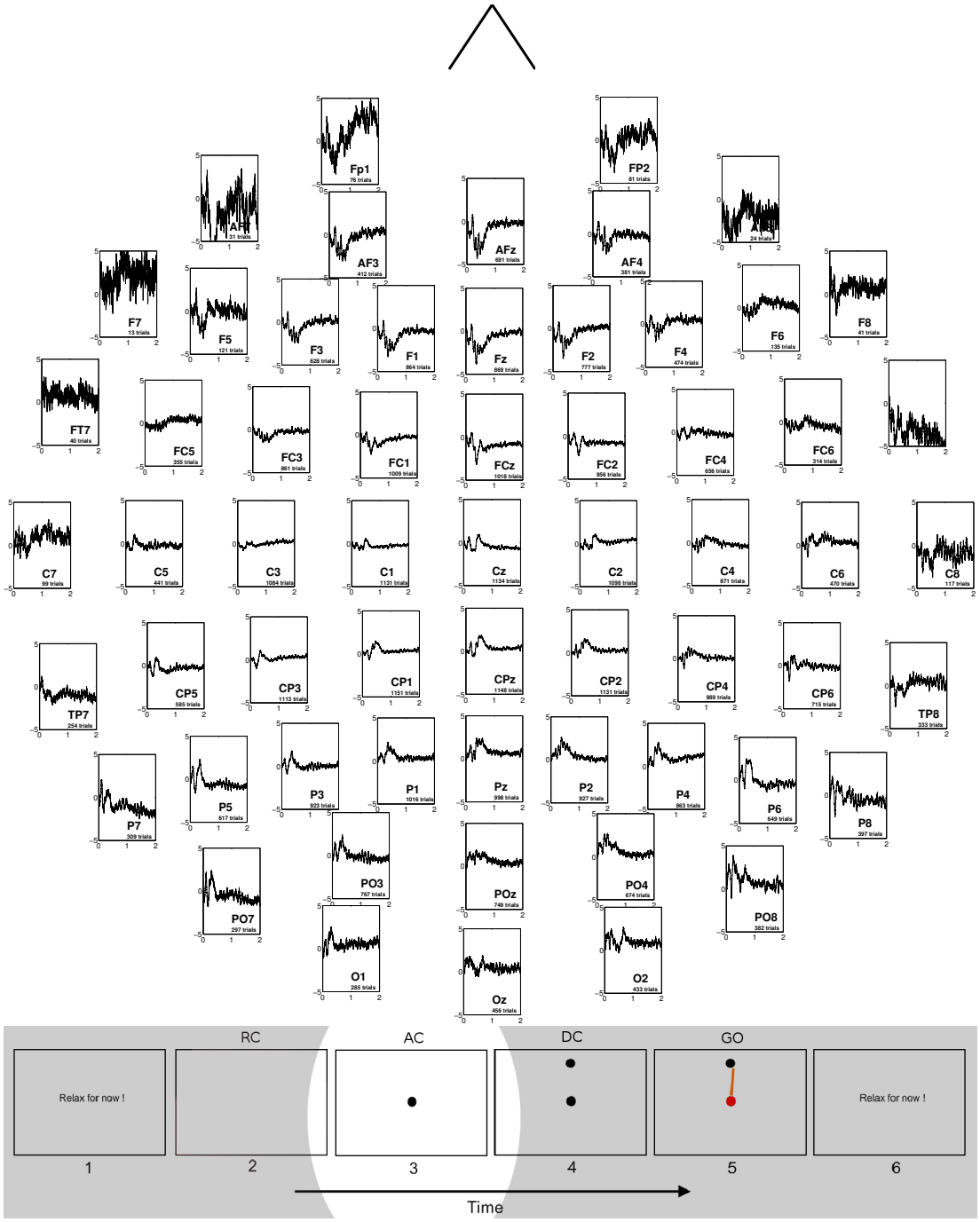

Figure 4.19. Spatial distribution of the time domain variations in surface EEG electrodes. Average CAR EEG (μV) across all of the trials from 8 subjects during the AC stage.

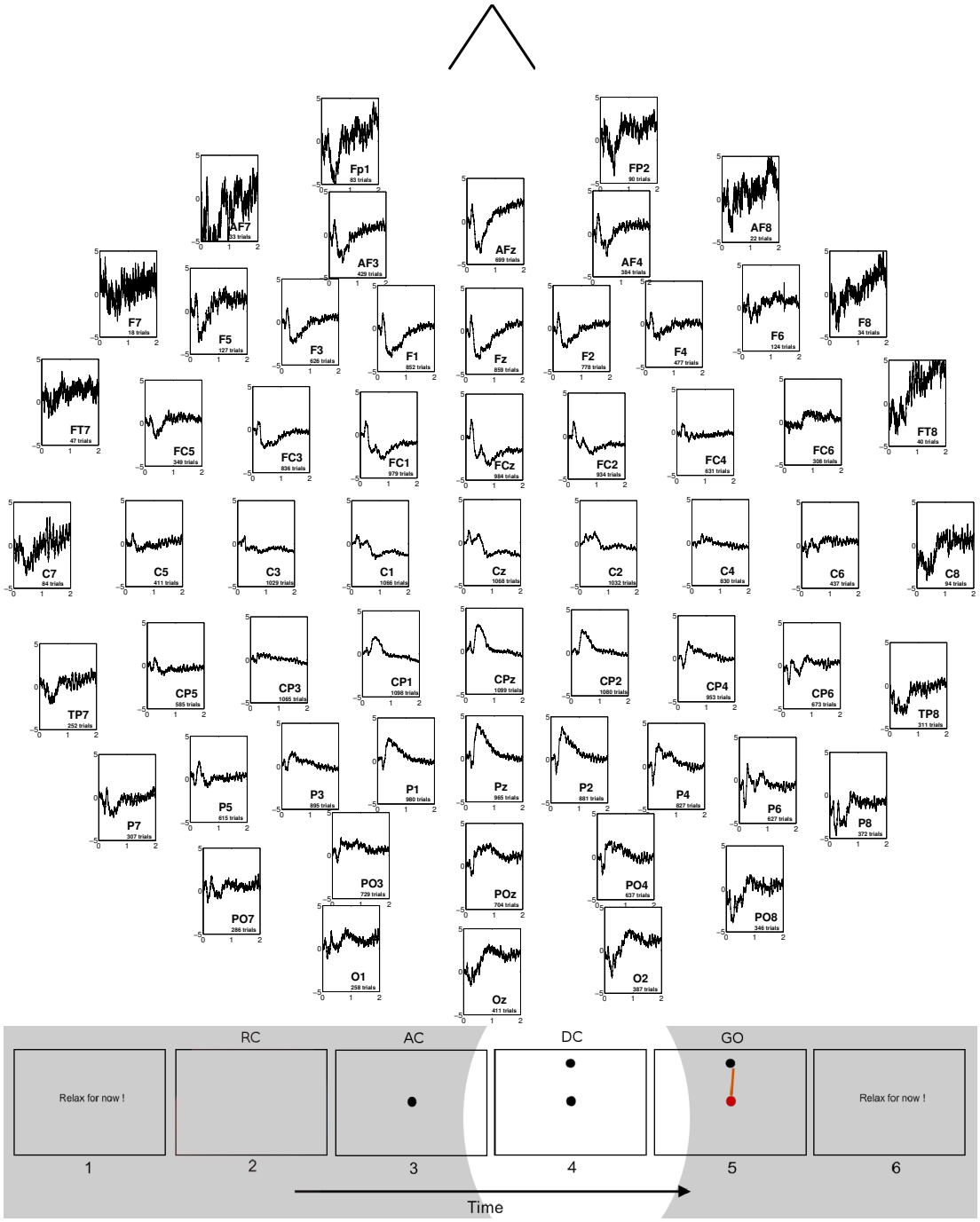

Figure 4.20. Spatial distribution of the time domain variations in surface EEG electrodes. Average CAR EEG (μV) across all of the trials from 8 subjects during the DC stage.

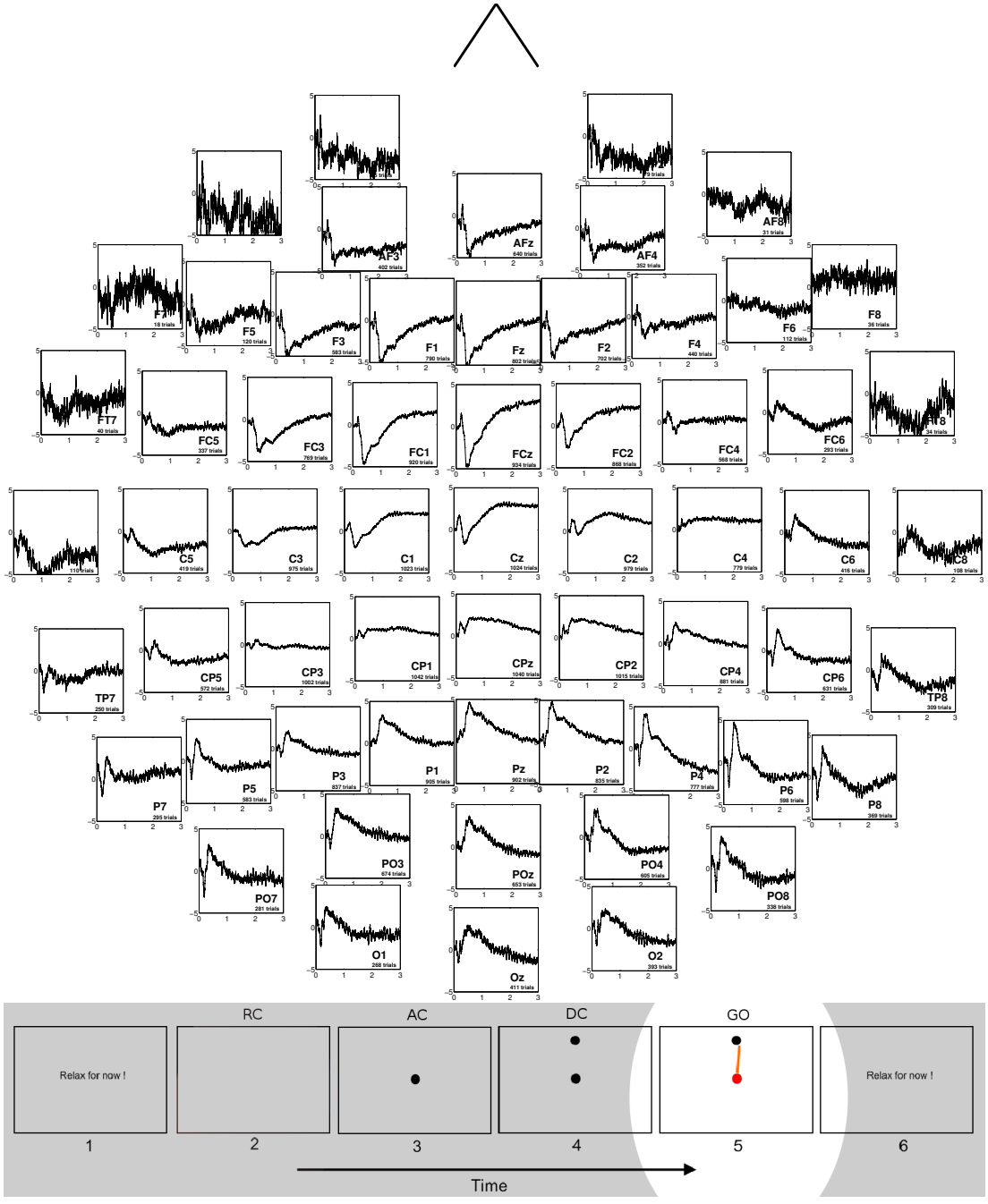

Figure 4.21. Spatial distribution of the time domain variations in surface EEG electrodes. Average CAR EEG (μV) across all of the trials from 8 subjects during the GO stage.

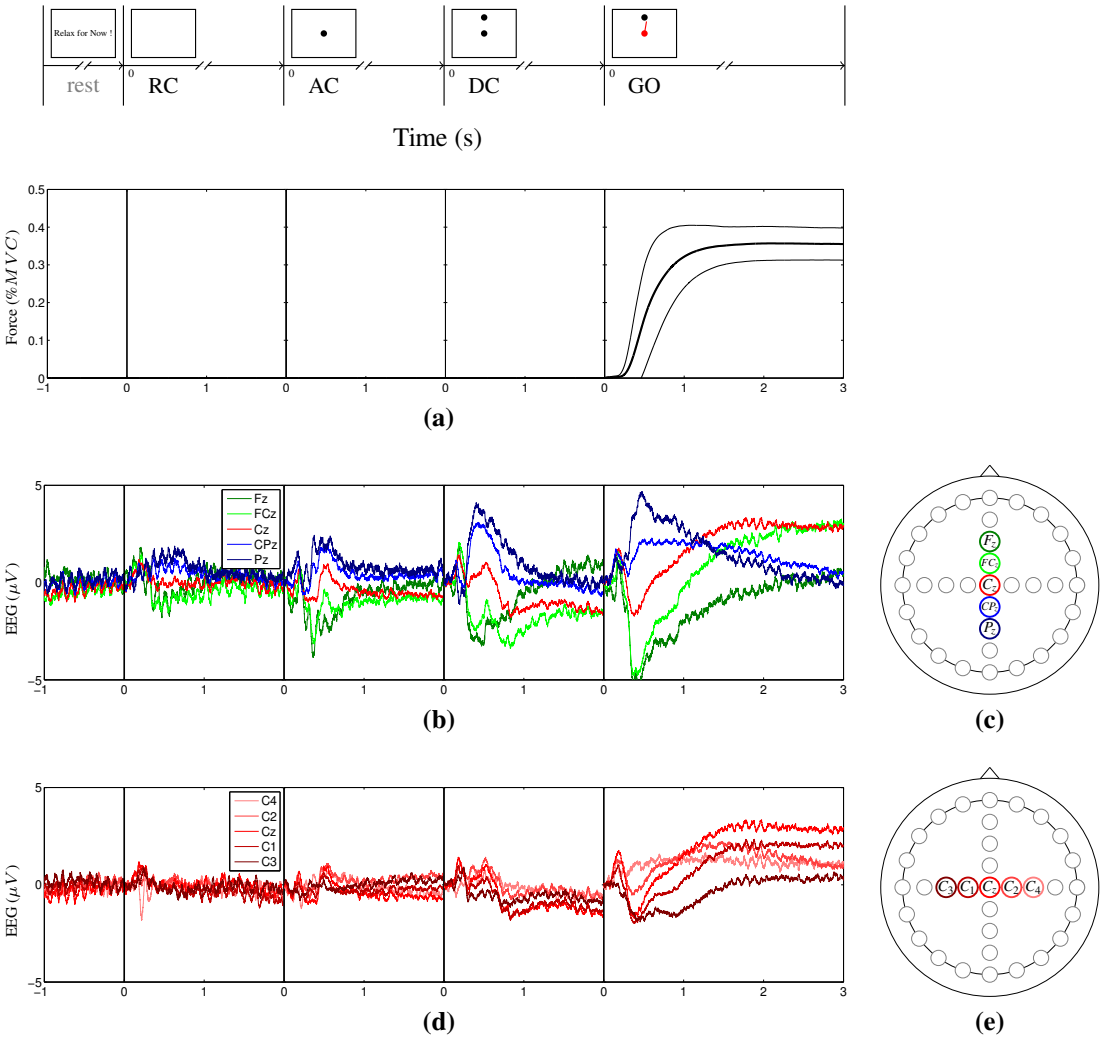

Figure 4.22. Spatial difference of the time domain average of the CAR EEG. Horizontal axes are time in seconds. Zeros from left to right indicate the presentation of visual cues: RC, AC, DC and GO (see Figure 3.5). a) The force development profile (mean $\pm$ 1 SD). b) Trend of EEG changes when moving from frontal to parietal regions from F_z, FC_z, C_z, and CP_z to P_z as depicted in (c). d) Trend of EEG changes when moving from ipsilateral to contralateral motor regions from C_4, C_2, C_z, and C_1 to C_3 as depicted in (e).

as follows:

RC (Rest) stage: The activity pattern changes from P-N in frontal regions to P in parietal regions, while in central regions the ipsilateral Negative Peak (N) changes to a Positive Peak (P) in contralateral side.

AC (Preparation) stage: The N-P-N-P pattern at C_z changes to P-N-P at P_z and to N-P-N at F_z. The central region ERPs are suppressed towards lateral electrodes.

DC (Planning) stage: The observed pattern of P-N-P-N at C_z changes to P-N-P towards parietal and is reduced to larger N-P-N towards frontal. Again, the central region ERPs are suppressed towards lateral electrodes. A sustained negativity is observed at C_z and C_4.

GO (Execution) stage: The P-N in C_z is followed by sustained positivity. It changes to P-N-P at P_z, and to N-P-N at F_z. In contralateral central area (C_3) this changes to a large negative peak, while on the ipsilateral side (C_4) this changes to a slight positive peak. A sustained positivity is observed at C_z and C_4.

4.2.3. Summary of Time Domain EEG Signatures

In the time domain, ERPs were observed after all visual cues in the form of positive and negative waveform peaks. The observed patterns, described earlier in Section 4.2, vary considerably as a function of electrode position and the time-course of trial. Notable feature are the tendencies towards negativity in the frontal recordings and positivity in the parietal recordings in both ear-lobe referenced (ELR) and, especially, common average referenced (CAR) EEG; however, many ERPs appear with different polarities in these regions. Sustained negativity during planning and sustained positivity during force maintenance is observed in all electrodes with ELR, and above ipsilateral and central motor cortical area in CAR EEG. The other observation is the relatively symmetric and midline-centric activity during the AC (preparation) and the DC (planning) stages, while the activity in GO stage (execution) is asymmetric with bolder contralateral activity.

4.3. Event-Related (De-)Synchronisations (ERD/ERS)

As described in Section 3.3, the time frequency characteristics of EEG have been extracted. Similar to the previous section, the time-frequency characteristics of ELR EEG are reviewed in Section 4.3.1 and subsequently the time-frequency characteristics of CAR EEG are reviewed in Section 4.3.2. For both ELR and CAR results, the patterns of activity are inspected by considering the trial-averaged time-frequency representation for 5 main single channels C_z, C_3, C_4, F_z, and P_z from a representative subject S3 in Sections 4.3.1.1 and 4.3.2.1. The spatial distribution maps of ERD/ERS are produced in Sections 4.3.1.2 and 4.3.2.2.

4.3.1. Event-Related (De-)Synchronisations in Ear-Lobe Referenced EEG

4.3.1.1. Temporal Features of Ear-Lobe Referenced ERD/ERS

By studying the statistically significant features in time-frequency distributions, the consistent features across subjects can be identified, as well as some subject-specific features. Figures 4.23, 4.24, 4.25, 4.26, and 4.27, show the ELR EEG normalised scalogram for electrodes C_z, C_3, C_4, F_z, and P_z for subject S3. The significance of time-frequency representations are determined by comparison to the average rest-time values before the RC, using permutation test and $p < 0.05$ significanc elevel (see Section 3.3.3.1 and Equation 3.4). There are transient (i.e. phasic or early) ERS after all visual cues. There are also both transient and sustained ERD following the visual cues in μ, β and γ bands. It should be noted that the average values, represented by colours at each frequency band, are representative of classic ERD/ERS obtained by averaging of the band-passed signal power (Graimann and Pfurtscheller, 2006). Significance analysis reveals that considerable regions of time-frequency representations show significant changes compared to rest-time. The relatively high ITC values, especially for transient low frequency ERS, is an indicator of EEG activity phase-locked to visual cues. For comprehensive visualisation of ERS/ERD for all subjects at the same time instance and a better comparison of inter-subject variability, see Appendix E.

The features that are observed in all electrodes are listed in Table 4.6. The table lists the features that can be seen in 5 or more out of 8 subjects by visual inspection of significant wavelet moduli at each frequency (1-50Hz, 1 Hz steps) for the transient and sustained segments of each execution stage (see Appendix E). This corresponds to 4.88% significance level (see Appendix D). When the white screen appears (RC) mild transient signatures of ERD can be seen between 22-26 Hz and 30-34 Hz. When the attention cue (AC) appears, a relatively strong transient ERS in 4-5 Hz and ERD in 17-36 Hz range happens. Directional cue (DC) induces ERS in 4-5 Hz and ERD in 18-32 Hz range, as well as a sustained ERD in the 18-27 Hz range. When the GO command appears and subjects actually start exerting force, considerable transient ERS in 4-5 Hz and ERD between 8-9 Hz and 17-22 Hz range is observed. The sustained features which correspond to maintaining the requested force level, include ERD between 14-31 Hz (see Table 4.6).

4.3.1.2. Spatial Features of Ear-Lobe Referenced ERD/ERS

While many EEG channels in central, frontal, and parietal regions and in ipsilateral and contralateral sites show similar time-frequency patterns, there are also local region-

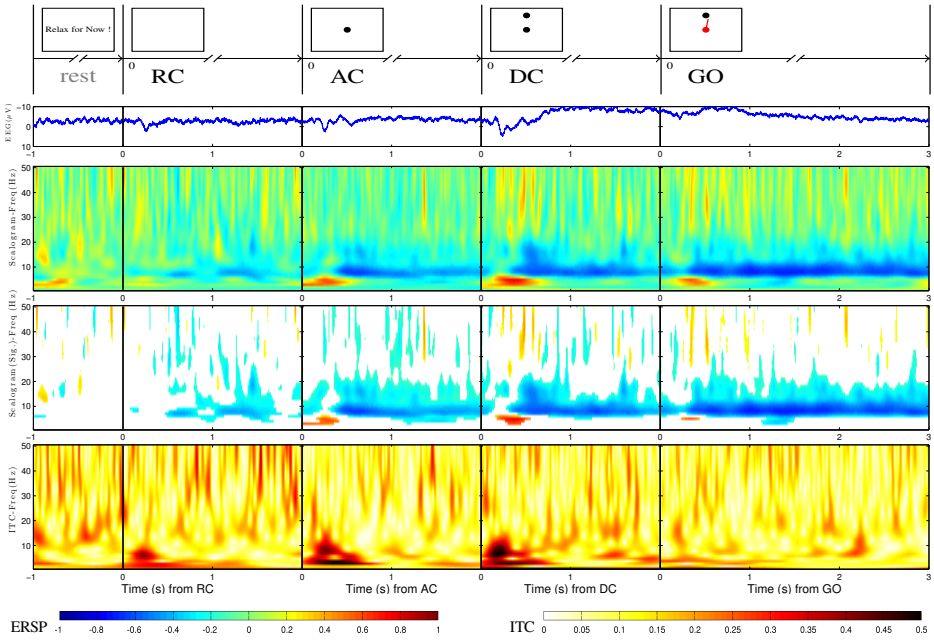

Figure 4.23. Time-frequency distribution for electrode C_z, for subject 3. Horizontal axes are time in seconds. Vertical axes are ELR EEG (μV) or Frequency (Hz). Zeros from left to right indicate the presentation of visual cues: RC, AC, DC and GO. Top: continuous wavelet transform (CWT) squared moduli (scalogram), normalised to pre-movement rest-time EEG. Dark blue shows 100% ERD and dark red 100% ERS. Middle: the same distribution with only statistically significant values retained. Bottom: inter-trial coherence (ITC).

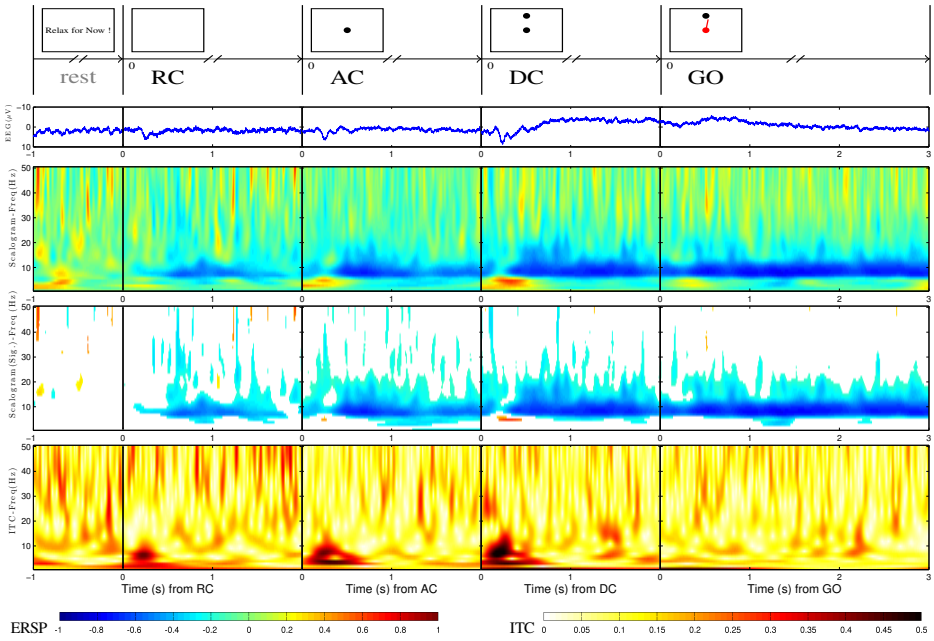

Figure 4.24. Time-frequency distribution for electrode C_3, for subject 3. Horizontal axes are time in seconds. Vertical axes are ELR EEG (μV) or Frequency (Hz). Zeros from left to right indicate the presentation of visual cues: RC, AC, DC and GO. Top: continuous wavelet transform (CWT) squared moduli (scalogram), normalised to pre-movement rest-time EEG. Dark blue shows 100% ERD and dark red 100% ERS. Middle: the same distribution with only statistically significant values retained. Bottom: inter-trial coherence (ITC).

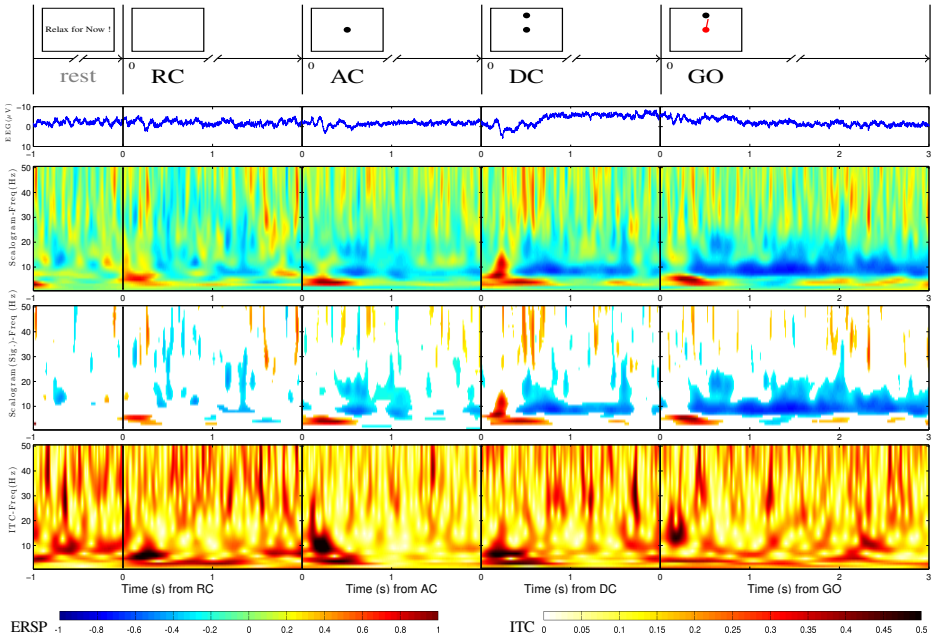

Figure 4.25. Time-frequency distribution for electrode C_4, for subject 3. Horizontal axes are time in seconds. Vertical axes are ELR EEG (μV) or Frequency (Hz). Zeros from left to right indicate the presentation of visual cues: RC, AC, DC and GO. Top: continuous wavelet transform (CWT) squared moduli (scalogram), normalised to pre-movement rest-time EEG. Dark blue shows 100% ERD and dark red 100% ERS. Middle: the same distribution with only statistically significant values retained. Bottom: inter-trial coherence (ITC).

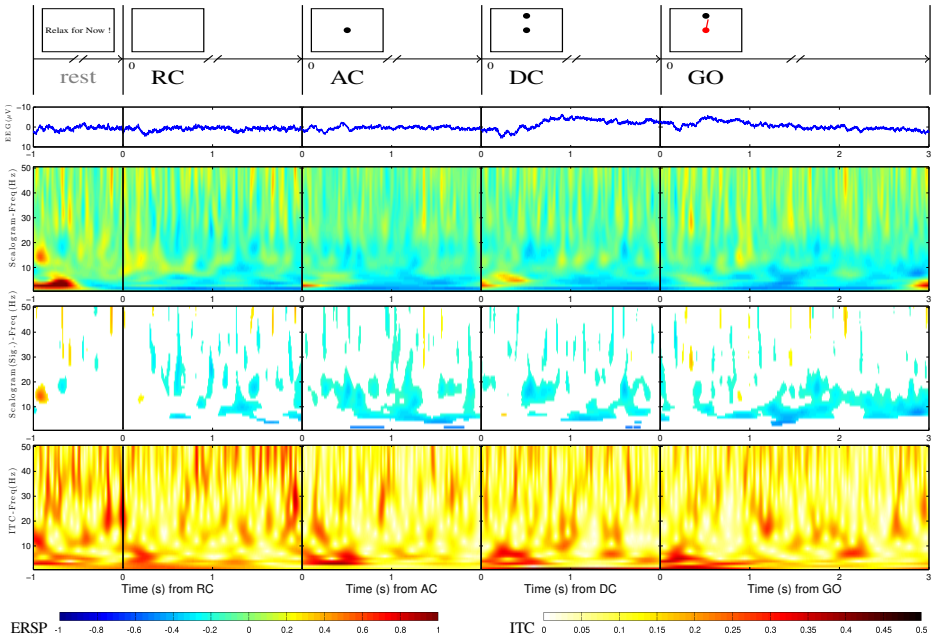

Figure 4.26. Time-frequency distribution for electrode F_z, for subject 3. Horizontal axes are time in seconds. Vertical axes are ELR EEG (μV) or Frequency (Hz). Zeros from left to right indicate the presentation of visual cues: RC, AC, DC and GO. Top: continuous wavelet transform (CWT) squared moduli (scalogram), normalised to pre-movement rest-time EEG. Dark blue shows 100% ERD and dark red 100% ERS. Middle: the same distribution with only statistically significant values retained. Bottom: inter-trial coherence (ITC).

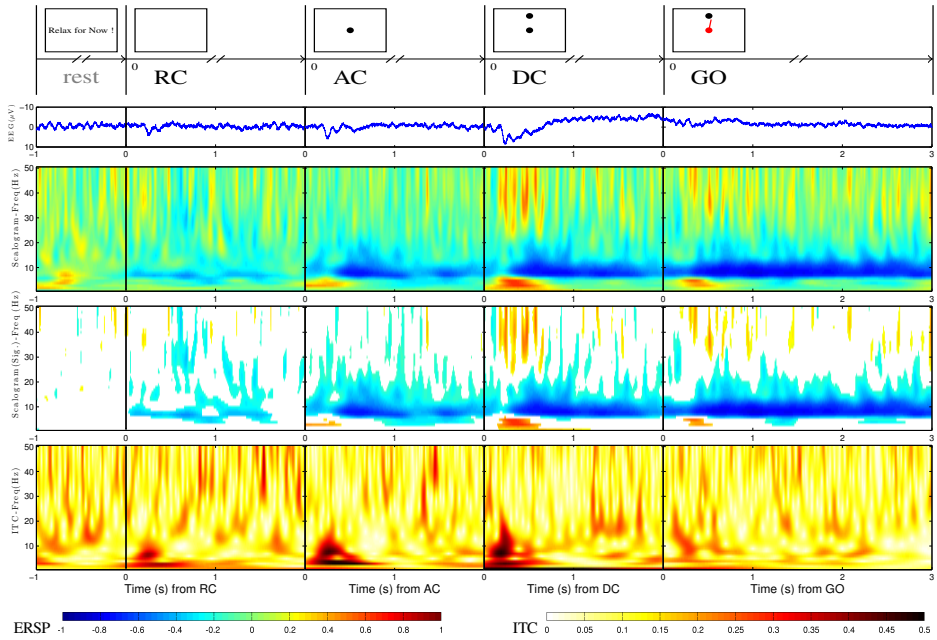

Figure 4.27. Time-frequency distribution for electrode P_z, for subject 3. Horizontal axes are time in seconds. Vertical axes are ELR EEG (μV) or Frequency (Hz). Zeros from left to right indicate the presentation of visual cues: RC, AC, DC and GO. Top: continuous wavelet transform (CWT) squared moduli (scalogram), normalised to pre-movement rest-time EEG. Dark blue shows 100% ERD and dark red 100% ERS. Middle: the same distribution with only statistically significant values retained. Bottom: inter-trial coherence (ITC).

specific characteristics in each EEG channel.

In order to obtain a broader perspective on ELR surface EEG activity, the spatial distribution maps of time-frequency representations can be studied. Figures 4.28, 4.29, 4.30 and 4.31 show the spatial variation of ELR surface EEG time-frequency features for Subject S3.

In order to summarise the results for all subjects, Table 4.7 lists the major significant ERD/ERS in ELR EEG for electrodes C_z, C_3, C_4, F_z, and P_z that are observed in the majority of subjects (5 or more out of 8). The table lists the features that can be seen

Table 4.6. Summary of statistically significant ERD/ERS in ELR EEG that appear in all C_z, C_3, C_4, F_z and P_z electrodes, in majority (5/8) of subjects .

RC		AC		DC		GO	
Transient	Sustained	Transient	Sustained	Transient	Sustained	Transient	Sustained
-[22,26]	none	+[4,5]	none	+[4,5]	-[18,27]	+[4,5]	-[14]
-[30,34]		-[17,36]		-[18,32]		-[8,9]	-[16,31]
						-[17,22]	

[a] + shows ERS and - shows ERD. Numbers are the frequency ranges in Hz.
[b] Transient means the first 0.5-1.0s after the cue where transient or phasic activity is observed. Sustained, indicates the sustained or tonic activity that lasts about 1.0-1.5s afterwards.

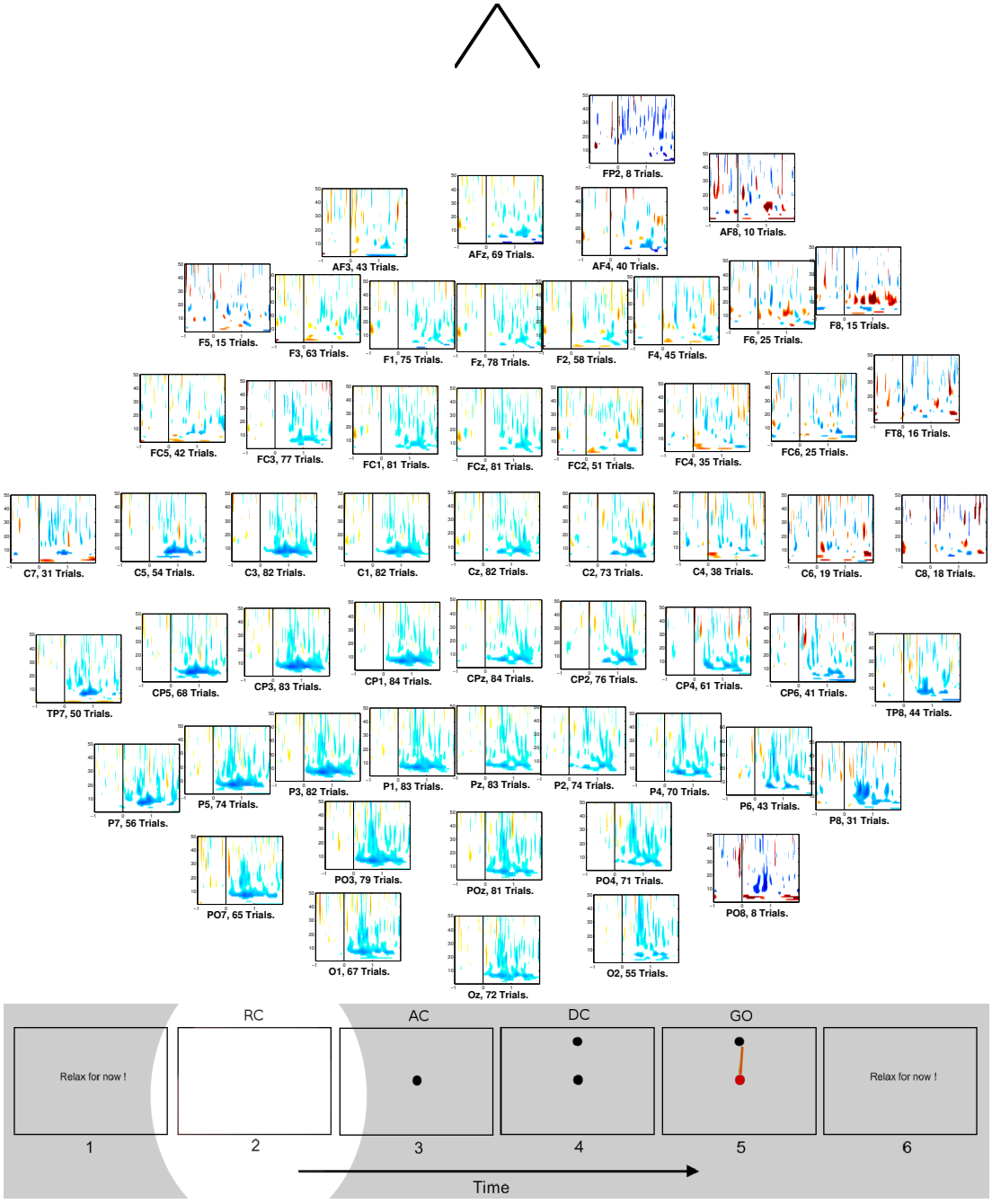

Figure 4.28. Spatial distribution of trial-averaged ELR EEG time-frequency distributions, from subject 3 and in time stage RC. For each electrode position the normalised continuous wavelet transform scalograms are plotted as described in Figure 4.3.

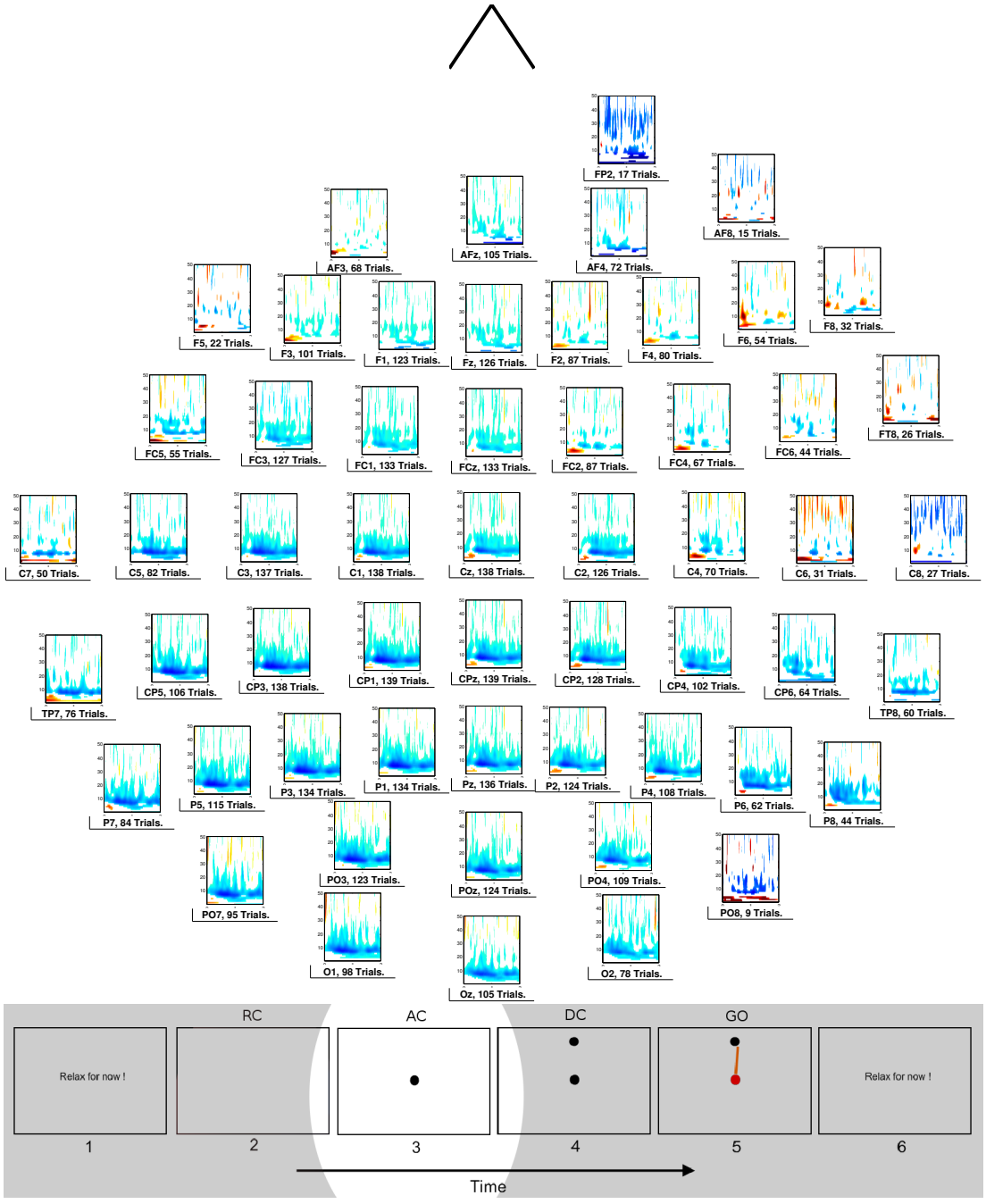

Figure 4.29. Spatial distribution of trial-averaged ELR EEG time-frequency distributions, from subject 3 and in time stage AC. For each electrode position the normalised continuous wavelet transform scalograms are plotted as described in Figure 4.3.

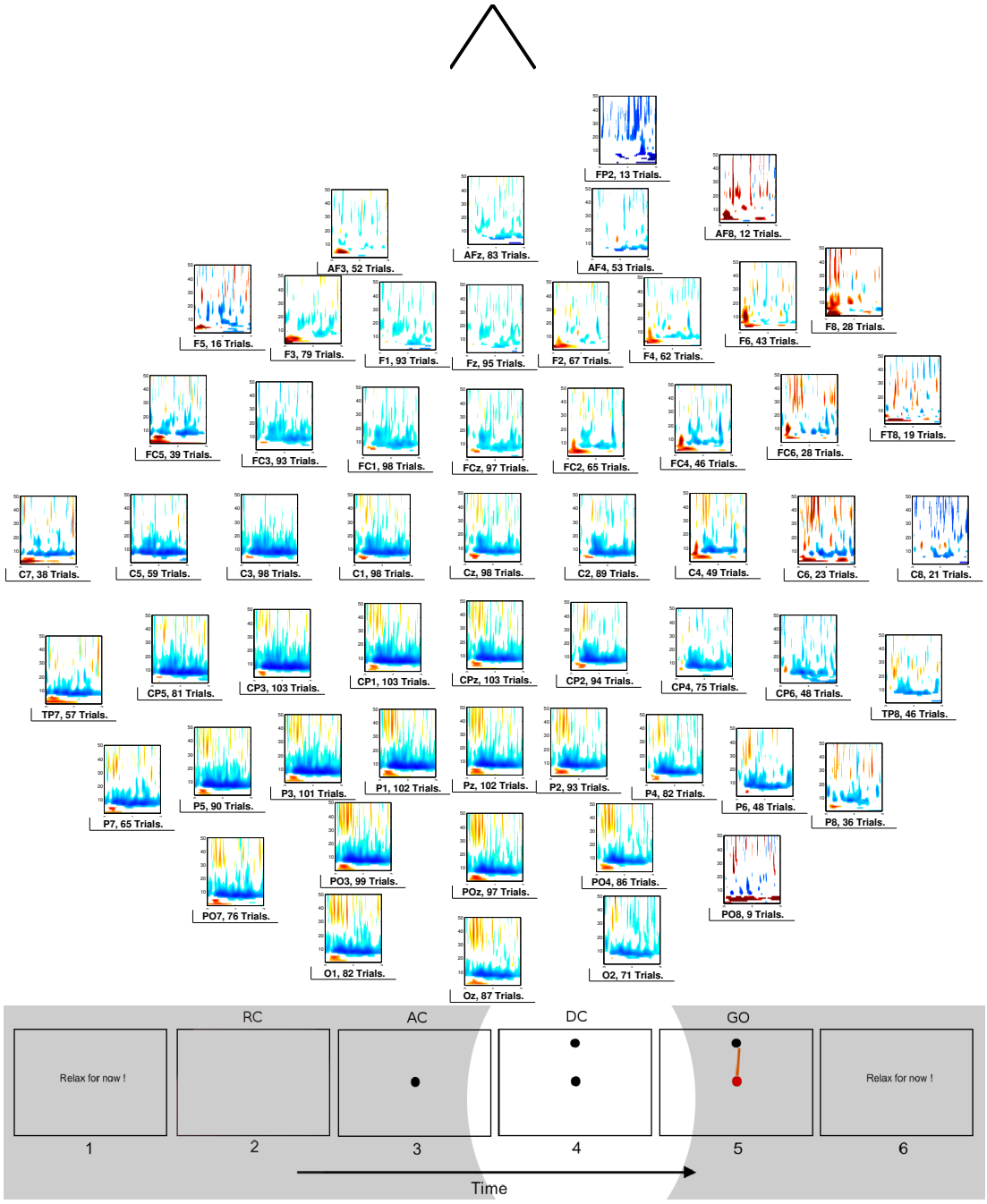

Figure 4.30. Spatial distribution of trial-averaged ELR EEG time-frequency distributions, from subject 3 and in time stage DC. For each electrode position the normalised continuous wavelet transform scalograms are plotted as described in Figure 4.3.

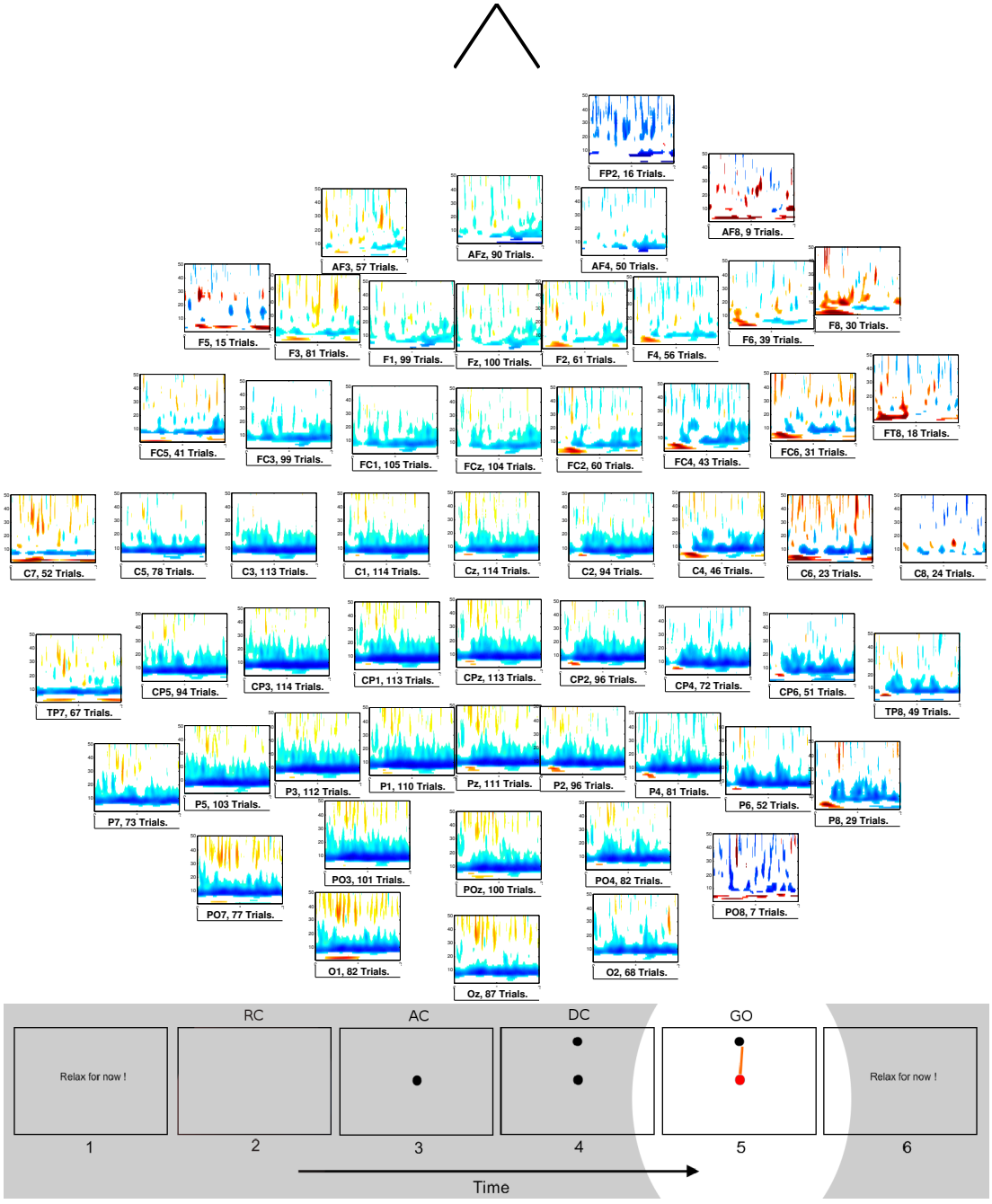

Figure 4.31. Spatial distribution of trial-averaged ELR EEG time-frequency distributions, from subject 3 and in time stage GO. For each electrode position the normalised continuous wavelet transform scalograms are plotted as described in Figure 4.3.

Table 4.7. Summary of statistically significant ERD/ERS in ELR EEG observed in majority (5/8) of subjects in electrodes C_z, C_3, C_4, F_z and P_z .

Task	RC		AC		DC		GO	
	Transient	Sustained	Transient	Sustained	Transient	Sustained	Transient	Sustained
C_z	-[7]	+[6,7]	+[2,4]	-[17,40]	+[2,4]	-[6]	+[2,5]	-[4,6]
	+[9,10]	-[24]	**+[5]**		**+[5]**	-[13,16]	-[8,34]	-[8,17]
	-[15,39]		+[6,8]		+[6]	**-[17,20]**		**-[18,24]**
	-[46,48]		-[14,19]		-[10,12]	-[21]		-[25,41]
			-[20,27]		-[14,19]	**-[22,24]**		
			-[28,33]		**-[20,21]**	-[25,50]		
			-[34,36]		-[22,50]			
			-[37,50]					
C_3	-[8,21]	+[15,16]	+[4]	-[1]	+[3,4]	-[6,13]	+[2,5]	-[1,2]
	-[22,33]	+[23-27]	**+[5]**	-[16,36]	**+[5]**	**-[14,36]**	-[6,41]	-[5,16]
	-[34-39]		+[6]		+[6]	-[37,48]		**-[17,30]**
	-[41,43]		-[7,19]		-[7,17]			-[31,41]
	-[45,46]		**-[20,36]**		**-[18,34]**			
	-[48,50]		-[37,50]		-[35,50]			
C_4	+[6]	-[15,19]	+[4,6]	-[1]	+[3,7]	-[8,18]	+[3,5]	-[4,15]
	-[16,21]	-[21,22]	-[8,10]	+[7]	-[8,12]	**-[19,23]**	-[7,18]	**-[16,23]**
	-[22,25]	+[25,28]	+[13,14]	-[19,27]	±[13]	-[24,33]	**-[19,22]**	-[24,39]
	-[26]	+35	-[15,18]		-[15,18]		-[23,32]	
	-[30,37]		**-[19,24]**		**-[19,24]**		+[41,50]	
			-[25,36]		-[25,34]			
F_z	-[22,34]	none	+[4,5]	none	+[4,5]	-[18,27]	+[4,6]	-[14]
			+[7]		-[18,47]	-[37,42]	-[8,9]	-[16,31]
			-[17,48]				-[17,22]	
P_z	-[5]	-[5]	+[3,6]	-[13,31]	+[1,5]	-[6,29]	+[3,5]	-[4,5]
	±[6]		-[7,47]		±[6,7]		-[6,32]	**-[6,7]**
	-[7,13]		-[50]		-[8,12]		+[36,50]	-[8,34]
	-[14,25]				-[16,32]			
	-[26,37]							

[a] + shows ERS, - shows ERD, and ± shows ERS followed by ERD. Numbers are frequency ranges in Hz and **bold** entries show observation of ERD/ERS in all of the subjects.

[b] Transient means the first 0.5-1.0s after the cue where transient or phasic activity is observed. Sustained, indicates the sustained or tonic activity that lasts about 1.0-1.5s after the transient stage.

[c] ERD/ERS in 5 of 8 subjects corresponds to 0.0488 significance level. Similarly, ERD/ERS in 8 of 8 subjects corresponds to 0.000046 significance level.

in 5 or more out of 8 subjects by visual inspection of significant wavelet moduli at each frequency (1-50Hz, 1 Hz steps) for the transient and sustained segments of each execution stage (see Appendix E). This corresponds to 4.88% significance level (see Appendix D). The table describes the transient ERD/ERS and sustained ERD/ERS after each visual cue. This is an abstraction of the results in Appendix E.

In addition to the aforementioned observed ERD/ERS for all electrodes (see Section 4.3.1.1), the following notable local features are observed. Other local features that are not explicitly highlighted below are mostly ERDs with extended frequency range of those listed in Table 4.6.

RC (Rest) stage: After RC there is ERS at 6Hz in C_4, at 9-10Hz in C_z and mixed ERD/ERS at 6Hz in P_z. The other dominant phenomenon is broad ERD from 7-8Hz in C_3 and P_z and from 15-22Hz in other electrodes up to 34-50Hz. In sustained RC stage, in addition to 6-7Hz ERS in C_z and high-β ERS in C_3 and C_4, there is low-β ERD in C_4 and ERS in C_3.

AC (Preparation) stage: After AC, in addition to common δ and θ band ERS in all electrodes, the dominant phenomenon is ERD in β and γ bands and also α ERD in C_3 and P_z. In C_4, high α ERS is seen. In sustained AC stage, β band ERD is seen in all electrodes, except for F_z.

DC (Planning) stage: After DC, the common δ and θ band ERS in all electrodes is present similar to the AC stage. The other patterns are very similar to the AC stage as well with α ERD more pronounced in C_z and C_4 and suppressed γ ERD in P_z. A mixed ERD/ERS at 6-7Hz is seen in P_z. In sustained DC stage, ERD is seen in the α, β and γ bands in all electrodes. This ERD is absent for α in C_z and F_z and for γ in C_4 and P_z.

GO (Execution) stage: After GO signal, the common δ and θ band ERS is present again, as in the AC and DC stages. ERD is seen in all electrodes in α, β and γ bands except the γ ERD in F_z and C_z. During sustained force generation, ERD is seen in θ, α, β and low-γ bands in general. Exceptions are in Fz with only β ERD and Pz with ERD in all bands but γ.

4.3.2. Event-Related (De-)Synchronisations in Common-Average Referenced EEG

4.3.2.1. Temporal Features of Common-Average Referenced ERD/ERS

Similar to ELR EEG, there are common and subject specific time-frequency features in CAR EEG as previously reported (Nasseroleslami et al., 2011a) and is presented here in full details. Figures 4.32, 4.33, 4.34, 4.35, and 4.36, show the CAR EEG normalised scalogram of electrode C_z, C_3, C_4, F_z, and P_z for subject S3. The significance of time-frequency representations are determined by comparison to the average rest-time values before the RC, using permutation test and $p < 0.05$ significance level (see Section 3.3.3.1 and Equation 3.4). As can be seen, there are transient δ and θ band ERS after all visual cues. There are also both transient and sustained ERD after the visual cues in μ, β and γ bands. It should be noted that the average values, represented by colours at each frequency band, are representative of classic ERD/ERS obtained by averaging of

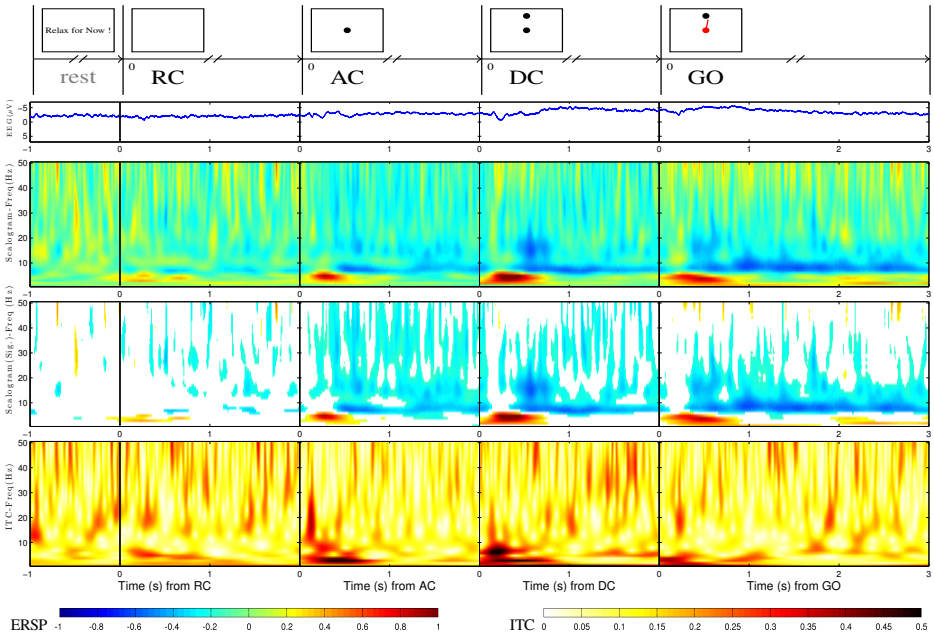

Figure 4.32. Time-frequency distribution for electrode C_z, for subject 3. Horizontal axes are time in seconds. Vertical axes are CAR EEG (μV) or Frequency (Hz). Zeros from left to right indicate the presentation of visual cues: RC, AC, DC and GO. Top: continuous wavelet transform (CWT) squared moduli (scalogram), normalised to pre-movement rest-time EEG. Dark blue shows 100% ERD and dark red 100% ERS. Middle: the same distribution with only statistically significant values retained. Bottom: inter-trial coherence (ITC).

the band-passed signal power (Graimann and Pfurtscheller, 2006). Significance analysis reveals that considerable regions of time-frequency representations show significant changes. The relatively high ITC values, especially for transient low frequency ERS, is an indicator of EEG activity phase-locked to visual cues. For comprehensive visualisation of ERS/ERD for all subjects at the same time and a better comparison of inter-subject variability, see Appendix E.

While it is very difficult to accurately describe the timings of ERD/ERS, it can be seen that δ and θ band transient ERS usually start no later than 100-200ms after the cue and last until 500-1000ms after the cue. For α, β and low-γ ERD, the onset of ERD is between 150-450ms and mostly in the 250-350ms range after the cues. By inspecting the patterns, the differences can mostly be attributed to differences between individuals and to some extent to ERD/ERS frequency bands rather than recording site or cue types. The ERDs usually vanish gradually or continue in the form of sustained ERD, thus specific offset time cannot be found for most ERDs.

The features that are observed in all electrodes are listed in Table 4.8. The table lists the features that can be seen in 5 or more out of 8 subjects by visual inspection of significant wavelet moduli at each frequency (1-50Hz, 1 Hz steps) for the transient and sustained segments of each execution stage (see Appendix E). This corresponds to 4.88% significance level (see Appendix D). When the white screen appears (RC) mild

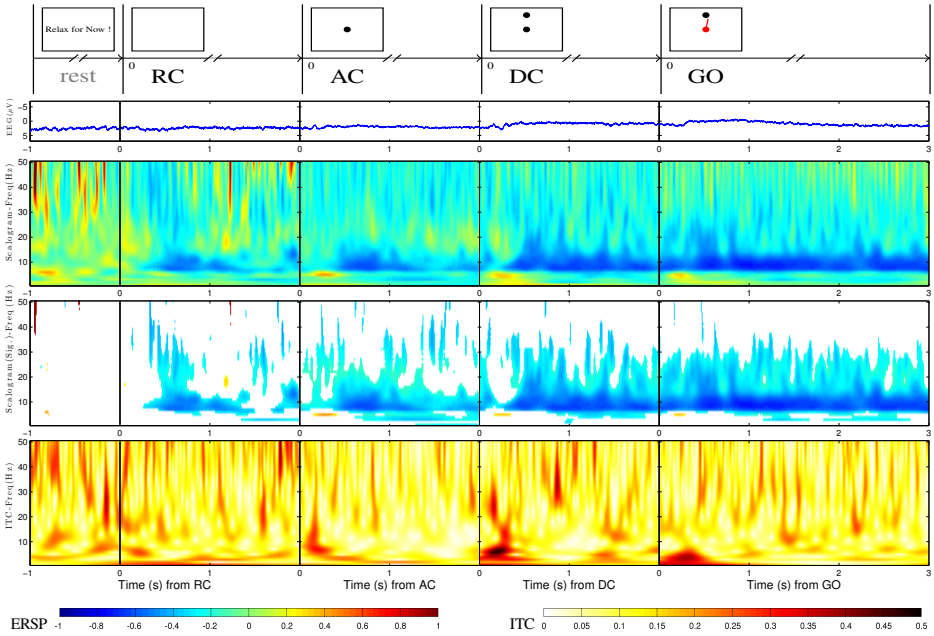

Figure 4.33. Time-frequency distribution for electrode C_3, for subject 3. Horizontal axes are time in seconds. Vertical axes are CAR EEG (μV) or Frequency (Hz). Zeros from left to right indicate the presentation of visual cues: RC, AC, DC and GO. Top: continuous wavelet transform (CWT) squared moduli (scalogram), normalised to pre-movement rest-time EEG. Dark blue shows 100% ERD and dark red 100% ERS. Middle: the same distribution with only statistically significant values retained. Bottom: inter-trial coherence (ITC).

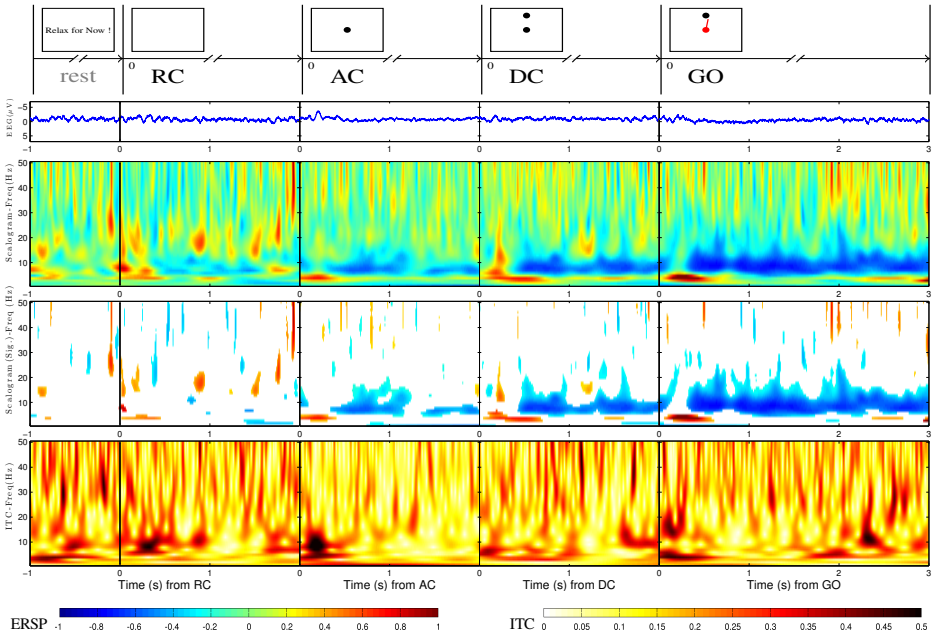

Figure 4.34. Time-frequency distribution for electrode C_4, for subject 3. Horizontal axes are time in seconds. Vertical axes are CAR EEG (μV) or Frequency (Hz). Zeros from left to right indicate the presentation of visual cues: RC, AC, DC and GO. Top: continuous wavelet transform (CWT) squared moduli (scalogram), normalised to pre-movement rest-time EEG. Dark blue shows 100% ERD and dark red 100% ERS. Middle: the same distribution with only statistically significant values retained. Bottom: inter-trial coherence (ITC).

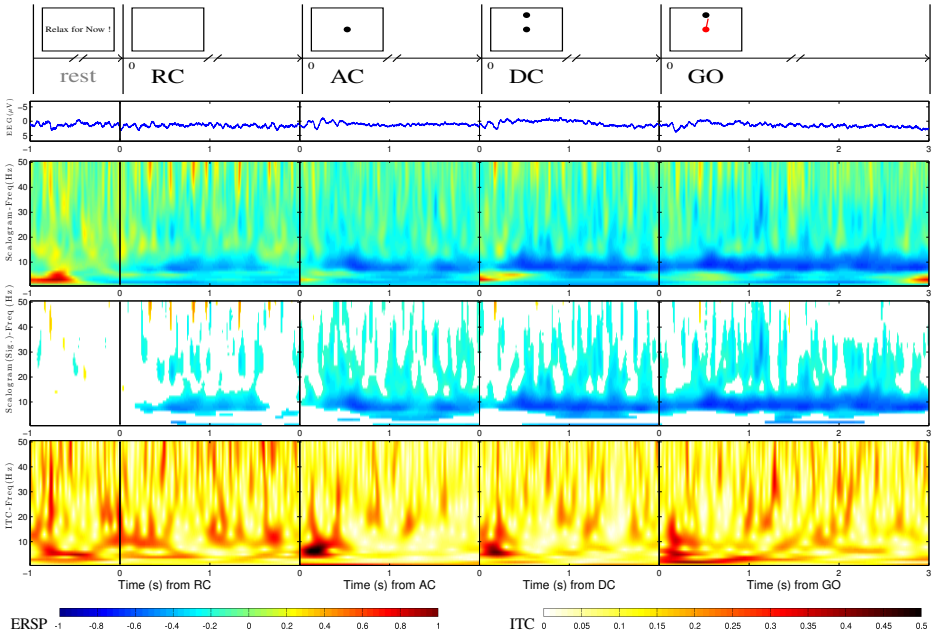

Figure 4.35. Time-frequency distribution for electrode F_z, for subject 3. Horizontal axes are time in seconds. Vertical axes are CAR EEG (μV) or Frequency (Hz). Zeros from left to right indicate the presentation of visual cues: RC, AC, DC and GO. Top: continuous wavelet transform (CWT) squared moduli (scalogram), normalised to pre-movement rest-time EEG. Dark blue shows 100% ERD and dark red 100% ERS. Middle: the same distribution with only statistically significant values retained. Bottom: inter-trial coherence (ITC).

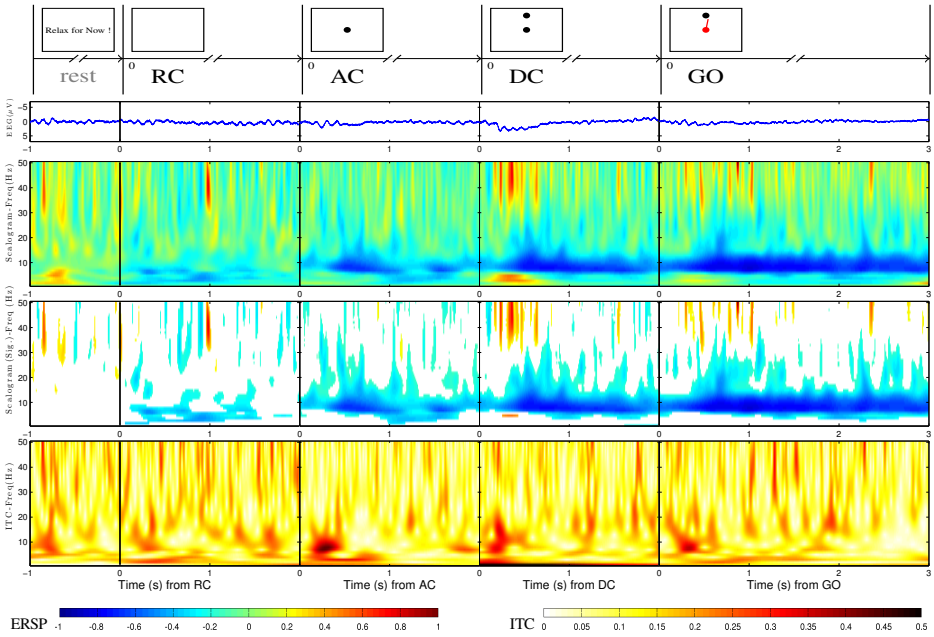

Figure 4.36. Time-frequency distribution for electrode P_z, for subject 3. Horizontal axes are time in seconds. Vertical axes are CAR EEG (μV) or Frequency (Hz). Zeros from left to right indicate the presentation of visual cues: RC, AC, DC and GO. Top: continuous wavelet transform (CWT) squared moduli (scalogram), normalised to pre-movement rest-time EEG. Dark blue shows 100% ERD and dark red 100% ERS. Middle: the same distribution with only statistically significant values retained. Bottom: inter-trial coherence (ITC).

Table 4.8. Summary of statistically significant ERD/ERS in CAR EEG that appear in all C_z, C_3, C_4, F_z and P_z electrodes, in majority (5/8) of subjects .

RC		AC		DC		GO	
Transient	Sustained	Transient	Sustained	Transient	Sustained	Transient	Sustained
-[24,36]	none	+5 -[8,10] -[15,33]	variable	-[9,10] -[13,35]	-[16,24]	-[8,37]	-[8,31]

[a] + shows ERS and - shows ERD. Numbers are frequency ranges in Hz.
[b] Transient means the first 0.5-1.0s after the cue where transient or phasic activity is observed. Sustained, indicates the sustained or tonic activity that lasts about 1.0-1.5s afterwards

transient signatures of ERD can be seen between 24-36 Hz, followed by sustained ERD or ERS (ERD or ERS is not consistent across subjects). When the attention cue (AC) appears, a relatively strong transient ERS at 5 Hz and ERD in 8-10 Hz and 15-33 Hz range happens. This is followed by sustained activity which is dependent on the electrode positions. Directional cue (DC) induces ERD in 9-10 Hz and 13-35 Hz ranges, as well as a sustained ERD in the 16-24 Hz range. When the GO command appears and subjects actually start exerting force, considerable transient ERD between 8-37 Hz is observed. The sustained features which correspond to maintaining the requested force level, include ERD between 8-31 Hz (see Table 4.8).

4.3.2.2. Spatial Features of Common-Average Referenced ERD and ERS

While many EEG channels show similar time-frequency patterns, there are also local region-specific characteristics in each EEG channel. The local features in CAR EEG are more pronounced compared to ELR ELR.

In order to obtain a broader perspective on CAR surface EEG activity, the spatial distribution maps of time-frequency representations can be studied. Figures 4.37, 4.38, 4.39 and 4.40 show the spatial variation of CAR surface EEG time-frequency features for Subject S3.

In order to summarise the results for all subjects, Table 4.9 lists the major significant ERD/ERS in CAR EEG for electrodes C_z, C_3, C_4, F_z, and P_z that are observed in the majority of subjects (5 or more out of 8). The table lists the features that can be seen in 5 or more out of 8 subjects by visual inspection of significant wavelet moduli at each frequency (1-50Hz, 1 Hz steps) for the transient and sustained segments of each execution stage (see Appendix E). This corresponds to 4.88% significance level (see Appendix D). The table describes the transient ERD/ERS and sustained ERD/ERS after each visual cue. This is an abstraction of the results in Appendix E.

In addition to the aforementioned observed ERD/ERS for all electrodes (see Sec-

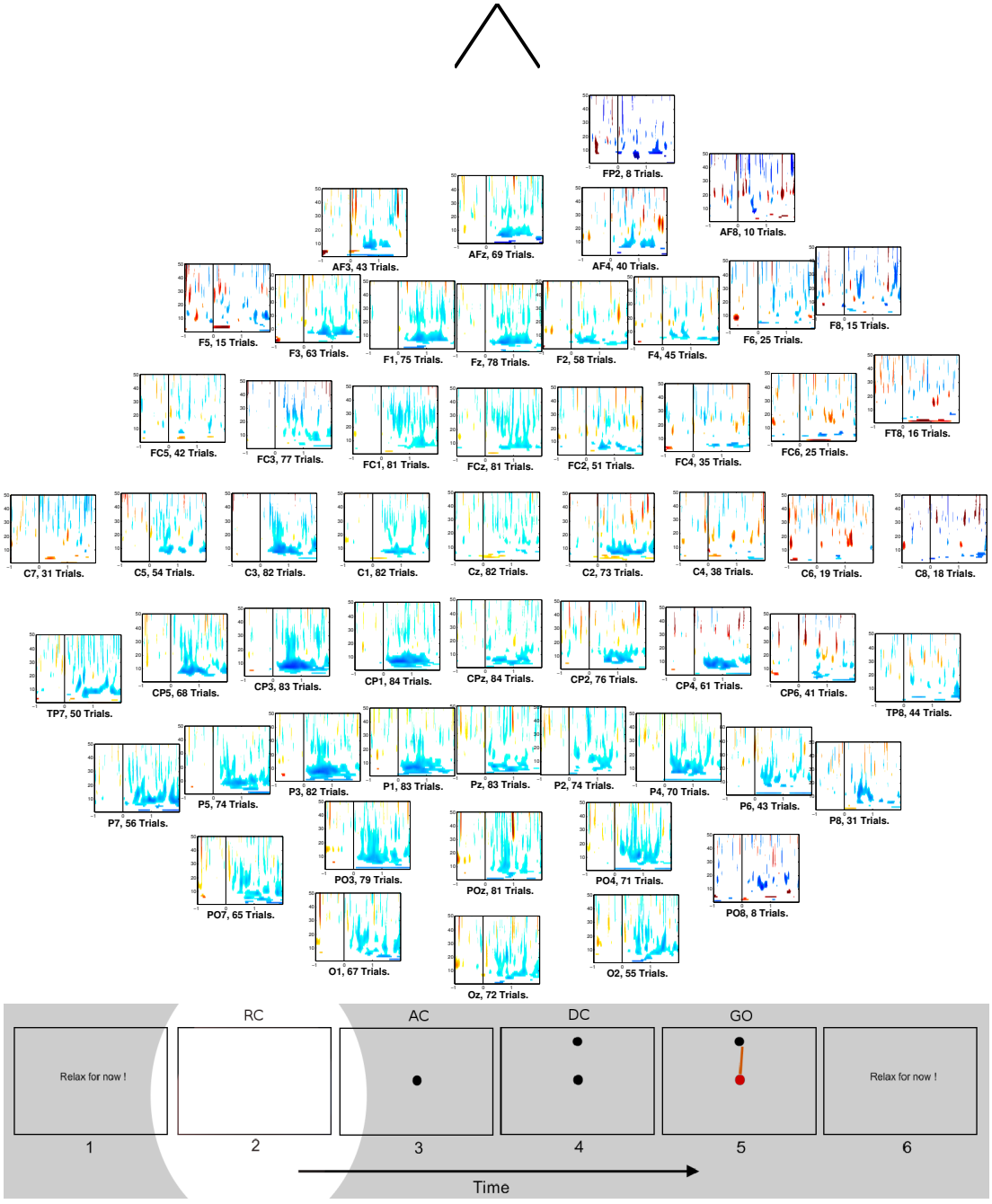

Figure 4.37. Spatial distribution of trial-averaged CAR EEG time-frequency distributions, from subject 3 and in time stage RC. For each electrode position the normalised continuous wavelet transform scalograms are plotted as described in Figure 4.13.

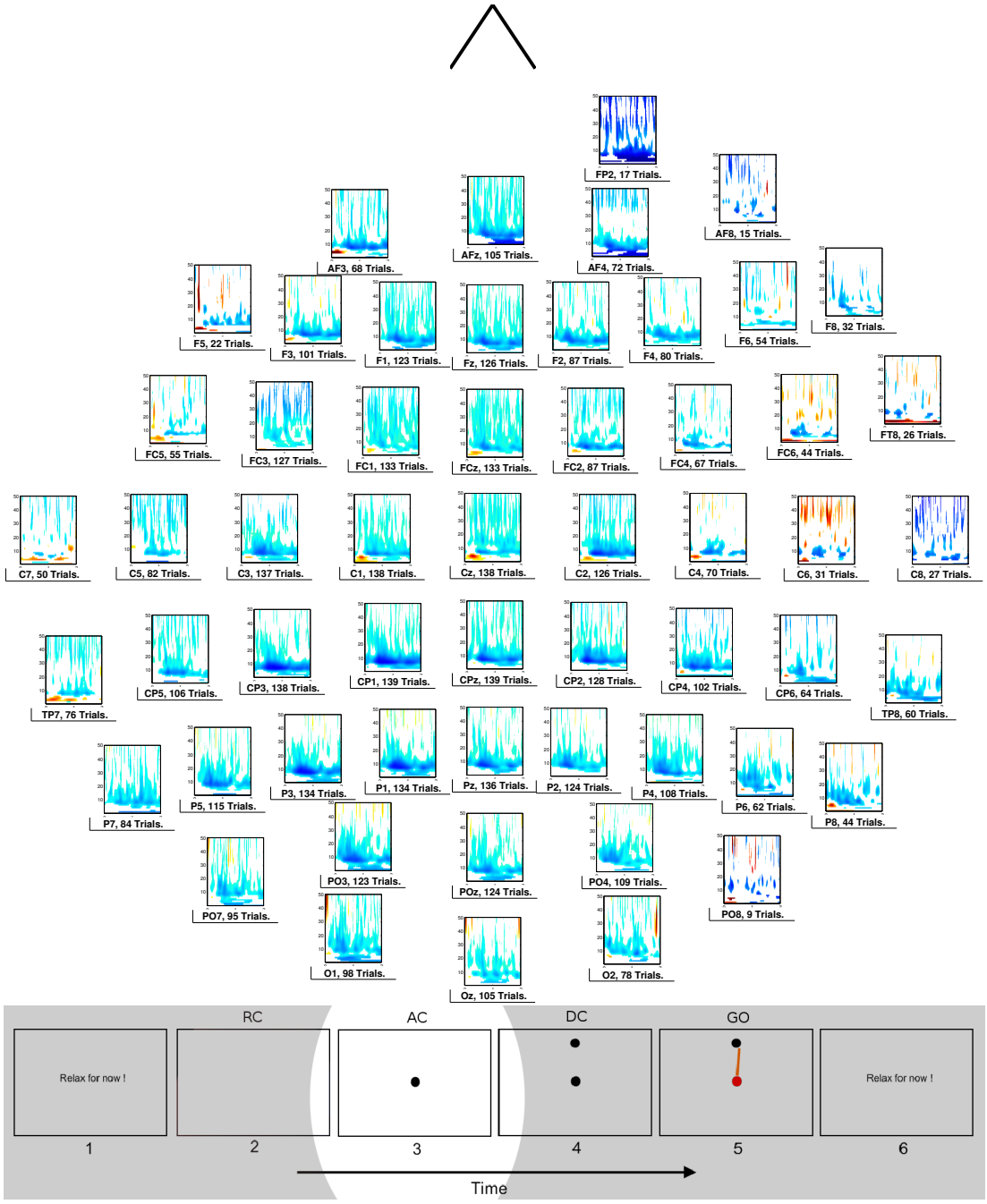

Figure 4.38. Spatial distribution of trial-averaged CAR EEG time-frequency distributions, from subject 3 and in time stage AC. For each electrode position the normalised continuous wavelet transform scalograms are plotted as described in Figure 4.13.

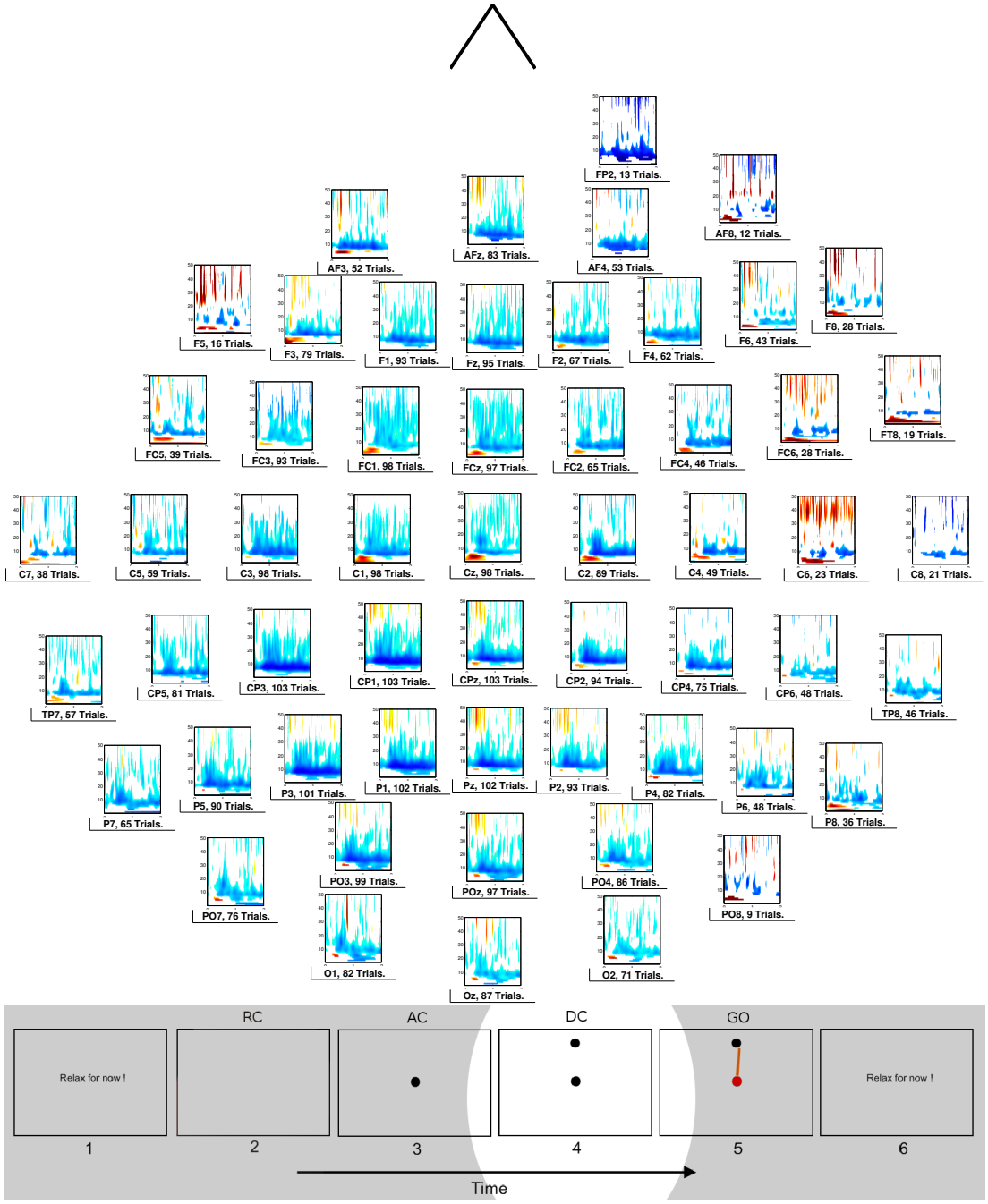

Figure 4.39. Spatial distribution of trial-averaged CAR EEG time-frequency distributions, from subject 3 and in time stage DC. For each electrode position the normalised continuous wavelet transform scalograms are plotted as described in Figure 4.13.

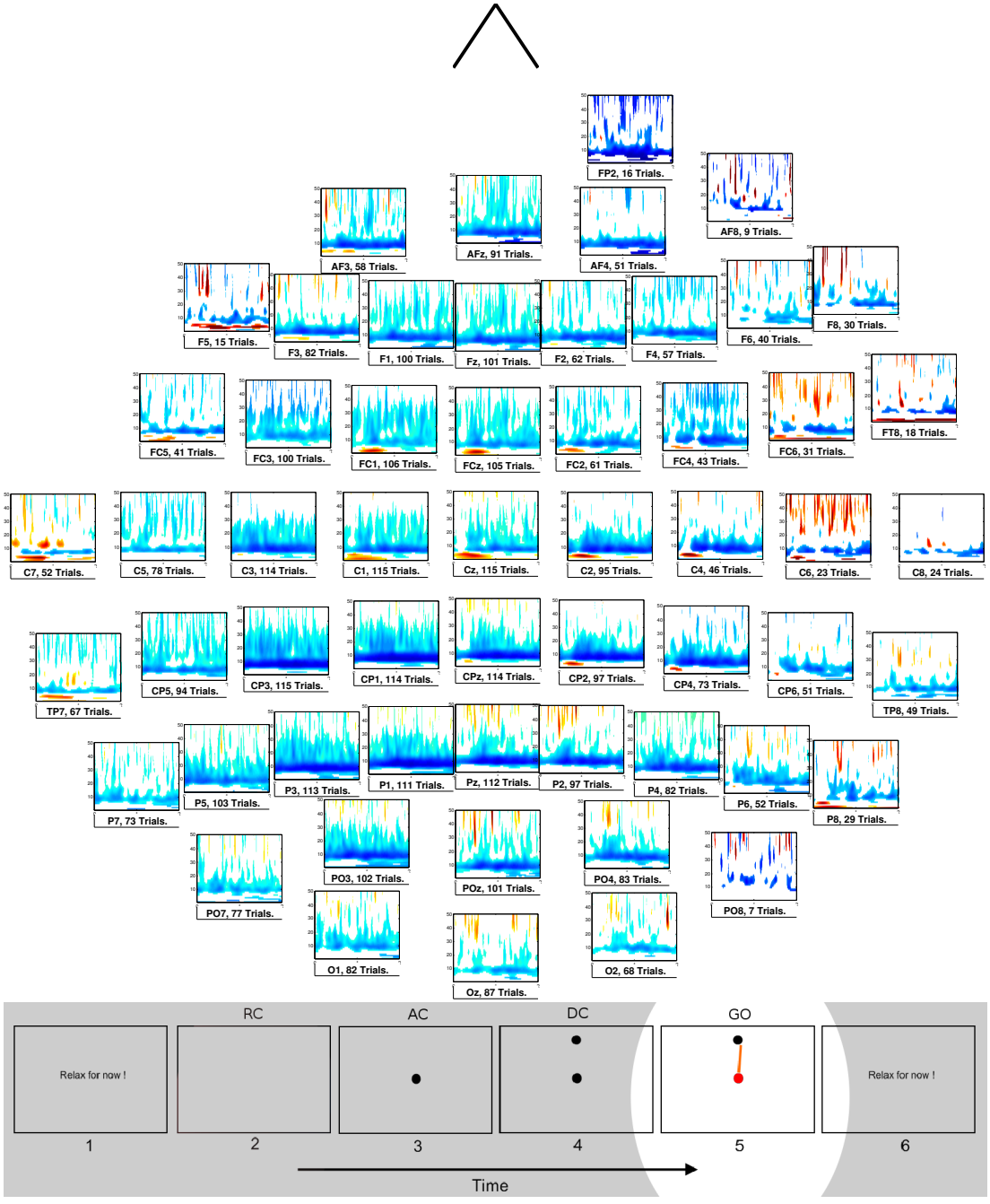

Figure 4.40. Spatial distribution of trial-averaged CAR EEG time-frequency distributions, from subject 3 and in time stage GO. For each electrode position the normalised continuous wavelet transform scalograms are plotted as described in Figure 4.13.

Table 4.9. Summary of statistically significant ERD/ERS in CAR EEG observed in majority (5/8) of subjects in electrodes C_z, C_3, C_4, F_z and P_z .

Task	RC		AC		DC		GO	
	Transient	Sustained	Transient	Sustained	Transient	Sustained	Transient	Sustained
C_z	+5 -[17,41]	+[8,9]	+3 -[8,10] -[14,15] **-[16,32]** -[33,50]	-2 -[17,46]	+[2,7] -[9,10] -[13,18] **-[19,35]** -[36,42]	-[16,45]	+[2,6] -[7,10] **-[11,35]** -[36,43]	-[1,7] **-[8,26]** -[27,50]
C_3	-6 **-7** -[8,42]	+[12,18]	-1 +[4,5] -[6,17] **-[18,50]**	-1 -3 -[14,45]	-[6,17] **-[18,38]** -[39,50]	-[1,2] -[7,15] **-[16,29]** -[30,41]	-1 -[6,10] **-[11,41]** -[42,50]	-[1,14] **-[15,35]** -[36,48]
C_4	-6 -[9,11] -[18,36]	+[14,19] +[36,43]	+[4,5] -[6,11] -[15,20] **-[21,26]** -[27,38]	-1 -[15,34]	+[3,5] -[6,13] $\pm$ [14,16] **-[17,28]** -[29,40]	-[1,2] -[6,21] **-[22,30]** -[31,35]	-1 -[5,13] **-[14,30]** -[31,50]	-[1,15] **-[16,31]** -[32,42]
F_z	+6 -[8,12] -[15,16] $\pm$ [21,27] -[28,39]	-5 -[18,24]	+[5,6] -[8,18] **-[19,30]** -[31,40]	-1 -[14-24]	+[2,7] -[8,17] **-[18,30]** -[31,47]	+5 -[9,37]	+[3,6] -[8,13] **-[14,41]** -[42,50]	-[1,4] **-[8,32]** -[33,40]
P_z	-[9,20] -[24,38]	none	+[3,6] -[7,33] -[37,46]	-1 -8 -[11,15] +[21,22]	+[2,7] -[8,35]	-5 -[13,24] +[36,50]	+[2,4] -[8,18] **-[19,24]** -[25,37] +[39,50]	-1 -[5,31] +[38,50]

[a] + shows ERS, - shows ERD, and $\pm$ shows ERS followed by ERD. Numbers are frequency ranges in Hz and **bold** entries show observation of ERD/ERS in all of the subjects.
[b] Transient means the first 0.5-1.0s after the cue where transient or phasic activity is observed. Sustained, indicates the sustained or tonic activity that lasts about 1.0-1.5s after the transient stage.
[c] ERD/ERS in 5 of 8 subjects corresponds to 0.0488 significance level. Similarly, ERD/ERS in 8 of 8 subjects corresponds to 0.000046 significance level.

tion 4.3.2.1), the following notable local features are observed. Other local features that are not explicitly highlighted below are mostly ERDs with extended frequency range of those listed in Table 4.8.

RC (Rest) stage: After readiness cue (RC), F_z and C_z show transient ERS at 5-6Hz and F_z shows a sequential ERS-ERD in 21-27 Hz range. ERD in 8-12 Hz is observed in all but C_z electrode. This is followed by sustained ERS at 8-9 Hz for C_z, 13-18 Hz for C_3 and C_4, and 35-43 Hz for C_4, while F_z shows sustained ERD in 18-24 Hz range.

AC (Preparation) stage: Succeeding the AC, γ band (30-50 Hz) ERD can be seen in different electrodes and most notably in C_z and especially C_3. There is sustained ERS, specifically in parietal electrode P_z between 21-22 Hz. The sustained activity in frontal F_z is ERD from 14 Hz to 24 Hz. This is also observed in central electrodes up to 34 Hz

and up to 46 Hz for C_z and C_3.

DC (Planning) stage: Directional cue, causes a notable ERS in 2-7 Hz for all electrodes except C_3. The common pattern of ERD between 13-35 Hz extends up to 50 Hz in F_z and C_3. F_z shows sustained ERS about 5 Hz while P_z shows ERD about 5 Hz. A sustained ERD between 7-15 Hz is observed in C_3, C_4, and F_z. There is also an ERS specific to parietal P_z between 36-50 Hz. Meanwhile, other electrodes show ERD in 25-36 Hz and up to 45 Hz in C_z and C_3.

GO (Execution) stage: The prominent low frequency ERS between 2-6 Hz is observed in C_z, F_z, and to some extent in P_z. While the common pattern of ERD between 8-37 Hz extends to 43 Hz in C_z and up to 50 Hz in C_3, C_4, and F_z; P_z shows an opposite ERS in gamma band (39-50 Hz). During the sustained force generation, there is ERD in the 2-7 Hz range in C_z, C_3, and C_4, and to some extent in F_z. The gamma band activity (31-50 Hz) in sustained GO stage appears as low gamma band ERD in (31-40 Hz) for C_4 and F_z and 30-50 Hz gamma band ERD in C_z and C_3. Again, P_z shows the different ERS pattern in 40-50 Hz gamma band.

4.3.3. Summary of Time-Frequency EEG Signatures

The features common to all electrodes in ELR EEG include transient β band ERD after all cues and sustained β band ERD after directional cue and during exertion. Low sustained α band ERD is seen during execution. Transient θ ERS is observed after attention cue, directional cue and GO.

The most pronounced local features are: (1) θ anf α band ERD in parietal regions (P_z) and central contralateral (C_3) in most stages of movement which is extended to central ipsilateral (C_4) during preparation and planning and extended to C_z during planning and execution, (2) sustained β ERD in preparation in all areas, exept frontal area (F_z), (3) sustained γ ERD in central areas (C_z, C_4, C_3) in planning and execution; transient γ ERD in C_z and C_3 extended to other areas during preparation and planning; transient γ ERS in parietal and central ipsilateral areas (C_4, P_z) during force development.

The features common to all electrodes in CAR EEG include transient β band ERD after all cues and sustained β band ERD after directional cue and during exertion. Low transient α band ERD is seen after the attention and directional cues. Transient and sustained α band ERD (μ rhythm ERD) is observed during force development and maintenance.

The most pronounced local features are: (1) δ and θ band (2-7 Hz) transient ERS in the central, frontal, and parietal regions (C_z, P_z, F_z), but less in the temporal regions,

after all cues, (2) transient and sustained γ band ERD (30-50 Hz) in regions other than the parietal area, observed in readiness, planning and execution stages, to different extents, especially during execution. The parietal area (e.g. P_z) shows γ band ERS before and during force generation.

The features common to all electrodes are very similar when comparing ELR and CAR. β-band features are essentially the same. The feature specific to CAR is the transient α ERD in preparation and planning. The feature specific to ELR is the transient 4-5Hz ERS during planning and execution. Comparing the local features in different recording sites in ELR and CAR, it can be seen that the localisation characteristic of CAR has chnaged the common transient θ ERS to a local feature, as mentioned above. CAR has also accentuated the γ band ERD/ERS distribution patterns when comparing ELR and CAR results. This trend holds for other features, explained in inis section. In cases where a feature, such as α ERD as described in this section earlier, is present in majority of electrodes except for few electrodes, ELR results may better indicate the location(s) where the features is not present, compared to CAR.

4.4. Directional Information in EEG

So far, the time and time-frequency signatures of EEG in planning and execution of isometric tasks have been reported regardless of the exertion direction. The next imminent question is:

How are the time and time-frequency features of EEG modulated by exertion direction ?

For this purpose, the signal features in the four direction groups (right, left, up and down) are compared against each other. A corresponding question is whether the inter-group variance (against within-group variance) of the observed features are statistically significant. In Sections 4.4.1 and 4.4.2 the inter-group variance of time and time-frequency features are presented and Section 4.4.3 shows the classification rates, using linear classifiers.

4.4.1. Inter-Class Variance of Event-Related Potentials

Figures 4.41, 4.42, 4.43, 4.44, and 4.45 show the ERPs for all subjects in 4 different directions, as well as the significance of inter-class variance for ear-lobe referenced EEG.

Figures 4.46, 4.47, 4.48, 4.49, and 4.50 show the ERPs for all subjects in 4 different directions, as well as the significance of inter-class variance for common-average referenced EEG.

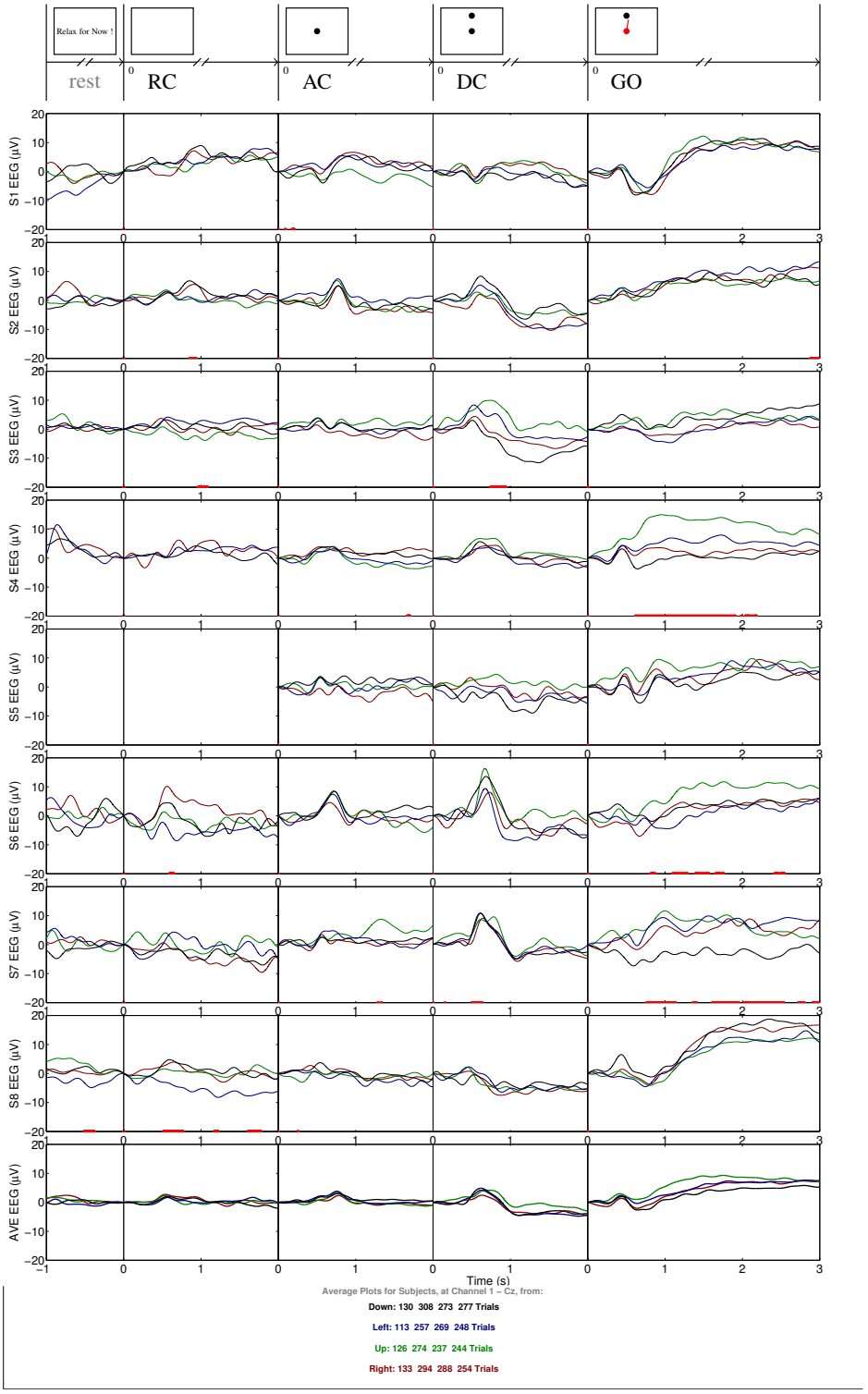

Figure 4.41. Trial-averaged event-related potentials (ERP) from ELR EEG (4 Hz low-pass filtered) for electrode C_z, for Subjects S1 (top panel) to S8, as well as the across-subject averaged values (bottom panel). Horizontal axes are time in seconds. Vertical axes are EEG (μV). Zeros from left to right indicate different stages of movement, as described in Figure 3.5 and the presentation of visual cues: RC, AC, DC and GO. Different colours show different directions and the thick red line below each individual subject's plot is the statistically significant (p-value<0.05) inter-class difference between the ERP of different directions. Average segments with too few acceptable trials are not plotted.

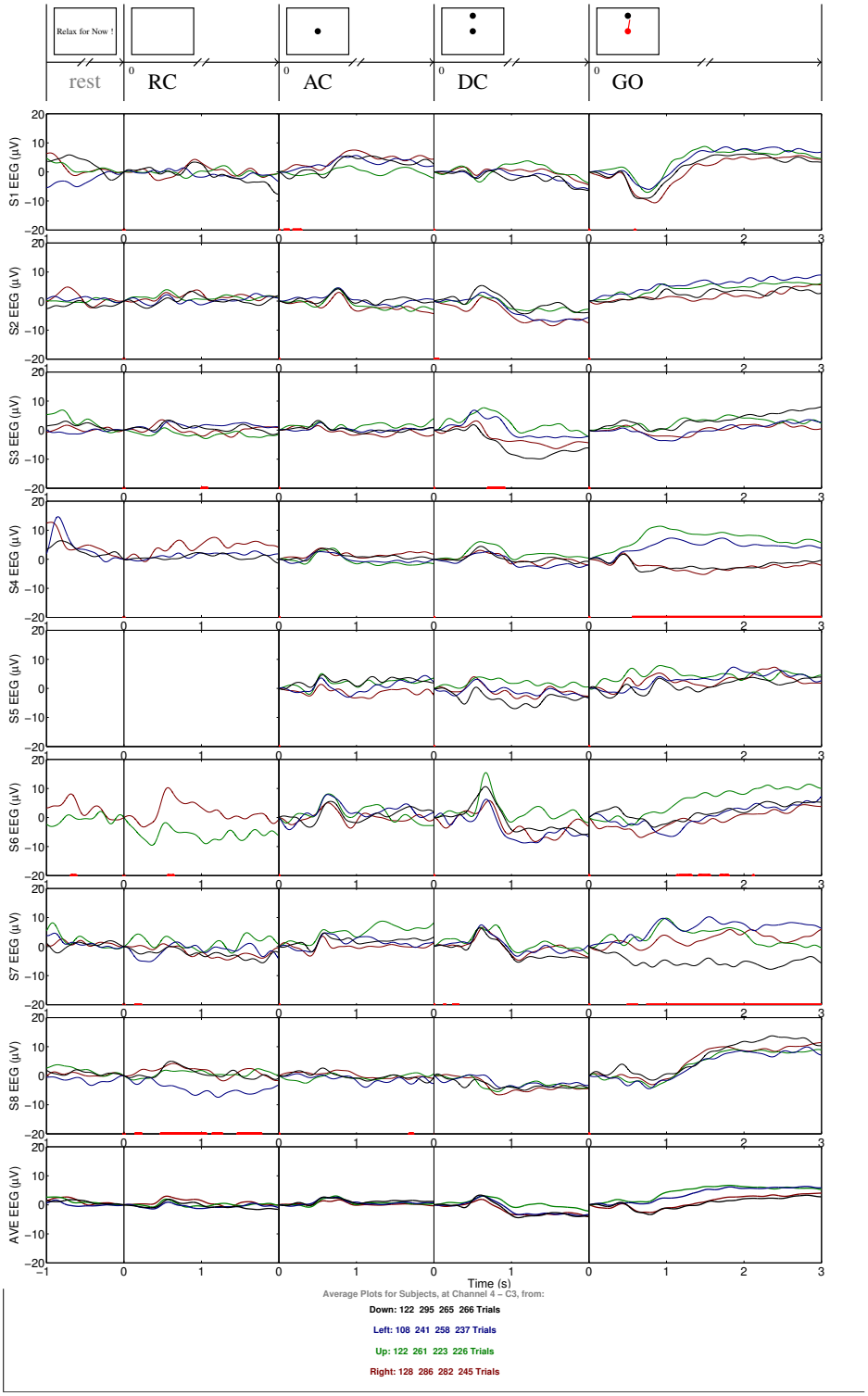

Figure 4.42. Trial-averaged event-related potentials (ERP) from ELR EEG (4 Hz low-pass filtered) for electrode C_3, for Subjects S1 (top panel) to S8, as well as the across-subject averaged values (bottom panel). Horizontal axes are time in seconds. Vertical axes are EEG (μV). Zeros from left to right indicate different stages of movement, as described in Figure 3.5 and the presentation of visual cues: RC, AC, DC and GO. Different colours show different directions and the thick red line below each individual subject's plot is the statistically significant (p-value<0.05) inter-class difference between the ERP of different directions. Average segments with too few acceptable trials are not plotted.

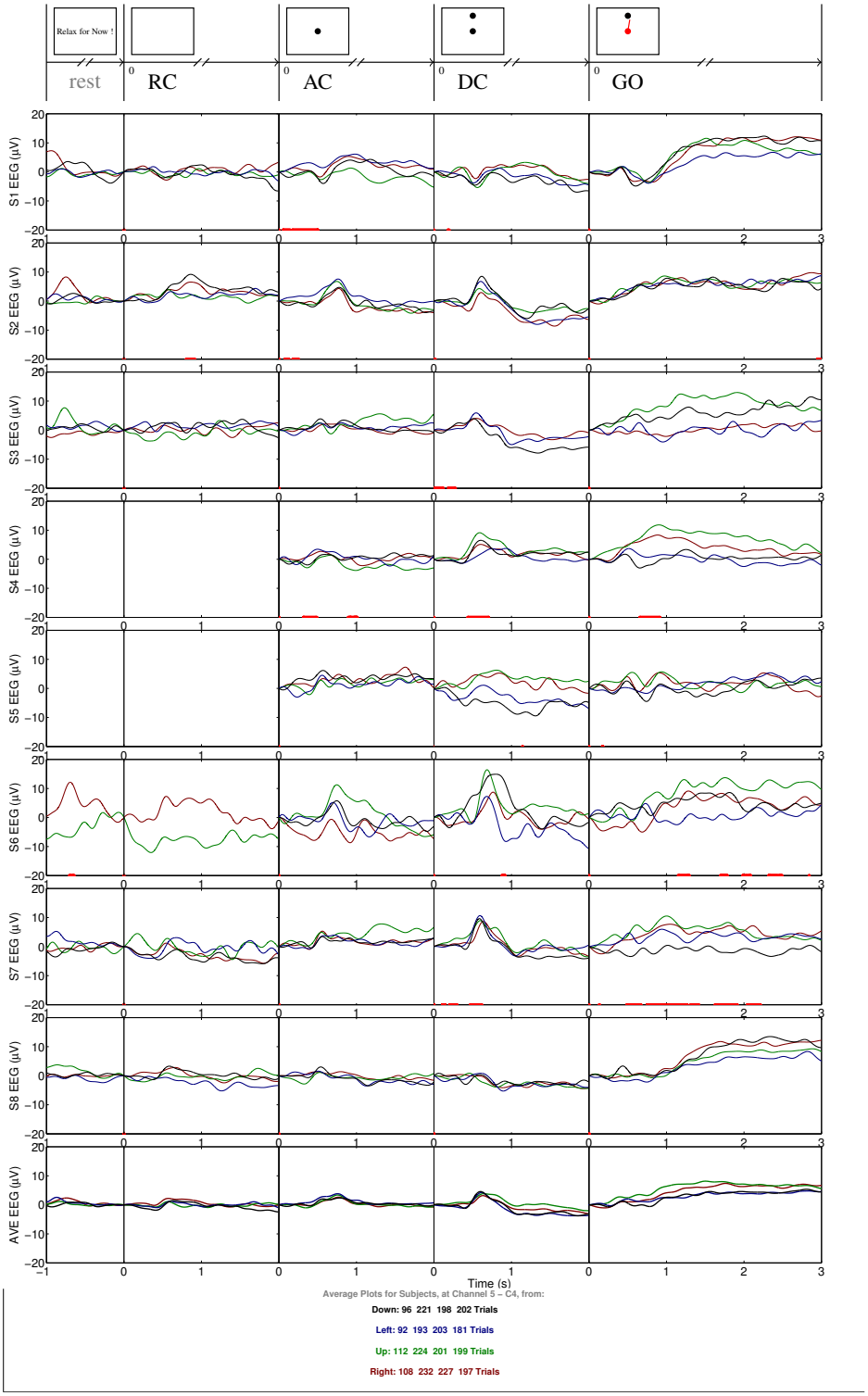

Figure 4.43. Trial-averaged event-related potentials (ERP) from ELR EEG (4 Hz low-pass filtered) for electrode C_4, for Subjects S1 (top panel) to S8, as well as the across-subject averaged values (bottom panel). Horizontal axes are time in seconds. Vertical axes are EEG (μV). Zeros from left to right indicate different stages of movement, as described in Figure 3.5 and the presentation of visual cues: RC, AC, DC and GO. Different colours show different directions and the thick red line below each individual subject's plot is the statistically significant (p-value<0.05) inter-class difference between the ERP of different directions. Average segments with too few acceptable trials are not plotted.

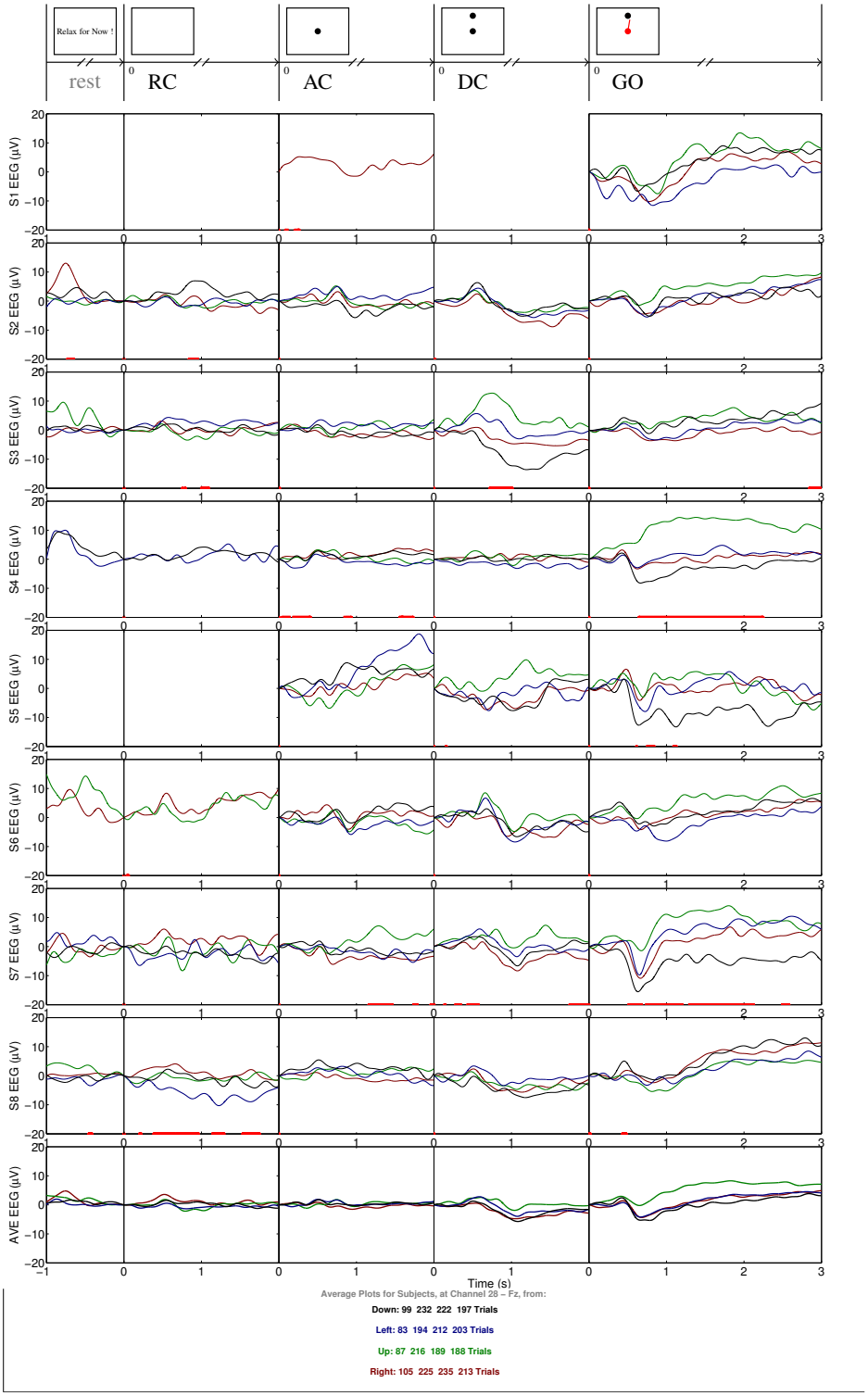

Figure 4.44. Trial-averaged event-related potentials (ERP) from ELR EEG (4 Hz low-pass filtered) for electrode F_z, for Subjects S1 (top panel) to S8, as well as the across-subject averaged values (bottom panel). Horizontal axes are time in seconds. Vertical axes are EEG (μV). Zeros from left to right indicate different stages of movement, as described in Figure 3.5 and the presentation of visual cues: RC, AC, DC and GO. Different colours show different directions and the thick red line below each individual subject's plot is the statistically significant (p-value<0.05) inter-class difference between the ERP of different directions. Average segments with too few acceptable trials are not plotted.

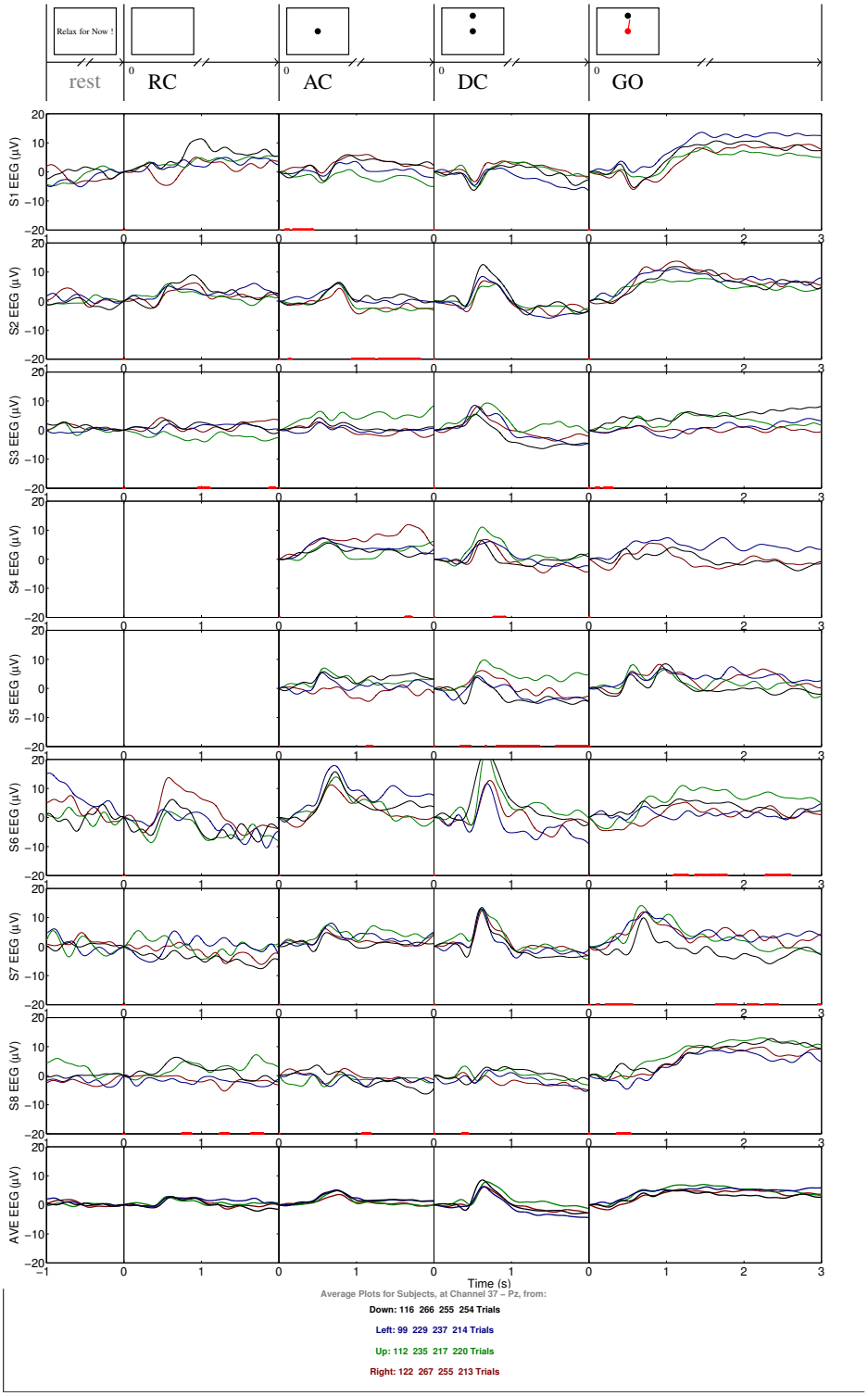

Figure 4.45. Trial-averaged event-related potentials (ERP) from ELR EEG (4 Hz low-pass filtered) for electrode P_z, for Subjects S1 (top panel) to S8, as well as the across-subject averaged values (bottom panel). Horizontal axes are time in seconds. Vertical axes are EEG (μV). Zeros from left to right indicate different stages of movement, as described in Figure 3.5 and the presentation of visual cues: RC, AC, DC and GO. Different colours show different directions and the thick red line below each individual subject's plot is the statistically significant (p-value<0.05) inter-class difference between the ERP of different directions. Average segments with too few acceptable trials are not plotted.

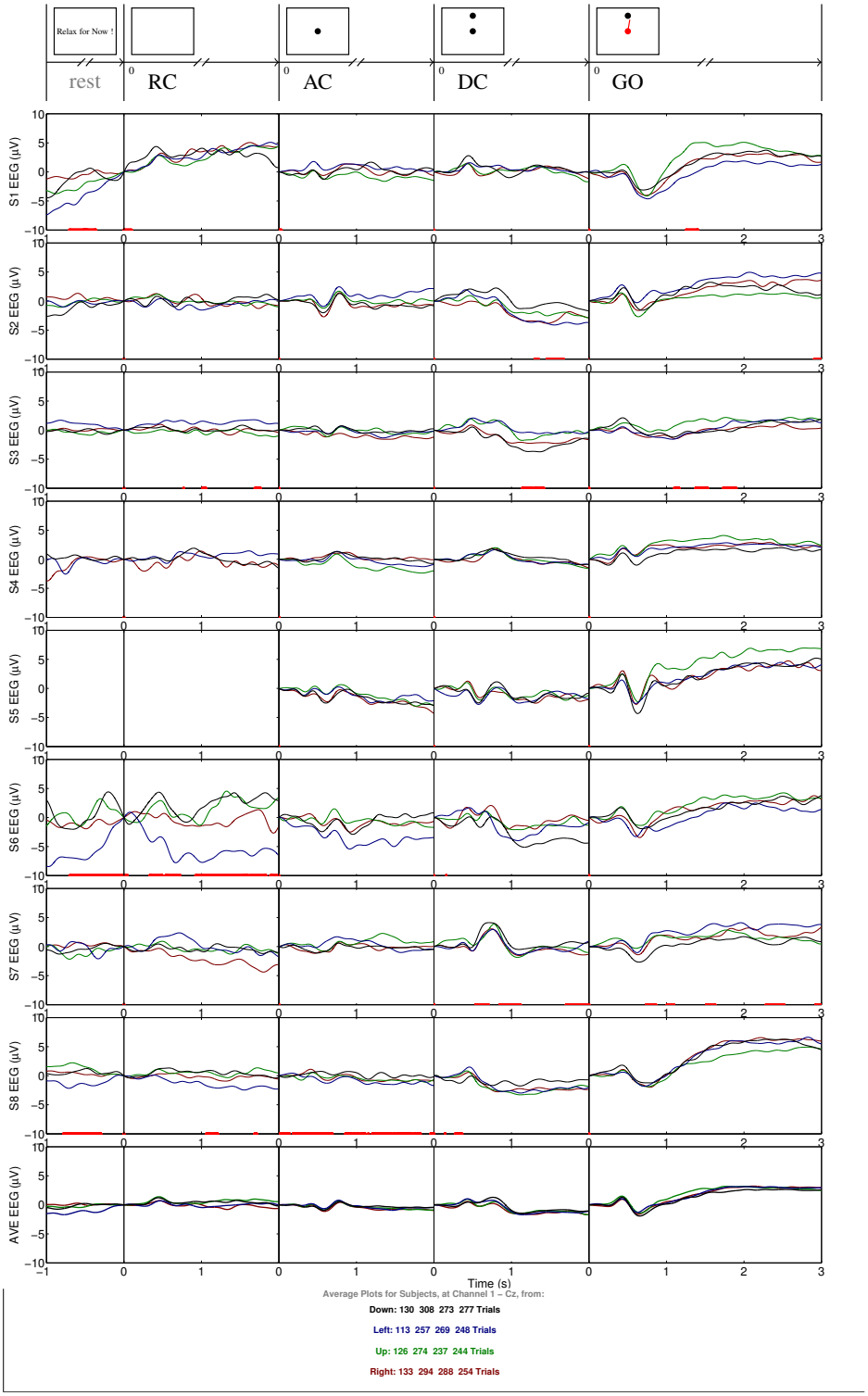

Figure 4.46. Trial-averaged event-related potentials (ERP) from CAR EEG (4 Hz low-pass filtered) for electrode C_z, for Subjects S1 (top panel) to S8, as well as the across-subject averaged values (bottom panel). Horizontal axes are time in seconds. Vertical axes are EEG (μV). Zeros from left to right indicate different stages of movement, as described in Figure 3.5 and the presentation of visual cues: RC, AC, DC and GO. Different colours show different directions and the thick red line below each individual subject's plot is the statistically significant (p-value<0.05) inter-class difference between the ERP of different directions. Average segments with too few acceptable trials are not plotted.

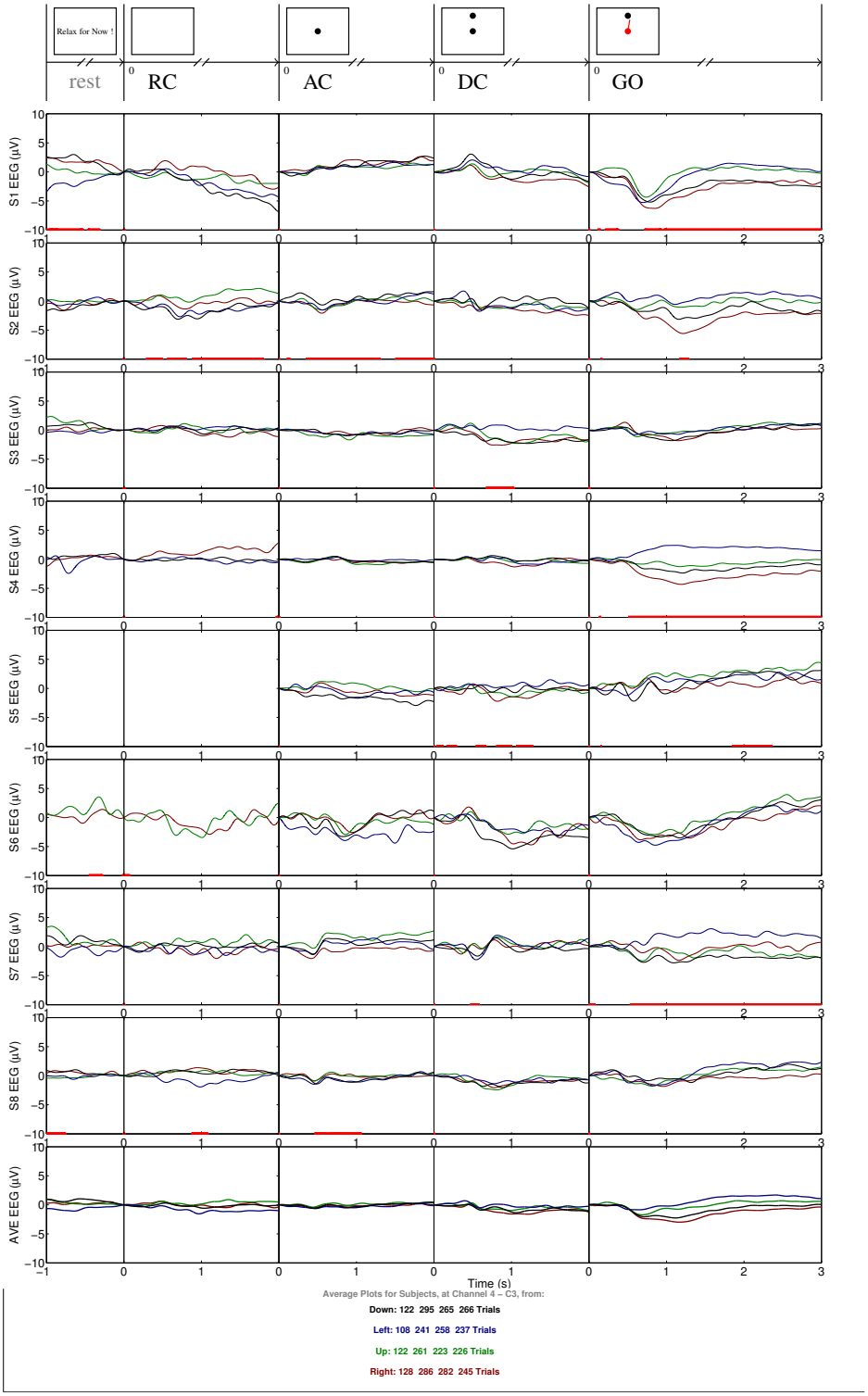

Figure 4.47. Trial-averaged event-related potentials (ERP) from CAR EEG (4 Hz low-pass filtered) for electrode C_3, for Subjects S1 (top panel) to S8, as well as the across-subject averaged values (bottom panel). Horizontal axes are time in seconds. Vertical axes are EEG (μV). Zeros from left to right indicate different stages of movement, as described in Figure 3.5 and the presentation of visual cues: RC, AC, DC and GO. Different colours show different directions and the thick red line below each individual subject's plot is the statistically significant (p-value<0.05) inter-class difference between the ERP of different directions. Average segments with too few acceptable trials are not plotted.

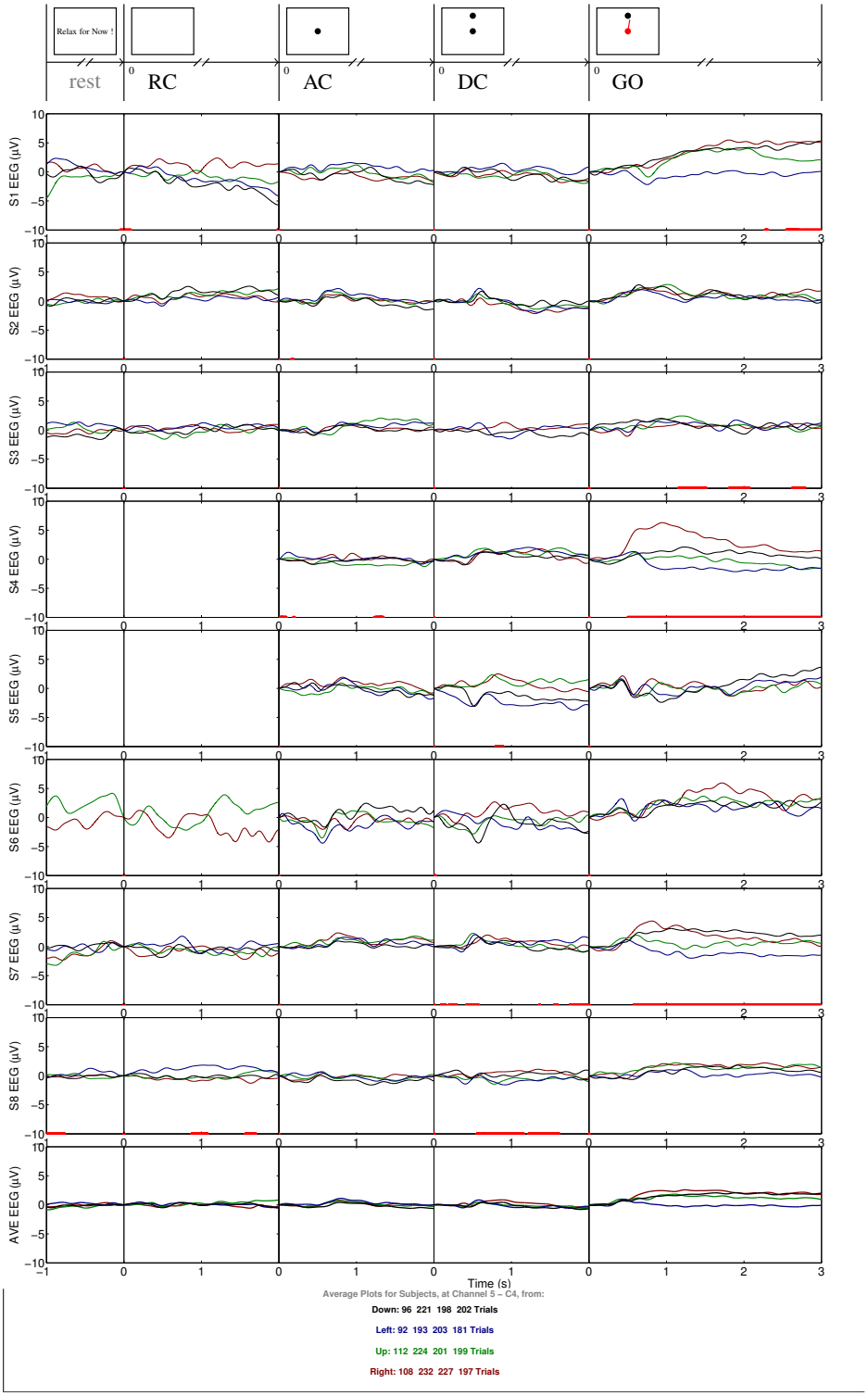

Figure 4.48. Trial-averaged event-related potentials (ERP) from CAR EEG (4 Hz low-pass filtered) for electrode C_4, for Subjects S1 (top panel) to S8, as well as the across-subject averaged values (bottom panel). Horizontal axes are time in seconds. Vertical axes are EEG (μV). Zeros from left to right indicate different stages of movement, as described in Figure 3.5 and the presentation of visual cues: RC, AC, DC and GO. Different colours show different directions and the thick red line below each individual subject's plot is the statistically significant (p-value<0.05) inter-class difference between the ERP of different directions. Average segments with too few acceptable trials are not plotted.

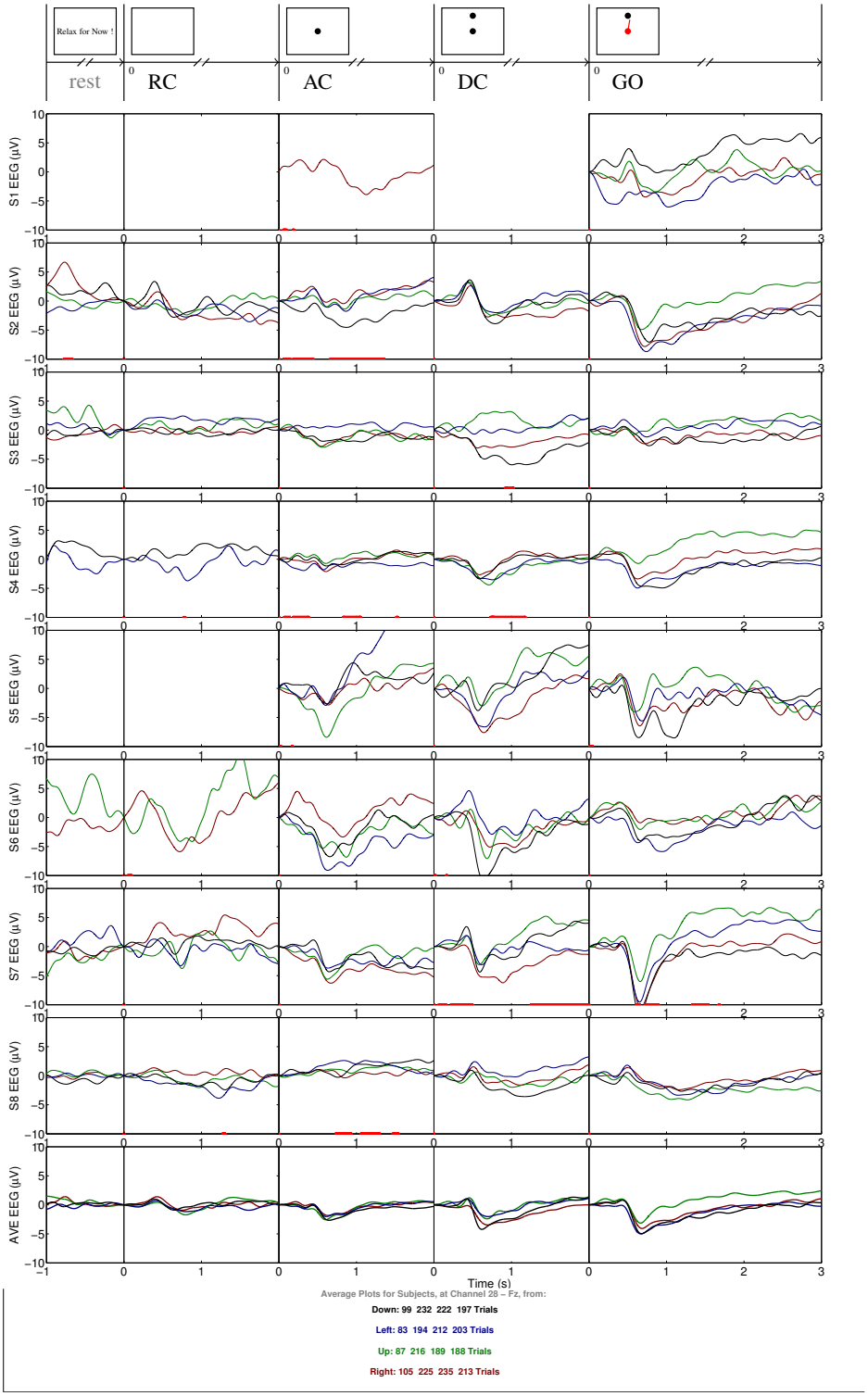

Figure 4.49. Trial-averaged event-related potentials (ERP) from CAR EEG (4 Hz low-pass filtered) for electrode F_z, for Subjects S1 (top panel) to S8, as well as the across-subject averaged values (bottom panel). Horizontal axes are time in seconds. Vertical axes are EEG (μV). Zeros from left to right indicate different stages of movement, as described in Figure 3.5 and the presentation of visual cues: RC, AC, DC and GO. Different colours show different directions and the thick red line below each individual subject's plot is the statistically significant (p-value<0.05) inter-class difference between the ERP of different directions. Average segments with too few acceptable trials are not plotted.

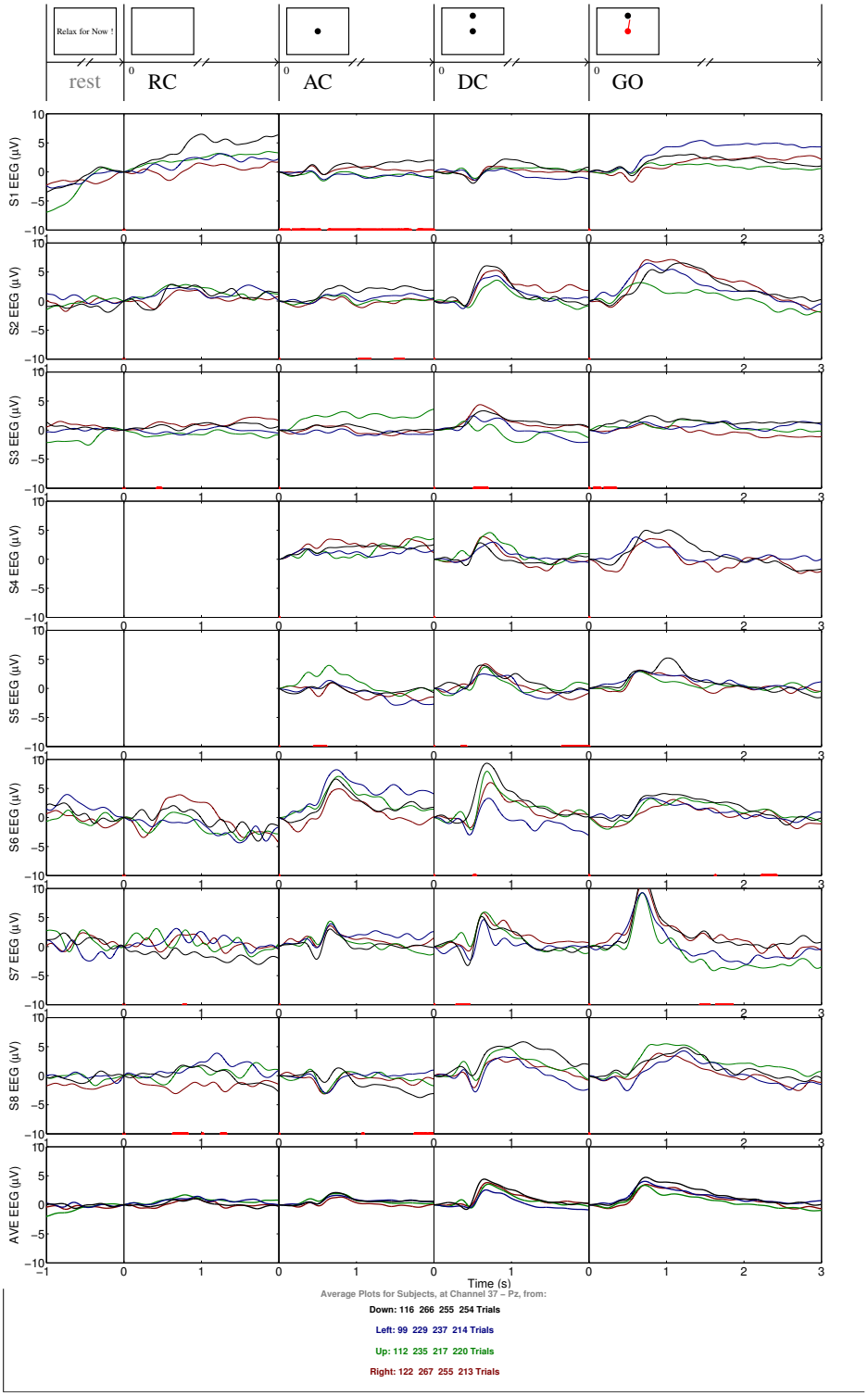

Figure 4.50. Trial-averaged event-related potentials (ERP) from CAR EEG (4 Hz low-pass filtered) for electrode P_z, for Subjects S1 (top panel) to S8, as well as the across-subject averaged values (bottom panel). Horizontal axes are time in seconds. Vertical axes are EEG (μV). Zeros from left to right indicate different stages of movement, as described in Figure 3.5 and the presentation of visual cues: RC, AC, DC and GO. Different colours show different directions and the thick red line below each individual subject's plot is the statistically significant (p-value<0.05) inter-class difference between the ERP of different directions. Average segments with too few acceptable trials are not plotted.

It can be seen from the inter-class differences in ELR ERPs, that only few subjects show significantly different (i.e. direction-dependent) ERPs during motor planning and execution. Compared to the RC and AC stages, in which no actual directional information exists and any reported differences are random, the planning and execution ERP values are not much different from chance level. However, in subjects who do show different ERPs, central electrodes give longer time spans of significantly different ERPs. In CAR EEG, the C_3 which is closest to the contralateral M1 regions of the arm muscles, shows the highest interclass difference during the physical exertion stage. In short, the direction-dependent variations of ERPs do not reach significance levels.

4.4.2. Inter-Class Variance of Time-Frequency Representations

Similar analysis can be performed on time-frequency coefficients (continuous Morlet wavelet transform moduli) to find the regions with significant inter-class variance.

Figures 4.51, 4.52, 4.53, 4.54, and 4.55 show the statistically significant inter-class difference in CWT scalograms for all subjects (4 different directions), using ear-lobe referenced EEG.

Figures 4.56, 4.57, 4.58, 4.59, and 4.60 show the statistically significant inter-class difference in CWT scalograms for all subjects (4 different directions), using common-average referenced EEG.

By carefully inspecting the significance levels of time-frequency representations it is seen that there are many scattered regions which show significant intergroup variance. However, in addition to this scattered subject-unspecific features, there are regions that exhibit more consistent inter-group variances across subjects (Previously reported, Nasseroleslami et al., 2011b; and reproduced in Figures 4.56, 4.57, 4.58, 4.59, and 4.60). Although the number of subjects who do show the significant values for each time-frequency point is lower than the significance level (5 out of 8 subjects), the observations may be summarised as follows: In central electrodes and to some extent F_z, especially in C_3, significant time-frequency features are seen in α and β bands (transient) and this happens during the motor execution or GO stage (See the black contoures, bottom panels of Figures 4.56 and 4.57). Contrarily, the P_z electrode shows significant values mostly during motor planning or DC stage (See the the black contour, bottom panel of Figure 4.60) and the values are in δ, θ and the α bands (transient). Again the direction-dependent variations of ERD/ERS do not reach significance level. The trends are considerably accentuated by common-average referencing.

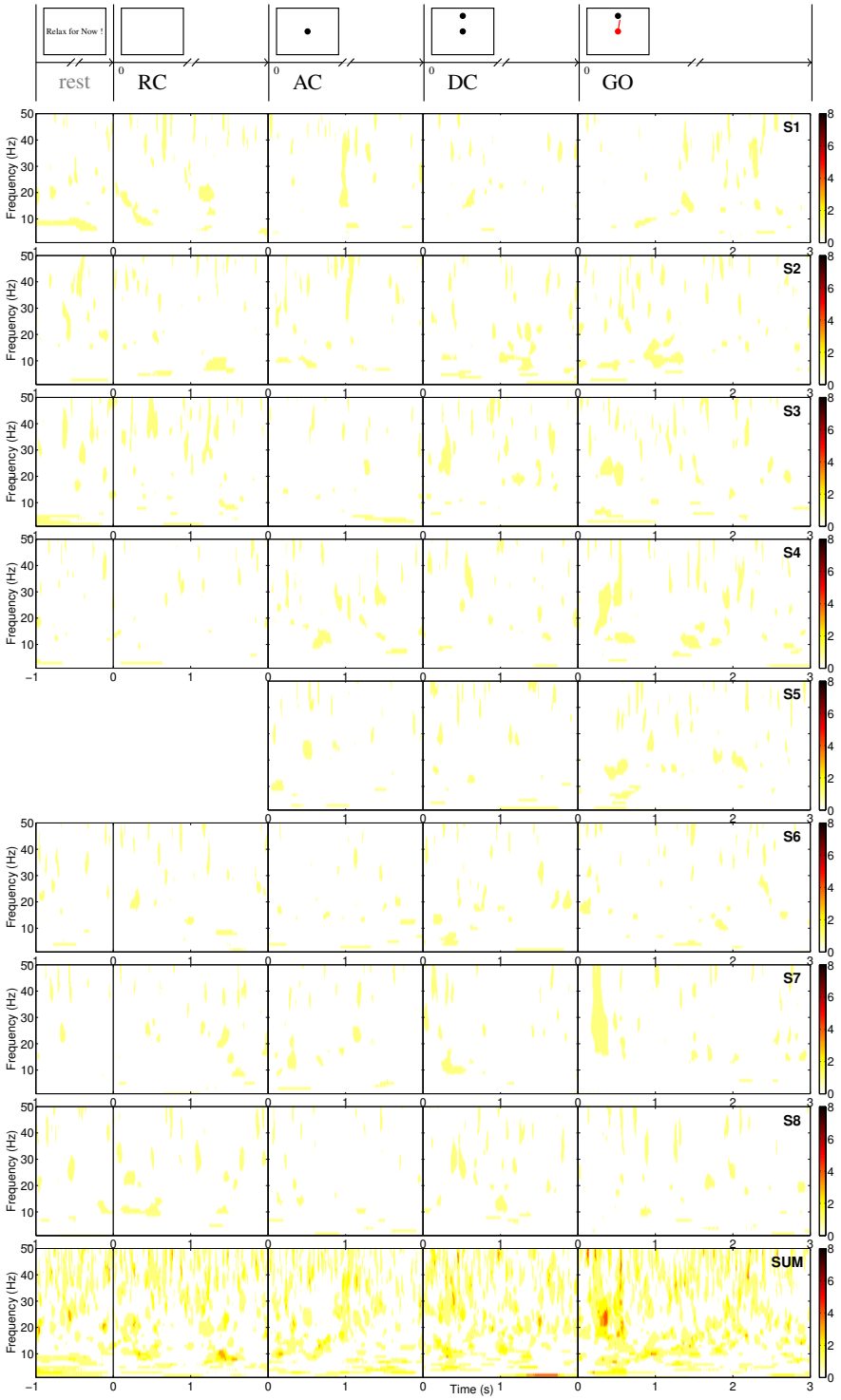

Figure 4.51. Regions of continuous Morlet wavelet transform scalograms for electrode C_z in which the coefficient values show statistically significant inter-group (for 4 directions) variance (p-value<0.05). ELR EEG is used. From top panels downward: Subjects S1 (top panel) to S8, as well as the overlapped regions (bottom panel) in which the number of subjects with significant difference is shown. Horizontal axes are time in seconds. Vertical axes show Frequency (Hz). Zeros from left to right indicate different stages of movement, as described in Figure 3.5 and the presentation of visual cues: RC, AC, DC and GO. Segments with too few acceptable trials are not plotted.

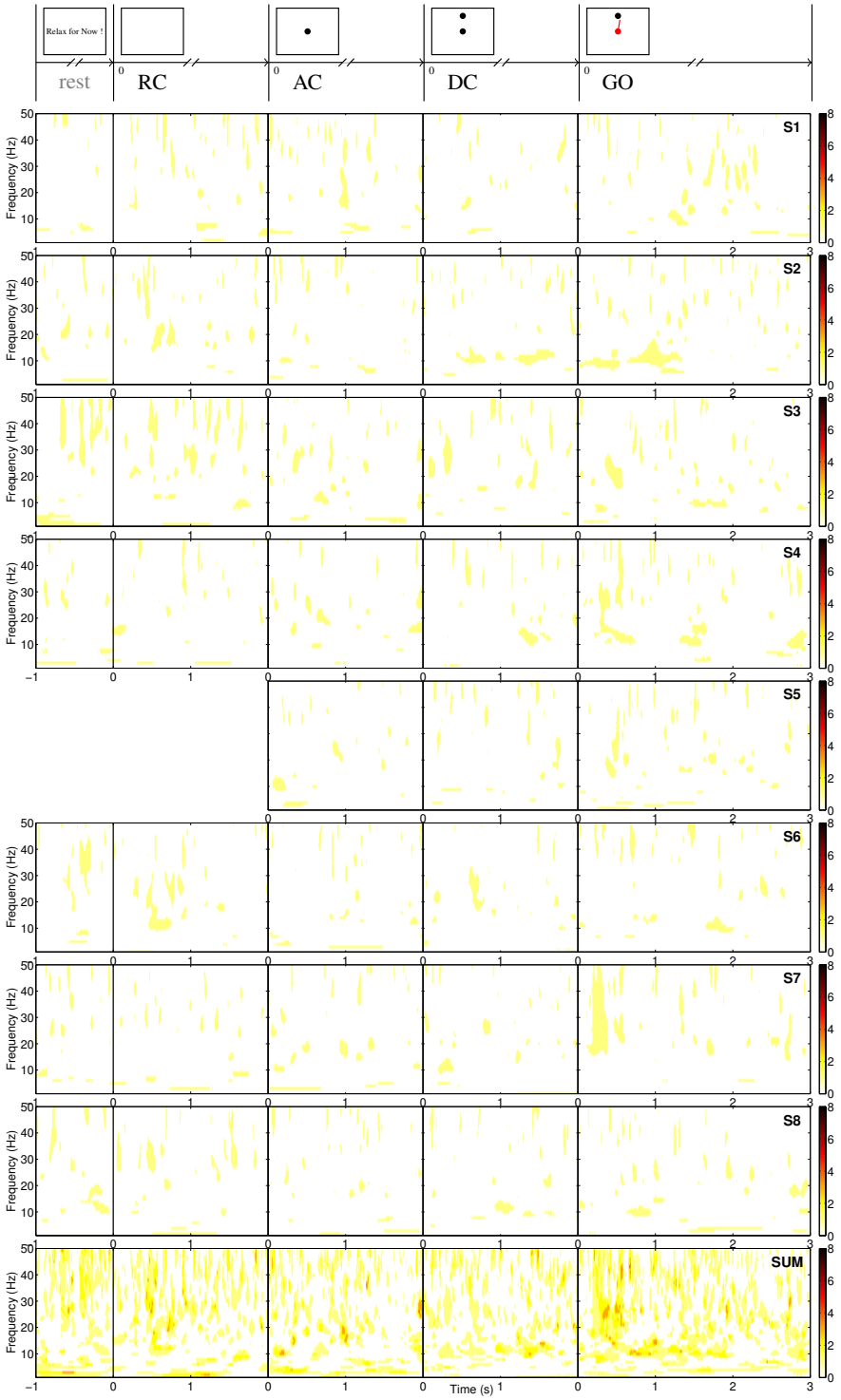

Figure 4.52. Regions of continuous Morlet wavelet transform scalograms for electrode C_3 in which the coefficient values show statistically significant inter-group (for 4 directions) variance (p-value<0.05). ELR EEG is used. From top panels downward: Subjects S1 (top panel) to S8, as well as the overlapped regions (bottom panel) in which the number of subjects with significant difference is shown. Horizontal axes are time in seconds. Vertical axes show Frequency (Hz). Zeros from left to right indicate different stages of movement, as described in Figure 3.5 and the presentation of visual cues: RC, AC, DC and GO. Segments with too few acceptable trials are not plotted.

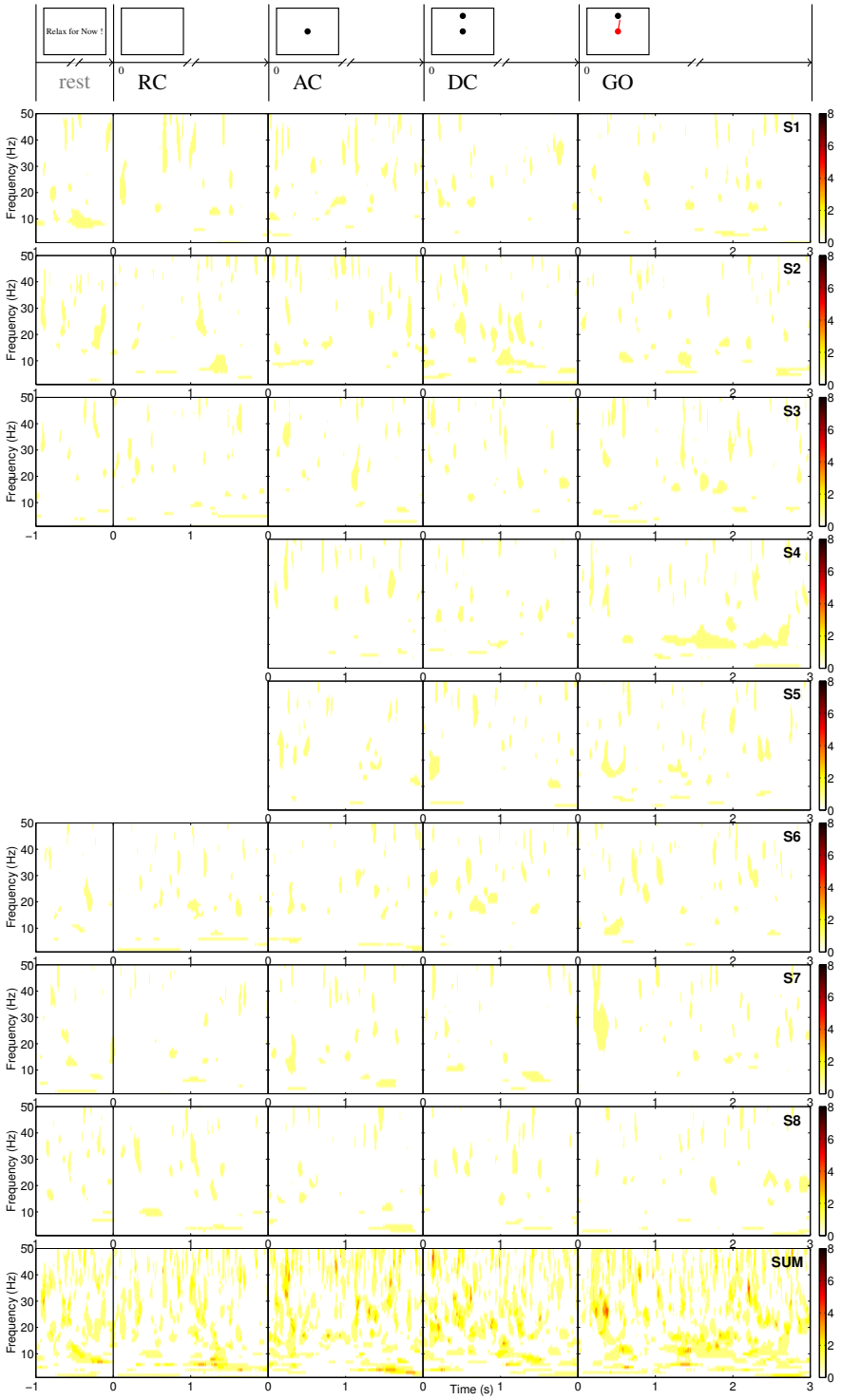

Figure 4.53. Regions of continuous Morlet wavelet transform scalograms for electrode C_4 in which the coefficient values show statistically significant inter-group (for 4 directions) variance (p-value<0.05). ELR EEG is used. From top panels downward: Subjects S1 (top panel) to S8, as well as the overlapped regions (bottom panel) in which the number of subjects with significant difference is shown. Horizontal axes are time in seconds. Vertical axes show Frequency (Hz). Zeros from left to right indicate different stages of movement, as described in Figure 3.5 and the presentation of visual cues: RC, AC, DC and GO. Segments with too few acceptable trials are not plotted.

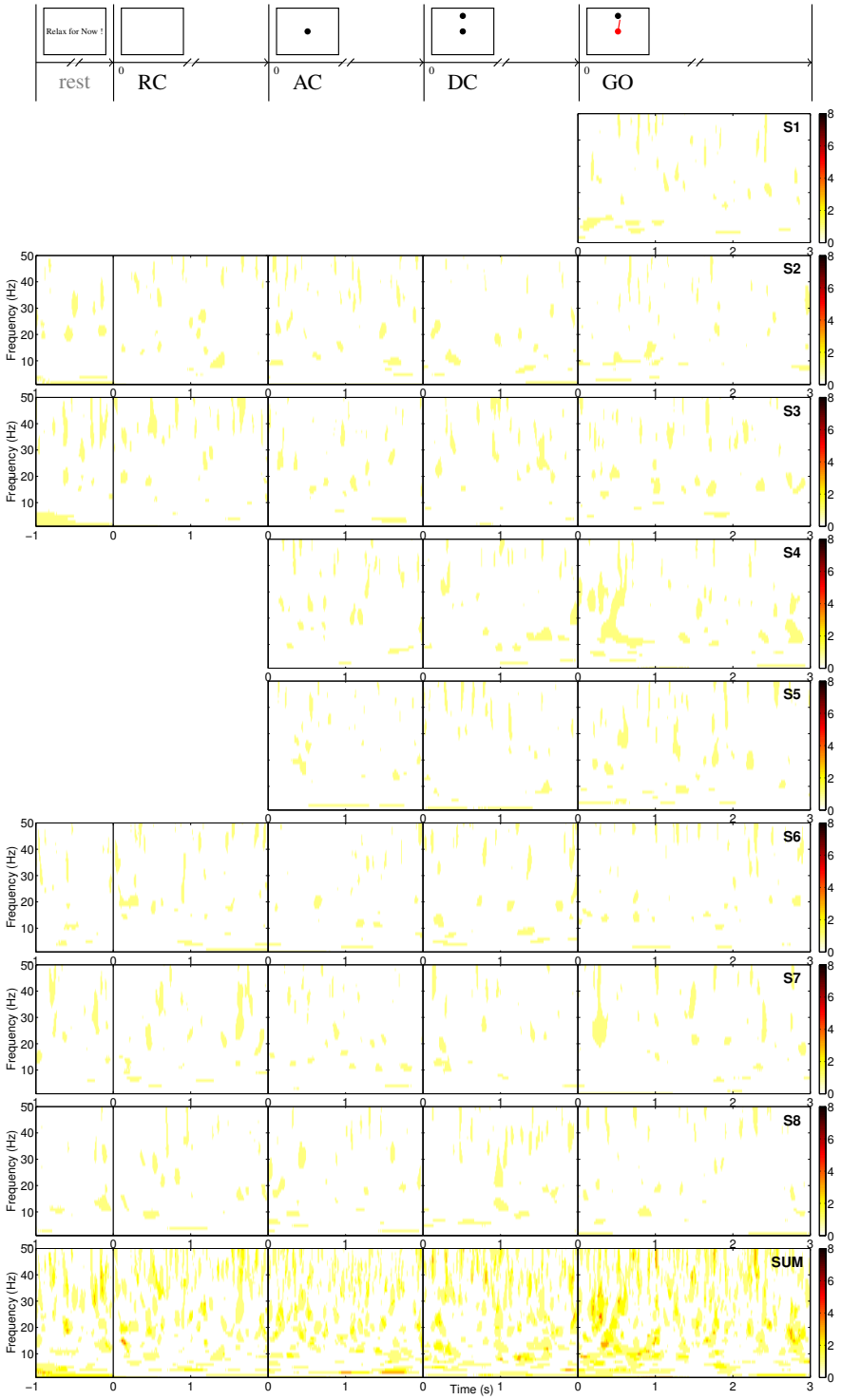

Figure 4.54. Regions of continuous Morlet wavelet transform scalograms for electrode F_z in which the coefficient values show statistically significant inter-group (for 4 directions) variance (p-value<0.05). ELR EEG is used. From top panels downward: Subjects S1 (top panel) to S8, as well as the overlapped regions (bottom panel) in which the number of subjects with significant difference is shown. Horizontal axes are time in seconds. Vertical axes show Frequency (Hz). Zeros from left to right indicate different stages of movement, as described in Figure 3.5 and the presentation of visual cues: RC, AC, DC and GO. Segments with too few acceptable trials are not plotted.

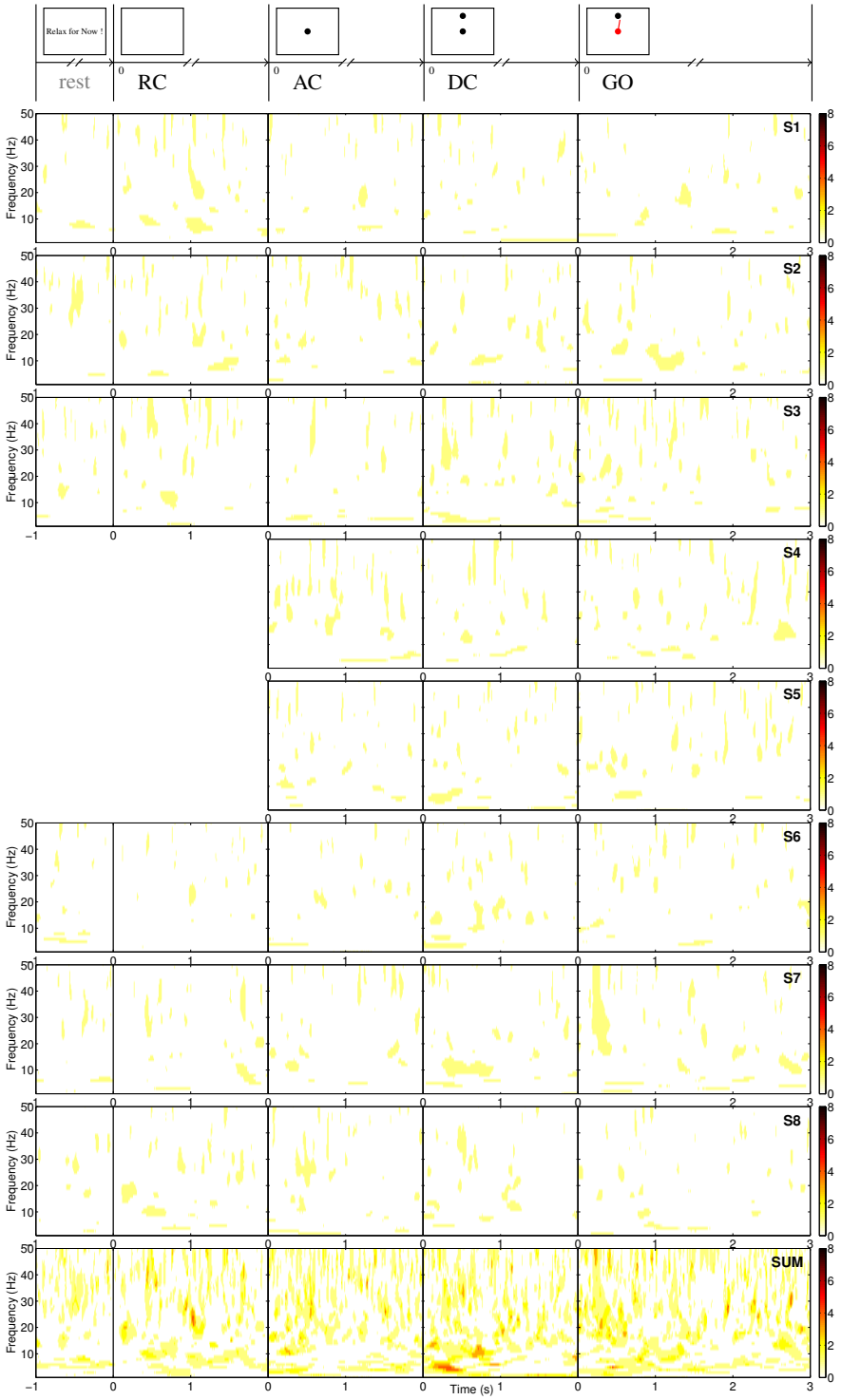

Figure 4.55. Regions of continuous Morlet wavelet transform scalograms for electrode P_z in which the coefficient values show statistically significant inter-group (for 4 directions) variance (p-value<0.05). ELR EEG is used. From top panels downward: Subjects S1 (top panel) to S8, as well as the overlapped regions (bottom panel) in which the number of subjects with significant difference is shown. Horizontal axes are time in seconds. Vertical axes show Frequency (Hz). Zeros from left to right indicate different stages of movement, as described in Figure 3.5 and the presentation of visual cues: RC, AC, DC and GO. Segments with too few acceptable trials are not plotted.

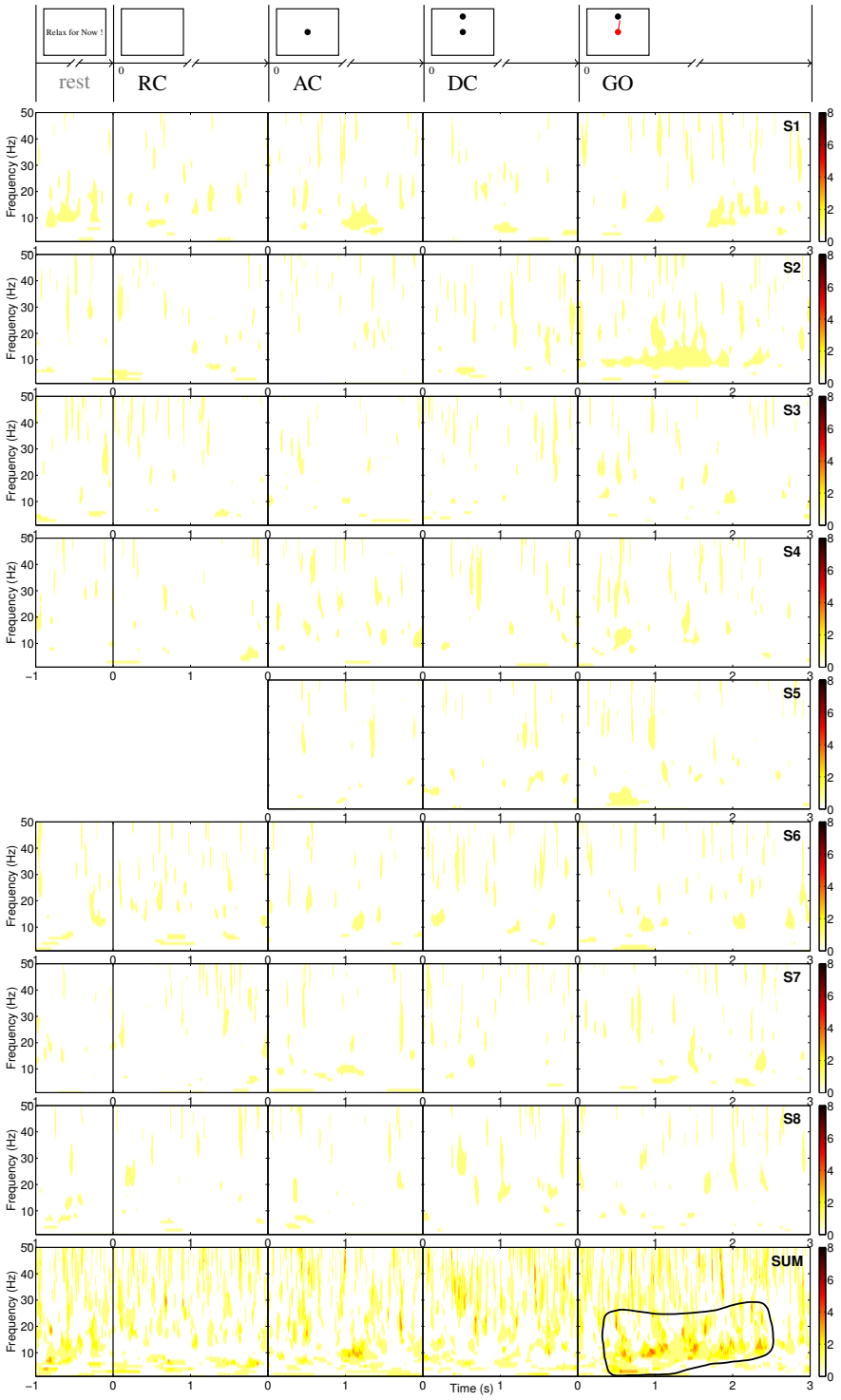

Figure 4.56. Regions of continuous Morlet wavelet transform scalograms for electrode C_z in which the coefficient values show statistically significant inter-group (for 4 directions) variance (p-value<0.05). CAR EEG is used. From top panels downward: Subjects S1 (top panel) to S8, as well as the overlapped regions (bottom panel) in which the number of subjects with significant difference is shown. Horizontal axes are time in seconds. Vertical axes show Frequency (Hz). Zeros from left to right indicate different stages of movement, as described in Figure 3.5 and the presentation of visual cues: RC, AC, DC and GO. Segments with too few acceptable trials are not plotted. The region where significant difference is observed in more subjects is indicated by black contour.

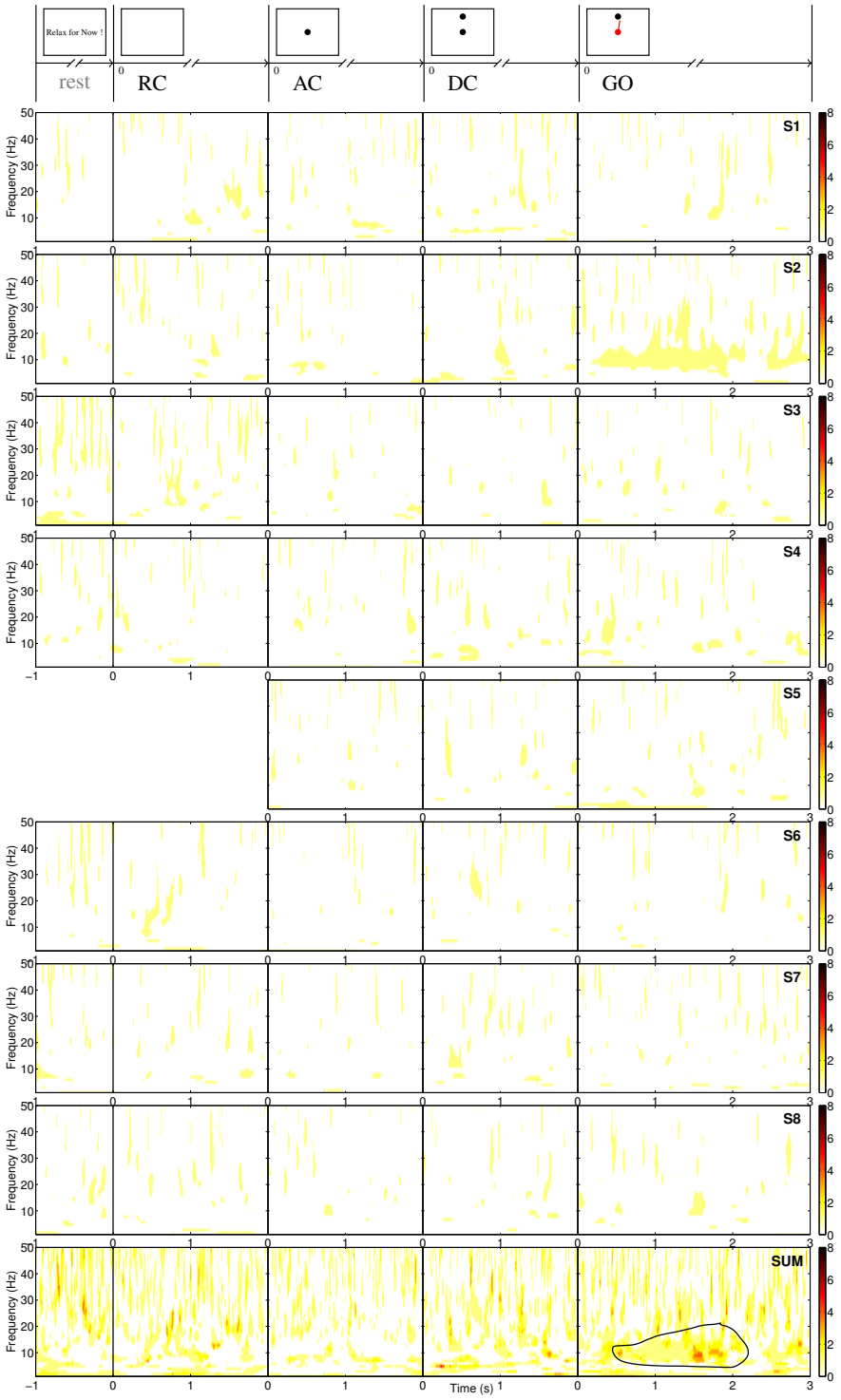

Figure 4.57. Regions of continuous Morlet wavelet transform scalograms for electrode C_3 in which the coefficient values show statistically significant inter-group (for 4 directions) variance (p-value<0.05). CAR EEG is used. From top panels downward: Subjects S1 (top panel) to S8, as well as the overlapped regions (bottom panel) in which the number of subjects with significant difference is shown. Horizontal axes are time in seconds. Vertical axes show Frequency (Hz). Zeros from left to right indicate different stages of movement, as described in Figure 3.5 and the presentation of visual cues: RC, AC, DC and GO. Segments with too few acceptable trials are not plotted. The region where significant difference is observed in more subjects is indicated by black contour.

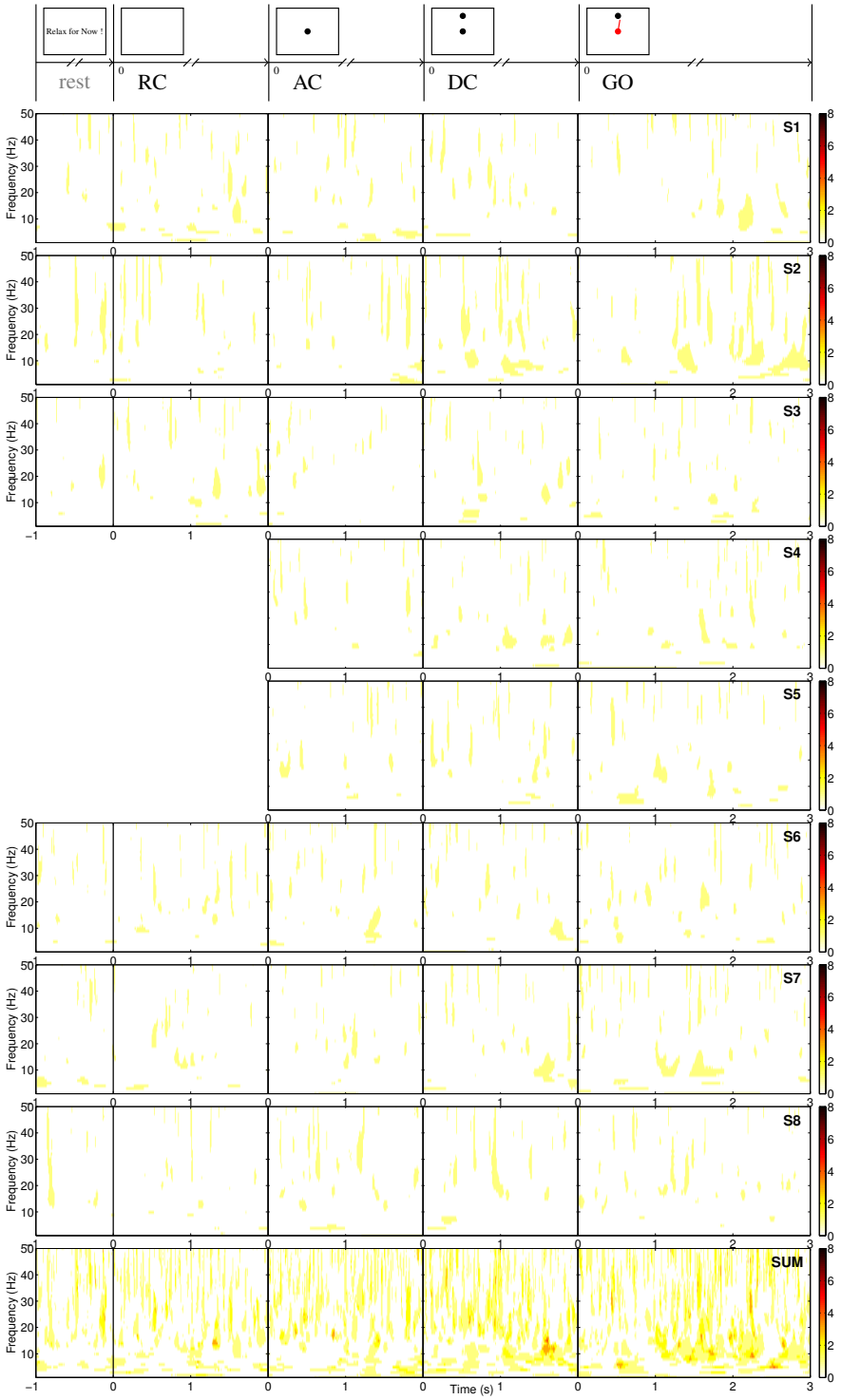

Figure 4.58. Regions of continuous Morlet wavelet transform scalograms for electrode C_4 in which the coefficient values show statistically significant inter-group (for 4 directions) variance (p-value<0.05). CAR EEG is used. From top panels downward: Subjects S1 (top panel) to S8, as well as the overlapped regions (bottom panel) in which the number of subjects with significant difference is shown. Horizontal axes are time in seconds. Vertical axes show Frequency (Hz). Zeros from left to right indicate different stages of movement, as described in Figure 3.5 and the presentation of visual cues: RC, AC, DC and GO. Segments with too few acceptable trials are not plotted.

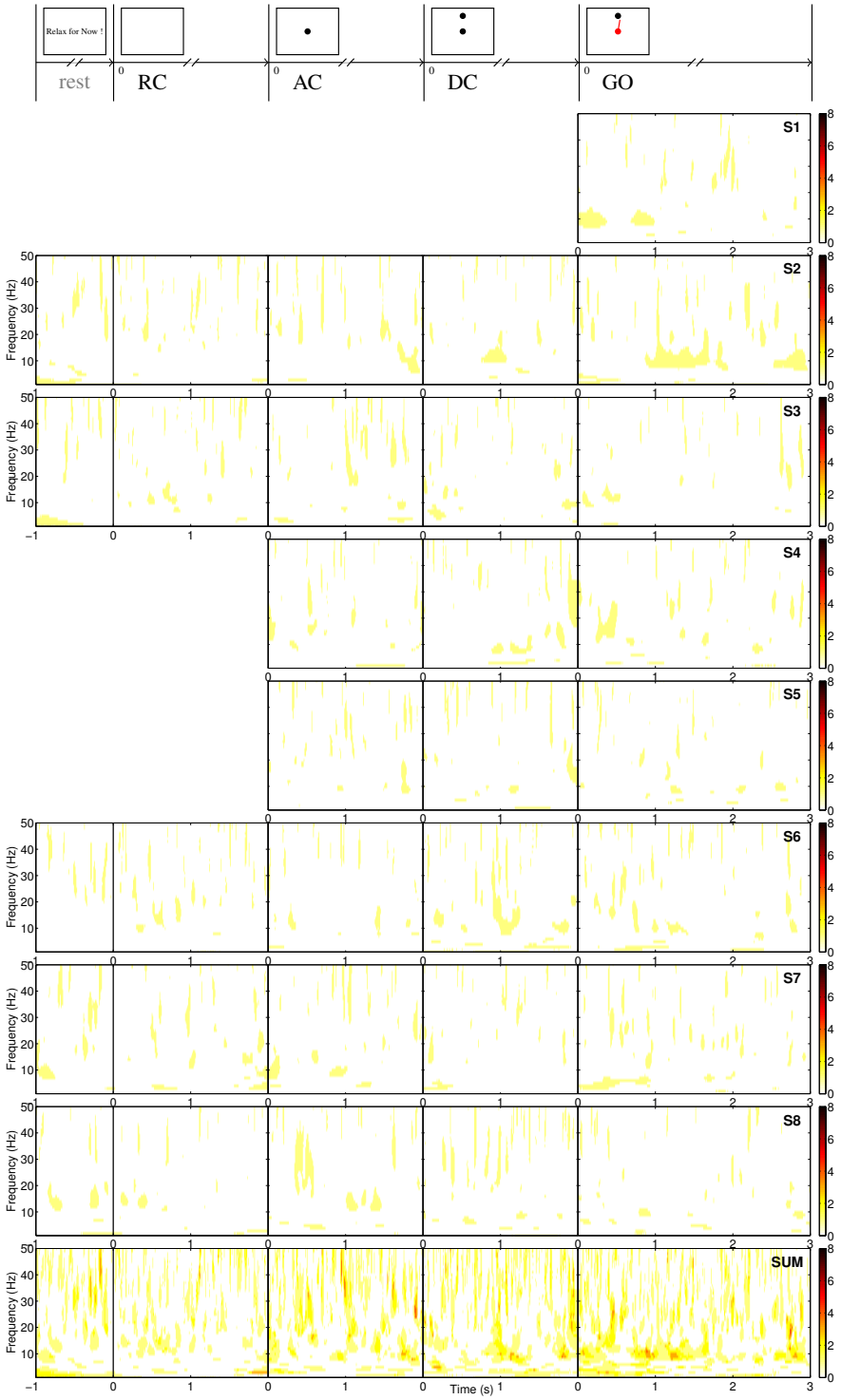

Figure 4.59. Regions of continuous Morlet wavelet transform scalograms for electrode F_z in which the coefficient values show statistically significant inter-group (for 4 directions) variance (p-value<0.05). CAR EEG is used. From top panels downward: Subjects S1 (top panel) to S8, as well as the overlapped regions (bottom panel) in which the number of subjects with significant difference is shown. Horizontal axes are time in seconds. Vertical axes show Frequency (Hz). Zeros from left to right indicate different stages of movement, as described in Figure 3.5 and the presentation of visual cues: RC, AC, DC and GO. Segments with too few acceptable trials are not plotted.

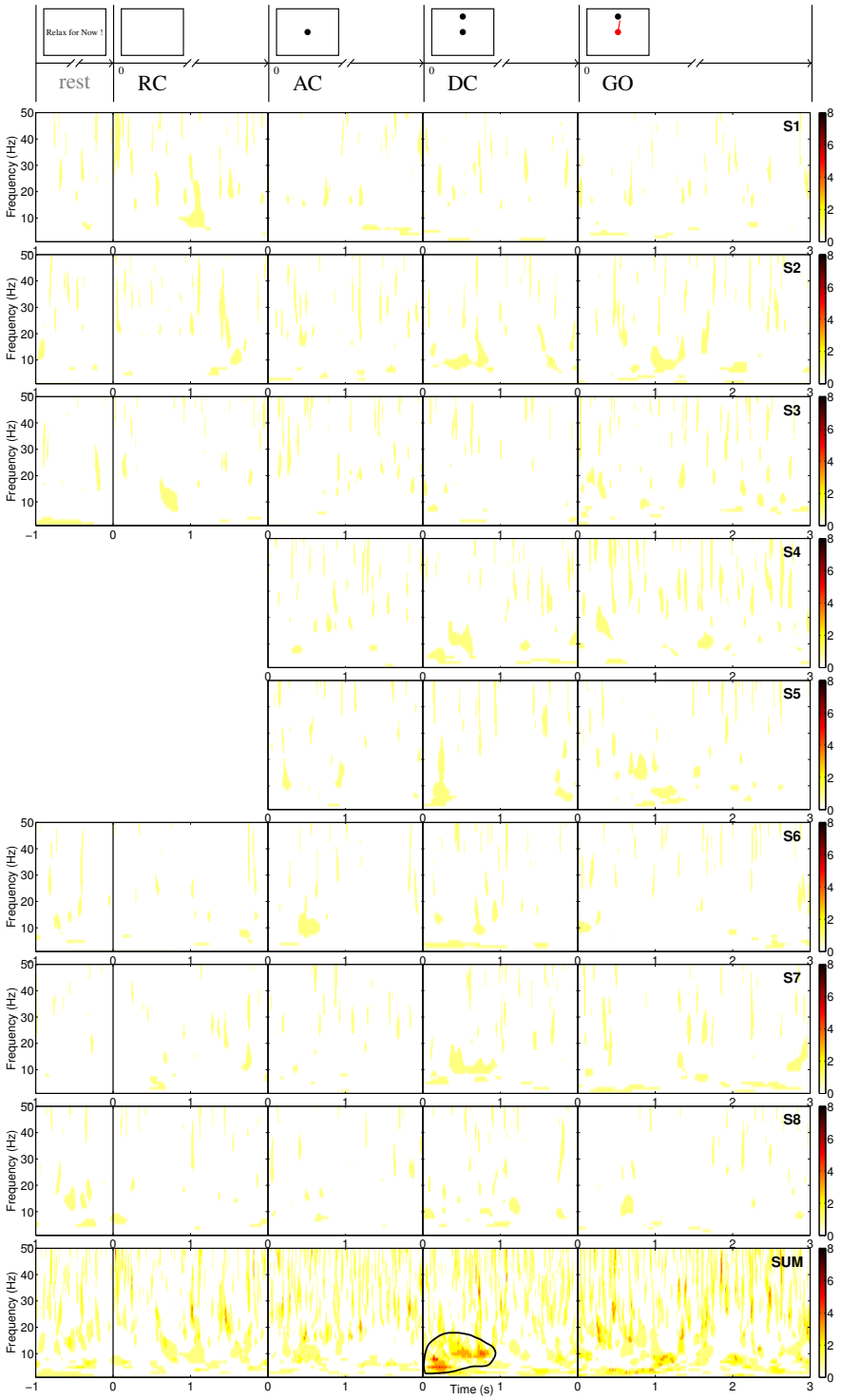

Figure 4.60. Regions of continuous Morlet wavelet transform scalograms for electrode P_z in which the coefficient values show statistically significant inter-group (for 4 directions) variance (p-value<0.05). CAR EEG is used. From top panels downward: Subjects S1 (top panel) to S8, as well as the overlapped regions (bottom panel) in which the number of subjects with significant difference is shown. Horizontal axes are time in seconds. Vertical axes show Frequency (Hz). Zeros from left to right indicate different stages of movement, as described in Figure 3.5 and the presentation of visual cues: RC, AC, DC and GO. Segments with too few acceptable trials are not plotted. The region where significant difference is observed in more subjects is indicated by black contour.

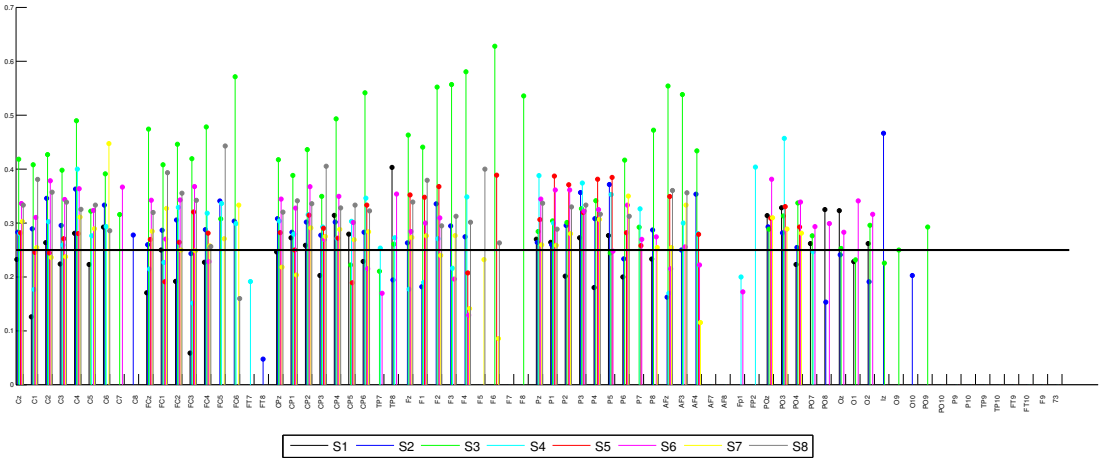

Figure 4.61. Classificatrion rates of exertion direction during DC (planning) stage, from baseline-adjusted unfiltered ELR EEG, using PCA dimension reduction and EDC classifiers. Colours show results from different subjects for the indicated electrodes. The 0.25% chance level for 4-direction groups is shown as a black horizontal line.

4.4.3. Information in Single EEG Channels

In order to see the directional information in single EEG channels, PCA dimension reduction and EDC or KNN classification of time-domain EEG is used (see Sections 3.3.4 and 3.3.5). A combination of different referencing (ELR, CAR, SL), different low-pass filtering (none, 4Hz, 8Hz, 12Hz, 25Hz and 50Hz), and different classifiers (EDC, KNN5) are used for classification (Leave-One-Out). The classification rates during planning and execution stages are visualised in Figures 4.61 and 4.62. The figures show the classification rates using unfiltered baseline-adjusted ELR EEG, PCA dimension-reduction and EDC classifiers. The details of results and also the mean classification rate values are listed in Table 4.10.

To better understand the directional information in different stages and to see the effect of different classification techniques, Table 4.11 provides a summary of mean and maximum statistically significant classification rate values for each method and each stage.

Finally, to succinctly see the directional information of EEG in each subject and on average, regardless of the method or position, the maximum values are listed. Table 4.12 show the maximum classification values in each subject (and subject average and maximum values) among different electrodes and classification methods.

4.4.4. Summary of the Directional Information in EEG

The following points can be underlined according to the presented results:

- The inter-class difference of time and time-frequency EEG features does not reach

Table 4.10. Single channel classification results (%) for individual subjects, electrodes and data segments, using the ELR-LPF0-DCR-ZPCA-EDC .

No.	Electrode	S1		S2		S3		S4		S5		S6		S7		S8		**Mean**	
		DC	GO	DC	GO	DC	GO	DC	GO	DC	GO	DC	GO	DC	GO	DC	GO	**DC**	**GO**
1	Cz	23	34	28	22	42	36	28	42	28	40	34	33	30	33	33	27	**36**	**36**
2	C1	13	37	29	34	41	41	18	42	25	29	31	32	25	36	38	21	**39**	**38**
3	C2	26	38	35	28	43	38	30	32	24	37	38	27	24	37	36	23	**38**	**37**
4	C3	22	31	30	35	40	35	26	42	27	38	34	30	24	36	34	35	**36**	**37**
5	C4	28	31	36	35	49	43	40	38	28	29	36	38	31	35	33	19	**38**	**38**
6	C5	22	31	0	0	32	37	28	50	0	0	32	26	29	50	33	16	**0**	**46**
7	C6	29	34	33	29	39	0	29	38	0	0	0	0	45	31	29	19	**39**	**36**
8	C7	0	0	0	0	32	27	0	0	0	0	37	33	0	0	0	0	**0**	**0**
9	C8	0	33	28	36	0	58	0	0	0	0	0	15	0	0	0	0	**0**	**58**
10	FCz	17	37	26	31	47	41	21	46	27	38	34	34	28	40	32	32	**38**	**40**
11	FC1	25	36	29	28	41	25	23	39	19	27	27	39	33	38	39	32	**38**	**38**
12	FC2	19	23	31	37	45	38	33	42	26	22	34	33	25	35	36	26	**37**	**37**
13	FC3	5.9	19	24	25	42	30	15	47	32	21	37	37	25	37	34	24	**38**	**40**
14	FC4	23	12	29	33	48	51	32	34	28	29	23	36	26	38	26	30	**48**	**41**
15	FC5	0	4	34	31	31	32	34	61	0	0	0	0	27	33	44	42	**39**	**51**
16	FC6	0	12	30	34	57	58	30	55	0	0	0	0	33	0	16	24	**57**	**57**
17	FT7	0	0	0	0	0	0	19	75	0	0	0	0	0	0	0	0	**0**	**75**
18	FT8	0	0	4.8	38	0	0	0	0	0	0	0	0	0	0	0	0	**0**	**0**
19	CPz	25	21	31	31	42	31	30	44	28	32	34	29	22	33	32	23	**36**	**38**
20	CP1	27	24	28	30	39	34	28	44	25	28	33	31	20	40	34	21	**35**	**39**
21	CP2	26	30	30	33	44	36	32	34	31	35	37	28	29	36	34	24	**36**	**35**
22	CP3	20	29	28	31	35	34	29	42	29	34	27	32	28	39	41	29	**38**	**36**
23	CP4	31	36	30	26	49	36	27	43	27	39	35	27	29	34	33	21	**39**	**38**
24	CP5	28	28	0	0	22	26	30	38	19	18	30	35	27	0	33	33	**0**	**36**
25	CP6	23	21	28	27	54	41	35	29	33	17	22	35	28	42	32	26	**54**	**39**
26	TP7	0	0	0	0	21	22	25	46	0	0	17	39	0	0	0	0	**0**	**42**
27	TP8	40	44	19	18	26	35	27	35	0	0	35	22	0	0	0	0	**38**	**44**
28	Fz	0	23	26	24	46	41	18	44	35	29	28	36	27	36	34	33	**38**	**38**
29	F1	0	14	18	36	44	41	19	48	35	26	30	39	28	45	38	31	**39**	**42**
30	F2	0	19	34	37	55	48	27	47	37	38	31	31	24	38	29	33	**42**	**42**
31	F3	0	0	29	30	56	46	22	49	0	0	20	39	28	37	31	34	**56**	**43**
32	F4	0	0	27	32	58	50	35	39	21	24	13	35	14	38	30	31	**46**	**42**
33	F5	0	0	0	0	0	0	0	0	0	0	0	0	23	24	40	30	**0**	**0**
34	F6	0	0	0	0	63	31	0	0	39	0	0	0	8.6	17	26	30	**63**	**0**
35	F7	0	0	0	0	0	0	0	0	0	0	0	0	0	0	0	0	**0**	**0**
36	F8	0	0	0	0	54	43	0	0	0	0	0	0	0	0	0	0	**54**	**43**
37	Pz	27	26	26	23	28	30	39	31	31	33	34	37	26	36	34	23	**36**	**35**
38	P1	26	28	26	26	30	39	30	38	39	40	36	29	26	40	29	23	**37**	**39**
39	P2	20	20	30	33	30	32	0	0	37	31	36	34	28	37	33	17	**35**	**35**
40	P3	27	32	36	28	33	38	37	35	32	35	32	27	0	0	33	23	**34**	**35**
41	P4	18	35	31	29	34	26	0	0	38	36	32	33	31	31	32	22	**35**	**35**
42	P5	28	34	37	0	24	23	35	26	38	36	25	25	0	0	0	0	**37**	**35**
43	P6	20	44	23	31	42	29	0	0	28	29	33	31	35	34	31	16	**37**	**39**
44	P7	0	0	0	0	29	30	33	45	26	18	27	31	0	0	0	0	**33**	**45**
45	P8	23	31	29	33	47	21	0	0	0	0	27	32	25	29	0	0	**47**	**32**
46	AFz	0	0	16	32	55	42	17	40	35	28	22	39	25	44	36	33	**46**	**41**
47	AF3	0	0	25	25	54	51	30	60	0	0	26	49	33	38	36	42	**45**	**50**
48	AF4	0	0	35	32	43	38	28	40	28	43	22	32	12	51	0	0	**39**	**43**
49	AF7	0	0	0	0	0	0	0	0	0	0	0	0	0	0	0	0	**0**	**0**
50	AF8	0	0	0	0	0	0	0	0	0	0	0	0	0	0	0	0	**0**	**0**
51	Fp1	0	0	0	0	0	0	20	0	0	0	17	38	0	0	0	0	**0**	**38**
52	FP2	0	0	0	0	0	0	40	0	0	0	0	42	0	0	0	0	**40**	**0**
53	POz	31	27	29	32	29	26	0	0	31	36	38	34	31	34	0	0	**38**	**34**
54	PO3	33	24	28	30	31	37	46	20	33	28	29	29	29	0	0	0	**37**	**37**
55	PO4	22	28	25	44	34	26	0	0	29	35	34	31	28	55	0	0	**34**	**41**
56	PO7	26	19	0	0	28	35	25	19	0	0	29	32	0	0	0	0	**0**	**35**
57	PO8	32	32	15	22	0	0	0	0	0	0	30	30	0	0	0	0	**0**	**0**
58	Oz	32	29	24	25	25	28	0	0	0	0	28	30	0	0	0	0	**0**	**0**
59	O1	23	21	0	0	23	32	0	0	0	0	34	31	0	0	0	0	**34**	**0**
60	O2	26	28	19	23	30	18	0	0	0	0	32	29	0	0	0	0	**0**	**0**
61	Iz	0	0	47	0	23	24	0	0	0	0	0	0	0	0	0	0	**0**	**0**
62	O9	0	0	0	0	25	30	0	0	0	0	0	0	0	0	0	0	**0**	**0**
63	O10	0	0	20	25	0	16	0	0	0	0	0	0	0	0	0	0	**0**	**0**
64	PO9	0	0	0	0	29	29	0	0	0	0	0	0	0	0	0	0	**0**	**0**
65	PO10	0	0	0	0	0	0	0	0	0	0	0	0	0	0	0	0	**0**	**0**
66	P9	0	0	0	0	0	0	0	0	0	0	0	0	0	0	0	0	**0**	**0**
67	P10	0	0	0	0	0	0	0	0	0	0	0	0	0	0	0	0	**0**	**0**
68	TP9	0	0	0	0	0	0	0	0	0	0	0	0	0	0	0	0	**0**	**0**
69	TP10	0	0	0	0	0	0	0	0	0	0	0	0	0	0	0	0	**0**	**0**
70	FT9	0	0	0	0	0	0	0	0	0	0	0	0	0	0	0	0	**0**	**0**
71	FT10	0	0	0	0	0	0	0	0	0	0	0	0	0	0	0	0	**0**	**0**
72	F9	0	0	0	0	0	0	0	0	0	0	0	0	0	0	0	0	**0**	**0**
73	73	0	0	0	0	0	0	0	0	0	0	0	0	0	0	0	0	**0**	**0**

See caption of table 4.11 for abbreviations of method. Values with no statistical significance (p-value>0.05) are shown in gray.

Table 4.11. Summary of classification results (%), using different classification methods .

No.	Method		DC 0.0-1.0s	DC 1.0-2.0s	DC 0.0-2.0s	GO 0.0-1.0s	GO 1.0-2.0s	GO 2.0-3.0s	GO 0.0-3.0s
1	ELR-LPF0-DCR-ZPCA-EDC	mean	40	39	39	40	40	38	40
		max	63@F6(S3)	61@F8(S3)	63@F6(S3)	68@FT7(S4)	75@FT7(S4)	70@FT7(S4)	75@FT7(S4)
2	ELR-LPF4-DCR-ZPCA-EDC	mean	40	39	39	40	39	38	40
		max	64@FC6(S3)	61@F8(S3)	60@F6(S3)	65@FT7(S4)	78@FT7(S4)	75@FT7(S4)	80@FT7(S4)
3	ELR-LPF8-DCR-ZPCA-EDC	mean	40	39	39	40	40	38	40
		max	64@FC6(S3)	61@F8(S3)	63@F6(S3)	63@FC5(S4)	78@FT7(S4)	72@FT7(S4)	82@FT7(S4)
4	ELR-LPF12-DCR-ZPCA-EDC	mean	39	39	39	40	40	37	40
		max	64@FC6(S3)	61@F8(S3)	63@F6(S3)	65@FT7(S4)	78@FT7(S4)	70@FT7(S4)	82@FT7(S4)
5	ELR-LPF25-DCR-ZPCA-EDC	mean	40	39	39	40	40	37	39
		max	64@FC6(S3)	61@F8(S3)	63@F6(S3)	68@FT7(S4)	78@FT7(S4)	70@FT7(S4)	78@FT7(S4)
6	ELR-LPF50-DCR-ZPCA-EDC	mean	40	39	39	40	40	37	40
		max	64@FC6(S3)	61@F8(S3)	65@F6(S3)	65@FT7(S4)	78@FT7(S4)	70@FT7(S4)	78@FT7(S4)
7	ELR-LPF0-DCR-ZPCA-KNN5-ds10	mean	39	38	38	40	39	38	40
		max	61@FC6(S3)	54@F8(S3)	56@AF3(S3)	66@FC5(S4)	72@FT7(S4)	60@FT7(S4)	69@AF3(S4)
8	ELR-LPF4-DCR-ZPCA-KNN5-ds10	mean	40	38	39	40	39	38	41
		max	64@FC6(S3)	50@C7(S6)	58@AF3(S3)	70@FC5(S4)	70@FT7(S4)	56@AF3(S4)	72@FT7(S4)
9	ELR-LPF8-DCR-ZPCA-KNN5-ds10	mean	40	37	39	39	39	38	40
		max	61@FC6(S3)	53@F4(S3)	58@AFz(S3)	70@FT7(S4)	72@FT7(S4)	55@FT7(S4)	72@FT7(S4)
10	ELR-LPF12-DCR-ZPCA-KNN5-ds10	mean	40	38	39	39	39	38	40
		max	61@FC6(S3)	53@F6(S3)	64@F8(S3)	68@FT7(S4)	72@FT7(S4)	57@FT7(S4)	71@AF3(S4)
11	ELR-LPF25-DCR-ZPCA-KNN5-ds10	mean	40	39	39	40	39	37	40
		max	61@FC6(S3)	54@F8(S3)	61@F8(S3)	72@FT7(S4)	70@FT7(S4)	60@FT7(S4)	68@AF3(S4)
12	ELR-LPF50-DCR-ZPCA-KNN5-ds10	mean	39	38	39	39	39	38	40
		max	61@FC6(S3)	54@F8(S3)	54@F3(S3)	69@FC5(S4)	70@FT7(S4)	57@FT7(S4)	70@FT7(S4)
13	CAR-LPF0-DCR-ZPCA-EDC	mean	37	38	38	41	40	39	40
		max	61@C6(S3)	52@C6(S3)	61@C6(S3)	77@FC5(S4)	71@F4(S4)	61@FC5(S4)	75@FC5(S4)
14	CAR-LPF4-DCR-ZPCA-EDC	mean	38	37	37	41	40	39	40
		max	64@F8(S3)	54@F8(S3)	52@C6(S3)	70@AF4(S4)	75@AF4(S4)	58@FC5(S4)	76@FC4(S4)
15	CAR-LPF8-DCR-ZPCA-EDC	mean	38	37	38	41	40	39	40
		max	64@F8(S3)	52@C6(S3)	54@AFz(S3)	69@FC5(S4)	73@F4(S4)	61@FC5(S4)	78@FC4(S4)
16	CAR-LPF12-DCR-ZPCA-EDC	mean	38	38	37	40	40	38	40
		max	58@AF3(S3)	52@C6(S3)	52@AFz(S3)	70@FC5(S4)	71@FC5(S4)	62@FC5(S4)	73@FC5(S4)
17	CAR-LPF25-DCR-ZPCA-EDC	mean	37	38	38	41	40	39	39
		max	57@F8(S3)	52@C6(S3)	52@C6(S3)	73@FC5(S4)	73@F4(S4)	62@FC5(S4)	73@AF4(S4)
18	CAR-LPF50-DCR-ZPCA-EDC	mean	38	38	38	41	40	38	40
		max	61@C6(S3)	52@C6(S3)	52@C6(S3)	76@FC5(S4)	71@F4(S4)	61@FC5(S4)	75@FC5(S4)
19	CAR-LPF0-DCR-ZPCA-KNN5-ds10	mean	37	37	38	42	41	39	41
		max	57@C6(S3)	52@CP6(S3)	52@C6(S3)	77@FC6(S4)	72@FC6(S4)	57@FC5(S4)	75@F4(S4)
20	CAR-LPF4-DCR-ZPCA-KNN5-ds10	mean	38	38	37	41	40	39	41
		max	61@C6(S3)	50@C5(S8)	57@C6(S3)	78@AF4(S4)	75@AF4(S4)	59@FC5(S4)	75@F4(S4)
21	CAR-LPF8-DCR-ZPCA-KNN5-ds10	mean	38	37	37	41	41	38	41
		max	61@C6(S3)	50@CP6(S3)	52@C6(S3)	78@FC6(S4)	69@FC5(S4)	58@FC5(S4)	78@F4(S4)
22	CAR-LPF12-DCR-ZPCA-KNN5-ds10	mean	38	36	37	42	41	40	41
		max	57@C6(S3)	50@CP6(S3)	57@C6(S3)	78@F4(S4)	68@AF4(S4)	61@FC5(S4)	78@F4(S4)
23	CAR-LPF25-DCR-ZPCA-KNN5-ds10	mean	37	37	37	42	41	40	41
		max	57@C6(S3)	48@CP6(S3)	61@C6(S3)	80@F4(S4)	71@F4(S4)	58@FC5(S4)	83@F4(S4)
24	CAR-LPF50-DCR-ZPCA-KNN5-ds10	mean	37	37	37	42	41	39	41
		max	57@C6(S3)	50@CP6(S3)	61@C6(S3)	78@FC6(S4)	72@FC6(S4)	59@FC5(S4)	78@F4(S4)
25	SL-LPF0-DCR-ZPCA-EDC	mean	38	36	37	38	37	36	37
		max	54@C6(S2)	47@CP4(S3)	44@F2(S5)	50@AFz(S3)	53@FCz(S1)	44@F1(S4)	58@FCz(S5)
26	SL-LPF4-DCR-ZPCA-EDC	mean	37	37	37	38	37	36	37
		max	47@P3(S6)	62@CP6(S2)	54@CP6(S2)	52@P2(S5)	53@FCz(S1)	44@AFz(S7)	53@F1(S4)
27	SL-LPF8-DCR-ZPCA-EDC	mean	37	38	37	38	37	36	37
		max	47@P3(S6)	69@CP6(S2)	48@FC2(S3)	52@P2(S5)	53@FCz(S1)	43@CP4(S7)	58@FCz(S5)
28	SL-LPF12-DCR-ZPCA-EDC	mean	38	37	37	38	37	36	37
		max	62@C6(S2)	47@CP4(S3)	44@F2(S5)	52@P2(S5)	53@FCz(S1)	43@P1(S1)	58@FCz(S5)
29	SL-LPF25-DCR-ZPCA-EDC	mean	37	36	37	38	37	36	37
		max	54@C6(S2)	53@CP4(S3)	44@F2(S5)	50@AFz(S3)	53@FCz(S1)	44@F1(S4)	58@FCz(S5)
30	SL-LPF50-DCR-ZPCA-EDC	mean	37	36	37	38	37	36	37
		max	54@C6(S2)	47@CP4(S3)	44@F2(S5)	50@AFz(S3)	53@FCz(S1)	44@F1(S4)	58@FCz(S5)
31	SL-LPF0-DCR-ZPCA-KNN5-ds10	mean	37	36	36	37	38	36	37
		max	54@FC3(S3)	52@C2(S5)	46@FC3(S3)	51@FC3(S4)	52@CP4(S1)	46@P1(S5)	46@PO4(S2)
32	SL-LPF4-DCR-ZPCA-KNN5-ds10	mean	37	38	37	37	37	36	37
		max	50@FC3(S3)	54@FC3(S3)	46@FC3(S3)	50@FCz(S5)	52@CP4(S1)	46@P1(S5)	48@C2(S3)
33	SL-LPF8-DCR-ZPCA-KNN5-ds10	mean	37	38	36	37	37	35	37
		max	54@FC3(S3)	50@C2(S5)	50@FC3(S3)	49@CP1(S4)	51@PO4(S2)	43@P1(S5)	45@PO4(S2)
34	SL-LPF12-DCR-ZPCA-KNN5-ds10	mean	37	37	36	38	38	36	36
		max	54@FC3(S3)	52@C2(S5)	50@FC3(S3)	46@FCz(S5)	54@PO4(S2)	49@P1(S5)	49@PO4(S2)
35	SL-LPF25-DCR-ZPCA-KNN5-ds10	mean	37	37	36	37	38	35	36
		max	54@FC3(S3)	52@C2(S5)	46@FC3(S3)	49@FC3(S4)	53@CP1(S4)	46@P1(S5)	46@PO4(S2)
36	SL-LPF50-DCR-ZPCA-KNN5-ds10	mean	37	37	36	37	38	35	36
		max	54@FC3(S3)	52@C2(S5)	46@FC3(S3)	47@FC3(S4)	52@CP4(S1)	46@P1(S5)	46@PO4(S2)

[1] ELR: ear-lobe referencing, CAR: common-average Referencing, SL: surface Laplacian, LPFn: low-pass filtering with n-Hz cut-off frequency (0:unfiltered), DCR: direct current removal (baseline adjustment), ZPCA: z-score adjustment and principal component analysis, EDC: euclidean distance classifier, KNN5: k^{th}-nearest neighbour classifier with k=5, ds10: downsampled by factor of 10.

[2] Only statistically significant values (p-value<0.05) are taken into account.

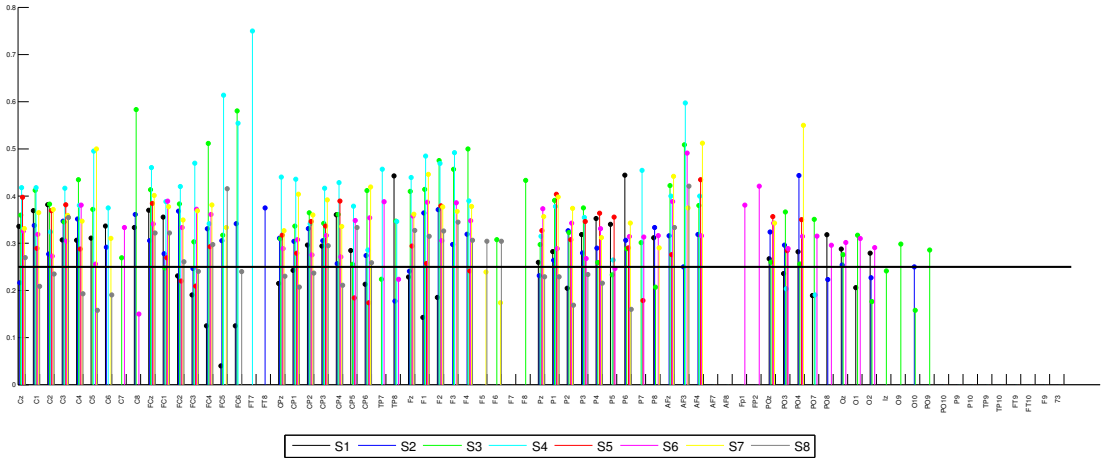

Figure 4.62. Classification rates of exertion direction during GO (execution) stage, from baseline-adjusted unfiltered ELR EEG, using PCA dimension reduction and EDC classifiers. Colours show results from different subjects for the indicated electrodes. The 0.25% chance level for 4-direction groups is shown as a black horizontal line.

Table 4.12. Maximum classification rates (%) for different subjects .

Subject	DC 0.0-1.0s	DC 1.0-2.0s	DC 0.0-2.0s	GO 0.0-1.0s	GO 1.0-2.0s	GO 2.0-3.0s	GO 0.0-3.0s
S1	40 @PO8 (M10)	45.9 @P1 (M32)	40.3 @TP8 (M1)	47.6 @F1 (M19)	52.9 @FCz (M25)	43.1 @P1 (M25)	50 @FCz (M25)
S2	61.5 @C6 (M28)	69.2 @CP6 (M27)	53.8 @CP6 (M26)	49.3 @PO4 (M13)	53.7 @PO4 (M34)	52.8 @C8 (M22)	52.8 @C8 (M19)
S3	64.3 @FC6 (M2)	60.7 @F8 (M1)	65.1 @F6 (M6)	54.4 @AF3 (M2)	64.5 @FC6 (M1)	54.8 @FC6 (M1)	62.5 @C8 (M6)
S4	47.8 @Pz (M23)	45.7 @PO3 (M3)	48.6 @PO3 (M2)	79.7 @F4 (M23)	77.5 @FT7 (M2)	75 @FT7 (M2)	83.1 @F4 (M23)
S5	49 @P5 (M1)	51.7 @C2 (M31)	48.4 @P7 (M15)	56.5 @AF4 (M1)	52.2 @CP6 (M15)	48.6 @P1 (M34)	57.7 @FCz (M25)
S6	50 @C7 (M8)	50 @C7 (M8)	46.7 @C7 (M3)	57.9 @FP2 (M4)	55 @C8 (M21)	51.2 @C5 (M13)	49.1 @AF3 (M1)
S7	45.3 @P4 (M13)	48 @P2 (M27)	46.7 @PO3 (M20)	59.4 @C5 (M2)	51.7 @C6 (M15)	55.2 @C6 (M19)	58.6 @C6 (M16)
S8	47.4 @F6 (M8)	51.9 @FC5 (M3)	49.1 @CP5 (M19)	52.2 @F5 (M6)	47.4 @CP3 (M34)	47.8 @F5 (M19)	47.8 @F6 (M3)
mean	**50.7 (±8.18)**	**52.9 (±8.14)**	**49.8 (±7.21)**	**57.1 (±9.98)**	**56.9 (±9.65)**	**53.6 (±9.54)**	**57.7 (±11.5)**
max	**64.3**	**69.2**	**65.1**	**79.7**	**77.5**	**75**	**83.1**

[1] See caption of table 4.11 for abbreviations of methods (M1, M2 and etc.).
[2] Values in parentheses, (± SD), show standard deviations.
[3] Only statistically significant values (p-value<0.05) are taken into account.

the significance level, but implies the partial involvement of some neural regions in processing of exertion direction in different stages of task.

- Common-average referencing (CAR) does not improve the inter-class difference of time domian EEG features, but accentuates the interclass difference of time-frequency EEG features.

- Applying Common-average referencing (CAR) and especially surface Laplacian (SL), both degrade the classification rates in the current time-domain classification methods.

- It can be seen that low pass filtering has no notable effect on average classification rates, in general. The unfiltered EEG or 4Hz Low Pass Filtering (LPF4) provide only slightly better classification rates for best-performing electrodes.

- KNN and EDC both show successful classification results.
- In all stages of movement, the average classification rates across all electrodes and in different stages of experiment are above the 25% chance level (28-33%).
- There are directional information in both transient and sustained stages of DC and GO.
- The best performing electrodes show relatively high classification rates in planning and execution (mean: 49.8% and 57.7%, max: 65.1% and 83.1%).
- The best performing electrode positions vary as a function of stage and classification method.
- The directional information exists in both transient and sustained stages of DC and GO. The GO stage shows slightly higher classification rates.

The ZPCA and EDC methods are also applied on the time-frequency distributions of each trial. That is, a feature vector is constructed by taking the 1-50Hz values of the scalogram every 10ms and vectorized into a feature vector similar to the feature vector of raw EEG. Then the processing stages and precudures for time-domain classification, were similarly applied to the time-frequency feature vectors as if they were time-domain EEG feature vectors. However, no notably better classification rates were found.

4.5. Chapter Summary

In this chapter, neurophysiological correlates resulting from the experiments and methods for investigating isometric exertion planning and execution were presented in form of ERPs (Section 4.2), and in terms of ERD/ERS (Section 4.3). Also, the extent of direction-dependent modulation of EEG features and EEG directional information were demonstrated. In next chapter, the results are discussed, interpreted and compared to previous studies and conclusions are made based on the presented evidence.

Chapter 5

Discussion and Conclusions

In this chapter the relevance of results to previous brain recording studies, interpretations of the results, potential impacts and limitations are summarised, reviewed and discussed. The key observations in the results are underlined in Section 5.1 and then the results are compared against previous studies in Section 5.2. In Section 5.3 the considerations and limitations are discussed followed by the potential interpretation of results and discussions in Section 5.4. The impact and significance of the results are underlined in Section 5.5, and followed by the direction of future work in Section 5.6. Section 5.7 summarises the chapter. Finally, a succinct message of the whole thesis is brought forward in Section 5.8.

5.1. Overview of Results

In this study, the EEG correlates of isometric arm exertions during preparation, planning, and execution of the task were explored. Common and local time and time-frequency features of EEG signals across 8 subjects were assessed. Time-domain waveforms and phase-locked activity in the form of ERD/ERS, similar to those in movement tasks or motor imagery (McFarland et al., 2000; Caldara et al., 2004; Neuper et al., 2006b), were observed. The ERP patterns in all the preparation, planning and execution stages were approximately similar to previous reports of isometric task execution ERPs (see Section 5.2.2.1). ERD/ERS patterns also resemble voluntary movements or motor imagery task ERD/ERS (see Section 5.2.2.2). Common-average referencing (CAR) localises the time and time-frequency signal characteristics. The EEG recordings also contain information about the direction of exertion of the task.

5.1.1. Time Domain EEG Signatures

The observation of the relatively symmetric and mid-line-centric activity during the AC (preparation) and the DC (planning) stages, but the asymmetric bolder contralateral activity in the GO stage (execution) is expected. This is compatible with the view of the relatively direct role of the contralateral motor cortex, due to corticospinal projections (Soteropoulos et al., 2011), in the execution of tasks and the participation of both ipsilateral and contralateral hemispheres in preparation, planning (Cisek and Kalaska, 2005) and execution (Schaal et al., 2004). However, direct interpretation of EEG results requires further source localisation of ERPs and ERD/ERSs.

5.1.2. Time-Frequency EEG Signatures

While many aspects of ELR and CAR time-frequency features of EEG are similar, CAR provides more local features with more pronounced region-dependent features. As shown in Section 4.3, the pattern of laterality mentioned in Section 5.1.1 can be found for time-frequency features as well, especially for β band desynchronisation.

The γ band ERS in the parietal area is observed before and during force generation when the direction of exertion is known. It can be inferred that this low-γ band ERS in the parietal area is induced by the directional content of the cue stimulus.

5.1.3. Directional Information in EEG

According to the classification results in Section 4.4.3, the motor related EEG in both the planning and execution stages of isometric tasks *do* contain information about the exertion direction. This directional information is not caused by cosine tuning, as the inter-class variances of ERPs and ERD/ERS do not reach significance level; this is despite the observation of cosine tuning in movement ERPs and ERS/ERD (Valsan, 2007) and both isometric and movement SUA (Cisek and Kalaska, 2005; Sergio et al., 2005). It is however noteworthy that this directional information is not present in all electrodes, but can be found only in specific EEG recording sites for each subject. This is not unusual as not all of the EEG recording sites reflect the neural activities of motor areas. Additionally, not all the motor areas necessarily reflect the exertion direction in their neural activity. Consequently, while the set of all recording sites contain the directional information of the task, this information is mostly in the best performing electrodes (with respect to their level of directional information) subset of the whole EEG electrode montage. As a result, the classification rate of the best performing electrode (a subset of montage) is equal or less than the rate for the whole montage. The whole electrode set would have classification rates equal to the best-performing electrode if other electrodes gave no contribution to

the information content. The whole electrode set would have higher information rates if the information from all of the EEG channels were appropriately combined together.

By comparing the best performing electrodes, the level of directional information in the transient and sustained segments of the planning and execution stages are not very different from each other. The GO stage shows slightly higher classification rates. It can be inferred that the underlying neural activities that contribute to directional information are present in both transient and sustained EEG activity, and both time windows contain directional information.

The planning stage also shows only a little less information compared to physical force production, i.e. 49.8% vs. 57.7% according to Table 4.12. This, together with inconsistent distribution of best-performing electrode location (also reported in Valsan, 2007) suggests that the contralateral M1 is probably neither the primary nor the only contributor to the directional information of ERPs in isometric exertion EEG. The fact that the best classification rate is observed at different recording sites and by different classification methods shows that the direction of exertion *is* reflected in EEG; however, the applied classification methods can only partially capture the underlying neurophysiological patterns.

5.2. Comparison of Results to Previous Studies

In this section, the findings are compared to previous research results on the neural correlates of isometric exertions, especially the EEG studies. Some studies (addressed in Sections 5.2.1 and 5.2.2) have used the readiness, planning and execution protocol, which are the most similar experiments to this study regarding the task protocol. Instruction-delay, an effective tool to distinguish between different stages of sensorimotor processing, is commonly employed in invasive recordings from primates. But due to the poor temporal resolution, it is less commonly used in other recordings such as human fMRI protocols. In the domain of EEG studies, the EEG features of interest for ERD/ERS are commonly measured in neurophysiological and BCI research studies; thus, there are few studies to date with systematic use of instruction-delay or similar protocols (see Chapter 2 and Section 5.2.2 for examples). Consequently, the majority of previous EEG studies report only the neural correlates in the execution or preparation stage. Partial comparison to some of these reports are possible with caution and consideration of the experimental condition.

5.2.1. Comparison to Single Cell Recording Studies

5.2.1.1. Comparison of Activity Patterns

The single cell recording studies, though usually recorded from non-human primates, give valuable information about the firing rates of cells in specific regions of the cerebral cortex during various motor tasks. Although the firing rate activity measures have not proved to generate ERD/ERS activity patterns they do provide measures of neural activity (with the assumption that the recorded oscillations come from the recording sites).

Cisek and Kalaska (2005) present a comprehensive study of motor and pre-motor activity of instruction-delay arm reaching tasks. During task execution both M1 and PM show transient activity, but only PM shows activities (in transient form) when attention and especially directional cues are presented to primates.

Isometric studies mostly address M1 activity during task execution (Sergio et al., 2005). There are both transient and sustained activities during force development and maintenance. There are a few studies that address PM activity in isometric tasks and practically no results for the planning stage of isometric exertions (Ashe 1997b and personal communication, John. F. Kalaska, Département de physiologie, Université de Montréal).

The involvement of ipsilateral and contralateral areas in different stages (see Section 5.1.1) is in agreement with single cell instruction-delay studies. In PMd areas there is considerable planning activity in both contralateral and ipsilateral sides, especially in the contralateral side. This activity is maintained during the execution of movement. In M1 activity is seen only during motor execution and not during planning. The activity in the contralateral side is considerably higher than the ipsilateral side (Cisek et al., 2003).

Although the appearance of sustained and transient EEG ERD/ERS, in different stages of the experiment, and some laterality patterns are very similar to transient and sustained single cell firing rates it is difficult to conclude if ERD/ERS are generated by the same sources. A preliminary interpretation would be to associate low frequency (2-7Hz) ERS to pre-motor areas (supplementary motor area (SMA) and, or PM), the μ and β band ERD to M1 and low-γ ERS to a source in the parietal cortex. This requires more spatially accurate EEG studies along with further establishment of ERD/ERS generation fundamentals (Pfurtscheller, 2006), for example through fMRI (Cooreman et al., 2011). Moreover, the current opinion about ERD/ERS sources and generation mechanisms (da Silva, 2006) does not confirm this.

5.2.1.2. Comparison of Directional Information

Compared to multi-joint control of artificial arms by invasive spike-activity-based BCIs (Velliste et al., 2008) the extracted information rate in this study is very low; however,

considering that the single channel classification rates are the lower bound of the directional information of the whole EEG montage and also the filtered nature of EEG, the directional information can be used for neuroscientific studies and for limited use in EEG-based BCI. Section 5.2.2.3 discusses the results against ECoG and non-invasive EEG/MEG studies.

5.2.2. Comparison to EEG, MEG, and ECoG studies

In this section, the observed ERPs are compared to previous EEG studies (Section 5.2.2.1). In addition to ERD/ERS studies using surface EEG, the MEG and ECoG studies can be used for comparison of time-frequency characteristics (Section 5.2.2.2) and directional information of the results (Section 5.2.2.3). These techniques can give more or less similar characteristics of oscillatory brain activity, especially in case of ECoG where the neural signal is affected by much lower level of spatial and temporal low-pass filtering.

5.2.2.1. Comparison of Motor-Related Potentials

In this section, the previous findings on motor-related potentials (MRP) during movement tasks and then during more relevant isometric tasks are used for comparison. These studies include a wide range from self-paced and reaction-time to instruction-delay or pre-cueing studies. In what follows, after a case-by-case comparison of ERPs, a summary of similarities and differences of ERP compared to previous studies is presented

While the general similarity of waveforms in AC and DC stages (see Section 3.2.3) in many electrode positions (roughly corresponding to non-informative and informative cues of MacKay and Bonnet, 1990) can be confirmed, the exact shape of ERP waveforms and their negativity and amplitude greatly depends on the planning stage and the spatial position of the electrodes, as shown in detail in Section 4.2. The potentials during motor execution at C_z are also very close to that of MacKay and Bonnet (1990), however, this does not hold for other electrodes. This can be due to different electrode positions and referencing methods in this study and the one by MacKay and Bonnet (1990). As discussed earlier, the frontal and parietal regions usually have reciprocal negativity and positivity features.

Wild-Wall et al. (2003) explored pre-cued, impeded finger movement tasks and different planning conditions. They come up with similar results with mid-line electrodes (especially parietal region) showing more pronounced variations in ERP magnitude. The other pre-cuing experiment on movement where spatial distribution of CNV is discussed (Leuthold and Jentzsch, 2009) reports similar spatial patterns compared to the present results: frontal negativity in early CNV (roughly corresponding to AC and DC in the

present experiment) and central negativity in late CNV. The waveform peaks with monotonically increasing or decreasing trend across 2D spatial map of surface EEG can be an indicator of a one dominant generating source; however this demands further source localisation studies on ERPs.

MRPs during self-paced isometric arm tasks are reported in the central electrodes (Oda et al., 1996; Shibata et al., 1997) and with the same pattern of waveform negativity and positivity peaks compared to Ulrich et al. (1998). The reported activity, including the negativity in frontal regions (Oda et al., 1996), matches the observations in this study during force generation. Despite the observations in this study, some of the published results on isometric finger force production report no notable positivity peaks (Slobounov and Ray, 1998). Reaction-time isometric studies (do Nascimento et al., 2005) report negativity before the cue, and a N-P pattern during execution at C_z. Imaginary reaction-time isometric exertions produce a similar pattern with the negativity peak partially suppressed (do Nascimento et al., 2006). The number of waveform peaks and their pattern is different from observations in this study, which is mostly due to different timing and cueing paradigms. Ulrich et al. (1998) present ERPs and LRP (lateralised readiness potentials) of pre-cued finger isometric tasks. This study shows planning and execution potentials in the form of single positivity for mid-line electrodes, followed by gradual negativity after planning and sustained positivity following the execution cue. Absence of positivity and negativity peak patterns can be attributed to constant and predictable between-cue and inter-trial intervals.

There is limited reference to the timings of the waveform positivities and negativities with respect to the visual cues in previous studies. By visual inspection of previous study results, a qualitative comparison is possible. For pre-cue/cue isometric finger force tasks, the results from Ulrich et al. (1998) show a large positivity peak in F_z, C_z and P_z after about 230ms of pre-cue. Compared to present results (Table 4.5) they are only close to the CAR positivity peak at C_3, 249ms after DC and the ELR positivity peak at Fz after 242ms of DC. Their results also show a positivity peak in F_z and C_z after about 230ms and in P_z after about 380ms of go-cue. No waveform peaks with timings comparable to this study were found. In another similar experiment results from Leuthold and Jentzsch (2009) shows a N-P-N pattern at C_z with approximate latencies of 150ms, 230ms and 350ms after the pre-cue. Among these waveforms, only the last negativity peak resembles the negative peak in the results 353ms after AC. Again, the predictability and timing of the cues are the main source of variability in the aforementioned and forthcoming discussions on variability sources.

The key similarities and differences of the present results compared to the aforementioned studies are briefly summarised:

1. Similar sustained negativity in motor planning and sustained positivity in motor execution over the central motor areas (Wilke and Lansing, 1973; Ulrich et al., 1998).

2. Similar trend of positivity in parietal recordings and negativity in frontal recordings in many ERP waveforms (Jahanshahi et al., 1995; Leuthold and Jentzsch, 2009).

3. Different and more complex waveforms, largely different waveform timings due to unpredictable cues in different stages in this experiment and the absence of many waveforms in previous studies due to different experiment design (Slobounov and Ray, 1998; Ulrich et al., 1998; do Nascimento et al., 2005, 2006; Leuthold and Jentzsch, 2009).

4. Different spatial variation of the observed features due to different EEG referencing and different experiment design (Wilke and Lansing, 1973; MacKay and Bonnet, 1990).

As discussed above, while the sustained negativity in the planning stages and the relative spatial distribution of frontal and central negativity of the results match the previous findings, relatively complex waveforms are observed in different stages of the trials. Part of this can be attributed to the random timing of the cues. The negativity or positivity peaks over spatial surface EEG maps are more location specific in common average referenced (CAR) EEG. The laterality of time-domain potentials as underlined in Section 5.1.1, is also in agreement with the proposed origins of Bereitschaftspotential (BP) or readiness potential (RP) components. BP components are observed mostly as premovement negativity in self-initiated movements similar to observations in this study; however BPs are maximal during self-initiated movements, and attenuated in cued experiments. The early and late phases (BP1 and BP2) are considered to originate from the SMA and contralateral M1 (Colebatch, 2007). This substantiates the previous argument in Section 5.2.1 that early symmetric components originate from the SMA during preparation, planning and execution and the large asymmetric components, including sustained potentials, originate from M1, and especially contralateral M1. However, it is again underlined that although there are similar trends between previous published results and the observations here, the comparison is not completely accurate; this is because the planning and execution initiation (instruction delay vs. reaction-time vs. self-paced) involving body parts (arm, fingers, foot), force magnitude or other parameters are not completely the same.

5.2.2.2. Comparison of Time-Frequency Signatures

The time-frequency EEG features of interest (ERD/ERS) are commonly measured by the neurophysiology and BCI research community. This means while there are well established ERD/ERS studies on movement tasks and motor imagery, there are few ECoG and EEG studies that explicitly address a separate planning-execution stage (see for example Hammon et al., 2008 that addresses directional information in planning and execution). There are relatively common trends of activity during various movements and isometric tasks (Graimann and Pfurtscheller, 2006; Waldert et al., 2009). MEG and EEG signatures of arm movements (Waldert et al., 2008), as well as ECoG signatures (Ball et al., 2009) show ERS in δ, θ, and high-γ bands (above 50 Hz) and ERD in α and β bands with most of the reported ERD/ERS on contralateral and to some extent ipsilateral motor areas. This is in agreement with general expectations of movement-related ERD/ERS (Graimann and Pfurtscheller, 2006; da Silva, 2006; Srinivasan et al., 2006)

The ECoG signatures (in terms of ERD/ERS) of non-directional sustained isometric contractions of body parts over several regions of the brain (Crone et al., 1998a,b) also show notable trends. There is α and β band ERD in transient and (to a lesser extent) sustained forms over the motor areas in both ipsilateral and, especially, contralateral sides. The low and high γ ERS has also been reported over contralateral motor areas.

In the execution stage, the same pattern for δ, θ, α, and β are seen in both EEG movement studies and ECoG isometric studies. In the γ band (30-50 Hz) the movement studies report ERD (McFarland et al., 2000; Caldara et al., 2004; Neuper et al., 2006b) while the sustained contraction ECoG study (Crone et al., 1998a,b) reports ERS. In this study, ERS is observed in parietal regions (P_z) and ERD is seen in other regions including ipsilateral and contralateral motor regions. The reported ERD in all bands during early isometric foot force generation in C_z (Masakado and Nielsen, 2008) is confirmed by the results for the α and β bands; however for the δ and θ bands ERS is observed. This changes to ERD during force maintenance. Attentional processing and force development-related changes may be responsible for this difference.

The reported μ band ERS in some neighbour electrodes along with the primary ERD (Pfurtscheller and Neuper, 1994) is not observed. This can be attributed to the large and extended regions of arm cortical motor regions.

The other observation is the sequential ERS and ERD in frontal regions (F_z) after the very beginning RC stage, and after DC in C_4. This is observed in part of the β band. A similar observation but with reverse order of appearance of ERS and ERD, and in a different experimental setup, has been reported (Graimann and Pfurtscheller, 2006).

It can be concluded that the readiness and planning stages share many common (and mostly transient) time-frequency features in isometric exertions; however, there are fea-

tures specific to each step. Execution can be described to have the most prominent ERD in the widest range of frequencies.

As mentioned earlier in Section 2.2.4.1, most EEG studies about isometric contractions or tasks have targeted corticomuscular coherence (CMC) features. This is the case from earliest findings (Conway et al., 1995) to more recent studies (Salenius and Hari, 2003). A relevant result may be the contralateral CMC in β band (Schoffelen et al., 2008) during wrist extension. Some studies also consider the effect of task or force parameters in CMC (Chakarov et al., 2009) but not explicitly as ERD/ERS over time. There are also reports on other frequency domain features, such as shift in peak frequency (Krause et al., 1983).

5.2.2.3. Comparison of Directional Information

The achieved rates of classification for exertion direction can be compared to similar studies in Table 2.3.

Compared to the self-paced arm movement ECoG study of Ball et al. (2009), for 4-classes, the same maximum classification rates are estimated. In comparison, the present classification rates are higher during planning, but not during execution. However, for the 5-class cued movement ECoG study of Reddy et al. (2009) the classification rates in the current study on average are lower.

In comparison to the 3-class instruction-delay movement study of Hammon et al. (2008) present results show matching or better directional information (considering the class difference). Compared to the cued 4-class arm movement EEG study of Waldert et al. (2008), there are higher average and maximum classification rates, but not against the whole-montage MEG results of the same study. In comparison to 4-class wrist movement EEG study of Valsan (2007), the current study shows higher average and lower maximum classification rates in the case of cued movements and lower average and higher maximum rates in case of self-paced movements. The results from this study show lower average or maximum classification rates compared to the motor imagery of Valsan (2007).

For better comparison of results from this study against previous studies Table 5.1 lists the extracted information from the classification in terms of relative entropy (Shannon, 1948), reported in bits/trial (Waldert et al., 2008). This facilitates the comparison of extracted information content for different studies regardless of the number of classes.

In the current study, the extracted directional information in planning is 0.2044 bits/trial on average and a maximum of 0.5137 bits/trial. In the execution stage, the average extracted information is 0.3467 bits/trial and up to the maximum of 1.077 bits/trial. In ECoG studies, the extracted information in plan and reach is on average 0.2993 and

Table 5.1. Comparison of extracted information from classification for present study against previous EEG, MEG and ECoG literature .

Study	recording method	Cue	decoded information	mean decoding accuracy	maximum decoding accuracy	mean bits/trial	max bits/trial
Valsan (2007)	1-ch EEG	cued	wrist movement direction	52.2% @4 class	85 % @ 4 class	0.2438	1.152
Valsan (2007)	1-ch EEG	self-paced	wrist movement direction	61.8% @4 class	75 % @ 4 class	0.4351	0.7925
Valsan (2007)	1-ch EEG	cued	wrist imaginary movement direction	72.2 % @ 4 class	95 % @ 4 class	0.7067	1.634
Hammon et al. (2008)	m-ch EEG	cued	arm movement direction	(58.85%,63.0%) @ 3 class plan/reach	n/a	(0.1962,0.2643)	n/a
Waldert et al. (2008)	CL m-ch EEG	cued	arm movement direction	55.0% @ 4 class	69.2% @ 4 class	0.2940	0.6210
Waldert et al. (2008)	m-ch MEG	cued	arm movement direction	67.0% @ 4 class	85.0% @ 4 class	0.5620	1.152
do Nascimento and Farina (2008)	1-ch EEG	cued	rate of imaginary foot force development	82.6% @ 2 class	91% @ 2 class	0.3332	0.5635
Gu et al. (2009)	1-ch EEG	cued	target imaginary foot torque	79.0% @ 2 class	100.0% @ 2 class	0.2585	1.0
Gu et al. (2009)	1-ch EEG	cued	rate of imaginary foot force development	82.5% @ 2 class	100.0% @ 2 class	0.3310	1.0
Ball et al. (2009)	CL m-ch ECoG	self-paced	arm movement direction	(45%, 75%) @ 4 class plan/total	(70%, 80%) @ 4 class plan/total	(0.1355,0.7925)	(0.6432,0.9611)
				(45%, 55%) @ 8 class plan/total	n/a	(0.4632,0.7439)	n/a
Reddy et al. (2009)	m-ch CL/IL ECoG	cued	arm movement direction & key press	73.5% @ 5 class	86.0 % @ 5 class	0.9577	1.4577
This Study	**1-ch EEG**	**cued**	**arm exertion direction**	**(49.8%, 57.7%) @ 4 class plan/exert**	**(65.1%, 83.1%)**	**(0.2044,0.3467)**	**(0.5137,1.077)**

[a] 1-ch: single channel, m-ch: multi-channel, IL: ipsilateral, CL: contralateral.
[b] The cited ECoG studies used subdural ECoG recordings.
[c] Information content relationship of Waldert et al. (2008) is used to convert classification rates (%) to information content (bits)

0.8630 bits/trial and the maximum levels are 0.6432 and 1.2004 bits/trial. For EEG studies the mean values are 0.1962 and 0.3809 bits/trial and the maximum level in execution is 0.9894 bits/trial. It is concluded that EEG of cued directional isometric tasks, during the execution stage, contain higher average directional information than EEG (and in some cases ECoG) of cued directional movement tasks (significant, one-tail t-test p=0.02767<0.05). The maximum rate of 1.054bits/trial is however smaller than the 1.152bits/trial value of Valsan (2007) and Waldert et al. (2008). The information level during planning (0.2044bits/trial) is higher than 0.1962bits/trial of movement planning (Hammon et al., 2008). These values fall within the expected range of information rates for non-invasive BCIs, i.e. less that 2 bits/trial per second in terms of transferred information (Daly and Wolpaw, 2008).

5.3. Considerations and Limitations of Study

5.3.1. Source and Nature of the Observed Brain Activity

It is important to take into account the potential visual stimulative effects of the experiment. The distance between the subject and monitor screen limits the visual angle to 5 degrees and minimises the eye-movement and movement artefacts. All the trials with traces of eye movements were rejected, and no trace of eye movements in the multichannel EEG of the accepted trials is expected.

Regarding the visual processing of cues it should be emphasised that the task is a visuomotor task because of the roles of cues and real time feedback of force on the screen. Consequently the visual processings cannot be completely removed from motor aspects of the task; however, it is noteworthy that the ERPs and ERD/ERSs observed after the cues are because of the attentional processings induced by the cues in the planning and execution of the requested task, and not the visual appearance of cues *per se*. In previous experiments (Valsan, 2007), there has been no specific time and time-frequency features when no reaction or task is requested from subjects and they just neglected visual cues. In case of simple small non-flashing cues, even when they start to move, there is no evoked potential, unless the target is attended by the subject (Guo et al., 2008b). In short, the visual components, if any, get their identity in the context of the visuomotor task. Additionally, it is observed that ERPs and ERD/ERS patterns are not of higher intensity in occipital areas over visual cortex (O_z and I_z electrodes); neither are the high frequency ERS/ERD in most frontal electrodes (e.g. AF_z) compared to motor cortical areas. Nevertheless, the term event-related potentials (ERP) are preferred and used over motor-related potentials (MRP) for the observed potentials.

The identified features related to isometric planning and execution are not available in the literature for this specific experiment paradigm. The accurate sources of ERD/ERS are not completely known and both thalamo-cortical loops (da Silva, 2006) and motor-cortical areas (Cooreman et al., 2011) have been suggested as generating sources of ERD/ERS. The author, however, suggests that the low frequency (2-7 Hz) ERS is mostly related to preparation, planning and initiation of motor tasks in SMA and PM; and the α and β band ERD is mostly related to the facilitation of motor command generation in M1 and PM. It is also known, however, that the observed ERD/ERS are not of a visual nature, as previously mentioned. More certain conclusions about the function and origin of oscillations require more sophisticated spatial analysis, source localisation studies on ERD/ERS and further experiments. The origin and mechanism of ERD/ERS plays a crucial role, especially for BCI rehabilitation.

The role of the active body part and direction-dependent active muscles needs to be underlined. As the averaged results for all directions are reported, the study does not highlight the spatio-temporal features specific to each direction. This makes the task similar to more complicated arm tasks where all the muscles are activated at the same time. It is noteworthy that motor parameters, such as direction and level of exerted force, are known to affect the signal amplitude only, and not the waveforms or essential ERD/ERS characteristics (do Nascimento et al., 2005, 2006; Valsan, 2007; Leuthold and Jentzsch, 2009; Waldert et al., 2009). Also, according to the inter-class variances for ERPs and ERD/ERSs in Sections 4.4.1 and 4.4.2, the observed activity type does not vary considerably between classes (i.e. directions). Consequently the reported features hold for all directions.

As mentioned earlier, the previous literature about ERD/ERS includes various experimental set-ups and different tasks (sustained contraction, reaching, manipulation and so forth). Consequently, the comparison of the present results to those reported in the literature should be considered as approximate and not as exact validation. This is of special importance as variability in the observed EEG has been reported (Graimann and Pfurtscheller, 2006; da Silva, 2006) and also taking into account the different neuro-circuitries and neuro-computations responsible for different motor tasks in the literature (Jordan and Wolpert, 1999; Shadmehr and Wise, 2005).

5.3.2. EEG Averaging and EEG Normalisation

The reported results are either observed for all subjects or in the "majority" (5 of 8) of subjects, which equals 0.0488 significance level. Averaging across subjects was avoided in this study. In some cases, significant ERD (e.g in late post-cue time windows) was seen in the majority of subjects, but a few subjects displayed significant ERS activity. In

such cases, although the activity is statistically significant, the interpretation of activity as ERS or ERD is directly related to the normalisation. By avoiding simple averaging, the dominant phenomenon is reported, and at the same time the issues related to normalisation are discussed in the next paragraph. Nevertheless, the reported phenomena are reasonably sound, firstly, because averaging is carried out over many trials (about 100 trials for 5 main electrodes, see Appendix E.1 for exact numbers) within subject datasets, and secondly because of careful artefact rejection and presence of some features in all 8 subjects. For BCI research, there are regions in time-frequency plane that show significant changes with respect to rest time. However not all of these regions show ERS or ERD in a specific and consistent fashion. These changes can be used for event-detection by employing techniques that do not rely on the relative increase or decrease (compared to rest-time) of spectral EEG features.

In this study, rest time EEG is used for normalisation of CWT moduli. While the subjects are assumed to be in rest during this time window, they may perform a physical or a mental task that is undetectable by the experimenter or by inspection of EEG or force data. The relatively high number of recorded trials for averaging lowers the chance of reflection of these activities in EEG. Some individual/subject-specific signal characteristics can be attributed to cognitive and psychological parameters affecting the subject's awareness during the experiment and how attentive the subject is in responses to cues. This considerably affects EEG features such as μ rhythm amplitude, when subjects have different levels of motor-readiness across trials and against different types of cues in comparison to other subjects. There is some evidence about cognitive-related EEG modulation (Compton et al., 2011) and test-retest variability of rest-time spectral EEG features (Fernández et al., 1993). Application of more sophisticated normalisation techniques can help reduce some of the observed variability in the data (Grandchamp and Delorme, 2011).

5.3.3. Classification Methods

While the applied classification methods give classification rates comparable to or better than movement task studies, it should be mentioned that the methods have major limitations.

The first major limitation of PCA dimension reduction and classification afterwards is that no discrimination is made between *class-dependent variance* and *class-independent variance* (Fukunaga, 1990). This can considerably deteriorate the classification rates.

The other issue is the inaccuracy that comes from shifted or time-warped ERPs or time-frequency features. This is because of the variability in human performance. Additionally, if the time or time frequency features contain suppressed features in small time

windows the present methods cannot efficiently take this suppressed or missing features into account.

While using the classification methods on scalogram values was not successful it is expected that time-frequency parameters will give good classification results with other techniques, as reported in previous EEG (Valsan, 2007) and ECoG (Chao et al., 2010) studies.

5.4. Interpretation of Results

5.4.1. Relevance to Research Hypotheses

According to the results and the discussions to this point, it may be concluded that there are consistent signal features associated with the planning and execution of isometric tasks as there are for movement tasks and movement imagery (McFarland et al., 2000; Caldara et al., 2004; Neuper et al., 2006b). Furthermore, the observed signal parameters in planning and execution are similar to those of movement or movement imagery (McFarland et al., 2000; Caldara et al., 2004; Neuper et al., 2006b), except for the minor difference discussed earlier (see Section 5.2.2). This is in agreement with the thesis hypotheses that isometric tasks are very similar to movements regarding the EEG signatures and can be used instead of movements in many applications (see Section 2.4.2.1).

The spatial distribution of the signal across the surface EEG map seems to be in agreement with the idea that the contralateral M1 is more active in execution; there is bilateral preparation/planning activity in M1, and there is bilateral preparation/planning/execution activity in PM. It is also suggested that parietal cortex is involved in direction-dependent sensorimotor integration when an isometric motor task is attempted.

The ERD/ERS does not only originate from the extrinsic coordinate change of the limb or from the pattern or intensity of the involved active muscles as they can be seen in planning and execution of arm isometric tasks. This is in agreement with the thesis hypotheses that ERD/ERS generation does not depend on extrinsic limb coordinates (see Section 2.4.2.1).

There is directional information in both stages of planning and execution, as hypothesised. This is of equal or slightly higher levels compared to movement EEG/MEG and even some ECoG studies; however, despite the previous hypothesis, the directional information does not come primarily from specific electrodes above M1, PM or SMA during planning and execution, but can be found in different electrodes in scattered patterns. This directional information does not originate from consistent direction-dependent modulation of ERP or ERD/ERS as in cosine-tuning in movements. The direction-dependent

modulation does not reach a statistically significant level.

Due to decreased motor task variability an improved directional decoding, in comparison to movement studies, is expected; the directional information is about the same level or slightly better than previous studies (Valsan, 2007; Waldert et al., 2008). This can be attributed to increased accuracy due to a less variable motor task, but also a simultaneous decrease in directional information due to a lack of coordinate change or physical target point. The classification method complexity and differences in experimental setups and paradigms suggest that further research is needed to verify this hypothesis.

5.4.2. Potential Oscillatory and Directional Tuning Mechanism

It seems that there are distinct and significant oscillatory characteristics in EEG associated with isometric motor task planning and execution. As some of these features are rather variable in ELR and CAR EEG and some of them are less variable across subjects, they can originate from different generators with different locations and distributions. Further ERP and ERS/ERD localisation studies are required to clarify this.

The other major concept to consider is the directional tuning (Georgopoulos et al., 1986) and is reported to be reflected in ECoG and EEG/MEG as well (Valsan, 2007; Waldert et al., 2009). However, by comparing the inter-class variance of ERPs and scalograms (see Sections 4.4.1 and 4.4.2) little directional tuning in the current experiments are noticed. While the directional tuning is observed in M1 and PM during movement (Cisek and Kalaska, 2005) and in M1 during isometric tasks (Sergio and Kalaska, 1998, 2003; Sergio et al., 2005) it seems that the directional (cosine) tuning in EEG is observed in movements and not in isometric tasks.

The absence of cosine tuning and presence of directional information in isometric task EEG implies that cosine tuning is not the only source of directional information. This is based on the negligible and non-significant level of tuning of ERP or ERD/ERS features, but relatively high directional information level comparable to movement tasks.

5.5. Significance, Contributions, and Impact

The significance and major contributions of thesis, are highlighted as follows. To the best of the author's knowledge, the present study is:

- The first EEG study to address ERD/ERS in the planning of directional isometric motor tasks.
- The first EEG study to address ERD/ERS in the execution stage of directional

isometric motor tasks. (Only limited ECoG data are available for sustained contractions.)

- The first study to extract directional information from isometric task execution where no extrinsic coordinate change has happened.
- The first study to extract directional information from isometric task planning where no overt or covert extrinsic coordinate change or muscle activity has happened.
- The re-examination of the existence of δ and θ transient ERS after an instruction cue; there is inconsistency in the literature in this regard. e.g. (e.g. Graimann and Pfurtscheller, 2006; Waldert et al., 2008; Valsan, 2007)
- The re-examination of low-γ ERS in parietal regions, and the first study to associate it to the direction of the task.
- The use of EEG ERPs and ERD/ERS to study laterality and approximate sources of brain activity in the planning and execution of isometric tasks.
- The reporting of the absence of cosine/directional tuning in isometric task EEG, in contrary to movement tasks.

In addition to the aforementioned points, the use of instruction delay or similar paradigms for more accurate neuroscientific studies is of importance. This study confirms that instruction-delay EEG studies are quite feasible and useful, and the results can be successfully interpreted to develop new understandings of the human motor system. More specific examples are the laterality and regions of activity during different planning and execution stages of the task.

Based on this knowledge, potential applications in targeted electrical brain stimulation would be to use EEG signatures as possible indicators for stimulation parameters. The frequency (δ, θ, β, γ), region of activity (frontal, parietal, central, ipsilateral/contralateral), polarity (ERD/ERS, positivity/negativity or cathode/anode stimulation) and the timing of the activity in EEG would be the first estimates for applying stimulation in rehabilitation protocols during a specific motor task.

Clinicians can use the reported EEG signatures as a measure to compare physiological and pathological patterns of motor-related EEG in the diagnostics of patients and healthy individuals. e.g. lack of gamma band ERS or ERD in parietal regions (which were shown to exist in healthy individuals), may be a symptom for a specific neurological disorder or disease.

The features identified in this study relate to isometric planning and execution, and therefore present additional insight into the EEG signatures previously described for point

to point movements and those generating joint/limb displacement. For clinical applications, it is likely that isometric training tasks, without the need for limb displacement (reaching, pointing and manipulation tasks), may provide a paradigm that is simpler to adapt to the needs of individual patients during the early stages of BCI-aided rehabilitation. First stage rehabilitation with isometric tasks are very similar to training with movement tasks, as they rely on mostly similar corticospinal pathways and both show similar EEG signatures. Besides, the difficulty in motor initiation, motor coordination, implementation of measurement and biofeedback during isometric task are considerably lower than movement tasks. Investigation of the observed signatures in acute stroke and other central nervous system (CNS) trauma conditions is of interest in this respect.

5.6. Future Works

Future work is expected to cover more accurate spatial analysis of the observed features using spatial filters (Van Veen et al., 1997), component analysis, and also more accurate time-frequency representations (e.g. Matching Pursuit, see Durka 2007) to localise the ERD/ERS sources more accurately in time, frequency and space. More advanced spatial analysis, including source localisation can identify the neuroanatomical regions active during different stages of motor tasks. Advanced time-frequency analyses can be used to more accurately investigate the timing of different ERPs and SMRs, while distinguishing more accurately between the ERD/ERS frequency contents during different stages of the task. Eventually this will amend the findings through source analysis.

However, given that a degree of inter-subject variability exists in the sample presented here, there is a need for caution in interpretation. Further studies aimed at determining the degree of inter-subject variability and the statistical significance of features of interest are therefore warranted. Similarly, the robustness of the reported observations is required to be explored through the use of a range of normalization techniques.

Finding various cortico-cortical and cortico-muscular coherence measures (Halliday et al., 1995) may also shed light on further cortical connectivities during isometric task planning and execution. A major further step would be to apply network analysis techniques (Lindsay and Rosenberg, 2011) to extract the causality information and direction of influence between different neuroanatomical brain regions such as the contralateral and ipsilateral M1, PM, and also SMA and parietal cortex.

Extension of the study to more complex experiments in which not only direction but also force magnitude, or rate of force development, is modulated can provide useful information about sensorimotor integration and its reflection in EEG.

From a clinical perspective, the study of subject groups with motor or sensory im-

pairments would be of considerable interest. An example of research in this area would be to distinguish between the ERPs and ERD/ERS that originate from sensory vs. motor processings or the combined sensorimotor integration. Knowing the exact sensory or motor correlates of ERPs and ERD/ERS in healthy and patient populations can help identify the exact neurological or sensorimotor impairments in patients, based on the pathological patterns of ERPs or ERD/ERS. In ideal case, these EEG-based diagnostics for sensorimotor impairments will be an addition to current EEG-based diagnostics (Benbadis et al., 2007) for cognitive and non-motor neurological or mental diseases.

The other area to explore would be the effect of motor learning, including adaptation to new kinematics maps, dynamics maps or tasks (Shadmehr and Wise, 2005) and the reflection of associated signals in EEG (Novakovic and Sanguineti, 2011; Perfetti et al., 2011). If there are specific activity patterns or oscillatory characteristics during motor learning the associated patterns can add to the understanding of sensorimotor processing and pave the way for potential tDCS interventions in future.

5.7. Chapter Summary

This chapter is the last chapter in the thesis. The results were briefly compared against previous, similar studies. After discussing the potential limitations and considerations, potential interpretations of the results according to the experiment characteristics and in regard to previous literature were summarised. Also the significant points of the study and how the future research topics can be expanded were mentioned. In the next section, the whole message of thesis is succinctly re-packed and this concludes the thesis.

5.8. Summary of Thesis Conclusions

- Instruction-delay protocols in movement and isometric tasks together with EEG analysis proves to be a useful tool for the study of human motor function.
- Isometric tasks in preparation, planning and execution stages show ERP and statistically significant ERD/ERS patterns very similar to movement and motor imagery; although no overt or covert change in limb coordinates or target-point happens. This suggests that the underlying generation mechanism is not exclusively a function of actual or imaginary length-dependent sensory activity.
- EEG accompanying an isometric task contains directional information in the planning and execution to the same extent as movement tasks; although no overt or

covert change in limb coordinates or target-points happen. However, despite movement ERPs or ERD/ERSs, the information does not seem to originate, consistently, from a specific source. This directional information is not a direct reflection of tuning of ERPs and ERD/ERS features. The cosine tuning of EEG features in isometric task planning and execution does not reach the significance level in the subject's group.

- The early interpretation of the activated brain regions and their laterality matches the current understanding of human motor function, but there is the need for further studies in this regard.

- Further investigating the reflection of the activity of different brain regions in EEG, as a function of different task stages and parameters are of benefit for clinical studies and for neuro-rehabilitation research.

Appendix A

Technical Recording Details

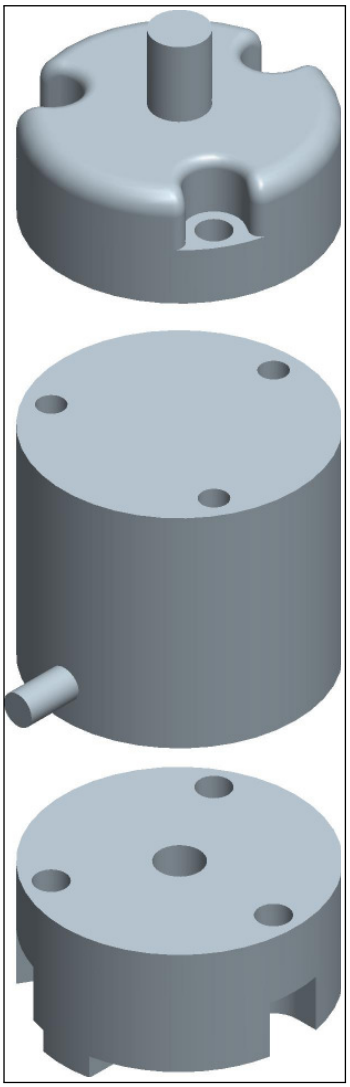

Figure A.1. Assembly of the top connector part, the force sensor (middle) and the bottom connector part.

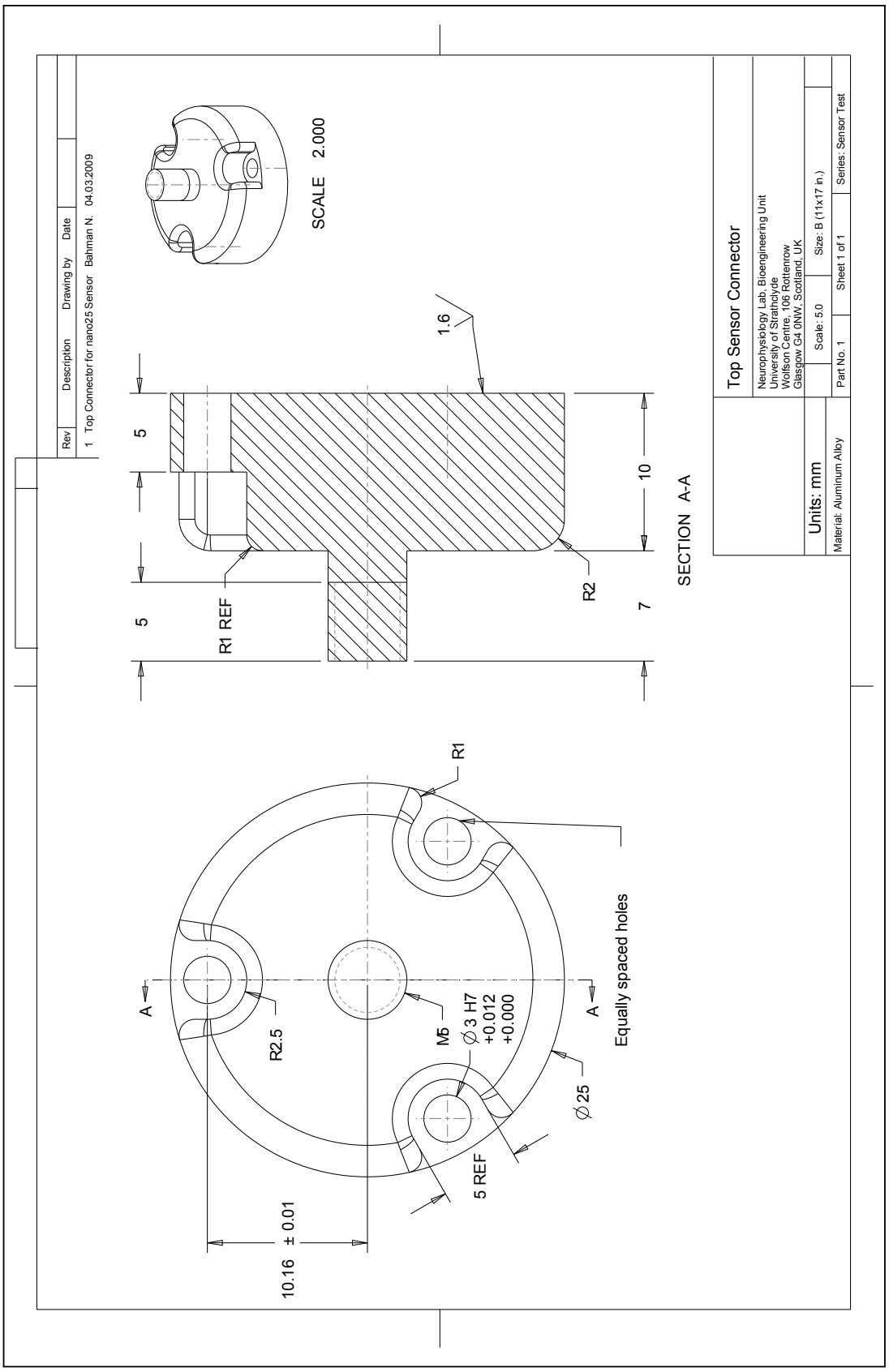

Figure A.2. Technical drawing for top connector part.

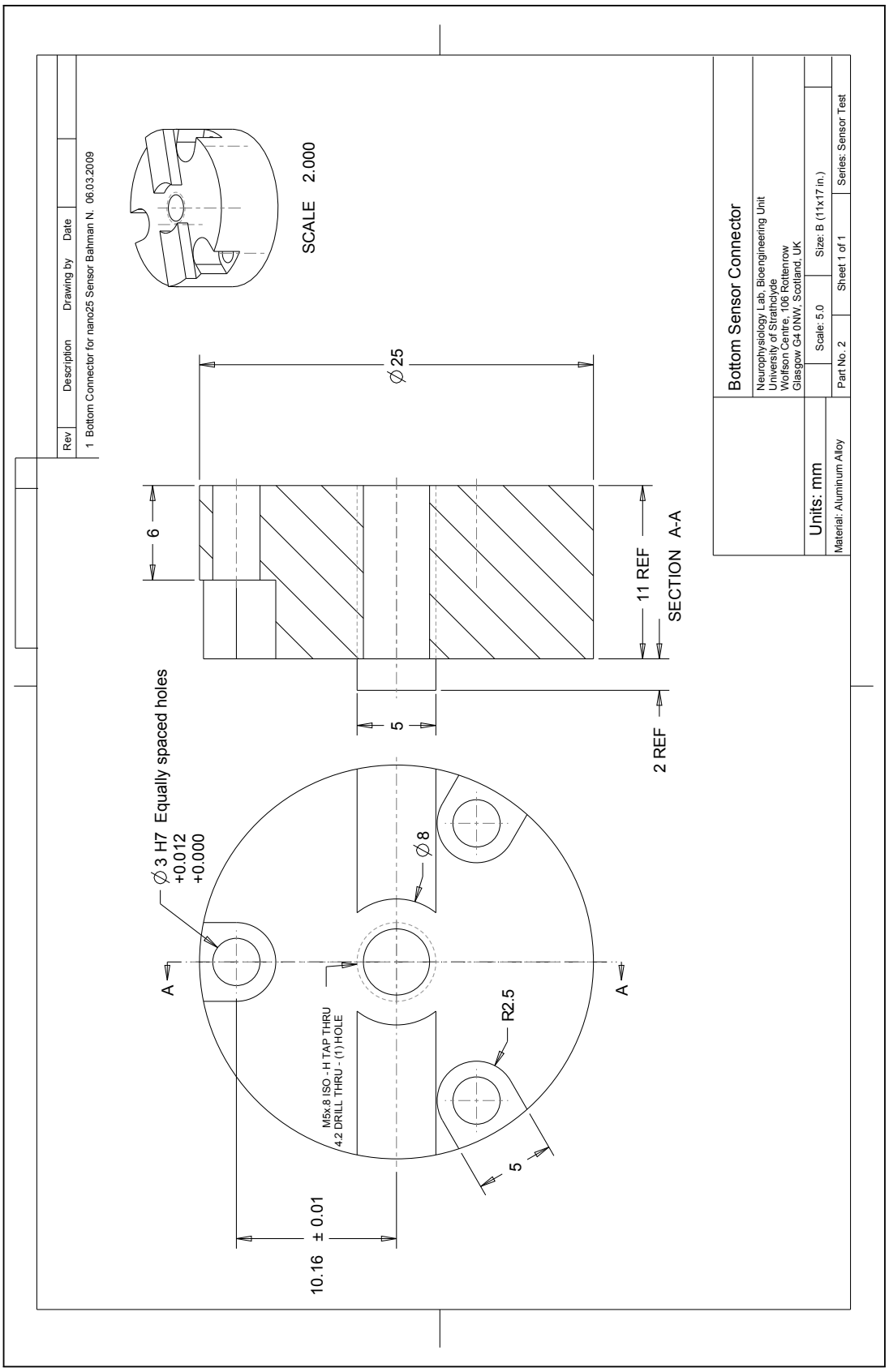

Figure A.3. Technical drawing for bottom connector part.

Events/Synchronisation Connection Cable, Version 2

Revision: 2009-07-03

Connections:

	I1	**O1**	**O2**
To/From	PC LPT Port	Synamps2 Event Port	CED Micro1401 Dig. In.
Plug/Socket Type	Male DB-25	Female DB-25	Female DB-25
	pin	pin	pin
GND	25	25	13
bit 0	2	8	21
bit 1	3	7	8
bit 2	4	6	20
bit 3	5	5	7
bit 4	6	4	19
bit 5	7	3	6
bit 6	8	2	18
bit 7	9	1	5, 23

Schematic:

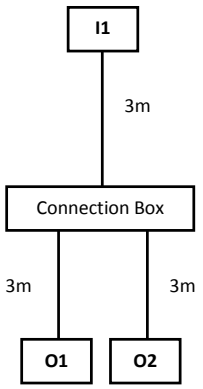

Figure A.4. Events cable: schematic and tables of connections to send cues from the visual stimuli computer to EEG and force recording systems.

Connection Box – Version3, 2009-07-08

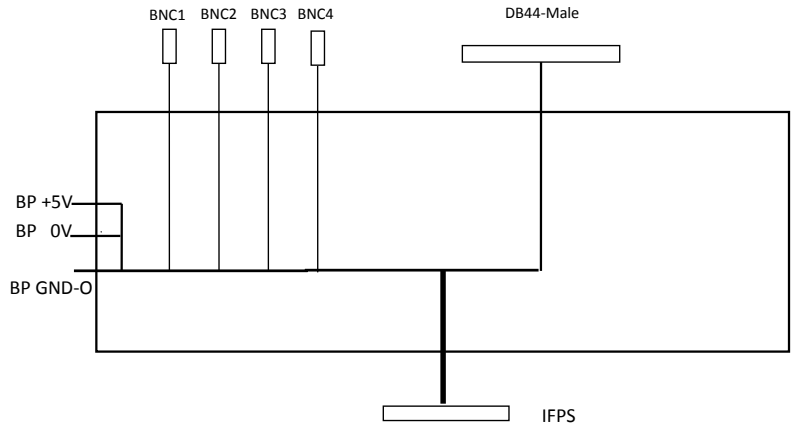

IFPS: 26-pin High Density D-Subminiature Connector, "INDUSTRY STANDARD FEMALE 26-PIN HIGH-DENSITY D-SUBMINIATURE" CONNECTOR

DB44 Male: 44-way Male high-density D-socket.

From (Connector-Pin#)	To (Connector-Pin#)	Description
IFPS-2	BP +5V	+5V Power Input from SA0 to IFPS
IFPS-4	DB44-Pin40	SG5 Positive Output from IFPS
IFPS-5	DB44-Pin38	SG4 positive Output from IFPS
IFPS-6	DB44-Pin36	SG3 positive Output from IFPS
IFPS-7	DB44-Pin34	SG2 positive Output from IFPS
IFPS-8	BNC4 I	SG1 positive Output from IFPS
IFPS-9	BNC2 I	SG0 positive Output from IFPS
IFPS-11	BP 0V	0V Power Input from SA0 to IFPS
IFPS-13	DB44-Pin39	SG5 Negative Output from IFPS
IFPS-14	DB44-Pin37	SG4 Negative Output from IFPS
IFPS-15	DB44-Pin35	SG3 Negative Output from IFPS
IFPS-16	DB44-Pin33	SG2 Negative Output from IFPS
IFPS-17	BNC3 I	SG1 Negative Output from IFPS
IFPS-18	BNC1 I	SG0 Negative Output from IFPS
IFPS-22	BP GND-O, all BNC-Xs O, DB44-Pin16 to DB44-Pin30	Ground
IFPS-Shell	GND	

* 4 BNC short connecting cables needed.

Figure A.5. Connection box: schematic and tables of connections to connect sensor interface box to the data acquisition box.

Appendix B

Software and GUI Tools

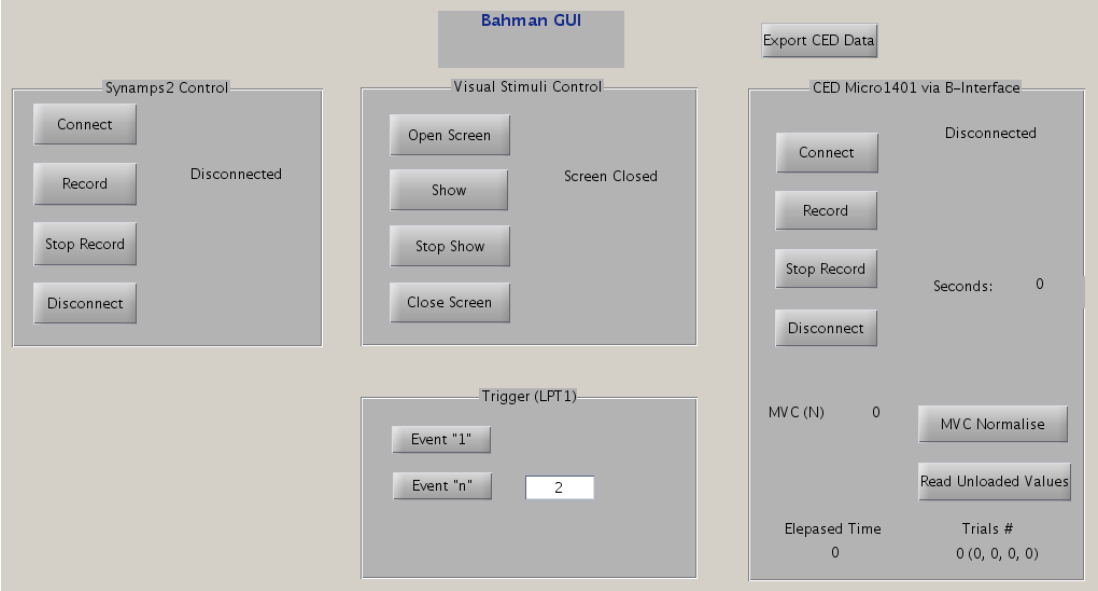

Figure B.1. Screenshot of the MATLAB GUI developed to control the visual stimuli and recording. *Synamps2 Control* panel is reserved for recording EEG and was not used. *Visual Stimuli Control* panel is used to open and close the visual stimuli screen and to start and stop showing the cues. It also shows the current screen status. *Trigger (LPT1)* panel is used to send fixed value (1) or arbitrary events to the LPT1 (parallel) port for testing purposes. *CED Micro1401 via B-Interface* panel is used to control the connection to the data acquisition box and recording the force signals, which is immediately visualised on the screen. It also shows the data acquisition box status and the recording time. The two buttons in the buttom are used to read the recorded values during unloaded condition (for callibration) and at maximum voluntary contraction (MVC) time (for normalisation). The MVC values, the elapased time and total trial numbers (right, forward, left, backward) are displayed. The *Export CED Data* button can be used to export the recorded data to file.

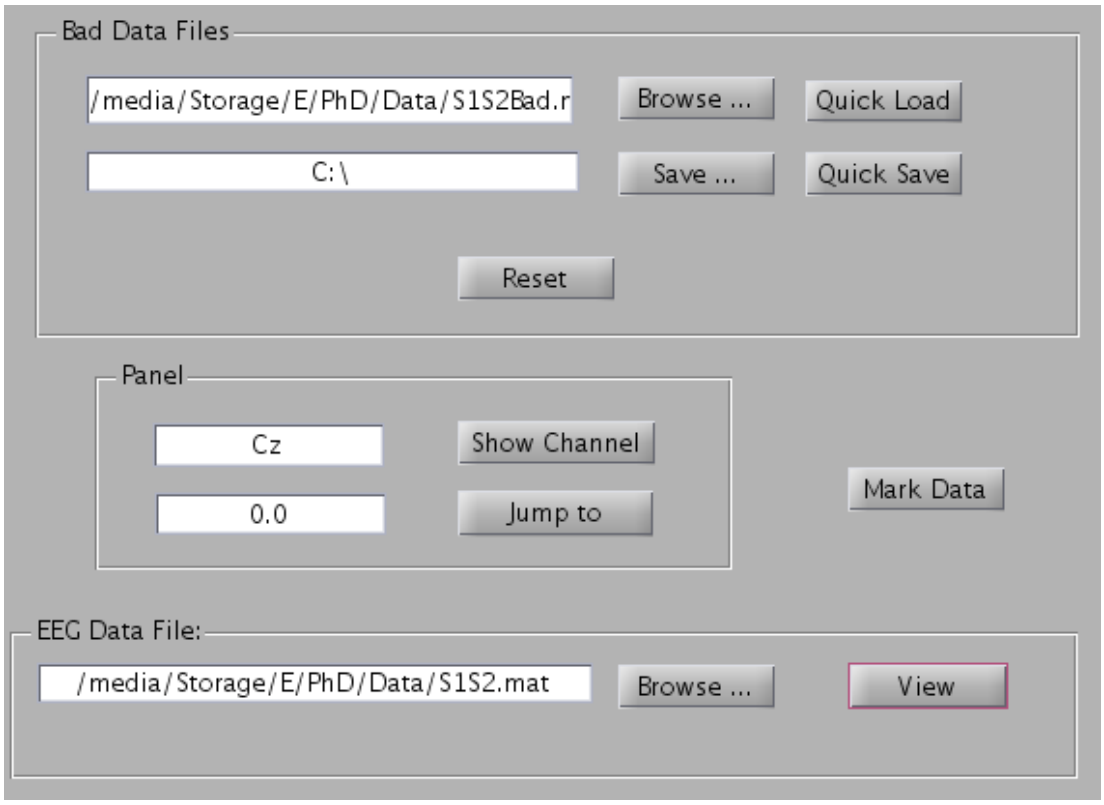

Figure B.2. Screenshot of the MATLAB GUI developed to visually inspect and mark (accept/reject) the recorded EEG and EMG data. The *EEG Data File* is loaded and displayed on a separate screen (see Figure B.3), the displayed channels and time on the screen are adjusted by the *panel*, and the interactive marking screen is activated by the *Mark Data* button. The bad/good marks for data are determined by the user interactively (Figure B.3), using mouse and keyboard and are stored separately as labels in *Bad Data Files*.

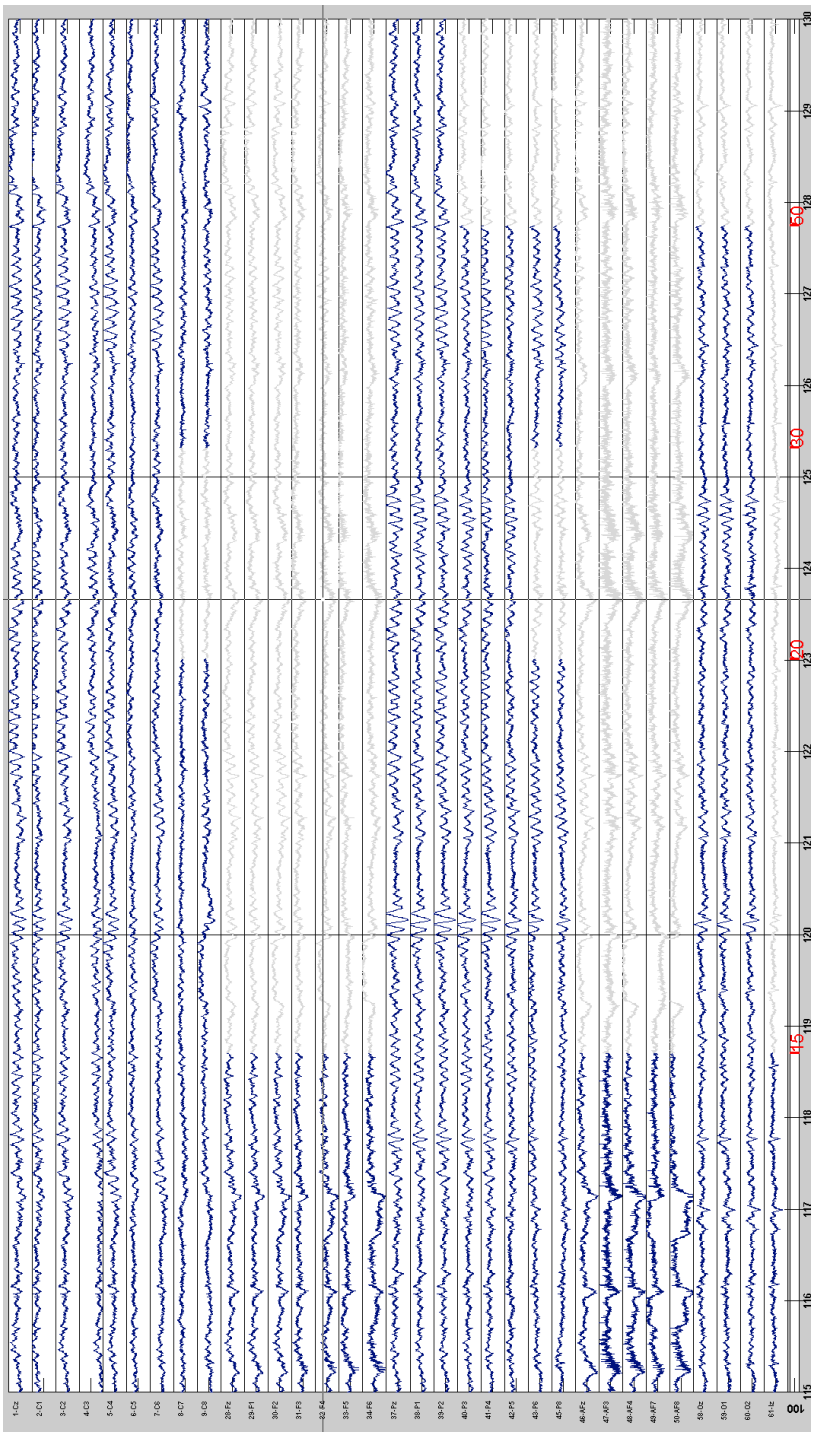

Figure B.3. Screenshot of the MATLAB GUI developed to visually inspect and mark (accept/reject) the recorded EEG and EMG data. The screen plots the raw signal segments marked as good in dark blue and segnments marked as bad in light grey. The timing in seconds and occurence of visual cues are displayed by numbers in the bottom panel where red 10, 15, 20, 30, 50 and 70 markers indicate the start of rest stage, RC, AC, DC, GO and end of trial, repectively (see Figure 3.5). The scale is shown in bold (100) and the channel numbers and labels are displayed. Not all the channels are shown in this figure, to provide better visual clarity.

Appendix C

Computational Implementations

C.1. Continuous Morlet Wavelet Transform

In order to inspect the EEG signals, the continuous wavelet transform coefficients as described in Equation (3.1) were computed. The Morlet mother wavelet was used for analysis, as formulated in Equation (C.1):

$$\psi(t) = \frac{1}{\sqrt{2\pi}} e^{-t^2/2 + j2\pi b_0 t} \tag{C.1}$$

The parameter $b_0 = 1$ was chosen by inspection, as it provides wide enough range before decaying to zero with respect to the period of oscillation. Its selection and design considerations are also discussed elsewhere (Durka, 2006). The Morlet wavelet is shown in Figure C.1.

Considering the definition of wavelet coefficients in Equation (3.1), and the property of the Morlet wavelet in Equation (C.1), where $\psi(-t) = \psi^*(t)$, the Equation (3.1) can be written as:

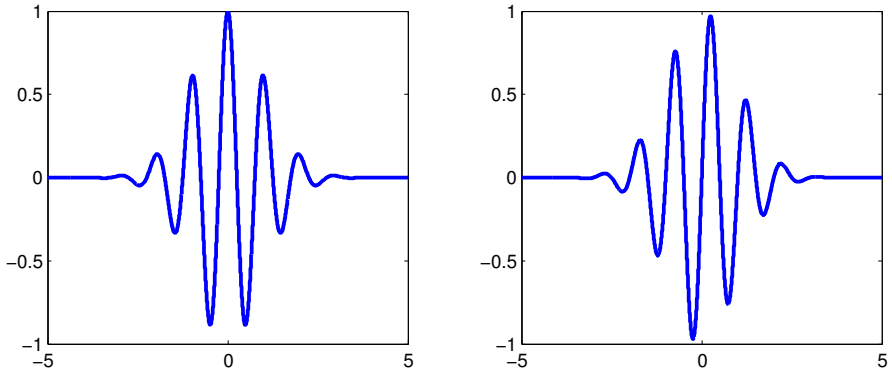

Figure C.1. Mother Morlet wavelet: real part (left), and imaginary part (right).

$$W(a,b) = \frac{1}{\sqrt{a}} \int_{-\infty}^{\infty} f(t)\psi\Big(\frac{b-t}{a}\Big)\mathrm{d}t \tag{C.2}$$

According to the definition of convolution by Oppenheim et al. (1999), the Equation (3.1) can be written as:

$$W(a,b) = \frac{1}{\sqrt{a}}(f * \psi_a)(b) \qquad , \qquad \psi_a(t) = \psi(\frac{t}{a}) \tag{C.3}$$

In order to compute the continuous wavelet transform coefficients in the discrete domain, not to be confused with Discrete Wavelet Transform (DWT) (Chui, 1992; Sanei and Chambers, 2007), first the wavelet is truncated to a finite number of points. A range of ± 4 periods was chosen as the wavelet amplitude decays to 3.35e-4 from 1. Finally, at each frequency (which is inversely proportional to a), the wavelet coefficients are given by convolution of the truncated approximation of the scaled wavelet and the signal.

This convolution should be computed at each frequency of interest. In order to make the formulation more efficient for parallel CPU and GPU computing, it is useful to reformulate the expression, so that the coefficients for all time shift values and each frequency can be computed in parallel. By zero-padding after the signal and wavelet to equalise the size of the truncated wavelet and the signal (equal to the convolution size, i.e. the sum of sizes minus one), taking the fast Fourier transform (FFT) of each, multiplication, and then the inverse FFT, convolution can be computed (from MATLAB® documentation):

```
X = fft([x zeros(1,length(y)-1)])
Y = fft([y zeros(1,length(x)-1)])
conv(x,y) = ifft(X.*Y)
```

C.2. Verification of Time-Frequency Representations

All the time-frequency representations including continuous Morlet wavelet transform, Wigner-Ville distribution, and matching pursuit (not used for final data analysis) were coded and compared against the Time-Frequency Toolbox for MATLAB® (Centre National de la Recherche Scientifique, Paris, France), using the following synthetic signals:

- Sine waves in the form of $y = a.sin(2.\pi.f_1.t) + b.sin(2.\pi.f_2.t) + c.sin(2.\pi.f_3.t)$.
- Sine waves in the form of $y = a.sin(2.\pi.b.t^2)$.

Appendix D

Supplementary Statistics

In an experiment, a statistical test is used to reject the null hypothesis $h_0 : \bar{X}_1 = \bar{X}_2$, with α significance level, in each subject.

It is of interest to find the overal probability p of getting $h_1 : \bar{X}_1 < \bar{X}_2$ (or $h_2 : \bar{X}_1 > \bar{X}_2$) in r or more out of n subjects, by chance. For this purpose the binomial probability distribution for r out of n subjects should be corrected for the family-wise error coming from multiple comparisons.

Based on the definition of h_0, h_1 and h_2, the confusion matrix for errors can be written as:

Table D.1. Confusion matrix of per-subject statistical test .

		Detected	
		h_1	$\sim h_1$
Actual	h_1	$1-\beta$	β
	$\sim h_1$	α	$1-\alpha$

[1] The table for h_2 is similar, with h_1 replaced by h_2.
[2] Type I error rate (the significance level) is α.
[3] Type II error rate (not known) is β.

If the outcome sequence $\vec{Y} =< y_1, y_2, ..., y_n >$ from n subjects takes the values $y_i \in \{h_0, h_1, h_2\}$, the probability of actual sequence $\vec{Y}_j$ being observed as the detected sequence $\vec{Y}_k$ is:

$$\begin{aligned}\Pr(\vec{Y}_j \to \vec{Y}_k) =& (1-\alpha)^{\#(y_{ji}=\sim h_1 \ \& \ y_{ki}=\sim h_1)} \\ & (\alpha)^{\#(y_{ji}=\sim h_1 \ \& \ y_{ki}=h_1)} \\ & (1-\beta)^{\#(y_{ji}=h_1 \ \& \ y_{ki}=h_1)} \\ & (\beta)^{\#(y_{ji}=h_1 \ \& \ y_{ki}=\sim h_1)}\end{aligned} \tag{D.1}$$

and the probability of observing $\vec{Y}_k$ is:

$$\Pr_o(\vec{Y}_k) = \sum_{\vec{Y}_j \in \{h_0,h_1,h_2\}^n} \Pr(\vec{Y}_j) \Pr(\vec{Y}_j \to \vec{Y}_k) \tag{D.2}$$

It can be assumed that the prior probability of h_0 is $u = 0.5$ and consequently the prior probability of h_1 and h_2 are $v_1 = 0.25$ and $v_2 = 0.25$, respectively. This is the chance level probability if the equality (h_0) and difference ($\sim h_0$) have equal probability of 0.5 and then the difference includes increase and decrease (h_1 and h_2) conditions with equal probbaility of 0.25 each.

we may write the probabilty of getting $\vec{Y}_j$ as:

$$\Pr(\vec{Y}_j) = {v_1}^{\#(y_{ji}=h_1)}(1-v_1)^{\#(y_{ji}=\sim h_1)} \tag{D.3}$$

Finally, the probability of getting r or more out of n subjects with h_1 is:

$$p = \sum_{\vec{Y}_k \in M} \Pr_o(\vec{Y}_k), \quad M = \{\vec{Y}_k \,|\#(y_{ki} = h_1) \geqslant r\} \tag{D.4}$$

The following table shows the p values for $r = 0, 1, 2, ..., 8$ for $n = 8$.

It can be seen that $\beta = 0$ provides the highest chance level probability; consequently, in the absence of accurate knowledge of the value for β, the conservative approach is to use $\beta = 0$ to avoid increased overal Type I errors.

Table D.2. Probability p of getting r or more times h_1 out of $n = 8$ subjects .

r	p							
	$v_1 = 0.33$ $\alpha = 0.00$ $\beta = 0.05$	$v_1 = 0.33$ $\alpha = 0.00$ $\beta = 0.00$	$v_1 = 0.33$ $\alpha = 0.05$ $\beta = 0.05$	$v_1 = 0.33$ $\alpha = 0.05$ $\beta = 0.00$	$v_1 = 0.25$ $\alpha = 0.00$ $\beta = 0.05$	$v_1 = 0.25$ $\alpha = 0.00$ $\beta = 0.00$	$v_1 = 0.25$ $\alpha = 0.05$ $\beta = 0.05$	$v_1 = 0.25$ $\alpha = 0.05$ $\beta = 0.00$
0	1.000000	1.000000	1.000000	1.000000	1.000000	1.000000	1.000000	1.000000
1	0.952459	0.960981	0.968135	0.974114	0.885733	0.899887	0.923668	0.933583
2	0.776213	0.804907	0.830873	0.854223	0.601003	0.632919	0.692041	0.719184
3	0.490350	0.531778	0.572186	0.611285	0.290602	0.321456	0.384537	0.416393
4	0.225403	0.258649	0.293600	0.329988	0.097236	0.113815	0.151257	0.172035
5	0.071928	0.087943	0.106090	0.126419	0.021951	0.027297	0.040651	**0.048785**
6	0.015030	0.019661	0.025317	0.032134	0.003191	0.004226	0.007088	0.008999
7	0.001846	0.002591	0.003570	0.004841	0.000270	0.000381	0.000722	0.000972
8	0.000101	0.000152	0.000225	0.000326	0.000010	0.000015	0.000032	**0.000046**

[1] The prior probability (chance level) of getting h_1 is v_1.
[2] Type I error rate (the significance level) is α.
[3] Type II error rate (not known) is β.
[4] Bold values show the maximum probability of getting 5 and 8 times h_1 observations out of 8 subjects by chnace, with the conservative assumptions of $\alpha = 0.05$ and $\beta = 0$, when change/no-change and increase/decrease have equal probability.

Appendix E

Supplementary Results

E.1. Detailed Experiment Statistics for Individual Subjects

Table E.1. Acceptable EEG epochs for subject 1 .

#	Electrode	RC	AC	DC	GO
1	Cz	58	140	129	131
2	C1	58	139	127	130
3	C2	57	139	129	131
4	C3	57	136	125	127
5	C4	55	126	121	124
6	C5	54	128	121	119
7	C6	44	104	106	107
8	C7	8	23	16	22
9	C8	10	19	15	21
10	FCz	31	74	82	100
11	FC1	31	65	76	90
12	FC2	28	64	73	91
13	FC3	5	18	17	21
14	FC4	6	21	22	24
15	FC5	6	15	15	25
16	FC6	5	13	10	16
17	FT7	0	0	0	0
18	FT8	0	0	0	0
19	CPz	60	151	142	135
20	CP1	61	152	143	136
21	CP2	60	150	143	135
22	CP3	61	153	143	136
23	CP4	60	147	140	136
24	CP5	53	141	136	123
25	CP6	49	127	118	122
26	TP7	0	0	0	0
27	TP8	21	58	62	70
28	Fz	5	13	12	35
29	F1	4	8	9	21
30	F2	4	8	12	27
31	F3	1	2	3	6
32	F4	1	3	7	11
33	F5	1	1	3	7
34	F6	1	1	3	10
35	F7	0	0	2	1
36	F8	0	0	0	0
37	Pz	56	146	137	131
38	P1	58	149	140	131
39	P2	50	136	129	127
40	P3	59	151	143	135
41	P4	53	132	122	122
42	P5	42	118	112	97
43	P6	40	87	75	90
44	P7	3	6	4	1
45	P8	19	59	60	77
46	AFz	1	3	1	13
47	AF3	1	0	0	2
48	AF4	1	0	1	9
49	AF7	1	0	0	0
50	AF8	1	0	1	11
51	Fp1	1	0	0	1
52	FP2	1	2	1	8
53	POz	59	142	137	131
54	PO3	55	145	134	123
55	PO4	54	121	121	117
56	PO7	21	47	42	37
57	PO8	17	44	40	44
58	Oz	30	69	65	66
59	O1	36	78	70	68
60	O2	21	48	42	43
61	Iz	0	1	1	1
62	O9	0	0	0	0
63	O10	1	0	1	2
64	PO9	0	0	0	0
65	PO10	0	0	0	0
66	P9	0	0	0	0
67	P10	0	0	0	0
68	TP9	0	0	0	0
69	TP10	0	0	0	0
70	FT9	0	0	0	0
71	FT10	0	0	0	0
72	F9	0	0	0	0
73	73	0	0	0	0

Total Trials: 228

Table E.2. Acceptable EEG epochs for subject 2 .

#	Electrode	RC	AC	DC	GO
1	Cz	115	187	159	148
2	C1	114	187	159	148
3	C2	115	187	159	148
4	C3	113	186	159	147
5	C4	111	184	157	148
6	C5	0	0	0	0
7	C6	87	145	123	120
8	C7	0	0	0	0
9	C8	25	52	36	36
10	FCz	110	179	154	144
11	FC1	111	181	157	144
12	FC2	109	182	157	144
13	FC3	108	179	152	142
14	FC4	99	165	139	133
15	FC5	31	45	44	36
16	FC6	31	51	56	41
17	FT7	0	0	0	0
18	FT8	15	23	21	16
19	CPz	115	188	159	148
20	CP1	115	189	159	148
21	CP2	115	189	159	148
22	CP3	111	187	155	144
23	CP4	115	189	159	148
24	CP5	0	0	0	0
25	CP6	113	188	159	146
26	TP7	0	0	0	0
27	TP8	49	90	72	62
28	Fz	103	169	152	137
29	F1	105	172	154	140
30	F2	97	166	146	132
31	F3	84	135	129	121
32	F4	62	106	102	94
33	F5	0	0	0	0
34	F6	0	0	0	0
35	F7	0	0	0	0
36	F8	0	0	0	0
37	Pz	114	189	159	147
38	P1	112	187	154	144
39	P2	114	188	159	147
40	P3	98	170	143	136
41	P4	114	188	159	145
42	P5	23	42	35	31
43	P6	99	167	137	124
44	P7	0	0	0	0
45	P8	73	138	108	96
46	AFz	78	132	123	114
47	AF3	62	98	96	92
48	AF4	62	103	99	91
49	AF7	0	0	0	0
50	AF8	0	0	0	0
51	Fp1	2	3	1	3
52	FP2	2	2	0	2
53	POz	114	185	157	142
54	PO3	101	168	142	125
55	PO4	112	186	157	142
56	PO7	0	0	0	0
57	PO8	103	179	150	130
58	Oz	103	165	141	126
59	O1	2	4	3	4
60	O2	112	187	157	141
61	Iz	12	17	15	11
62	O9	0	0	0	0
63	O10	101	167	143	124
64	PO9	0	0	0	0
65	PO10	0	0	0	0
66	P9	0	0	0	0
67	P10	0	0	0	0
68	TP9	0	0	0	0
69	TP10	0	0	0	0
70	FT9	0	0	0	0
71	FT10	0	0	0	0
72	F9	0	0	0	0
73	73	0	0	0	0

Total Trials: 223

Table E.3. Acceptable EEG epochs for subject 3 .

#	Electrode	RC	AC	DC	GO
1	Cz	82	138	98	115
2	C1	82	138	98	115
3	C2	73	126	89	95
4	C3	82	137	98	114
5	C4	38	70	49	46
6	C5	54	82	59	78
7	C6	19	31	23	23
8	C7	31	50	38	52
9	C8	18	27	21	24
10	FCz	81	133	97	105
11	FC1	81	133	98	106
12	FC2	51	87	65	61
13	FC3	77	127	93	100
14	FC4	35	67	46	43
15	FC5	42	55	39	41
16	FC6	25	44	28	31
17	FT7	0	0	0	0
18	FT8	16	26	19	18
19	CPz	84	139	103	114
20	CP1	84	139	103	114
21	CP2	76	128	94	97
22	CP3	83	138	103	115
23	CP4	61	102	75	73
24	CP5	68	106	81	94
25	CP6	41	64	48	51
26	TP7	50	76	57	67
27	TP8	44	60	46	49
28	Fz	78	126	95	101
29	F1	75	123	93	100
30	F2	58	87	67	62
31	F3	63	101	79	82
32	F4	45	80	62	57
33	F5	15	22	16	15
34	F6	25	54	43	40
35	F7	0	0	0	0
36	F8	15	32	28	30
37	Pz	83	136	102	112
38	P1	83	134	102	111
39	P2	74	124	93	97
40	P3	82	134	101	113
41	P4	70	108	82	82
42	P5	74	115	90	103
43	P6	43	62	48	52
44	P7	56	84	65	73
45	P8	31	44	36	29
46	AFz	69	105	83	91
47	AF3	43	68	52	58
48	AF4	40	72	53	51
49	AF7	2	9	8	12
50	AF8	10	15	12	9
51	Fp1	4	11	10	13
52	FP2	8	17	13	16
53	POz	81	124	97	101
54	PO3	79	123	99	102
55	PO4	71	109	86	83
56	PO7	65	95	76	77
57	PO8	8	9	9	7
58	Oz	72	105	87	87
59	O1	67	98	82	82
60	O2	55	78	71	68
61	Iz	48	72	62	58
62	O9	46	69	56	57
63	O10	15	21	19	19
64	PO9	29	48	41	35
65	PO10	0	0	0	0
66	P9	0	0	0	0
67	P10	0	0	0	0
68	TP9	0	0	0	0
69	TP10	0	0	0	0
70	FT9	0	0	0	0
71	FT10	0	0	0	0
72	F9	0	0	0	0
73	73	0	0	0	0

Total Trials: 220

Table E.4. Acceptable EEG epochs for subject 4 .

#	Electrode	RC	AC	DC	GO
1	Cz	32	150	164	146
2	C1	32	150	164	146
3	C2	31	150	162	145
4	C3	32	149	162	144
5	C4	11	70	75	71
6	C5	24	111	123	109
7	C6	15	73	75	72
8	C7	0	0	0	0
9	C8	0	5	8	7
10	FCz	31	147	163	139
11	FC1	31	147	163	139
12	FC2	29	145	161	138
13	FC3	30	133	152	132
14	FC4	4	37	44	41
15	FC5	17	101	110	101
16	FC6	15	92	107	101
17	FT7	10	40	47	40
18	FT8	0	0	0	0
19	CPz	28	141	158	134
20	CP1	33	147	161	140
21	CP2	30	139	149	129
22	CP3	31	150	164	144
23	CP4	11	59	70	56
24	CP5	29	143	155	140
25	CP6	12	45	52	42
26	TP7	26	130	142	116
27	TP8	14	62	66	52
28	Fz	28	141	158	132
29	F1	28	141	158	132
30	F2	26	135	155	130
31	F3	23	127	148	126
32	F4	10	55	66	59
33	F5	2	14	14	15
34	F6	0	0	0	0
35	F7	2	12	14	14
36	F8	0	0	0	0
37	Pz	9	56	67	54
38	P1	18	92	100	82
39	P2	0	3	2	3
40	P3	28	137	155	124
41	P4	0	0	0	0
42	P5	28	131	153	121
43	P6	0	0	0	0
44	P7	25	124	144	110
45	P8	0	0	0	0
46	AFz	22	125	153	120
47	AF3	15	87	110	77
48	AF4	11	68	82	60
49	AF7	0	0	0	0
50	AF8	0	0	0	0
51	Fp1	5	23	35	17
52	FP2	8	32	52	20
53	POz	0	0	0	0
54	PO3	18	59	70	59
55	PO4	0	0	0	0
56	PO7	19	57	77	63
57	PO8	0	0	0	0
58	Oz	0	0	0	0
59	O1	0	6	6	6
60	O2	0	0	0	0
61	Iz	0	0	0	0
62	O9	0	0	0	0
63	O10	0	0	0	0
64	PO9	0	0	0	0
65	PO10	0	0	0	0
66	P9	0	0	0	0
67	P10	0	0	0	0
68	TP9	0	0	0	0
69	TP10	0	0	0	0
70	FT9	0	0	0	0
71	FT10	0	0	0	0
72	F9	0	0	0	0
73	73	0	0	0	0

Total Trials: 221

Table E.5. Acceptable EEG epochs for subject 5 .

#	Electrode	RC	AC	DC	GO
1	Cz	9	110	110	83
2	C1	9	110	110	83
3	C2	6	92	90	65
4	C3	9	104	107	76
5	C4	8	74	82	66
6	C5	0	0	0	0
7	C6	0	0	0	0
8	C7	0	0	0	0
9	C8	0	0	0	0
10	FCz	5	92	89	52
11	FC1	5	92	89	52
12	FC2	5	89	87	50
13	FC3	4	70	78	43
14	FC4	4	61	64	41
15	FC5	0	0	0	0
16	FC6	0	0	0	0
17	FT7	0	0	0	0
18	FT8	0	0	0	0
19	CPz	10	117	124	104
20	CP1	10	117	124	104
21	CP2	10	115	124	104
22	CP3	10	117	124	104
23	CP4	10	101	114	95
24	CP5	4	23	37	38
25	CP6	0	24	27	23
26	TP7	0	0	0	0
27	TP8	0	0	0	0
28	Fz	2	66	71	34
29	F1	2	67	69	35
30	F2	2	61	68	29
31	F3	0	11	10	3
32	F4	2	52	53	29
33	F5	0	0	0	0
34	F6	0	23	18	11
35	F7	0	0	0	0
36	F8	0	9	6	6
37	Pz	11	117	124	104
38	P1	11	117	124	104
39	P2	11	117	124	104
40	P3	11	114	122	104
41	P4	11	106	118	99
42	P5	10	89	104	90
43	P6	6	61	78	62
44	P7	5	26	31	28
45	P8	0	0	0	0
46	AFz	2	62	63	29
47	AF3	0	0	0	0
48	AF4	1	40	43	23
49	AF7	0	0	0	0
50	AF8	0	1	1	0
51	Fp1	0	1	0	0
52	FP2	0	7	6	3
53	POz	11	110	123	101
54	PO3	11	114	121	102
55	PO4	11	109	123	100
56	PO7	2	16	16	12
57	PO8	0	0	0	0
58	Oz	0	2	4	4
59	O1	1	11	12	8
60	O2	0	0	0	0
61	Iz	0	0	0	0
62	O9	0	0	0	0
63	O10	0	0	0	0
64	PO9	0	0	0	0
65	PO10	0	0	0	0
66	P9	0	0	0	0
67	P10	0	0	0	0
68	TP9	0	0	0	0
69	TP10	0	0	0	0
70	FT9	0	0	0	0
71	FT10	0	0	0	0
72	F9	0	0	0	0
73	73	0	0	0	0

Total Trials: 222

Table E.6. Acceptable EEG epochs for subject 6 .

#	Electrode	RC	AC	DC	GO
1	Cz	39	114	116	138
2	C1	39	114	116	138
3	C2	38	111	111	132
4	C3	31	95	96	115
5	C4	20	54	55	63
6	C5	12	34	34	43
7	C6	1	2	2	2
8	C7	9	26	30	36
9	C8	6	14	14	20
10	FCz	26	108	111	132
11	FC1	27	109	111	131
12	FC2	26	105	105	123
13	FC3	18	69	68	86
14	FC4	11	29	35	36
15	FC5	5	14	14	15
16	FC6	0	2	2	2
17	FT7	0	0	0	0
18	FT8	0	0	0	0
19	CPz	47	120	119	142
20	CP1	47	120	119	143
21	CP2	47	119	117	138
22	CP3	46	118	115	139
23	CP4	40	104	103	118
24	CP5	35	95	93	112
25	CP6	27	63	65	65
26	TP7	19	48	53	67
27	TP8	27	63	65	76
28	Fz	24	98	102	123
29	F1	24	99	100	124
30	F2	21	84	84	108
31	F3	16	52	51	70
32	F4	10	27	31	46
33	F5	4	10	12	14
34	F6	1	3	5	5
35	F7	0	1	2	3
36	F8	0	0	0	0
37	Pz	47	120	119	142
38	P1	47	120	119	142
39	P2	47	120	119	143
40	P3	47	118	118	142
41	P4	46	117	117	139
42	P5	45	116	117	138
43	P6	45	116	117	140
44	P7	19	69	63	83
45	P8	40	113	113	136
46	AFz	21	71	79	103
47	AF3	16	41	43	57
48	AF4	12	34	36	57
49	AF7	5	13	15	18
50	AF8	0	1	1	2
51	Fp1	10	26	29	42
52	FP2	5	11	12	19
53	POz	47	120	118	143
54	PO3	47	120	118	142
55	PO4	47	120	118	143
56	PO7	29	82	75	92
57	PO8	47	120	117	142
58	Oz	41	110	106	126
59	O1	30	88	85	100
60	O2	47	120	117	141
61	Iz	0	0	0	0
62	O9	0	0	0	0
63	O10	6	17	16	21
64	PO9	0	0	0	0
65	PO10	0	0	0	0
66	P9	0	0	0	0
67	P10	0	0	0	0
68	TP9	0	0	0	0
69	TP10	0	0	0	0
70	FT9	0	0	0	0
71	FT10	0	0	0	0
72	F9	0	0	0	0
73	73	0	0	0	0

Total Trials: 224

Table E.7. Acceptable EEG epochs for subject 7 .

#	Electrode	RC	AC	DC	GO
1	Cz	68	167	166	148
2	C1	67	165	166	148
3	C2	68	165	166	148
4	C3	65	156	161	142
5	C4	68	165	165	147
6	C5	14	44	38	32
7	C6	19	42	38	29
8	C7	0	0	0	0
9	C8	0	0	0	0
10	FCz	64	166	166	147
11	FC1	62	163	163	143
12	FC2	63	165	165	146
13	FC3	60	156	162	141
14	FC4	63	162	164	139
15	FC5	15	51	48	42
16	FC6	10	35	30	27
17	FT7	0	0	0	0
18	FT8	0	0	0	0
19	CPz	69	165	166	150
20	CP1	68	162	163	146
21	CP2	71	166	166	150
22	CP3	62	141	150	125
23	CP4	71	164	164	146
24	CP5	12	24	26	17
25	CP6	62	140	142	124
26	TP7	0	0	0	0
27	TP8	0	0	0	0
28	Fz	52	148	151	130
29	F1	51	146	153	130
30	F2	52	142	151	122
31	F3	46	137	142	117
32	F4	34	90	93	82
33	F5	19	53	57	46
34	F6	11	29	36	23
35	F7	0	0	0	0
36	F8	0	0	0	0
37	Pz	66	143	159	129
38	P1	60	127	144	108
39	P2	63	149	158	131
40	P3	9	19	23	6
41	P4	62	147	150	125
42	P5	2	4	3	1
43	P6	57	129	140	105
44	P7	0	0	0	0
45	P8	20	43	55	31
46	AFz	35	110	111	86
47	AF3	14	47	55	40
48	AF4	18	46	53	41
49	AF7	3	8	9	4
50	AF8	0	3	3	3
51	Fp1	2	5	4	3
52	FP2	3	5	3	3
53	POz	29	68	72	35
54	PO3	17	38	45	21
55	PO4	13	29	32	20
56	PO7	0	0	0	0
57	PO8	12	30	30	15
58	Oz	4	5	8	2
59	O1	0	0	0	0
60	O2	0	0	0	0
61	Iz	0	0	0	0
62	O9	0	0	0	0
63	O10	0	0	0	0
64	PO9	0	0	0	0
65	PO10	0	0	0	0
66	P9	0	0	0	0
67	P10	0	0	0	0
68	TP9	0	0	0	0
69	TP10	0	0	0	0
70	FT9	0	0	0	0
71	FT10	0	0	0	0
72	F9	0	0	0	0
73	73	0	0	0	0

Total Trials: 220

Table E.8. Acceptable EEG epochs for subject 8 .

#	Electrode	RC	AC	DC	GO
1	Cz	102	128	126	115
2	C1	102	128	126	115
3	C2	102	128	126	115
4	C3	94	121	121	110
5	C4	101	128	126	114
6	C5	34	42	36	38
7	C6	59	73	70	63
8	C7	0	0	0	0
9	C8	0	0	0	0
10	FCz	96	119	122	115
11	FC1	96	119	122	115
12	FC2	96	119	121	115
13	FC3	88	109	114	104
14	FC4	94	114	117	111
15	FC5	60	74	79	77
16	FC6	68	77	75	75
17	FT7	0	0	0	0
18	FT8	0	0	0	0
19	CPz	98	127	128	113
20	CP1	96	125	126	111
21	CP2	97	125	128	114
22	CP3	88	109	111	95
23	CP4	97	123	128	109
24	CP5	46	53	57	48
25	CP6	53	64	62	58
26	TP7	0	0	0	0
27	TP8	0	0	0	0
28	Fz	86	108	118	110
29	F1	84	108	116	108
30	F2	69	94	95	92
31	F3	41	63	64	58
32	F4	48	61	63	62
33	F5	12	21	25	23
34	F6	20	25	19	23
35	F7	0	0	0	0
36	F8	0	0	0	0
37	Pz	67	91	98	83
38	P1	64	90	97	83
39	P2	65	90	97	83
40	P3	56	80	90	77
41	P4	50	65	79	65
42	P5	2	2	1	2
43	P6	16	27	32	25
44	P7	0	0	0	0
45	P8	0	0	0	0
46	AFz	63	83	86	84
47	AF3	52	71	73	76
48	AF4	18	18	17	20
49	AF7	0	1	1	1
50	AF8	5	4	4	6
51	Fp1	5	7	4	6
52	FP2	6	5	3	8
53	POz	0	0	0	0
54	PO3	0	0	0	0
55	PO4	0	0	0	0
56	PO7	0	0	0	0
57	PO8	0	0	0	0
58	Oz	0	0	0	0
59	O1	0	0	0	0
60	O2	0	0	0	0
61	Iz	0	0	0	0
62	O9	0	0	0	0
63	O10	0	0	0	0
64	PO9	0	0	0	0
65	PO10	0	0	0	0
66	P9	0	0	0	0
67	P10	0	0	0	0
68	TP9	0	0	0	0
69	TP10	0	0	0	0
70	FT9	0	0	0	0
71	FT10	0	0	0	0
72	F9	0	0	0	0
73	73	0	0	0	0

Total Trials: 260

Table E.9. Statistics on exertion direction for individual subjects based on acceptable force profiles .

Subject No.	Right	Up	Left	Down	Sum
S1	55	51	47	47	200
S2	46	57	54	35	192
S3	45	38	47	62	192
S4	47	42	56	68	213
S5	53	50	47	55	205
S6	47	46	48	68	209
S7	48	37	50	71	206
S8	61	48	51	53	213
Average	50.25	46.125	50	57.375	203.75
Total	402	369	400	459	1630

Trials with acceptable force profiles are taken into account. For analyses of EEG and EMG, the acceptability of the corresponding signal is also considered.

E.2. Details of ERD/ERS Across Subjects

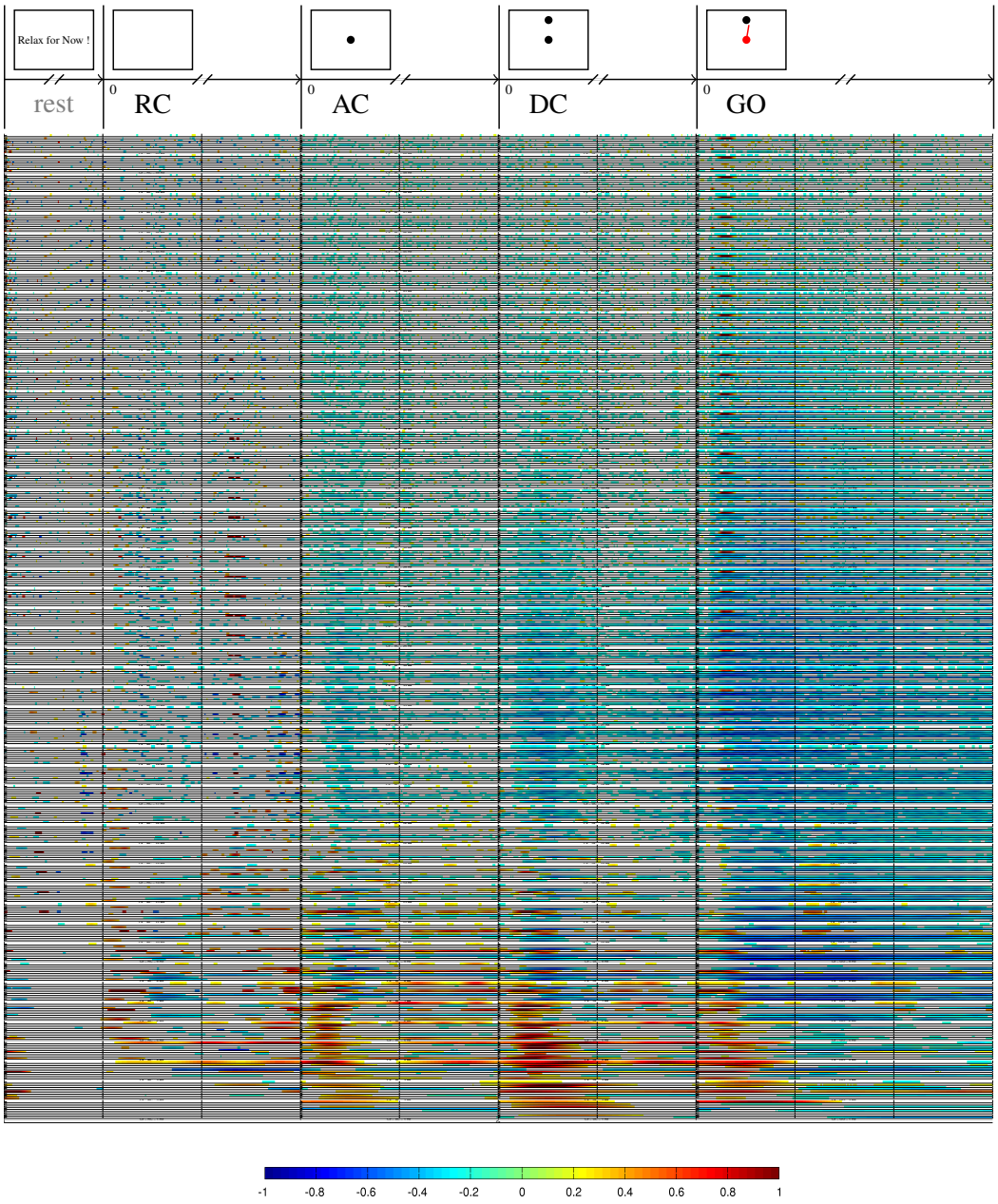

Figure E.1. ELR EEG time-frequency distribution for electrode C_z, showing statistically significant normalised (to pre-movement rest-time EEG) continuous Morlet wavelet transform (NCWT) scalograms from all subjects. Horizontal axes are time in seconds. Thicker blocks show different stages of experiment (from left to right the visual cues: RC, AC, DC, GO) and smaller x-axis chunks equal 1.0s. Vertical axes are frequencies (Hz), stacked from all subjects. Dark blue shows 100% ERD and dark red 100% ERS with respect to rest-time EEG.

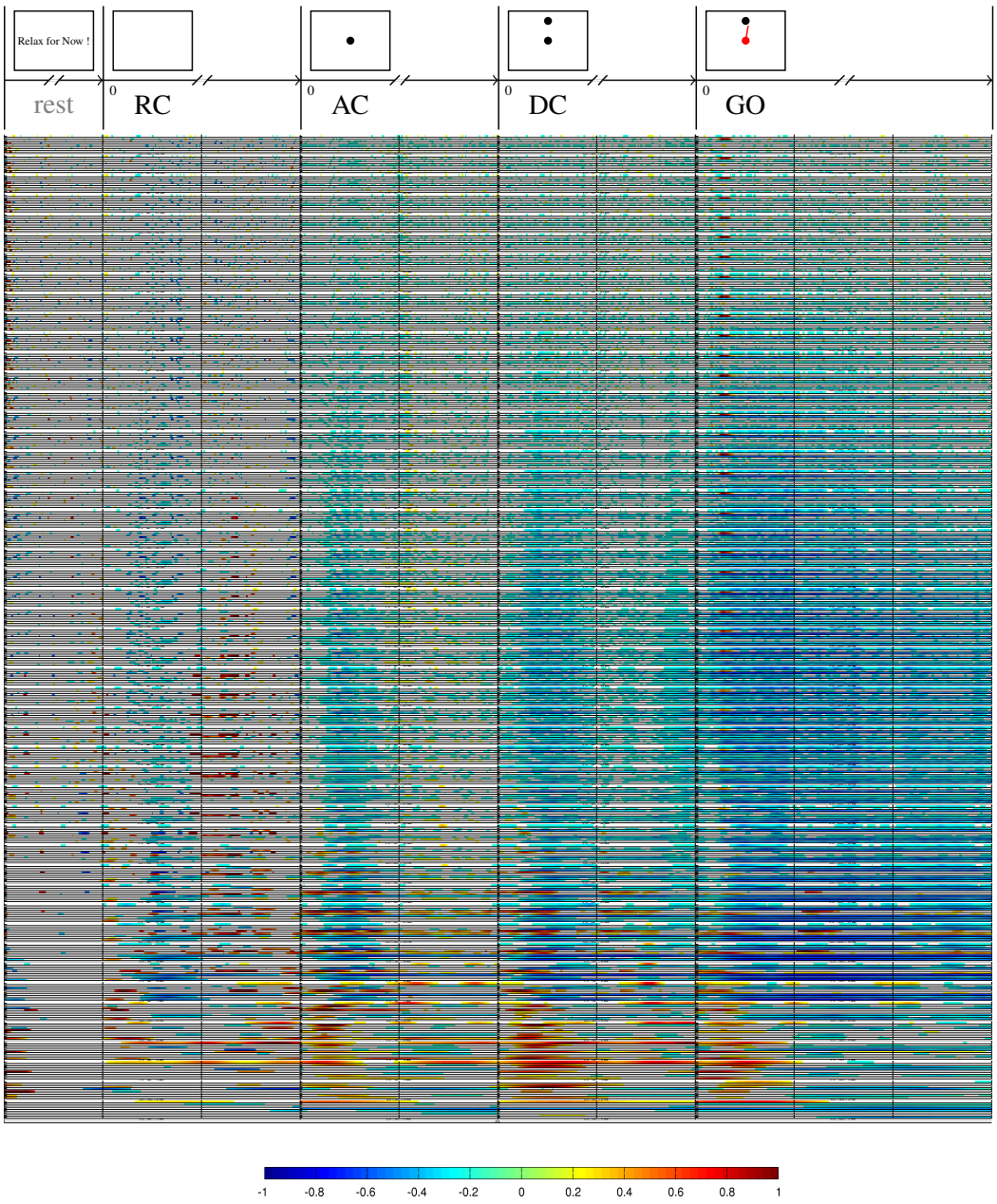

Figure E.2. ELR EEG time-frequency distribution for electrode C_3, showing statistically significant normalised (to pre-movement rest-time EEG) continuous Morlet wavelet transform (NCWT) scalograms from all subjects. Horizontal axes are time in seconds. Thicker blocks show different stages of experiment (from left to right the visual cues: RC, AC, DC, GO) and smaller x-axis chunks equal 1.0s. Vertical axes are frequencies (Hz), stacked from all subjects. Dark blue shows 100% ERD and dark red 100% ERS with respect to rest-time EEG.

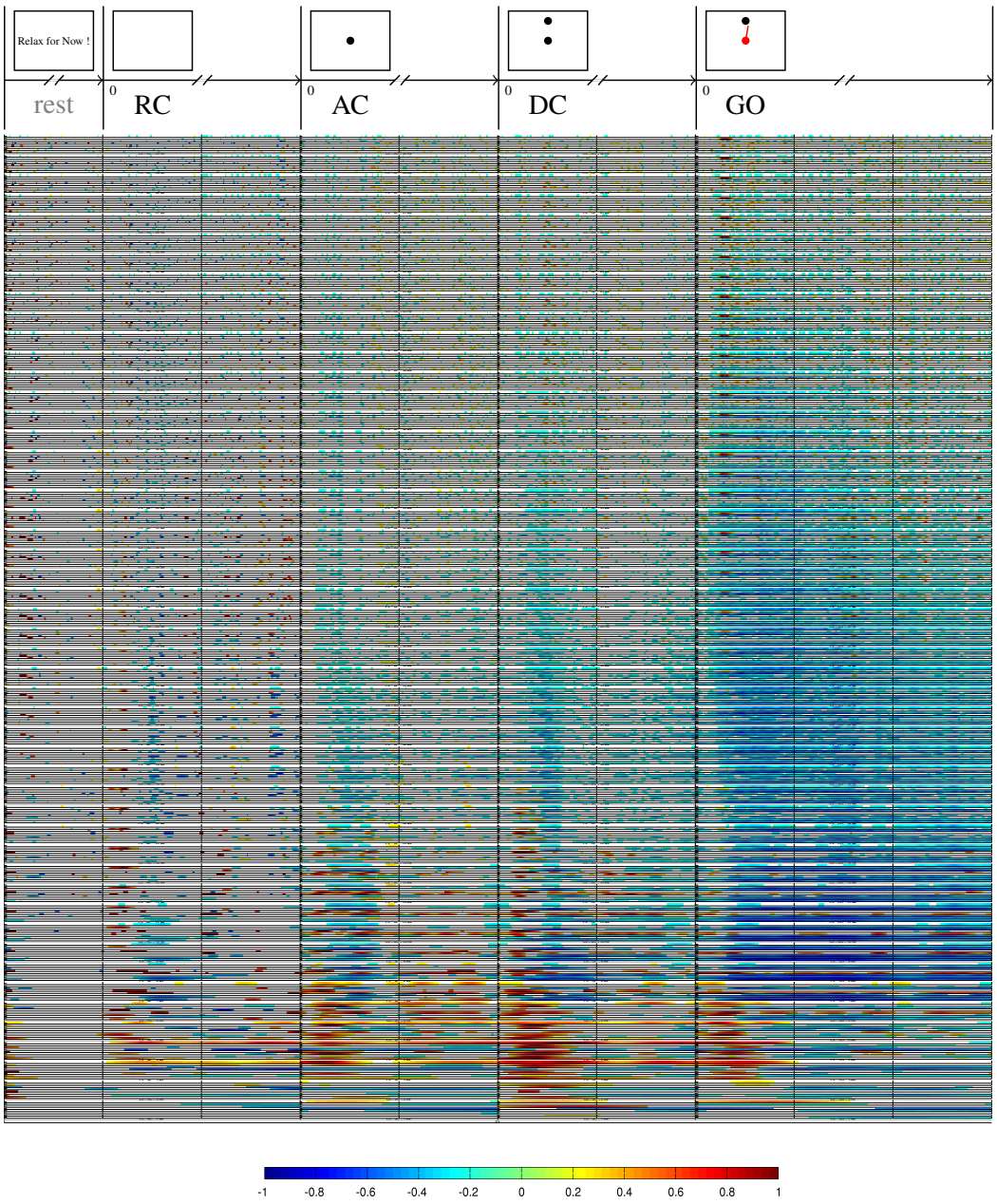

Figure E.3. ELR EEG time-frequency distribution for electrode C_4, showing statistically significant normalised (to pre-movement rest-time EEG) continuous Morlet wavelet transform (NCWT) scalograms from all subjects. Horizontal axes are time in seconds. Thicker blocks show different stages of experiment (from left to right the visual cues: RC, AC, DC, GO) and smaller x-axis chunks equal 1.0s. Vertical axes are frequencies (Hz), stacked from all subjects. Dark blue shows 100% ERD and dark red 100% ERS with respect to rest-time EEG.

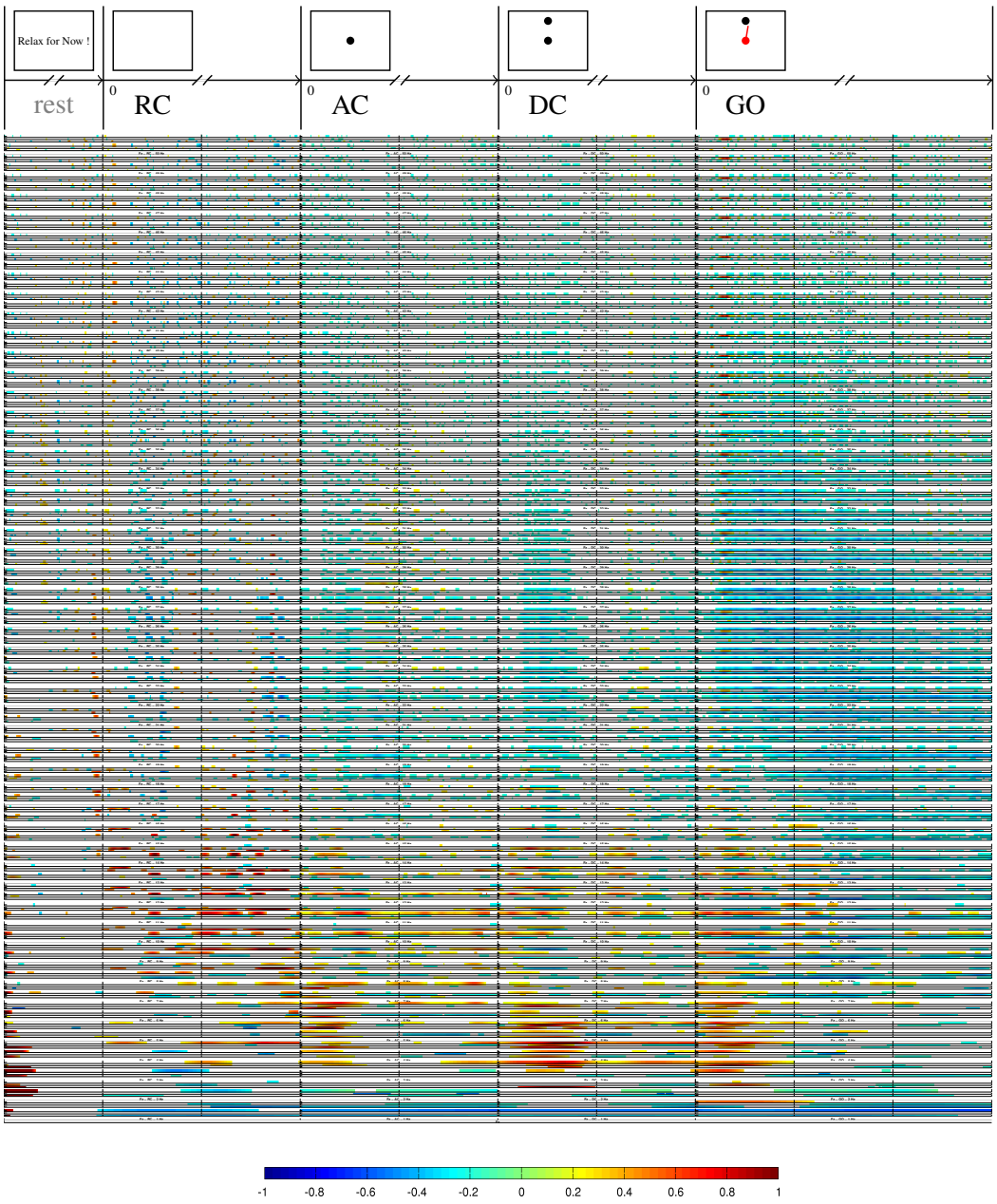

Figure E.4. ELR EEG time-frequency distribution for electrode F_z, showing statistically significant normalised (to pre-movement rest-time EEG) continuous Morlet wavelet transform (NCWT) scalograms from all subjects. Horizontal axes are time in seconds. Thicker blocks show different stages of experiment (from left to right the visual cues: RC, AC, DC, GO) and smaller x-axis chunks equal 1.0s. Vertical axes are frequencies (Hz), stacked from all subjects. Dark blue shows 100% ERD and dark red 100% ERS with respect to rest-time EEG.

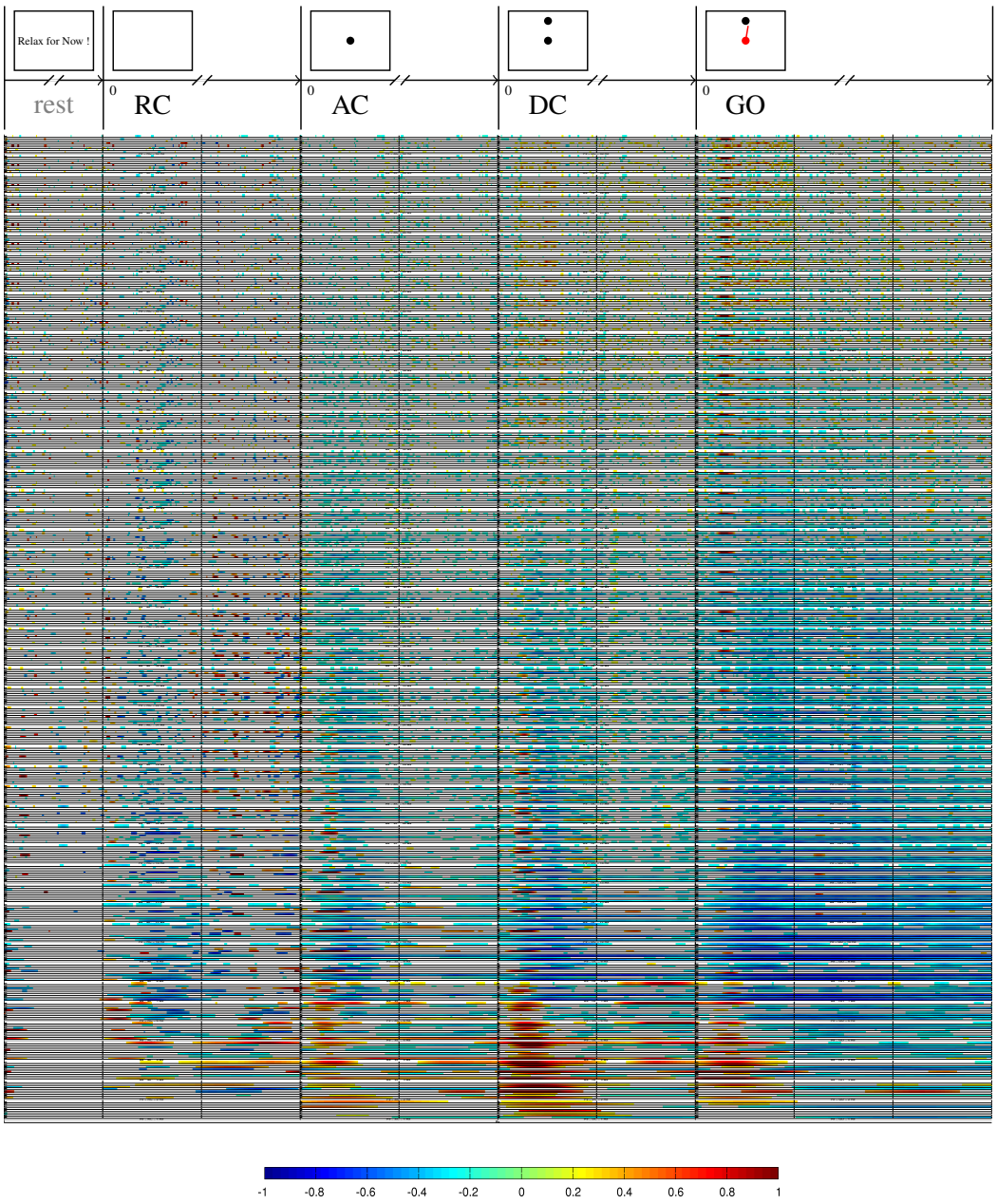

Figure E.5. ELR EEG time-frequency distribution for electrode P_z, showing statistically significant normalised (to pre-movement rest-time EEG) continuous Morlet wavelet transform (NCWT) scalograms from all subjects. Horizontal axes are time in seconds. Thicker blocks show different stages of experiment (from left to right the visual cues: RC, AC, DC, GO) and smaller x-axis chunks equal 1.0s. Vertical axes are frequencies (Hz), stacked from all subjects. Dark blue shows 100% ERD and dark red 100% ERS with respect to rest-time EEG.

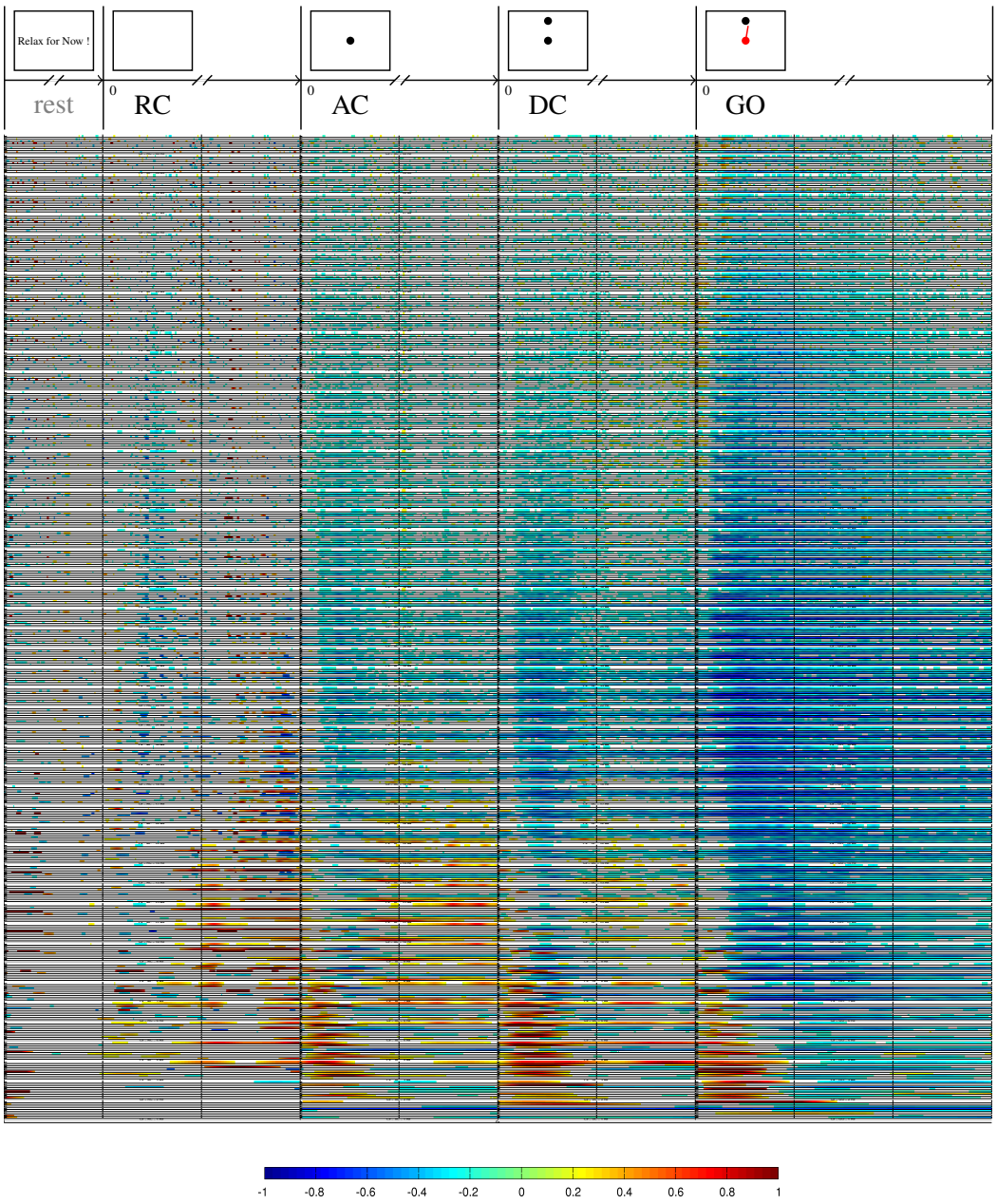

Figure E.6. CAR EEG time-frequency distribution for electrode C_z, showing statistically significant normalised (to pre-movement rest-time EEG) continuous Morlet wavelet transform (NCWT) scalograms from all subjects. Horizontal axes are time in seconds. Thicker blocks show different stages of experiment (from left to right the visual cues: RC, AC, DC, GO) and smaller x-axis chunks equal 1.0s. Vertical axes are frequencies (Hz), stacked from all subjects. Dark blue shows 100% ERD and dark red 100% ERS with respect to rest-time EEG.

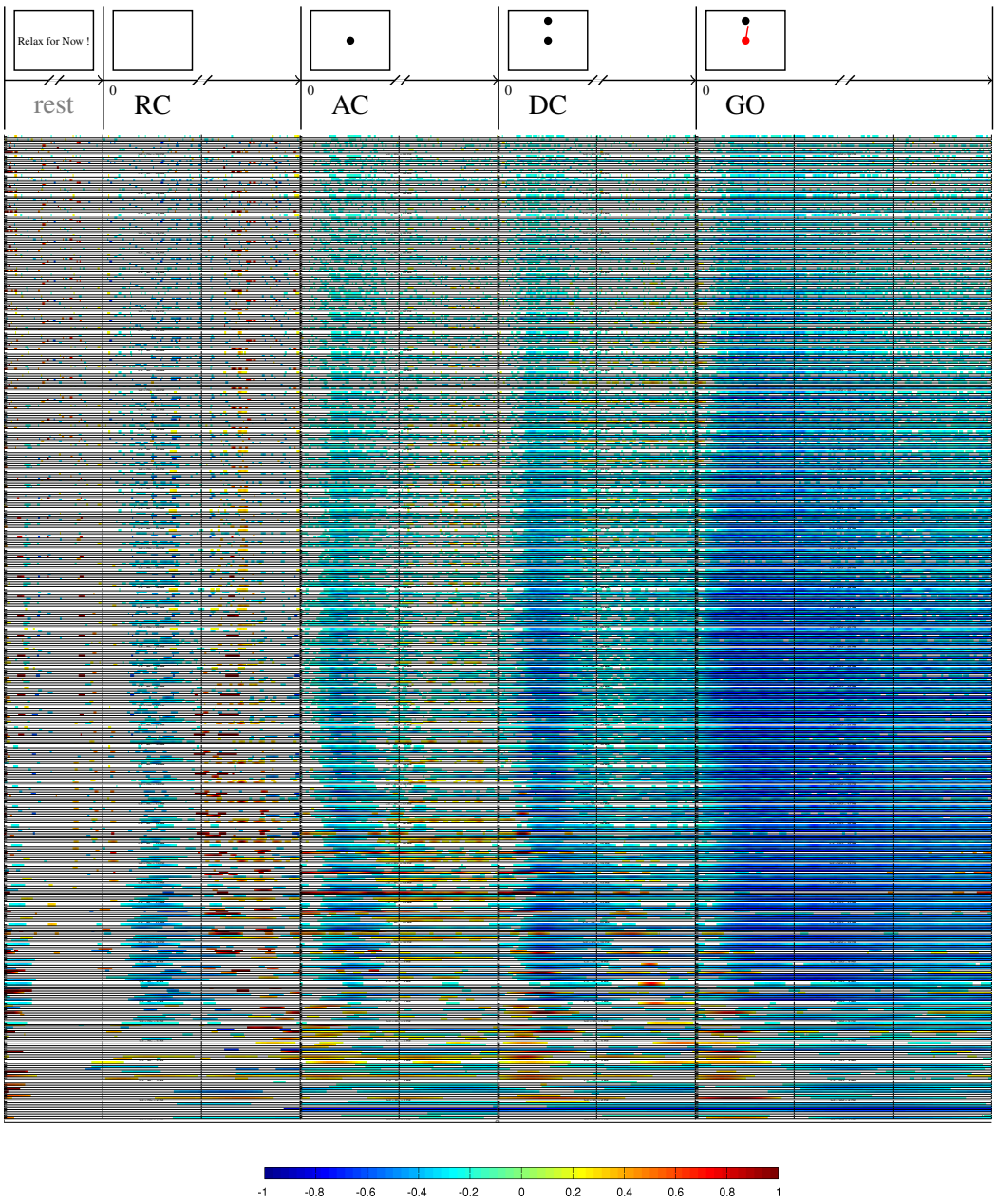

Figure E.7. CAR EEG time-frequency distribution for electrode C_3, showing statistically significant normalised (to pre-movement rest-time EEG) continuous Morlet wavelet transform (NCWT) scalograms from all subjects. Horizontal axes are time in seconds. Thicker blocks show different stages of experiment (from left to right the visual cues: RC, AC, DC, GO) and smaller x-axis chunks equal 1.0s. Vertical axes are frequencies (Hz), stacked from all subjects. Dark blue shows 100% ERD and dark red 100% ERS with respect to rest-time EEG.

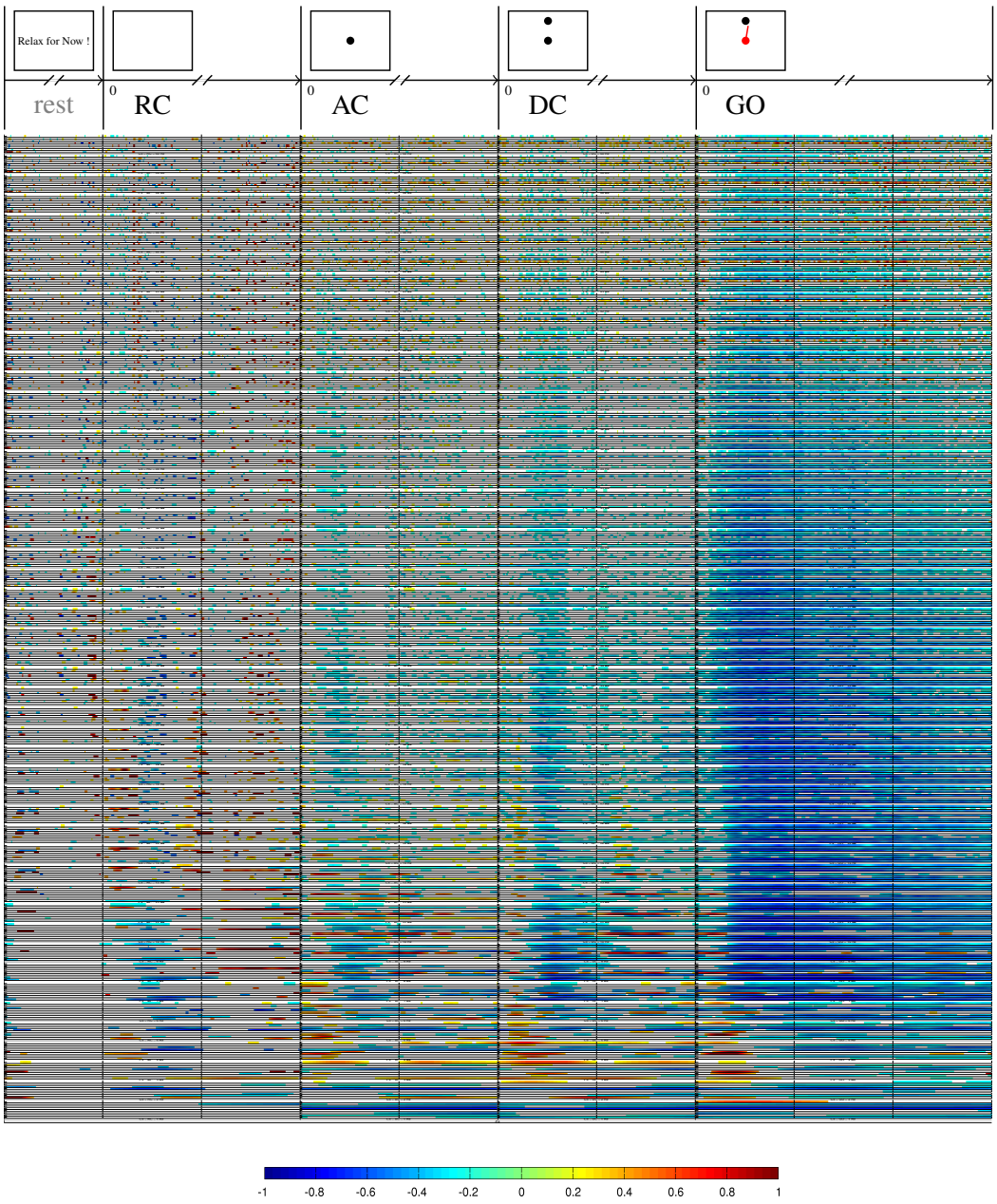

Figure E.8. CAR EEG time-frequency distribution for electrode C_4, showing statistically significant normalised (to pre-movement rest-time EEG) continuous Morlet wavelet transform (NCWT) scalograms from all subjects. Horizontal axes are time in seconds. Thicker blocks show different stages of experiment (from left to right the visual cues: RC, AC, DC, GO) and smaller x-axis chunks equal 1.0s. Vertical axes are frequencies (Hz), stacked from all subjects. Dark blue shows 100% ERD and dark red 100% ERS with respect to rest-time EEG.

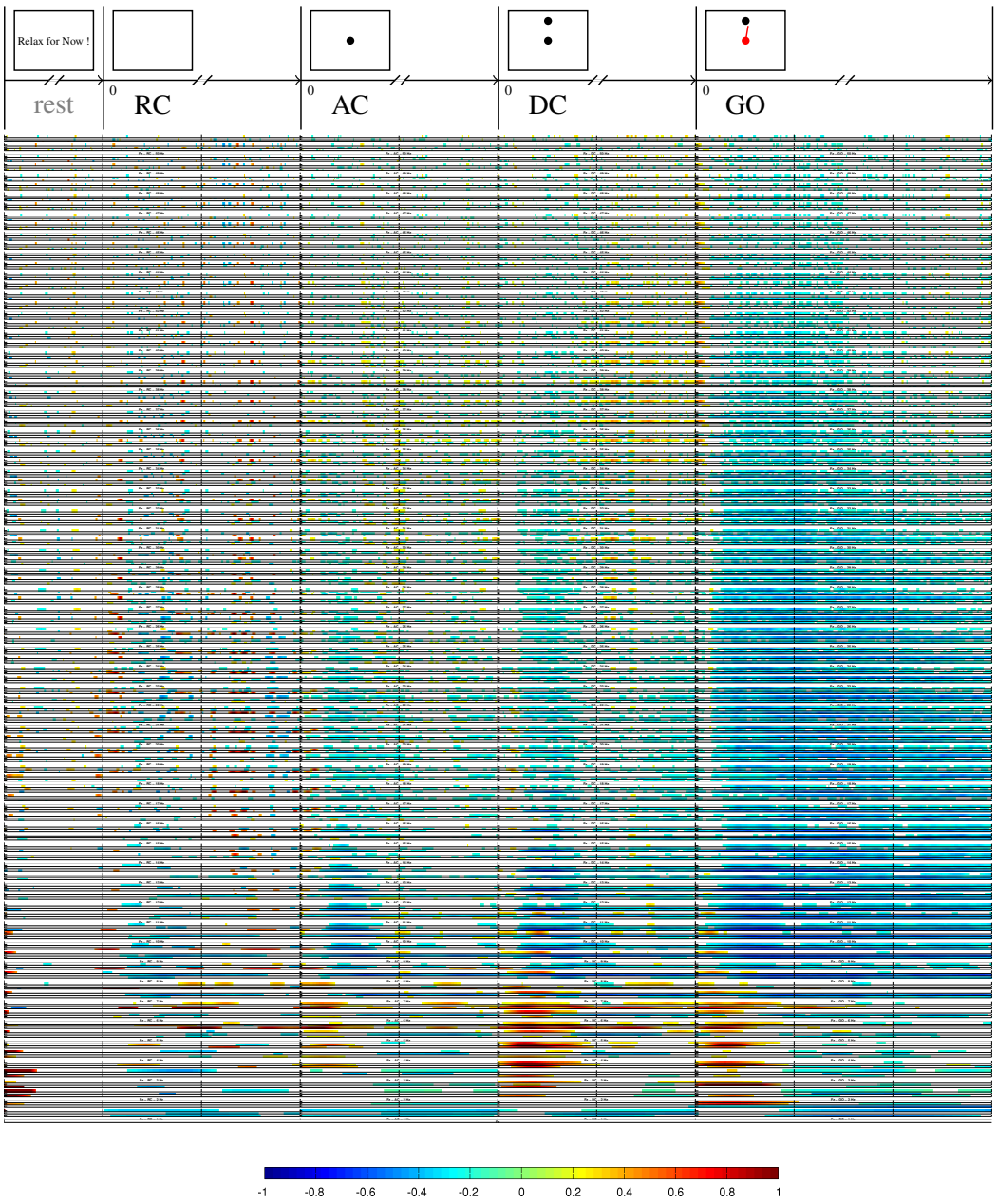

Figure E.9. CAR EEG time-frequency distribution for electrode F_z, showing statistically significant normalised (to pre-movement rest-time EEG) continuous Morlet wavelet transform (NCWT) scalograms from all subjects. Horizontal axes are time in seconds. Thicker blocks show different stages of experiment (from left to right the visual cues: RC, AC, DC, GO) and smaller x-axis chunks equal 1.0s. Vertical axes are frequencies (Hz), stacked from all subjects. Dark blue shows 100% ERD and dark red 100% ERS with respect to rest-time EEG.

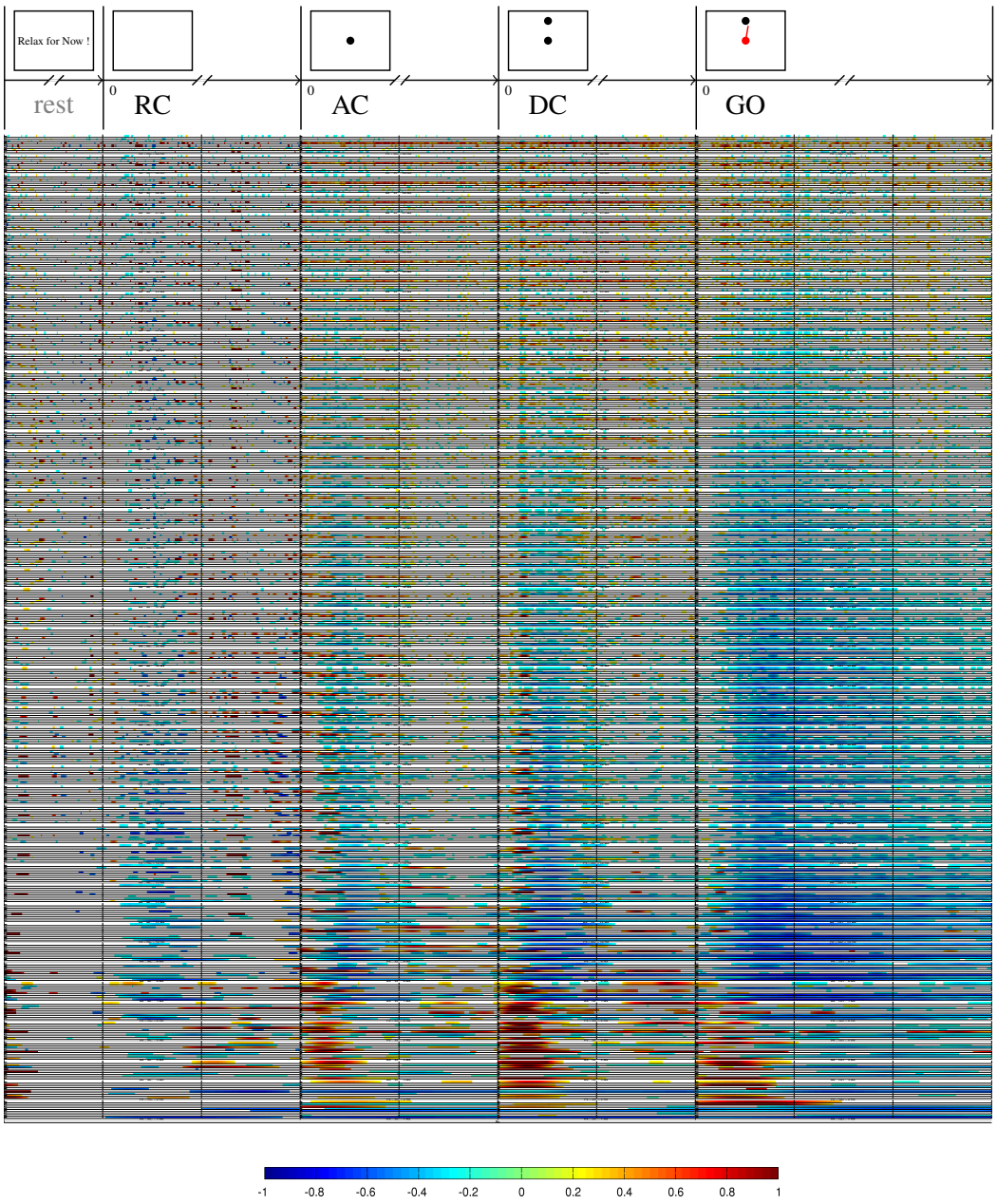

Figure E.10. CAR EEG time-frequency distribution for electrode P_z, showing statistically significant normalised (to pre-movement rest-time EEG) continuous Morlet wavelet transform (NCWT) scalograms from all subjects. Horizontal axes are time in seconds. Thicker blocks show different stages of experiment (from left to right the visual cues: RC, AC, DC, GO) and smaller x-axis chunks equal 1.0s. Vertical axes are frequencies (Hz), stacked from all subjects. Dark blue shows 100% ERD and dark red 100% ERS with respect to rest-time EEG.

Appendix F

Publications

Posters/Abstracts:

1. Nasseroleslami, B., Lakany, H., and Conway, B. A. (2011a). Time-Frequency EEG signatures of arm isometric exertions. Abstract/Poster, Glasgow Neuroscience Day 2011, Glasgow, Scotland, UK.

2. Nasseroleslami, B., Lakany, H., and Conway, B. A. (2011b). EEG signatures and directional information in planning and execution of arm isometric exertions," Abstract/Poster, Scottish Neuroscience Day 2011, Aberdeen, Scotland, UK.

Peer-reviewed Conference Papers:

1. Nasseroleslami, B., Lakany, H., and Conway, B. A. (2011a). Event-related (de-)synchronisation in arm isometric exertions: A wavelet analysis. In Proc. IEEE Symp. Computational Intelligence, Cognitive Algorithms, Mind, and Brain (CCMB), pages 1--7.

2. Nasseroleslami, B., Lakany, H., and Conway, B. A. (2011b). Identification of time-frequency EEG features modulated by force direction in arm isometric exertions. In Proc. 5th Int Neural Engineering (NER) IEEE/EMBS Conf, pages 422--425.

In Preparation:

1. Nasseroleslami, B., Lakany, H., and Conway, B. A. (In preparation). EEG signatures of directional arm isometric exertions in planning and execution.

2. Nasseroleslami, B., Lakany, H., and Conway, B. A. (In preparation). Directional information in EEG during planning and execution of arm isometric exertions.

3. Nasseroleslami, B., Lakany, H., and Conway, B. A. (In preparation). Event-related (de-)synchronisation in experiments with consecutive cues.

Appendix G

Ethics

Participant Information Sheet

University of Strathclyde
Bioengineering Unit
Neurophysiology Lab

Title of the study:
EEG Signatures of Directional Arm Isometric Exertions

Introduction

This experiment is conducted by Bahman Nasseroleslami, a doctoral student at University of Strathclyde, Bioengineering Unit, as part of his doctoral research experiment.

Bahman Nasseroleslami, PhD Student
Neurophysiology Lab, Bioengineering Unit, University of Strathclyde
Wolfson Centre, 106 Rottenrow, Glasgow G4 0NW, Scotland, UK
Tel: +44 141 548 4691, Fax: +44 141 552 6098, Mobile: +44 7532 271 398
E-Mail: bahman.nasseroleslami@strath.ac.uk

What is the purpose of this investigation?

This Experiment is designed to study how human brain works during exertion of force by arm/wrist. It investigates if the changes in brain activity during exertion of different forces van be detected. The results can be used for Brain-Computer Interfacing and for Neuro-Rehabilitation.

Do you have to take part?

For this purpose you are asked to sit on a chair and grab a manipulandum in your right hand and exert force according to instructions and cues on the computer screen. During the experiment, you will be wearing a cap. Your brain activity will be recorded by the electrodes on the cap. A conductive gel fills the gap between the cap electrodes and your scalp. This is called Electroencephalography (EEG). Some other electrodes are used to record the activity of your arm muscles (electromyography or EMG). After the experiment a towel and shampoo will be provided for washing your head.

Participation is completely voluntary. You are completely free to decide if you want to participate or not. There will be no consequences if you refuse to participate or if you withdraw from participation at any time before or during the experiment, for any reason.

What will you do in the project?

You will sit for the experiment, as described in previous section.

EEG:
Recording the activity of your brain is easily affected by blinking, jaw clench, swallowing, looking to left/right or by moving your head. For this reason, the recording will be most useful if you limit any of these tasks for the relaxation period between the experiment trials.

Last updated: 23/2/2009

Figure G.1. Subject information sheet (page 1).

Task:
You are asked to exert force in horizontal plane while holding the manipulandum with your right hand. The direction of requested force is forward, backward, to the right or to the left.
The figure shows the time course of appearance of cues on the computer screen. Cues always appear in the described order, after each other. However the durations between appearance of cues are random.

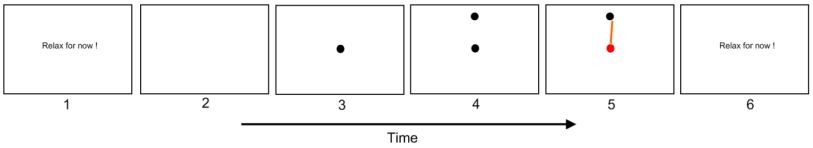

1. In relaxation time you are free to relax, blink, swallow, move and relax.
2. The white screen is the start of trial. You don't need to do anything. You can relax, but you are asked not to swallow, blink, move, and so forth.
3. When the black circle in the centre of screen appears, you should get prepared for instructional cues.
4. Appearance of the second black circle tells you what the direction of force, that you are going to exert, is. You shouldn't exert any physical force in this stage yet.
5. Here you are asked to exert force on the manipulandum in the direction shown in previous stage. You can see the direction and magnitude of your force on the screen in real time. The force indicator should approximately reach the circle.
6. The trial is finished and you can relax.

Site: University of Strathclyde, Bioengineering Unit, Neurophysiology Lab.
Duration: About 3.5 hours
Compensation/Payments: None.

Why have you been invited to take part?
For this experiment normal and healthy male or female participants are recruited. Participants with no neural, psychiatric, or musculoskeletal impairment or disease are included. No specific skill is required for the experiment. Participants need to have normal sight and upper limb function.

What are the potential risks to you in taking part?
Recording Equipments are medical grade devices, electrically isolated and periodically inspected. Consequently no risk is predicted regarding the electrical or recording aspects. If you are allergic to EEG conductive gel or EMG abrasive gels and pads, please inform the experimenter. This should not be the case if you have had your EEG recorded before.
There is no specific requirement/consideration prior to experiment.

What happens to the information in the project?
Your personal information will not be disclosed to individuals out of our research group without your permission, unless required by law. Your anonymous recording results will be used in reports and scientific publications without any identifiable information included. Your experiment results will be stored on the computers and servers of the University of Strathclyde and experimenter's personal computer.

Last updated: 23/2/2009

Figure G.2. Subject information sheet (page 2).

The University of Strathclyde is registered with the Information Commissioner's Office who implements the Data Protection Act 1998. All personal data on participants will be processed in accordance with the provisions of the Data Protection Act 1998.

Thank you for reading this information – please ask any questions if you are unsure about what is written here.

What happens next?
If you are happy with taking part, you are asked to sign the accompanying consent form for confirmation.
You can ask to be informed If the results are published.

This investigation was granted ethical approval by the University of Strathclyde ethics committee, by Bioengineering Unit Departmental Ethics Committee.

If you have any questions/concerns, during or after the investigation, or wish to contact an independent person to whom any questions may be directed or further information may be sought from, please contact:

Secretary to the University Ethics Committee
University of Strathclyde
McCance Building, 16 Richmond Street, Glasgow G1 1XQ, Scotland, UK.
Telephone: +44 141 548 2752
Email: ethics@strath.ac.uk

Researcher Contact Details:
Bahman Nasseroleslami, PhD Student
Neurophysiology Lab, Bioengineering Unit, University of Strathclyde
Wolfson Centre, 106 Rottenrow, Glasgow G4 0NW, Scotland, UK
Tel: +44 141 548 4691, Fax: +44 141 552 6098, Mobile: +44 7532 271 398
E-Mail: bahman.nasseroleslami@strath.ac.uk

Chief Investigator Details:

Bernard A. Conway, PhD, Professor and Head of Department,
Bioengineering Unit, University of Strathclyde
Wolfson Centre, 106 Rottenrow, Glasgow G4 0NW, Scotland, UK.
Tel: +44 141 548 3316, Fax: +44 141 552 6098,
E-Mail: b.a.conway@strath.ac.uk

Heba Lakany, PhD, Senior Lecturer,
Bioengineering Unit, University of Strathclyde
Wolfson Centre, 106 Rottenrow, Glasgow G4 0NW, Scotland, UK.
Tel: +44 141 548 3487, Fax: +44 141 552 6098,
E-Mail: heba.lakany@strath.ac.uk

Last updated: 23/2/2009

Figure G.3. Subject information sheet (page 3).

Consent Form

University of Strathclyde
Bioengineering Unit
Neurophysiology Lab

Title of the study:
EEG Signatures of Directional Arm Isometric Exertions

University of Strathclyde Glasgow

- I confirm that I have read and understood the information sheet for the above project and the researcher has answered any queries to my satisfaction.
- I understand that my participation is voluntary and that I am free to withdraw from the project at any time, without having to give a reason and without any consequences.
- I understand that I can withdraw my data from the study at any time.
- I understand that any information recorded in the investigation will remain confidential and no information that identifies me will be made publicly available.
- I consent to being a participant in the project

I (PRINT NAME)	Hereby agree to take part in the above project
Signature of Participant:	Date

Last updated: 23/2/2009

Figure G.4. Subject consent form.

Bibliography

Allison, B. Z., McFarland, D. J., Schalk, G., Zheng, S. D., Jackson, M. M., and Wolpaw, J. R. (2008). Towards an independent brain-computer interface using steady state visual evoked potentials. *Clin Neurophysiol*, 119(2):399--408.

Andersen, R. A., Musallam, S., and Pesaran, B. (2004). Selecting the signals for a brain-machine interface. *Curr Opin Neurobiol*, 14(6):720--726.

Ashe, J. (1997a). Force and the motor cortex. *Behav Brain Res*, 87(2):255--269.

Ashe, J. (1997b). Force and the motor cortex. *Behav Brain Res*, 86(1):1--15.

Association, W. M. (2001). World medical association declaration of helsinki. ethical principles for medical research involving human subjects. *Bull World Health Organ*, 79(4):373--374.

Axford, P. (2010). Transcranial sinusoidal direct current stimulation and its effects on inter-muscular coherence. In *Strathclyde Engineering Research Day*.

Babiloni, C., Carducci, F., Cincotti, F., Rossini, P. M., Neuper, C., Pfurtscheller, G., and Babiloni, F. (1999). Human movement-related potentials vs desynchronization of eeg alpha rhythm: a high-resolution eeg study. *Neuroimage*, 10(6):658--665.

Bagesteiro, L. B. and Sainburg, R. L. (2002). Handedness: dominant arm advantages in control of limb dynamics. *J Neurophysiol*, 88(5):2408--2421.

Ball, T., Schulze-Bonhage, A., Aertsen, A., and Mehring, C. (2009). Differential representation of arm movement direction in relation to cortical anatomy and function. *J Neural Eng*, 6(1):016006.

Basso, D., Pesarin, F., Salmaso, L., and Solari, A. (2009). *Permutation Tests for Stochastic Ordering and ANOVA*. Lecture Notes in Statistics. Springer.

Benbadis, S., Husain, A., Kaplan, P., and Tatum, W. (2007). *Handbook of EEG Interpretation*. Springer Demos Medic Series. Demos Medical Publishing.

Berardelli, A., Hallett, M., Rothwell, J. C., Agostino, R., Manfredi, M., Thompson, P. D., and Marsden, C. D. (1996). Single-joint rapid arm movements in normal subjects and in patients with motor disorders. *Brain*, 119 (Pt 2):661--74. 0006-8950 (Print) Journal Article Review.

Birbaumer, N. (2006). Breaking the silence: brain-computer interfaces (bci) for communication and motor control. *Psychophysiology*, 43(6):517--532.

Birbaumer, N. and Cohen, L. G. (2007). Brain-computer interfaces: communication and restoration of movement in paralysis. *J Physiol*, 579(Pt 3):621--636.

Birbaumer, N., Hinterberger, T., Kübler, A., and Neumann, N. (2003). The thought-translation device (ttd): neurobehavioral mechanisms and clinical outcome. *IEEE Trans Neural Syst Rehabil Eng*, 11(2):120--123.

Birbaumer, N., Murguialday, A. R., and Cohen, L. (2008). Brain-computer interface in paralysis. *Curr Opin Neurol*, 21(6):634--638.

Birbaumer, N., Weber, C., Neuper, C., Buch, E., Haapen, K., and Cohen, L. (2006). Physiological regulation of thinking: brain-computer interface (bci) research. *Prog Brain Res*, 159:369--391.

Boashash, B., editor (2003). *time-frequency signal analysis and processing: a comprehensive reference*. Elsevier.

Bradberry, T. J., Gentili, R. J., and Contreras-Vidal, J. L. (2010). Reconstructing three-dimensional hand movements from noninvasive electroencephalographic signals. *J Neurosci*, 30(9):3432--3437.

Bradberry, T. J., Gentili, R. J., and Contreras-Vidal, J. L. (2011). Fast attainment of computer cursor control with noninvasively acquired brain signals. *J Neural Eng*, 8(3):036010.

Bradberry, T. J., Rong, F., and Contreras-Vidal, J. L. (2009). Decoding center-out hand velocity from meg signals during visuomotor adaptation. *Neuroimage*, 47(4):1691--1700.

Brainard, D. H. (1997). The psychophysics toolbox. *Spat Vis*, 10(4):433--436.

Bretz, F., Hothorn, T., Westfall, P., and Westfall, P. H. (2011). *Multiple Comparisons Using R*. A Chapman & Hall book. CRC PressINC.

Brown, J. M. and Gilleard, W. (1991). Transition from slow to ballistic movement: development of triphasic electromyogram patterns. *European journal of applied physiology and occupational physiology*, 63(5):381--6. 0301-5548 (Print) Journal Article.

Brown, S. H. and Cooke, J. D. (1981). Amplitude- and instruction-dependent modulation of movement-related electromyogram activity in humans. *The Journal of Physiology-London*, 316:97--107. 0022-3751 (Print) Journal Article Research Support, Non-U.S. Gov't.

Caldara, R., Deiber, M.-P., Andrey, C., Michel, C. M., Thut, G., and Hauert, C.-A. (2004). Actual and mental motor preparation and execution: a spatiotemporal erp study. *Exp Brain Res*, 159(3):389--399.

Cambiaghi, M., Velikova, S., Gonzalez-Rosa, J. J., Cursi, M., Comi, G., and Leocani, L. (2010). Brain transcranial direct current stimulation modulates motor excitability in mice. *Eur J Neurosci*, 31(4):704--709.

Chakarov, V., Naranjo, J. R., Schulte-Mönting, J., Omlor, W., Huethe, F., and Kristeva, R. (2009). Beta-range eeg-emg coherence with isometric compensation for increasing modulated low-level forces. *J Neurophysiol*, 102(2):1115--1120.

Chao, Z. C., Nagasaka, Y., and Fujii, N. (2010). Long-term asynchronous decoding of arm motion using electrocorticographic signals in monkeys. *Front Neuroeng*, 3:3.

Chui, C. K. (1992). *An Introduction to Wavelets*. Academic Press.

Cifrek, M., Medved, V., Tonković, S., and Ostojić, S. (2009). Surface emg based muscle fatigue evaluation in biomechanics. *Clin Biomech (Bristol, Avon)*, 24(4):327--340.

Cisek, P., Crammond, D. J., and Kalaska, J. F. (2003). Neural activity in primary motor and dorsal premotor cortex in reaching tasks with the contralateral versus ipsilateral arm. *J Neurophysiol*, 89(2):922--942.

Cisek, P. and Kalaska, J. F. (2002). Simultaneous encoding of multiple potential reach directions in dorsal premotor cortex. *J Neurophysiol*, 87(2):1149--1154.

Cisek, P. and Kalaska, J. F. (2004). Neural correlates of mental rehearsal in dorsal premotor cortex. *Nature*, 431(7011):993--996.

Cisek, P. and Kalaska, J. F. (2005). Neural correlates of reaching decisions in dorsal premotor cortex: specification of multiple direction choices and final selection of action. *Neuron*, 45(5):801--814.

Cohen, L. (1995). *Time-Frequency Analysis*. Prentice Hall Signal Processing Series. Prentice Hall PTR.

Colebatch, J. G. (2007). Bereitschaftspotential and movement-related potentials: origin, significance, and application in disorders of human movement. *Mov Disord*, 22(5):601--610.

Compton, R. J., Arnstein, D., Freedman, G., Dainer-Best, J., and Liss, A. (2011). Cognitive control in the intertrial interval: evidence from eeg alpha power. *Psychophysiology*, 48(5):583--590.

Conway, B. A., Halliday, D. M., Farmer, S. F., Shahani, U., Maas, P., Weir, A. I., and Rosenberg, J. R. (1995). Synchronization between motor cortex and spinal motoneuronal pool during the performance of a maintained motor task in man. *J Physiol*, 489 (Pt 3):917--924.

Cooreman, C., Sclocco, R., Tana, M. G., Vanderperren, K., Visani, E., Panzica, F., Franceschetti, S., Van Huffel, S., Cerutti, S., and Bianchi, A. M. (2011). Bold correlates of alpha and beta eeg-rhythm during a motor task. In *Proc. 5th Int Neural Engineering (NER) IEEE/EMBS Conf*, pages 25--28.

Crammond, D. J. and Kalaska, J. F. (2000). Prior information in motor and premotor cortex: activity during the delay period and effect on pre-movement activity. *J Neurophysiol*, 84(2):986--1005.

Crone, N. E., Miglioretti, D. L., Gordon, B., and Lesser, R. P. (1998a). Functional mapping of human sensorimotor cortex with electrocorticographic spectral analysis. ii. event-related synchronization in the gamma band. *Brain*, 121 (Pt 12):2301--2315.

Crone, N. E., Miglioretti, D. L., Gordon, B., Sieracki, J. M., Wilson, M. T., Uematsu, S., and Lesser, R. P. (1998b). Functional mapping of human sensorimotor cortex with electrocorticographic spectral analysis. i. alpha and beta event-related desynchronization. *Brain*, 121 (Pt 12):2271--2299.

Cui, R. Q. and Deecke, L. (1999). High resolution dc-eeg analysis of the bereitschaftspotential and post movement onset potentials accompanying uni- or bilateral voluntary finger movements. *Brain Topogr*, 11(3):233--249.

da Silva, F. H. L. (2006). Event-related neural activities: what about phase? *Prog Brain Res*, 159:3--17.

Daly, J. J. and Wolpaw, J. R. (2008). Brain-computer interfaces in neurological rehabilitation. *Lancet Neurol*, 7(11):1032--1043.

Decety, J. (1996). The neurophysiological basis of motor imagery. *Behav Brain Res*, 77(1-2):45--52.

Delorme, A. and Makeig, S. (2004). Eeglab: an open source toolbox for analysis of single-trial eeg dynamics including independent component analysis. *J Neurosci Methods*, 134(1):9--21.

do Nascimento, O. F. and Farina, D. (2008). Movement-related cortical potentials allow discrimination of rate of torque development in imaginary isometric plantar flexion. *IEEE Trans Biomed Eng*, 55(11):2675--2678.

do Nascimento, O. F., Nielsen, K. D., and Voigt, M. (2005). Relationship between plantar-flexor torque generation and the magnitude of the movement-related potentials. *Exp Brain Res*, 160(2):154--165.

do Nascimento, O. F., Nielsen, K. D., and Voigt, M. (2006). Movement-related parameters modulate cortical activity during imaginary isometric plantar-flexions. *Exp Brain Res*, 171(1):78--90.

Dobkin, B. H. (2007). Brain-computer interface technology as a tool to augment plasticity and outcomes for neurological rehabilitation. *J Physiol*, 579(Pt 3):637--642.

Donchin, E., Spencer, K. M., and Wijesinghe, R. (2000). The mental prosthesis: assessing the speed of a p300-based brain-computer interface. *IEEE Trans Rehabil Eng*, 8(2):174--179.

Drissi, H., Regragui, F., Antoine, J. P., and Bennouna, M. (2000). Wavelet transform analysis of visual evoked potentials: some preliminary results. *ITBM-RBM*, 21(2):84 -- 91.

Duda, R. O., Hart, P. E., and Stork, D. G. (2000). *Pattern Classification*. Wiley-Interscience, 2nd edition.

Durka, P. (2007). *Matching Pursuit and unification in EEG analysis*. Artech House.

Durka, P. J. (2006). Time-frequency microstructure and statistical significance of erd and ers. *Prog Brain Res*, 159:121--133.

Durka, P. J., Zygierewicz, J., Klekowicz, H., Ginter, J., and Blinowska, K. J. (2004). On the statistical significance of event-related eeg desynchronization and synchronization in the time-frequency plane. *IEEE Trans Biomed Eng*, 51(7):1167--1175.

Ehrsson, H. H., Geyer, S., and Naito, E. (2003). Imagery of voluntary movement of fingers, toes, and tongue activates corresponding body-part-specific motor representations. *J Neurophysiol*, 90(5):3304--3316.

Erfon, B. and Tibshirani, R. J. (1993). *An Introduction to the bootstrap*. Chapman and Hall/CRC, London.

Fagg, A. H., Hatsopoulos, N. G., de Lafuente, V., Moxon, K. A., Nemati, S., Rebesco, J. M., Romo, R., Solla, S. A., Reimer, J., Tkach, D., Pohlmeyer, E. A., and Miller, L. E. (2007). Biomimetic brain machine interfaces for the control of movement. *J Neurosci*, 27(44):11842--11846.

Farwell, L. A. and Donchin, E. (1988). Talking off the top of your head: toward a mental prosthesis utilizing event-related brain potentials. *Electroencephalogr Clin Neurophysiol*, 70(6):510--523.

Fernández, T., Harmony, T., Rodríguez, M., Reyes, A., Marosi, E., and Bernal, J. (1993). Test-retest reliability of eeg spectral parameters during cognitive tasks: I. absolute and relative power. *Int J Neurosci*, 68(3-4):255--261.

Feurra, M., Bianco, G., Santarnecchi, E., Del Testa, M., Rossi, A., and Rossi, S. (2011). Frequency-dependent tuning of the human motor system induced by transcranial oscillatory potentials. *J Neurosci*, 31(34):12165--12170.

Fukunaga, K. (1990). *Introduction to statistical pattern recognition*. Morgan Kaufmann, second edition.

Gaal, G. (1993). Calculation of movement direction from firing activities of neurons in intrinsic co-ordinate systems defined by their preferred directions. *J Theor Biol*, 162(1):103--30. 0022-5193 (Print) Journal Article.

Georgopoulos, A. P., Kettner, R. E., and Schwartz, A. B. (1988). Primate motor cortex and free arm movements to visual targets in three-dimensional space. ii. coding of the direction of movement by a neuronal population. *J Neurosci*, 8(8):2928--2937.

Georgopoulos, A. P., Schwartz, A. B., and Kettner, R. E. (1986). Neuronal population coding of movement direction. *Science*, 233(4771):1416--9. 0036-8075 (Print) Journal Article.

Graimann, B., Allison, B., and Pfurtscheller, G. (2010). *BRAIN–COMPUTER INTERFACES: Revolutionizing Human–Computer Interaction*, chapter Brain–Computer Interfaces: A Gentle Introduction, pages 1--27. Springer-Verlag.

Graimann, B. and Pfurtscheller, G. (2006). Quantification and visualization of event-related changes in oscillatory brain activity in the time-frequency domain. *Prog Brain Res*, 159:79--97.

Grandchamp, R. and Delorme, A. (2011). Single-trial normalization for event-related spectral decomposition reduces sensitivity to noisy trials. *Front Psychol*, 2:236.

Green, A. M. and Kalaska, J. F. (2011). Learning to move machines with the mind. *Trends Neurosci*, 34(2):61--75.

Grychtol, B., Lakany, H., Valsan, G., and Conway, B. A. (2010). Human behavior integration improves classification rates in real-time bci. *IEEE Trans Neural Syst Rehabil Eng*, 18(4):362--368.

Gu, Y., do Nascimento, O. F., Lucas, M.-F., and Farina, D. (2009). Identification of task parameters from movement-related cortical potentials. *Med Biol Eng Comput*, 47(12):1257--1264.

Guo, F., Hong, B., Gao, X., and Gao, S. (2008a). A brain computer interface based on motion-onset veps. *Conf Proc IEEE Eng Med Biol Soc*, 2008:4478--4481.

Guo, F., Hong, B., Gao, X., and Gao, S. (2008b). A brain-computer interface using motion-onset visual evoked potential. *J Neural Eng*, 5(4):477--485.

Halliday, D. M., Rosenberg, J. R., Amjad, A. M., Breeze, P., Conway, B. A., and Farmer, S. F. (1995). A framework for the analysis of mixed time series/point process data--theory and application to the study of physiological tremor, single motor unit discharges and electromyograms. *Prog Biophys Mol Biol*, 64(2-3):237--278.

Hamel-Paquet, C., Sergio, L. E., and Kalaska, J. F. (2006). Parietal area 5 activity does not reflect the differential time-course of motor output kinetics during arm-reaching and isometric-force tasks. *J Neurophysiol*, 95(6):3353--3370.

Hammon, P. S., Makeig, S., Poizner, H., Todorov, E., and de Sa, V. R. (2008). Predicting reaching targets from human eeg. *IEEE Signal Processing Magazine*, 25(1):69--77.

Hanakawa, T., Immisch, I., Toma, K., Dimyan, M. A., Gelderen, P. V., and Hallett, M. (2003). Functional properties of brain areas associated with motor execution and imagery. *J Neurophysiol*, 89(2):989--1002.

Hatsopoulos, N. G. and Donoghue, J. P. (2009). The science of neural interface systems. *Annu Rev Neurosci*, 32:249--266.

Haykin, S. S. (1999). *Neural networks : a comprehensive foundation*. Prentice Hall, Upper Saddle River, NJ, 2nd edition. Simon Haykin. ill. ; 25 cm.

He, B. and Liu, Z. (2008). Multimodal functional neuroimaging: Integrating functional mri and eeg/meg. *IEEE Reviews in Biomedical Engineering*, 1:23--40.

Hebb, D. (1949). *The organization of behavior*. Wiley & Sons.

Herman, P., Prasad, G., McGinnity, T. M., and Coyle, D. (2008). Comparative analysis of spectral approaches to feature extraction for eeg-based motor imagery classification. *IEEE Trans Neural Syst Rehabil Eng*, 16(4):317--326.

Hermens, H. J., Freriks, B., Disselhorst-Klug, C., and Rau, G. (2000). Development of recommendations for semg sensors and sensor placement procedures. *J Electromyogr Kinesiol*, 10(5):361--374.

Hink, R. F., Deecke, L., and Kornhuber, H. H. (1983). Force uncertainty of voluntary movement and human movement-related potentials. *Biol Psychol*, 16(3-4):197--210.

Hlawatsch, F. and Auger, F. (2008). *Time-frequency analysis: concepts and methods*. Digital signal and image processing series. ISTE.

Hoffman, D. S. and Strick, P. L. (1999). Step-tracking movements of the wrist. iv. muscle activity associated with movements in different directions. *J Neurophysiol*, 81(1):319--33. 0022-3077 (Print) Clinical Trial Journal Article.

Hunter, T., Sacco, P., Nitsche, M. A., and Turner, D. L. (2009). Modulation of internal model formation during force field-induced motor learning by anodal transcranial direct current stimulation of primary motor cortex. *J Physiol*, 587(Pt 12):2949--2961.

Huysmans, M. A., de Looze, M. P., Hoozemans, M. J. M., van der Beek, A. J., and van Dieën, J. H. (2006). The effect of joystick handle size and gain at two levels of required precision on performance and physical load on crane operators. *Ergonomics*, 49(11):1021--1035.

Hwang, E. J. and Shadmehr, R. (2005). Internal models of limb dynamics and the encoding of limb state. *Journal of Neural Engineering*, 2(3):S266--78. 1741-2560 (Print) Journal Article Review.

Izenman, A. J. (2008). *Modern Multivariate Statistical Techniques: Regression, Classification, and Manifold Learning*. Springer Texts in Statistics. Springer.

Jahanshahi, M., Jenkins, I. H., Brown, R. G., Marsden, C. D., Passingham, R. E., and Brooks, D. J. (1995). Self-initiated versus externally triggered movements. i. an investigation using measurement of regional cerebral blood flow with pet and movement-related potentials in normal and parkinson's disease subjects. *Brain*, 118 (Pt 4):913--933.

Jin, Y., Kemp, A. S., Huang, Y., Thai, T. M., Liu, Z., Xu, W., He, H., and Potkin, S. G. (2011). Alpha eeg guided tms in schizophrenia. *Brain Stimul*.

Jolliffe, I. (2002). *Principal Component Analysis*. Springer, 2 edition.

Jordan, M. and Wolpert, D. (1999). Computational motor control. In Gazzaniga, M., editor, *The cognitive neuroscience*, pages 601--620. MIT Press, Cambridge, MA.

Kettner, R. E., Schwartz, A. B., and Georgopoulos, A. P. (1988). Primate motor cortex and free arm movements to visual targets in three-dimensional space. iii. positional gradients and population coding of movement direction from various movement origins. *J Neurosci*, 8(8):2938--47. 0270-6474 (Print) Journal Article.

Kornhuber, H. H. and Deecke, L. (1965). Hirnpotentialänderungen bei Willkürbewegungen und passiven Bewegungen des Menschen: Bereitschaftspotential und reafferente Potentiale. *Pflügers Arch*, 284:1--17.

Krause, G., Ullsperger, P., Beyer, L., and Gille, H. G. (1983). Changes in eeg power density spectrum during static muscle work. *Eur J Appl Physiol Occup Physiol*, 51(1):61--66.

Lacourse, M. G., Orr, E. L. R., Cramer, S. C., and Cohen, M. J. (2005). Brain activation during execution and motor imagery of novel and skilled sequential hand movements. *Neuroimage*, 27(3):505--519.

Lazzaro, V. D., Profice, P., Pilato, F., Dileone, M., Oliviero, A., and Ziemann, U. (2010). The effects of motor cortex rtms on corticospinal descending activity. *Clin Neurophysiol*, 121(4):464--473.

Lebedev, M. A. and Nicolelis, M. A. L. (2006). Brain-machine interfaces: past, present and future. *Trends Neurosci*, 29(9):536--546.

Lei, A. A. and Trapani, V. C. (2000). *Atlas of Electromyography*. Oxford University Press.

Leuthardt, E. C., Schalk, G., Roland, J., Rouse, A., and Moran, D. W. (2009). Evolution of brain-computer interfaces: going beyond classic motor physiology. *Neurosurg Focus*, 27(1):E4.

Leuthold, H. and Jentzsch, I. (2009). Planning of rapid aiming movements and the contingent negative variation: are movement duration and extent specified independently? *Psychophysiology*, 46(3):539--550.

Lin, S.-T., Gheewala, M., Wolfe, J. C., Dani, J. A., and Shih, W.-C. (2011). A flexible optrode for deep brain neurophotonics. In *Proc. 5th Int Neural Engineering (NER) IEEE/EMBS Conf*, pages 700--703.

Lindsay, K. A. and Rosenberg, J. R. (2011). Identification of directed interactions in networks. *Biol Cybern*, 104(6):385--396.

Ljubisavljevic, M. (2006). Transcranial magnetic stimulation and the motor learning-associated cortical plasticity. *Exp Brain Res*, 173(2):215--222.

Lv, J., Li, Y., and Gu, Z. (2010). Decoding hand movement velocity from electroencephalogram signals during a drawing task. *Biomed Eng Online*, 9:64.

MacKay, W. A. and Bonnet, M. (1990). Cnv, stretch reflex and reaction time correlates of preparation for movement direction and force. *Electroencephalogr Clin Neurophysiol*, 76(1):47--62.

Martin, K., Jacobs, S., and Frey, S. H. (2011). Handedness-dependent and -independent cerebral asymmetries in the anterior intraparietal sulcus and ventral premotor cortex during grasp planning. *Neuroimage*, 57(2):502--512.

Masakado, Y. and Nielsen, J. B. (2008). Task-and phase-related changes in cortico-muscular coherence. *Keio J Med*, 57(1):50--56.

McFarland, D. J., Krusienski, D. J., and Wolpaw, J. R. (2006). Brain-computer interface signal processing at the wadsworth-center: mu and sensorimotor beta rhythms. *Prog Brain Res*, 159:411--419.

McFarland, D. J., Miner, L. A., Vaughan, T. M., and Wolpaw, J. R. (2000). Mu and beta rhythm topographies during motor imagery and actual movements. *Brain Topogr*, 12(3):177--186.

McFarland, D. J., Sarnacki, W. A., and Wolpaw, J. R. (2010). Electroencephalographic (eeg) control of three-dimensional movement. *J Neural Eng*, 7(3):036007.

Mehring, C., Rickert, J., Vaadia, E., de Oliveira, S. C., Aertsen, A., and Rotter, S. (2003). Inference of hand movements from local field potentials in monkey motor cortex. *Nat Neurosci*, 6(12):1253--1254.

Merletti, R. and Parker, P. A. (2004). *Electromyography: Physiology, Engineering, and Noninvasive Applications*. IEEE Press - John Wiley and Sons.

Mima, T. and Hallett, M. (1999). Corticomuscular coherence: a review. *J Clin Neurophysiol*, 16(6):501--511.

Minev, I. R., Chew, D. J., Delivopoulos, E., Fawcett, J. W., and Lacour, S. P. (2011). Evaluation of an elastomer based gold microelectrode array for neural recording applications. In *Proc. 5th Int Neural Engineering (NER) IEEE/EMBS Conf*, pages 482--485.

Misiti, M., Misiti, Y., Oppenheim, G., and Poggi, J.-M. (2007). *Wavelets and their Applications*. ISTE, London.

Moore, D., McCabe, G., and Craig, B. (2010). *Introduction to the Practice of Statistics*. Macmillan Higher Education.

Morash, V., Bai, O., Furlani, S., Lin, P., and Hallett, M. (2008). Classifying eeg signals preceding right hand, left hand, tongue, and right foot movements and motor imageries. *Clin Neurophysiol*, 119(11):2570--2578.

Nasseroleslami, B., Lakany, H., and Conway, B. A. (2011a). Event-related (de-)synchronisation in arm isometric exertions: A wavelet analysis. In *Proc. IEEE Symp. Computational Intelligence, Cognitive Algorithms, Mind, and Brain (CCMB)*, pages 1--7.

Nasseroleslami, B., Lakany, H., and Conway, B. A. (2011b). Identification of time-frequency eeg features modulated by force direction in arm isometric exertions. In *Proc. 5th Int Neural Engineering (NER) IEEE/EMBS Conf*, pages 422--425.

Neuper, C., Müller-Putz, G. R., Scherer, R., and Pfurtscheller, G. (2006a). Motor imagery and eeg-based control of spelling devices and neuroprostheses. *Prog Brain Res*, 159:393--409.

Neuper, C., Wörtz, M., and Pfurtscheller, G. (2006b). Erd/ers patterns reflecting sensorimotor activation and deactivation. *Prog Brain Res*, 159:211--222.

Novakovic, V. and Sanguineti, V. (2011). Adaptation to constant-magnitude assistive forces: kinematic and neural correlates. *Exp Brain Res*, 209(3):425--436.

Oda, S., Shibata, M., and Moritani, T. (1996). Force-dependent changes in movement-related cortical potentials. *J Electromyogr Kinesiol*, 6(4):247--252.

Onton, J. and Makeig, S. (2006). Information-based modeling of event-related brain dynamics. *Prog Brain Res*, 159:99--120.

Oppenheim, A. V., Schafer, R. W., and Buck, J. R. (1999). *Discrete-Time Signal Processing*. Prentice Hall.

Patestas, M. A. and Gartner, L. P. (2006). *a textbook of neuroanatomy*. Blackwell.

Pease, W. S. (2007). *Johnson's Practical Electromyography*. Lippincott Williams & Wilkins.

Pelli, D. G. (1997). The videotoolbox software for visual psychophysics: transforming numbers into movies. *Spat Vis*, 10(4):437--442.

Pellionisz, A. (1988). Tensorial aspects of the multidimensional massively parallel sensorimotor function of neuronal networks. *Prog Brain Res*, 76:341--54. Ns 22999/ns/ninds Journal Article Research Support, U.S. Gov't, P.H.S. Review Netherlands.

Pellionisz, A. and Llinas, R. (1979). Brain modeling by tensor network theory and computer simulation. the cerebellum: distributed processor for predictive coordination. *Neuroscience*, 4(3):323--48. Journal Article Research Support, U.S. Gov't, P.H.S. England.

Perfetti, B., Moisello, C., Landsness, E. C., Kvint, S., Lanzafame, S., Onofrj, M., Di Rocco, A., Tononi, G., and Ghilardi, M. F. (2011). Modulation of gamma and theta spectral amplitude and phase synchronization is associated with the development of visuo-motor learning. *J Neurosci*, 31(41):14810--14819.

Pfurtscheller, G. (2006). The cortical activation model (cam). *Prog Brain Res*, 159:19--27.

Pfurtscheller, G. and Aranibar, A. (1977). Event-related cortical desynchronization detected by power measurements of scalp eeg. *Electroencephalogr Clin Neurophysiol*, 42(6):817--826.

Pfurtscheller, G. and da Silva, F. H. L. (1999). Event-related eeg/meg synchronization and desynchronization: basic principles. *Clin Neurophysiol*, 110(11):1842--1857.

Pfurtscheller, G., Müller, G. R., Pfurtscheller, J., Gerner, H. J., and Rupp, R. (2003). 'thought'--control of functional electrical stimulation to restore hand grasp in a patient with tetraplegia. *Neurosci Lett*, 351(1):33--36.

Pfurtscheller, G. and Neuper, C. (1994). Event-related synchronization of mu rhythm in the eeg over the cortical hand area in man. *Neurosci Lett*, 174(1):93--96.

Pfurtscheller, G. and Neuper, C. (2006). Future prospects of erd/ers in the context of brain-computer interface (bci) developments. *Prog Brain Res*, 159:433--437.

Power, S. D., Falk, T. H., and Chau, T. (2010). Classification of prefrontal activity due to mental arithmetic and music imagery using hidden markov models and frequency domain near-infrared spectroscopy. *J Neural Eng*, 7(2):26002.

Reddy, C. G., Reddy, G. G., Kawasaki, H., Oya, H., Miller, L. E., and Howard, M. A. (2009). Decoding movement-related cortical potentials from electrocorticography. *Neurosurg Focus*, 27(1):E11.

Reis, J., Robertson, E., Krakauer, J. W., Rothwell, J., Marshall, L., Gerloff, C., Wassermann, E., Pascual-Leone, A., Hummel, F., Celnik, P. A., Classen, J., Floel, A., Ziemann, U., Paulus, W., Siebner, H. R., Born, J., and Cohen, L. G. (2008). Consensus: "can tdcs and tms enhance motor learning and memory formation?". *Brain Stimulat*, 1(4):363--369.

Romero, D. H., Lacourse, M. G., Lawrence, K. E., Schandler, S., and Cohen, M. J. (2000). Event-related potentials as a function of movement parameter variations during motor imagery and isometric action. *Behav Brain Res*, 117(1-2):83--96.

Salenius, S. and Hari, R. (2003). Synchronous cortical oscillatory activity during motor action. *Curr Opin Neurobiol*, 13(6):678--684.

Sanei, S. and Chambers, J. A. (2007). *EEG signal processing*. Wiley-Interscience.

Santucci, D. M., Kralik, J. D., Lebedev, M. A., and Nicolelis, M. A. L. (2005). Frontal and parietal cortical ensembles predict single-trial muscle activity during reaching movements in primates. *Eur J Neurosci*, 22(6):1529--1540.

Schaal, S., Sternad, D., Osu, R., and Kawato, M. (2004). Rhythmic arm movement is not discrete. *Nat Neurosci*, 7(10):1136--1143.

Schalk, G., Kubánek, J., Miller, K. J., Anderson, N. R., Leuthardt, E. C., Ojemann, J. G., Limbrick, D., Moran, D., Gerhardt, L. A., and Wolpaw, J. R. (2007). Decoding two-

dimensional movement trajectories using electrocorticographic signals in humans. *J Neural Eng*, 4(3):264--275.

Scherer, R., Schloegl, A., Lee, F., Bischof, H., Jansa, J., and Pfurtscheller, G. (2007). The self-paced graz brain-computer interface: methods and applications. *Comput Intell Neurosci*, page 79826.

Schieber, M. (2011). Changing circuits that control the fingers: Dissociating motor cortex from the motor. In *Physiological Society Abstract*, page 557, Cambridge, UK. The Physiological Society.

Schieber, M. H. and Santello, M. (2004). Hand function: peripheral and central constraints on performance. *J Appl Physiol*, 96(6):2293--2300.

Schoffelen, J.-M., Oostenveld, R., and Fries, P. (2008). Imaging the human motor system's beta-band synchronization during isometric contraction. *Neuroimage*, 41(2):437--447.

Schwartz, A. B., Kettner, R. E., and Georgopoulos, A. P. (1988). Primate motor cortex and free arm movements to visual targets in three-dimensional space. i. relations between single cell discharge and direction of movement. *J Neurosci*, 8(8):2913--27. 0270-6474 (Print) Journal Article.

Scott, S. H. and Norman, K. E. (2003). Computational approaches to motor control and their potential role for interpreting motor dysfunction. *Curr Opin Neurol*, 16(6):693--8. Journal Article Research Support, Non-U.S. Gov't Review England.

Sergio, L. E., Hamel-Paquet, C., and Kalaska, J. F. (2005). Motor cortex neural correlates of output kinematics and kinetics during isometric-force and arm-reaching tasks. *J Neurophysiol*, 94(4):2353--78. 0022-3077 (Print) Journal Article.

Sergio, L. E. and Kalaska, J. F. (1998). Changes in the temporal pattern of primary motor cortex activity in a directional isometric force versus limb movement task. *J Neurophysiol*, 80(3):1577--1583.

Sergio, L. E. and Kalaska, J. F. (2003). Systematic changes in motor cortex cell activity with arm posture during directional isometric force generation. *J Neurophysiol*, 89(1):212--28. 0022-3077 (Print) Journal Article.

Shadmehr, R. and Wise, S. P. (2005). *The computational neurobiology of reaching and pointing : a foundation for motor learning*. Computational neuroscience. MIT Press, Cambridge, MA. Reza Shadmehr and Steven P. Wise. ill. ; 26 cm. A Bradford book.

Shannon, C. E. (1948). A mathematical theory of communication. *The Bell System Technical Journal*, 27:379–423, 623–656.

Shibasaki, H. and Hallett, M. (2006). What is the bereitschaftspotential? *Clin Neurophysiol*, 117(11):2341--2356.

Shibasaki, H. and Kato, M. (1975). Movement-associated cortical potentials with unilateral and bilateral simultaneous hand movement. *J Neurol*, 208(3):191--199.

Shibata, M., Oda, S., and Moritani, T. (1997). The relationships between movement-related cortical potentials and motor unit activity during muscle contraction. *J Electromyogr Kinesiol*, 7(2):79--85.

Siegel, M., Donner, T. H., and Engel, A. K. (2012). Spectral fingerprints of large-scale neuronal interactions. *Nat Rev Neurosci*, 13(2):121--134.

Siemionow, V., Yue, G. H., Ranganathan, V. K., Liu, J. Z., and Sahgal, V. (2000). Relationship between motor activity-related cortical potential and voluntary muscle activation. *Exp Brain Res*, 133(3):303--311.

Sinkkonen, J., Tiitinen, H., and Näätänen, R. (1995). Gabor filters: an informative way for analysing event-related brain activity. *J Neurosci Methods*, 56(1):99--104.

Slobounov, S., Johnston, J., Chiang, H., and Ray, W. (2002). Movement-related eeg potentials are force or end-effector dependent: evidence from a multi-finger experiment. *Clin Neurophysiol*, 113(7):1125--1135.

Slobounov, S. M. and Ray, W. J. (1998). Movement-related potentials with reference to isometric force output in discrete and repetitive tasks. *Exp Brain Res*, 123(4):461--473.

Society, A. C. N. (2006). Guidelines for standard electrode position nomenclature. acns.2006.

Soteropoulos, D., Edgley, S., and Baker, S. (2011). Ipsilateral corticospinal contributions to control of the forelimb in monkey. In *Physiological Society Abstracts*, pages 81--82, Cambridge, UK. The Physiological Society.

Srinivasan, R., Winter, W. R., and Nunez, P. L. (2006). Source analysis of eeg oscillations using high-resolution eeg and meg. *Prog Brain Res*, 159:29--42.

Stagg, C. J. and Nitsche, M. A. (2011). Physiological basis of transcranial direct current stimulation. *Neuroscientist*, 17(1):37--53.

Stieglitz, T., Rubehn, B., Henle, C., Kisban, S., Herwik, S., Ruther, P., and Schuettler, M. (2009). Brain-computer interfaces: an overview of the hardware to record neural signals from the cortex. *Prog Brain Res*, 175:297--315.

Tatum, W. O., Dworetzky, B. A., and Schomer, D. L. (2011). Artifact and recording concepts in eeg. *J Clin Neurophysiol*, 28(3):252--263.

Thut, G., Veniero, D., Romei, V., Miniussi, C., Schyns, P., and Gross, J. (2011). Rhythmic tms causes local entrainment of natural oscillatory signatures. *Curr Biol*, 21(14):1176--1185.

Todorov, E. (2004). Optimality principles in sensorimotor control. *Nat Neurosci*, 7(9):907--15. 1097-6256 (Print) Journal Article Research Support, U.S. Gov't, P.H.S. Review.

Torrence, C. and Compo, G. P. (1998). A practical guide to wavelet analysis. *Bull. Amer. Meteor. Soc.*, 79(1):61--78.

Ulrich, R., Leuthold, H., and Sommer, W. (1998). Motor programming of response force and movement direction. *Psychophysiology*, 35(6):721--728.

Valsan, G. (2007). *Brain Computer Interface using detection of movement intent*. PhD thesis, University of Starthclyde.

Valsan, G., Grychtol, B., Lakany, H., and Conway, B. A. (2009). The strathclyde brain computer interface. *Conf Proc IEEE Eng Med Biol Soc*, 2009:606--609.

van Drongelen, W. (2006). *Signal Processing for Neuroscientists*. Academic Press.

van Gerven, M., Farquhar, J., Schaefer, R., Vlek, R., Geuze, J., Nijholt, A., Ramsey, N., Haselager, P., Vuurpijl, L., Gielen, S., and Desain, P. (2009). The brain-computer interface cycle. *J Neural Eng*, 6(4):041001.

Van Veen, B. D., van Drongelen, W., Yuchtman, M., and Suzuki, A. (1997). Localization of brain electrical activity via linearly constrained minimum variance spatial filtering. *IEEE Trans Biomed Eng*, 44(9):867--880.

Velliste, M., Perel, S., Spalding, M. C., Whitford, A. S., and Schwartz, A. B. (2008). Cortical control of a prosthetic arm for self-feeding. *Nature*, 453(7198):1098--1101.

Vialatte, F.-B., Maurice, M., Dauwels, J., and Cichocki, A. (2010). Steady-state visually evoked potentials: focus on essential paradigms and future perspectives. *Prog Neurobiol*, 90(4):418--438.

Ville, J. (1958). *Theory and Applications of the Notion of Complex Signal*. Rand.

Waldert, S., Pistohl, T., Braun, C., Ball, T., Aertsen, A., and Mehring, C. (2009). A review on directional information in neural signals for brain-machine interfaces. *J Physiol Paris*, 103(3-5):244--254.

Waldert, S., Preissl, H., Demandt, E., Braun, C., Birbaumer, N., Aertsen, A., and Mehring, C. (2008). Hand movement direction decoded from meg and eeg. *J Neurosci*, 28(4):1000--1008.

Walter, W. G., Cooper, R., Aldrige, V. J., McCallum, W. C., and Winter, A. L. (1964). Contingent negative variation: An electric sign of sensorimotor association and expectancy in the human brain. *Nature*, 203:380--384.

Werner, W., Bauswein, E., and Fromm, C. (1991). Static firing rates of premotor and primary motor cortical neurons associated with torque and joint position. *Exp Brain Res*, 86(2):293--302.

Wild-Wall, N., Sangals, J., Sommer, W., and Leuthold, H. (2003). Are fingers special? evidence about movement preparation from event-related brain potentials. *Psychophysiology*, 40(1):7--16.

Wilke, J. T. and Lansing, R. W. (1973). Variations in the motor potential with force exerted during voluntary arm movements in man. *Electroencephalogr Clin Neurophysiol*, 35(3):259--265.

Wolpaw, J. R. (2007). Brain-computer interfaces as new brain output pathways. *J Physiol*, 579(Pt 3):613--619.

Wolpaw, J. R., Birbaumer, N., McFarland, D. J., Pfurtscheller, G., and Vaughan, T. M. (2002). Brain-computer interfaces for communication and control. *Clin Neurophysiol*, 113(6):767--791.

Wolpaw, J. R. and McFarland, D. J. (2004). Control of a two-dimensional movement signal by a noninvasive brain-computer interface in humans. *Proc Natl Acad Sci U S A*, 101(51):17849--17854.

Yuan, H., Perdoni, C., and He, B. (2010). Relationship between speed and eeg activity during imagined and executed hand movements. *J Neural Eng*, 7(2):26001.

Zander, T. O., Lehne, M., Ihme, K., Jatzev, S., Correia, J., Kothe, C., Picht, B., and Nijboer, F. (2011). A dry eeg-system for scientific research and brain-computer interfaces. *Front Neurosci*, 5:53.